POLYCYCLIC COMPOUNDS OF MANGANESE

By

NADA REGINATO, B.Sc., M.Sc.

A Thesis

Submitted to the School of Graduate Studies

in Partial Fulfillment of the Requirements

for the Degree

Doctor of Philosophy

McMaster University

POLYCYCLIC COMPOUNDS OF MANGANESE

Dedicated to my family,

my dad, the late Tarcisio, my mom AnnaMaria,

my sister Lisa, my little brother Marco and

my fiancé, Kevin

DOCTOR OF PHILOSOPHY (2003) McMaster University

(Chemistry) Hamilton, Ontario

TITLE: Polycyclic Compounds of Manganese

AUTHOR: Nada Reginato, B.Sc., M.Sc. (McMaster University)

SUPERVISOR: Professor M. J. McGlinchey

NUMBER OF PAGES: XVIII, 258

ABSTRACT

This dissertation focuses on the synthesis, characterization and reactivity of several types of arene manganese systems.

The reaction of potassium *tert*-butoxide with [(η^6-trindane)Mn(CO)$_3$][BF$_4$], **58c**, was investigated in attempts to functionalize **58c** at the benzylic positions. It was demonstrated that complex **58c** undergoes three C-H insertions and a haptotropic shift when treated with potassium *tert*-butoxide. As well, other trindane complexes including [(η^6-trindane)Mn(CO){P(OMe)$_3$}$_2$][BF$_4$], **98**, and [(η^6-trindane)Re(CO)$_3$][PF$_6$], **99**, have been synthesized in hopes of alkylating the *exo* benzylic positions and develop an organometallic route to sumanene, a key fragment of C_{60} that has not yet been synthesized. The former compound, **98**, was characterized by X-ray crystallography.

In order to probe the generality of the novel reaction exhibited by the trindane system, other [(arene)Mn(CO)$_3$]$^+$ systems were studied in which the arene is bicyclic or tricyclic and possesses attached 5-, 6- or 7-membered rings. In particular, the syntheses of [(η^6-indane)Mn(CO)$_3$][BF$_4$], **84**, [(η^6-tetralin)Mn(CO)$_3$][PF$_6$], **103**, and [(η^6-dibenzosuberane)Mn(CO)$_3$][BF$_4$], **102**, and their reactions with potassium *tert*-butoxide in the presence of donor ligands are presented. The products of these reactions were characterized by infrared and ^{1}H, ^{13}C and ^{31}P NMR spectroscopy and mass spectrometry.

The molecular dynamics of two hexaethylbenzene (HEB) complexes, [(η^6-HEB)Mn(CO)$_3$][BF$_4$], **147**, and (η^6-HEB)Mn(CO)$_2$Br, **148**, were examined using low-temperature NMR spectroscopy. The activation barrier ($\Delta G^{\neq}$) for ethyl rotation for **147** was determined to be ~ 11.5 kcal mol^{-1}. Crystallographic data was obtained for **148**,

which demonstrated the 1,3,5-*distal*-2,4,6-*proximal* geometry, a feature common to transition metal HEB complexes.

Finally, extended Hückel molecular orbital (EHMO) calculations were carried out for four polycyclic frameworks ligated to organometallic fragments: *anti*-dibenzpentalene, **157**, and *syn*-dibenzpentalene, **158**; fluoradenyl, **159**, and fluoranthene, **160**. Each of these systems exhibited unique dynamic behaviour, which are interpreted using a molecular orbital rationale.

ACKNOWLEDGEMENTS

I wish to express my deepest gratitude to my supervisor Dr. M. J. McGlinchey for his guidance and support throughout the course of my graduate career. He has provided an enjoyable approach to research along with his patience and understanding. I would also like to thank the members of my Ph.D. thesis committee, Dr. Harold Stöver and Dr. John Valliant for their ideas, valuable input and support throughout my thesis.

I would also like to thank the facilities staff in the Department of Chemistry, including Dr. Don Hughes (NMR), Brian Sayer (NMR) and George Timmins for their assistance, advice, and training on the NMR instruments. Thanks also to Dr. Jim Britten for his assistance in solving X-ray structures, answering many of the questions I had and taking the time to demonstrate how crystallography works. I would like to thank the ladies in the Chemistry Department office for their help, kindness and generosity.

To everyone with whom I worked with in the MJM lab, both past and present members, Dr. Sonya Balduzzi, Dr. Hari Gupta, Dr. Pippa Lock, Dr. Yannick Ortin, Dr. Mark Stradiotto, Stacey Brydges, John Kaldis, Laura Harrington and Frank Ogini. Thank you for making the lab an enjoyable place in which to work in, your advice and friendship will be cherished.

I would like to thank Dr. Nadine Merkley for her friendship. Thanks for all those timeless moments and great memories, graduate school related or not. You have been a friend who has always understood and listened to me. To Katrina, Linda, Sheila (and family), Gina and Anna for providing a constant ear, advice and support, but most

importantly for providing an outlet outside my science world. I would like to thank all my friends for their continuous support over the years.

Finally, a special thanks goes out to my Mom, my sister Lisa and my brother Marco for their unconditional love, support, patience and belief in me. There are no appropriate words to express my gratitude for what you have all done and endured. I know I can always count on all of you. I love you all, your constant encouragement and faith in me got me to where I am today.

I would like to thank my fiancé, Kevin for coming into my life when you did. Thank you for your continuous support throughout my thesis, especially spending numerous hours reading it and keeping me on track. You are my best friend; I look forward to spending an eternity with you.

I would like to thank my Dad, even though he is not here today, he has always told me to shoot for the stars. His belief in me and constant encouragement, support and love throughout the years, has made me who I am and has gotten me to where I am today. I love you and (you are always in my heart forever) Sempre nei miei pensieri e nel mio cuore, ti amo.

TABLE OF CONTENTS

Chapter Two: Manganese Complexes of Trindane

Chapter Three: Haptotropic Shifts of Manganese Tricarbonyl Moieties in Bi- and Tricyclic Arenes Possessing Five-, Six- and Seven-Membered Rings

LIST OF FIGURES

LIST OF SCHEMES

LIST OF TABLES

LIST OF ABBREVIATIONS

MeCN	Acetonitrile
Å	Ångstrom
π^*	Antibonding orbital
ν_{co}	Carbonyl stretching frequency
Cp	Cyclopentadienyl, C_5H_5
DFT	Density functional theory
FVP	Flash vacuum pyrolysis
$\Delta G^{\neq}$	Gibbs Free Energy of Activation
Hz	Hertz
HEB	Hexaethylbenzene, C_6Et_6
HMB	Hexamethylbenzene, C_6Me_6
H	Hydrogen
Δ	Heat
IR	Infrared spectroscopy
K	Temperature, Kelvin
kcal	kilocalories
L	Ligand
M	Metal
Me	Methyl
$[M]^+$	Parent ion mass (mass spectrometry)
m/z	mass to charge ratio (mass spectrometry)
MS	Mass spectrometry
MHz	Megahertz
mol	Mole
NMR	Nuclear Magnetic Resonance
Nu	Nucleophile
ML_n	Organometallic fragment
p	para
ppm	Parts per million
Ph	Phenyl
PTSA	*p*-Toluenesulfonic acid
t-BuOK	Potassium *tert*-butoxide
PES	Potential Energy Surface
T	Temperature
THF	Tetrahydrofuran
TFA	Trifluoroacetic acid
cm^{-1}	Reciprocal centrimeters (wavenumbers)

CHAPTER ONE

Introduction

1.1 Organometallic Chemistry: An Overview

Organometallic chemistry involves the combination of metal-containing molecular fragments with organic substances, thus forming organometallic compounds. First investigated by W. C. Zeise in the nineteenth century, it is today a well-developed and continually growing field leading to the discovery of new reactions, as well as novel and unique structures. It is not only intellectually challenging, but is also of enormous practical importance in organic synthesis, and plays a key role in industry, particularly with respect to catalysis. In 1827, W. C. Zeise synthesized an ethene complex of platinum, **1**, and, over the next century and a quarter, a number of other transition metal compounds were discovered. However, it was not until 1952 with the discovery of ferrocene, **2**,[1] a remarkably stable compound, that this area of chemistry began to flourish.

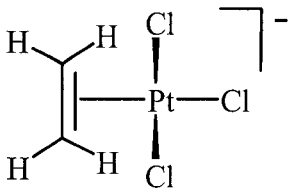

$[PtCl_3(\eta^2\text{-}C_2H_4)]^-$, **1**

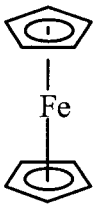

$Fe(\eta^5\text{-}C_5H_5)_2$, **2**

Organometallic compounds (or complexes) are defined as molecules that possess metal-carbon bonds. Nowadays, this class of compounds contains organic moieties that range from alkyl substituents to alkenes, alkynes, carbonyl groups, aromatics,

heterocycles, and many more. In general, organic fragments form two types of compounds with transition metals: those that contain metal-carbon σ-bonds, and those in which the organic molecule interacts with the metal *via* their π-electrons. In many cases both bonding situations may occur in the same molecule. Among other factors, the stability of an organometallic compound is related to the number of valence electrons provided by the metal and the ligand(s). The majority of stable transition metal complexes follow the 18-electron rule, which states that "a stable complex is obtained when the sum of the metal d-electrons, the electrons donated by the ligands, and the overall charge of the complex equals 18".[2] The focus of this thesis will be on organic moieties π-complexed to transition metals, in particular, arene manganese complexes.

1.2 Transition Metal Arene Complexes

There is a plethora of transition metal arene complexes documented in the literature. A very brief overview of transition metal complexes is given, although the main focus will be on manganese arene complexes. An arene is defined as a six-membered ring consisting of sp^2 carbon atoms, the simplest one being benzene (C_6H_6).[3] Arenes, such as benzene and its derivatives, can form complexes with transition metals in a variety of bonding arrangements. The most common mode of coordination for arenes to transition metals is the η^6 (hexahapto) form. However, η^4 and η^2 complexes are also known modes of coordination as exemplified by compounds **3** and **4**, respectively. [4,5] Hapticity, as originally defined by Cotton,[6] refers to the number of carbon atoms attached to the metal atom. Thus, each of the cyclopentadienyl rings in ferrocene is bonded in a

pentahapto (η^5) fashion, while a hexahapto (η^6) ligand denotes that six carbon atoms are bonded to the metal atom, as in compound **5**.

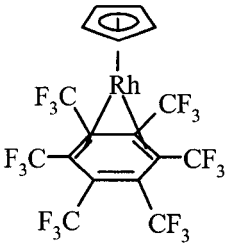

(η^4-$C_6(CF_3)_6$)Rh(η^5-C_5H_5), **3**

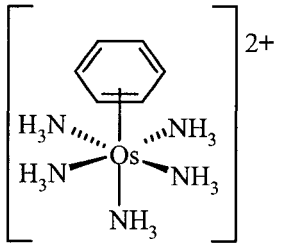

$[Os(NH_3)_5(\eta^2\text{-}C_6H_6)]^{2+}$, **4**

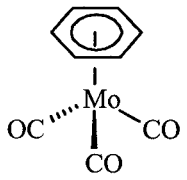

(η^6-C_6H_6)$Mo(CO)_3$, **5**

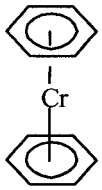

(η^6-C_6H_6)$_2$Cr, **6**

Bis(arene) metal complexes, such as **6**, or arene half-sandwich complexes of the type [(arene)ML_n, where L = CO, PR_3, etc.], such as **5**, have been synthesized for a wide variety of arene-metal combinations, including polyalkylated benzenes, as in (1,3,5-$Me_3C_6H_3$)$W(CO)_3$,[7] hormonal steroids such as the estradiol complex, **7**,[8] or polycyclic aromatics such as the triphenylene system, **8**.[9] Arene complexes are known in several forms: as neutral compounds, such as the parent chromium compound (C_6H_6)$Cr(CO)_3$;[10] as anionic species, typified by the vanadium complex $V(C_6H_6)_2^-$;[11] or as cations, as in the iron-containing mixed sandwich compound $[(C_5H_5)Fe(C_6H_6)]^+$.[12] Arenes are not restricted to binding to single metal sites but, for example, are also known to be sited on metal triangles, as in the face-capped μ_3-η^2:η^2:η^2-arene species of the trinuclear complexes $M_3(CO)_9(\mu_3\text{-}\eta^2\text{:}\eta^2\text{:}\eta^2\text{-}C_6H_6)$, where M = Ru and Os.[13]

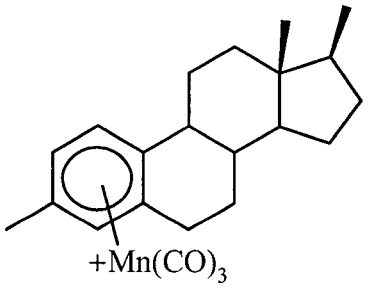

7

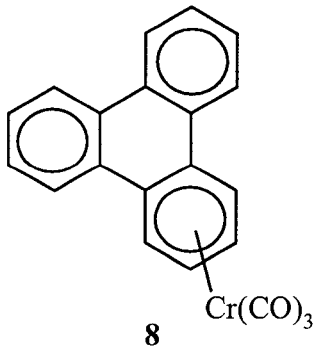

8

There are several, well-established, preparative methods for transition metal arene complexes. Typical synthetic routes are:

1) Arene and a complex of a reduced metal:[14]

$$Cr(CO)_6 + C_6H_6 \xrightarrow{n\text{-}Bu_2O} (C_6H_6)Cr(CO)_3 \qquad \textbf{1.1}$$

$$(\eta^5\text{-}C_5H_5)_2Fe + C_6H_6 \xrightarrow{AlCl_3} [(\eta^5\text{-}C_5H_5)Fe(C_6H_6)]^+ \qquad \textbf{1.2}$$

2) Arene, metal salt and a reducing agent:[15]

$$CrCl_3 + Al + C_6H_6 + AlCl_3 \longrightarrow [(C_6H_6)_2Cr]^+ \xrightarrow[KOH]{S_2O_4^{2-}} [(C_6H_6)_2Cr] \qquad \textbf{1.3}$$

3) Synthesis by ligand exchange:[16]

$$(C_6H_6)Cr(CO)_3 + 1,3,5\text{-}Me_3C_6H_3 \xrightarrow{\Delta} (1,3,5\text{-}Me_3C_6H_3)Cr(CO)_3 \qquad \textbf{1.4}$$

4) Synthesis from dienes:[17]

$$1,3\text{-cyclohexadiene} + RuCl_3 \longrightarrow [(C_6H_6)RuCl(\mu\text{-}Cl)]_2 \qquad \textbf{1.5}$$

5) Synthesis from metal carbonyls:[18]

$$C_6H_6 + MnCl(CO)_5 \xrightarrow{AlCl_3} [(\eta^6\text{-}C_6H_6)Mn(CO)_3][AlCl_4] \qquad \textbf{1.6}$$

Metal vapor synthesis is another useful method for the synthesis of arene complexes not accessible by the standard routes outlined above. Thus, cocondensation of chromium vapor, benzene and hexafluorobenzene onto a liquid nitrogen cooled surface yields the surprisingly stable mixed sandwich $(C_6H_6)Cr(C_6F_6)$.[19]

Arenes are known to coordinate preferentially to low-valent metals; hence metals (as salts) in higher oxidation states are often reduced in the presence of the ligand.[3] Herein, the remainder of the chapter will focus on cationic metal arene complexes, specifically arene manganese tricarbonyl complexes.

1.3 Cationic Metal Arene Complexes

The first report of a cationic metal arene complex was by Hein in the 1920's.[20] The compound was subsequently identified by Zeiss and Tsutsui as the bis(benzene)chromium cation, $[(C_6H_6)_2Cr]^+$.[21] In the 1950's Fischer and Hafner demonstrated that cationic π-aromatic complexes could be prepared under reducing conditions in the presence of a strong Lewis acid.[22] Today this method is referred to as the Fischer-Hafner reaction, and is commonly used for the synthesis of π-arene complexes (see Equation 1.3). Numerous metal arene complexes have been prepared utilizing this method, such as $[(\eta^6\text{-arene})FeCp]^+$ and $[(\eta^6\text{-arene})Mn(CO)_3]^+$. Cationic transition metal arene complexes, in particular cationic arene manganese tricarbonyl complexes display specific types of arene reactivity attributable to the presence of the metal fragment; this will be further discussed in Section 1.4.

1.3.1 Synthesis of Cationic Manganese Arene Complexes

There are generally three direct synthetic methods used for the preparation of cationic arene manganese tricarbonyl complexes. All methods involve the formation of the $[Mn(CO)_5]^+$ intermediate followed by coordination to the arene of interest (Scheme 1.1). The difference between the three methods lies in the conditions for generating $[Mn(CO)_5]^+$.

$$Mn(CO)_5Br \xrightarrow[1,\ 2,\ \text{or}\ 3]{\text{method}} [Mn(CO)_5]^+ \xrightarrow{\text{arene}} [(\eta^6\text{-arene})Mn(CO)_3]^+$$

Scheme 1.1: General scheme for the preparation of $[(\eta^6\text{-arene})Mn(CO)_3]^+$.

Fischer and Hafner[4] developed the original method which involves heating $Mn(CO)_5Br$ and the arene in the presence of a Lewis acid, $AlCl_3$. However, this route has its limitations with arenes containing reactive functional groups. When heated in a hydrocarbon solvent, the $[Mn(CO)_5]^+$ intermediate is formed through halide abstraction by the aluminum chloride (Equation 1.7); subsequent coordination to an arene, and loss of two carbonyl ligands, furnishes $[(\eta^6\text{-arene})Mn(CO)_3]^+$.

$$[Mn(CO)_5Br] + AlCl_3 \longrightarrow [Mn(CO)_5]^+ + AlCl_3Br^- \qquad \textbf{1.7}$$

A second method pioneered by Pauson,[23] also involves the formation of the $[Mn(CO)_5]^+$ intermediate, which is generated by halide abstraction using silver(I) ion (Equation 1.8).

$$[Mn(CO)_5Br] + Ag^+ \longrightarrow [Mn(CO)_5]^+ + AgBr \qquad \textbf{1.8}$$

This favoured synthetic process involves treating $Mn(CO)_5Br$ with a stoichiometric amount of $AgBF_4$ in CH_2Cl_2 under argon or nitrogen with the exclusion of light. After

heating under reflux for 30 min, the solution is treated with the arene and the reaction is maintained at reflux for 16 h. The reactive intermediate [$Mn(CO)_5^+$] (which is generated *in situ*) is formed by halide abstraction from $Mn(CO)_5Br$, ultimately giving rise to [(η^6-arene)$Mn(CO)_3$]$^+$. This method facilitates the coordination of the arene unit to the $Mn(CO)_3^+$ fragment under relatively mild conditions inhibiting any side reactions or isomerisation of the arene ring substituents. This method, referred to as the silver(I) method, has allowed the class of cationic arene manganese complexes to be extended and has been successful in allowing the coordination of the $Mn(CO)_3^+$ fragment to arenes containing electron-donating alkoxyl and alkyl subsituents[24], indoles[25] and aromatic steroids.[8, 26]

[(Arene)$Mn(CO)_3$]$^+$ complexes can also be generated by allowing the arene to react with $Mn(CO)_5(ClO_4)$ or $Mn(CO)_3(acetone)_3^+$ and heating under reflux in dichloromethane. The perchlorato complex, $Mn(CO)_5(ClO_4)$, is prepared in high yields (75 - 94 %), by treating $Mn_2(CO)_{10}$ in TFAA with $HClO_4$ at 0 °C.[27] This perchlorate complex has been used to synthesize cationic arene manganese tricarbonyl complexes under relatively mild conditions (i.e., heating the Mn(CO)5(ClO4) under reflux with the arene in CH_2Cl_2 for 2 - 20 h). The (arene)$Mn(CO)_3^+$ complex spontaneously precipitates out of the boiling CH_2Cl_2 solution.[27d]

In 1984, a third method of preparing [(η^6-arene)$Mn(CO)_3$]$^+$ complexes was established which also involves the generation of the [$Mn(CO)_5$]$^+$ intermediate, but *via* direct oxidation of [$Mn_2(CO)_{10}$] with a strong acid in trifluoroacetic (TFA) anhydride, as seen in Equation 1.9.[28]

$$[Mn_2(CO)_{10}] + 2H^+ + (CF_3CO)_2O \longrightarrow 2[Mn(CO)_5]^+ + H_2 \quad \textbf{1.9}$$

This method utilizes strong acidic conditions with the following starting materials $[Mn_2(CO)_{10}]$, $[Mn(CO)_5Br]$ or $[Mn_2(CO)_8(\mu\text{-}Cl)_2]$, to generate $[Mn(CO)_5]^+$.

The method of choice has been shown to depend on three factors that would influence the coordinating ability of the arene of interest.[29] These factors are: acid-sensitivity of the arene, the electronic character of the arene, and the presence of lone pair-bearing heteratoms on the arene. The electronic character of the arene is the most influential of the three, since the $Mn(CO)_3^+$ moiety is highly electronegative and withdraws electron density from the ring. Consequently, electron-donating substituents on the arene ring are favoured, and the presence of electron-withdrawing or electronegative substituents on the arene results in weak, if any, coordination to the $Mn(CO)_3^+$ fragment. Another factor, which must also be taken into consideration, is the acid sensitivity of the aromatic substrates. The acidic nature of the three reactions varies, however, the silver(I) approach utilizes stoichiometric amounts of a mild and highly halide-specific Lewis acid which is unlikely to react with most arenes. The other protocols employ an excess of strong Lewis or Brønsted acid, which will destabilize some arenes.

In summary, the Fischer-Hafner method is practical and does not require an inert atmosphere. The TFA anhydride synthesis involves the harshest conditions and caution must be implemented when using TFA anhydride. As previously stated, the Ag(I) approach is the mildest of the three and is extremely useful when using acid-sensitive arenes. Nonetheless, the reaction is carried out under inert conditions and in the dark.

The above synthetic methods have been successful for the preparation of monocyclic arenes, however, they are not necessarily applicable to the synthesis of polycyclic arenes. For instance, the attempted preparation of $(\eta^6$-naphthalene$)Mn(CO)_3^+$ *via* the Fischer-Hafner method afforded instead the $(\eta^6$-tetralin$)Mn(CO)_3^+$ complex.[30] Attempts to coordinate polycyclic arenes to the $Mn(CO)_3^+$ moiety by these methods yielded only trace amounts of the desired complex, or hydrogenated products. However, when all reagents are thoroughly dried, the Ag(I) method is an efficient method for producing a number of naphthalene-type manganese complexes. These complexes readily undergo displacement by donor solvents such as acetonitrile (Equation 1.10).[31]

$$(\text{polycyclic arene})Mn(CO)_3^+ + 3MeCN \longrightarrow (MeCN)_3Mn(CO)_3^+ + \text{polycyclic arene} \quad \textbf{1.10}$$

The ease with which these naphthalene-type manganese complexes undergo arene displacement by donor solvents has made them excellent manganese tricarbonyl transfer (MTT) agents.[31] Synthetically, this has opened the door to otherwise unavailable polycyclic manganese complexes through a remarkably mild procedure.

The synthetic utility of cationic arene manganese complexes is evident from their reactivity with carbon-based nucleophiles, thus giving rise to compounds with new carbon-carbon bonds.[29]

1.4 General Reactivity Patterns of Arene Manganese Tricarbonyl Complexes

It is generally found that arene manganese tricarbonyl complexes salts are pale yellow, usually crystalline, solids and are soluble in polar organic solvents. They are air- and moisture-stable in the solid state but, in solution, they undergo slow decomposition in presence of air. Cationic arene manganese complexes are commonly characterized by

infrared spectroscopy, which exhibits carbonyl stretching frequencies generally above 2000 cm^{-1}.

Complexation of the $Mn(CO)_3^+$ moiety to the arene imparts unique reactivity to the complexed arene system (Figure 1.1). Coordination of the metal fragment to the arene opens the door to synthetic transformations not possible with the arene alone. The reactivity is attributed to the electron-withdrawing properties of the $Mn(CO)_3^+$ unit.

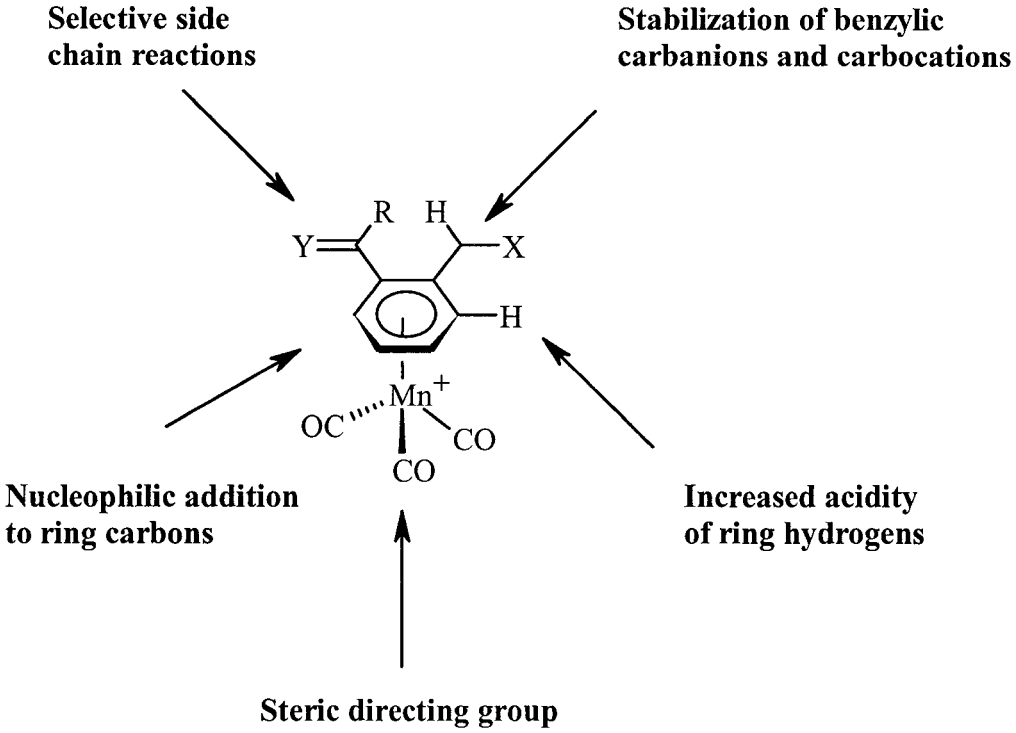

Figure 1.1: Reactivity of arene manganese tricarbonyl cationic complexes.

Cationic (arene)$Mn(CO)_3^+$ complexes are more electrophilic compared to neutral (arene)$Cr(CO)_3$ complexes. However, (arene)$Cr(CO)_3$ chemistry has been much more extensively developed than that of (arene)$Mn(CO)_3^+$ compounds. The relative reactivity of different arene-metal complexes towards nucleophilic addition compares as follows:

$[(C_6H_6)_2Fe]^{2+}$ (2 x 10^8) > $[(C_6H_6)_2Ru]^{2+}$ (6 x 10^6) > $[(C_6H_6)Mn(CO)_3]^+$ (1.1 x 10^4) > $[(C_6H_6)Mn(CO)_2(PPh_3)]^+$ (160) > $[(C_6H_6)Fe(C_5H_5)]^+$ (1) > $(C_6H_6)Cr(CO)_3$ (very low). [32]

Not only do the arene hydrogen atoms have increased acidity and are thus susceptible to deprotonation, but the arene is also prone to nucleophilic addition reactions. Typically nucleophiles attack on the *exo* face of the arene ring relative to the $Mn(CO)_3$ fragment.[33] The site of attack is dependent on the nature of the arene substituents. A variety of nucleophiles that have been used, including Grignard reagents, ketone enolates, malonates and hydrides. [33,34] Other nucleophiles that have not been as thoroughly investigated are hydroxyl, cyano and azido anions.[34]

1.4.1 Reactivity of Arene Manganese Tricarbonyl Complexes

Nucleophiles react with (arene)$Mn(CO)_3^+$ compounds in several ways: (i) by addition to the arene ring, (ii) by attack at the metal with displacement of a carbonyl ligand, (iii) by attack at the metal with liberation of arene, and (iv) by addition to the carbon atom of a carbonyl group.[35]

(i) Nucleophilic addition to the arene:

Addition of a nucleophile to the arene ring of (η^6-arene)$Mn(CO)_3^+$ occurs in a stereoselective manner giving rise to *exo*-cyclohexadienyl complexes which are quite stable.

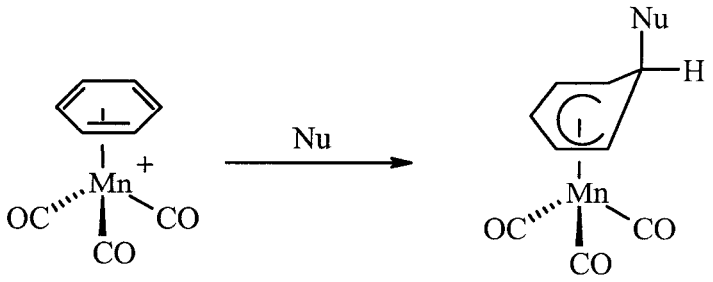

9 **10** **1.11**

Early work by Wilkinson and Pauson on the addition of nucleophiles involved treatment of **9** with LiMe, LiPh and hydride donors (such as $NaBH_4$ and $LiAlH_4$) and afforded the cyclohexadienyl complex, **10**, in poor yields.[36] Compound **10** (when Nu = H[37] or Ph[38]) was characterized by X-ray crystallography. However, other products were isolated that implied that attack had occurred on the carbonyl ligand. Walker and Mawby demonstrated that the addition of an enolate anion, $(EtO_2C)_2CH^-$ in ethanol at room temperature occurred *exo* to the arene ring of $[(C_6H_6)Mn(CO)_3][BF_4]$.[35] The formation of the cyclohexadienyl compound was evident from the carbonyl stretches at 2030, 1960 and 1948 cm^{-1} (in pentane), which are shifted to lower wavenumbers in comparison to those of the cationic precursor (2080, 2026 cm^{-1} in acetone).[35] A similar reaction occurred between $[(C_6H_6)Mn(CO)_3][BF_4]$ and the acetylacetonate anion giving rise to $[(\eta^5\text{-}C_6H_6CH(COMe)_2)Mn(CO)_3]$. The synthetic utility of arene manganese carbonyl complexes was examined by treatment with C-donor nucleophiles to probe arene functionalization. Grignard reagents (MgMeCl, MgEtCl, MgPhBr) and ester or ketone enolates ($NaCH(CO_2Et)_2$, $LiCH_2CO_2Bu^t$) were found to add efficiently, furnishing stable cyclohexadienyl complexes in high yields.[32] Decomplexation of the metal moiety from the cyclohexadienyl complexes occurs under oxidative conditions, using stoichiometric

quantities of the Jones reagent (CrO_3/H_2SO_4/acetone), producing the functionalized arene in high yields (Equation 1.12).[39]

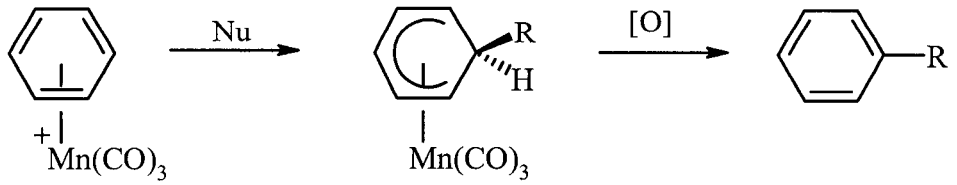

1.12

11 **12**

Nu = PhLi, MeLi, RMgBr, ketone enolates, malonates, $LiAlH_4$

Another technique used to isolate the functionalized arene is to treat **10** with acid in acetonitrile, which converts the manganese compound to $[Mn(CO)_3(MeCN)_3]^+$ and liberates the arene.[32] However, these methods are not always very successful. A more efficient protocol involves double nucleophilic addition, whereby decomplexation is achieved by simply stirring in the presence of oxygen (Equation 1.13).[40]

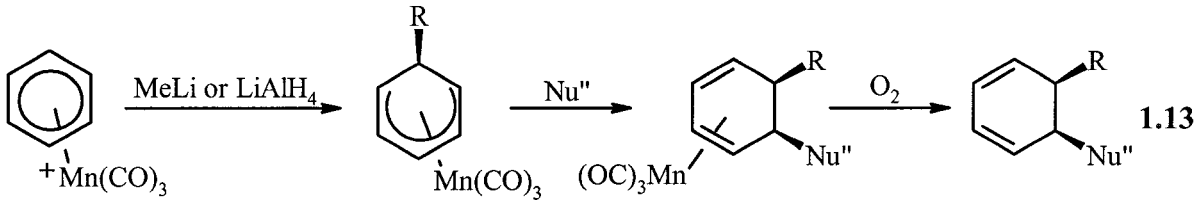

1.13

R = H or Me

Numerous C-donors have been allowed to react with $(\eta^6\text{-arene})Mn(CO)_3^+$ yielding thermally stable, relatively air-stable cyclohexadienyl compounds, from which the functionalized arene may be isolated by ready removal of the manganese fragment. This allows the synthesis of arenes not accessible by classical organic transformations, or any other method. The beauty of utilizing arene manganese carbonyl compounds is that

the nucleophilic addition can be monitored using infrared spectroscopy by observing the shifts of the carbonyl bands.

The examples stated above demonstrate the addition of "classical" nucleophiles to the arene ring of cationic (η^6-arene)tricarbonylmanganese complexes. On the other hand, organometallic nucleophiles such as lithiated (arene)$Cr(CO)_3$ have been treated with cationic arene manganese complexes leading to the formation of homo- and heteropolymetallic complexes.[41] These types of reactions have allowed the elegant syntheses of novel, hetero di-, tri- and tetrametallic complexes (**13** and **14**).[42] The addition of 2-lithioacetonitrile to (η^6-benzene)$Mn(CO)_3^+$ furnished the mononuclear complex **15**, dinuclear complex **16**, and trinuclear complex **17** in the ratio 80:18:2.[43] Other interesting multimetallic systems are structures **18** and **19**, which were synthesized by nucleophilic addition of $NaRe(CO)_5$ or $Na_2Os(CO)_4$ to the (η^6-benzene)$Mn(CO)_3^+$ complex, respectively.[44]

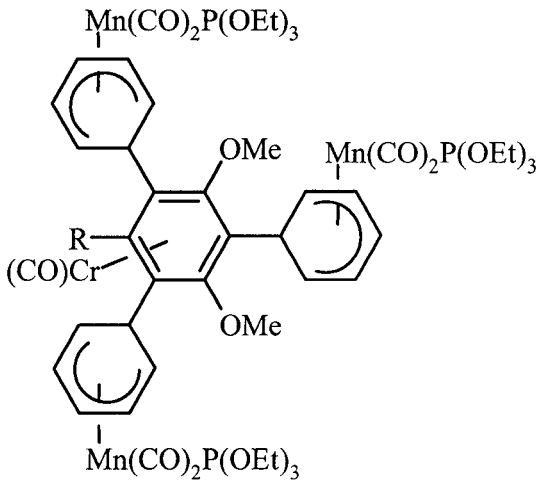

13 R = H (36 %)
14 R = OMe (33 %)

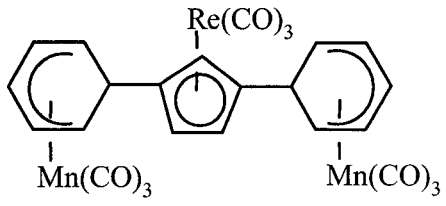

18

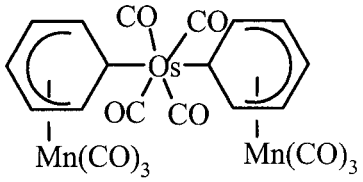

19

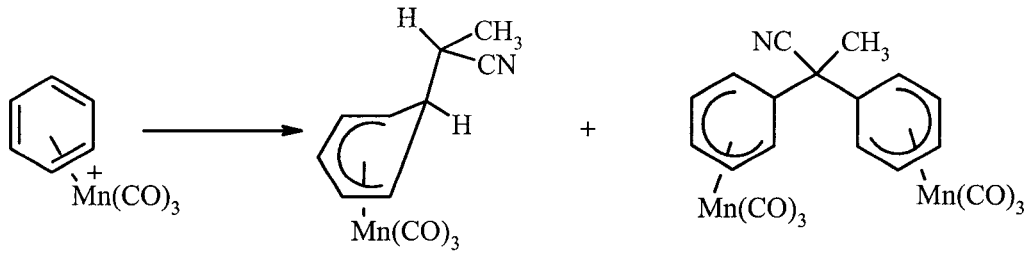

15 **16**

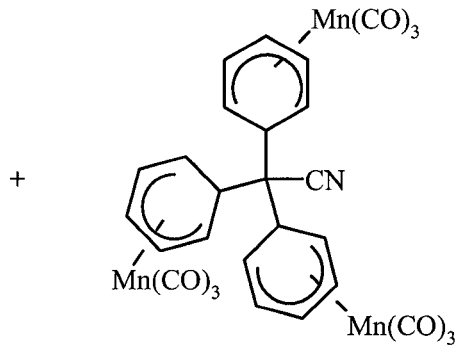

17

Another synthetic application of arene manganese carbonyl complexes involves the functionalization of aromatic steroids. For instance, Sweigart and co-workers have demonstrated that the A-ring in the aromatic steroids estrone 3-methyl ether or β-estradiol 3,17-dimethyl ether readily coordinates to $Mn(CO)_3^+$, thereby activating the A-ring towards nucleophilic attack and giving rise to the dienyl complex.[8] The dienyl complex can be demetallated and rearomatized, and one is left with a functionalized steroid. Other examples include the synthesis and electrophilic reactivity of manganese tricarbonyl complexes of the C-ring aromatic diterpenoid methyl *O*-methylpodocarpate.[26]

Non-nucleophilic bases such as potassium *tert*-butoxide, potassium hydride, and $LiNPr^i_2$ have been shown to deprotonate benzylic hydrogen atoms on the arene. Eyman *et al.* reported the synthesis and reactivity of the cyclohexadienyl complex, $(\eta^5\text{-}C_6Me_5(CH_2))Mn(CO)_3$, **20**, obtained from monodeprotonation of $(C_6Me_6)Mn(CO)_3^+$ by

KH.[45] The structure of **20** was established by X-ray crystallography confirming the presence of the exocyclic methylene group. Gladfelter further investigated the generality of deprotonating benzylic protons of other alkyl-arene manganese complexes, arene = toluene, C_6H_5Et, $C_6H_5Pr^i$. These manganese complexes when treated with excess potassium *tert*-butoxide yielded the air- and moisture-sensitive cyclohexadienyl complexes, $(\eta^5\text{-}C_6H_5(CH_2))Mn(CO)_3$, $(\eta^5\text{-}C_6H_5(CHCH_3))Mn(CO)_3$ and $(\eta^5\text{-}C_6H_5(CMe_2))Mn(CO)_3$ (see Equations 1.14 and 1.15).[46]

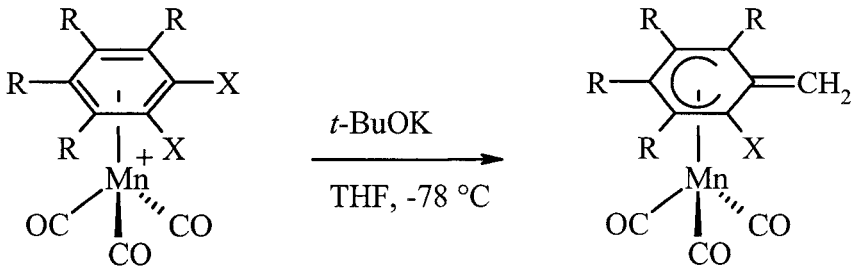

1.14

21a: X = R = Me
21b: X = Me, R = H

22a: X = R = Me
22b: X = Me, R = H

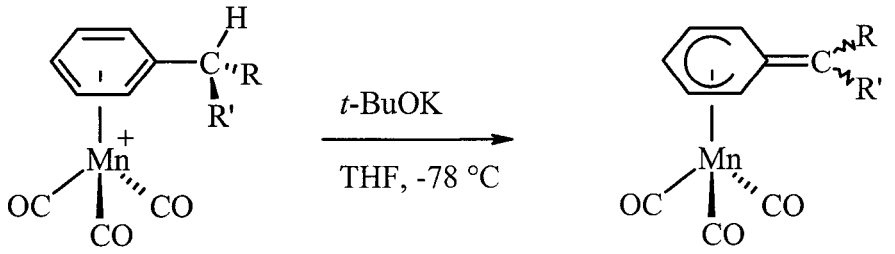

1.15

23a: R = R' = H
23b: R = H, R' = Me
23c: R = R' = Me

24a: R = R' = H
24b: R = H, R' = Me
24c: R = R' = Me

The isolation and identification of these cyclohexadienyl complexes demonstrates the potential for functionalization of the benzylic positions of arene systems including

multiple alkylations (see section 1.5.1, Astruc's methodololgy), and/or arene ring functionalization.

Compound **22a** was alkylated when treated with $CF_3SO_3CH_3$ affording the ethylpentamethylbenzene complex. Treatment of **24a** with Br_2 yielded the bromomethyl complex, $[(C_6H_5CH_2Br)Mn(CO)_3]^+$.

(ii) CO replacement:

The replacement of carbonyl ligands in arene manganese complexes is a known reaction. It has been well established that conversion of $(C_6Me_6)Mn(CO)_3^+$ into $(C_6Me_6)Mn(CO)_2X$ (X = Cl, Br,or I) requires either photolysis or use of trimethylamine N-oxide (Me_3NO) to induce loss of a carbonyl ligand.[47] The halide complexes have been shown to be useful precursors to other complexes (equations 1.16 and 1.17).

$$(C_6Me_6)Mn(CO)_2I + NaBH_4 \longrightarrow (C_6Me_6)Mn(CO)_2H \qquad \textbf{1.16}$$

$$(C_6Me_6)Mn(CO)_2Br + MeLi \longrightarrow (C_6Me_6)Mn(CO)_2Me \qquad \textbf{1.17}$$

Also, phosphines or phosphites readily substitute CO ligands either under photolytic conditions or by treatment with Me_3NO in the presence of PR_3 yielding $[(\eta^6\text{-arene})Mn(CO)_2PR_3]^+$.[48] Upon the replacement of a carbonyl by a phosphine or phosphite there is an increase in the electron density on the metal and the electrophilicity of the arene ring is reduced in comparison to that of the tricarbonyl cationic precursor. However, altering the electronic effect of the metal has a profound effect on the reactivity of these manganese complexes towards a variety of synthetically useful nucleophiles.

The substitution of two carbonyl groups has been carried out by utilizing the trimethylamine N-oxide procedure with $[(\eta^6\text{-arene})Mn(CO)_3]^+$ or $[(\eta^6\text{-arene})$-

$Mn(CO)_2PR_3]^+$ and the ligand of interest. This method has allowed the preparation of bis-phosphines or bis-phosphites with both cations, and also the formation of chelate complexes of the general formula, $[(\eta^6\text{-arene})Mn(CO)(PPh_2(CH_2)_nPPh_2)]^+$, where n = 1-3, by starting from the monsubstituted phosphine cation $[(\eta^6\text{-arene})\text{-}Mn(CO)_2(PPh_2(CH_2)_nPPh_2)]^+$.[49]

(iii) Nucleophilic attack on the metal with loss of the arene:

When $[(C_6H_6)Mn(CO)_3][BPh_4]$ was heated under reflux in acetonitrile, the arene was displaced and $[Mn(CO)_3(NCMe)_3][BPh_4]$ was isolated as a crystalline product.[35] Analogous reactions were performed with other cationic arene manganese complexes, where the arenes used were toluene, *p*-xylene and mesitylene. The rate of arene displacement was seen to decrease with increasing substitution on the arene, and was attributed to stronger bonding between the arene and the metal, or increasing hindrance to attack of the incoming acetonitrile.[35]

(iv) Nucleophilic addition to the carbon atom of a carbonyl group:

Cationic complexes, $[(arene)Mn(CO)_3]^+$ (arene = C_6H_6, C_6Me_6, mesitylene) react with methoxide in methanol to yield rather unstable esters $(arene)Mn(CO)_2CO_2Me$.[35] Angelici and Blacik reported that analogous compounds of the type $(arene)Mn(CO)_2CONHR$ (arene = C_6Me_6, mesitylene, toluene, *p*-xylene, durene and R = H, C_6H_{11}) were formed by treatment of $[(arene)Mn(CO)_3]^+$ with amines.[50]

1.5 Ligand Deprotonation Reactions

It is known that the benzylic hydrogen atoms of cyclic π-polyene ligands coordinated to electrophilic transition metal moieties, especially those that contain

carbonyl groups and/or cationic metal fragments, are moderately acidic. It has been clearly demonstrated that coordinating the manganese tricarbonyl moiety to an arene results in superior electrophilic activation, compared to that of the chromium and ruthenium analogues.[51] Deprotonation at benzylic carbons of π-coordinated arenes has been demonstrated for various metal fragments ($Mn(CO)_3^+$,[52] $FeCp^+$,[53] $Cr(CO)_3$[54]).

π-Coordination of a metal moiety to an arene with benzylic carbons facilitates base-catalyzed replacement of a hydrogen atom for an alkyl group. For instance, a steroidal chromium tricarbonyl complex substitutes a $-CH_2OH$ group at the benzylic position (C6) for a hydrogen atom, as seen in Scheme 1.2.[55] The strong electron-withdrawing properties of the $Cr(CO)_3$ moiety render the arene electrophilic, such that it becomes susceptible to deprotonation by a base followed by the addition of an electrophile. The hydrogen that is replaced is *exo* with respect to the metal moiety, that is, on the opposite (anti) side to the metal fragment.

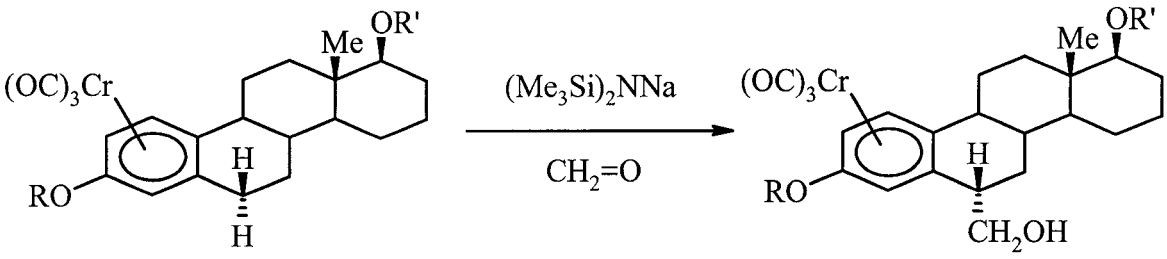

Scheme 1.2: Transition metal-promoted deprotonation at an *exo*-benzylic site.

See section 1.4.1 for other deprotonation reactions investigated by Eyman and Gladfelter separately.

1.5.1 Astruc's Methodology

Astruc[56] has devised an elegant methodology for synthesizing hexa-functionalized transition-metal-arene complexes in one step. It involves the deprotonation of *exo*-benzylic positions of the ligand followed by alkylation. In a typical reaction, $[(C_6Me_6)Fe(C_5H_5)]^+$, **25**, when treated with potassium *tert*-butoxide (*t*-BuOK) and excess methyl iodide (or benzyl bromide), gave rise to the cation $[(C_6Et_6)Fe(C_5H_5)]^+$, **26**, (or $[(C_6(CH_2CH_2Ph)_6)Fe(C_5H_5)]^+$) formed *via* a series of zwitterionic intermediates, as depicted in Scheme 1.3.

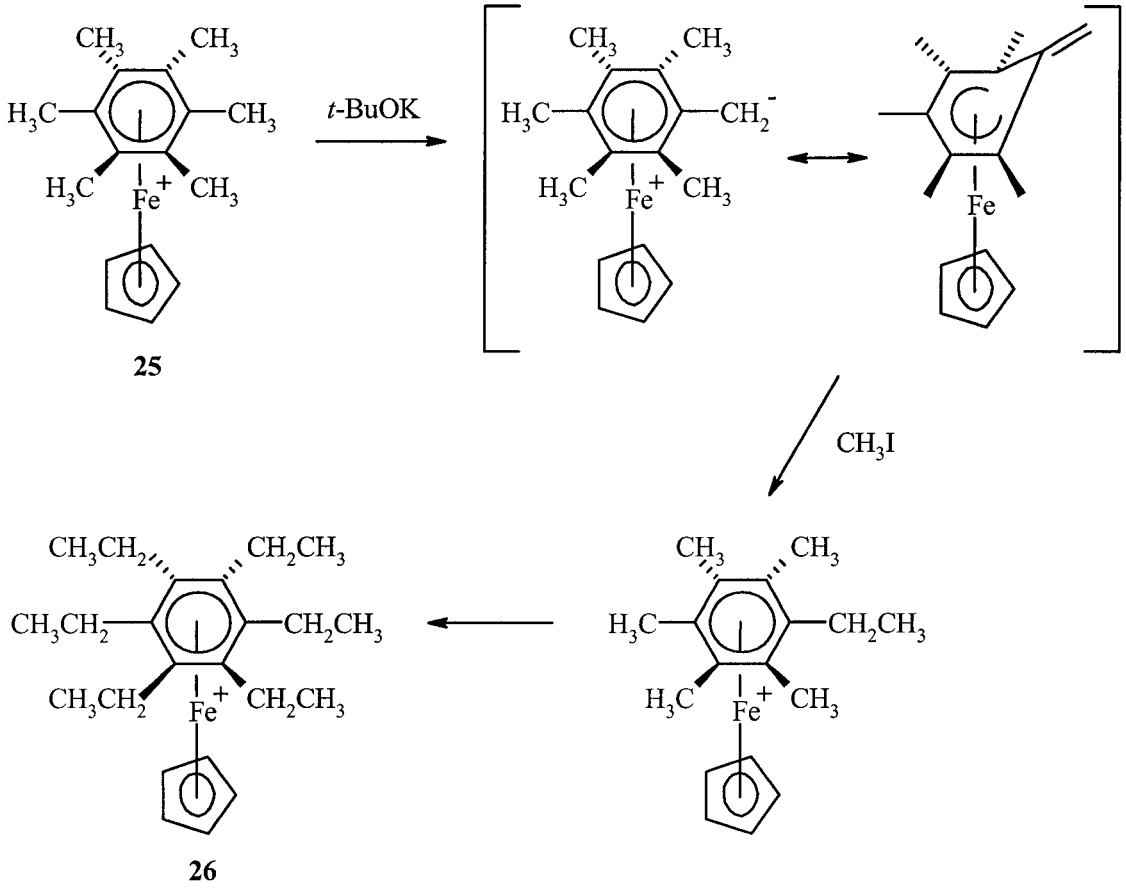

25 **26**

Scheme 1.3: Metal-assisted transformation of the C_6Me_6 ligand into a C_6Et_6 ligand.

The formation of $[(\eta^6\text{-arene})FeCp]^+$ by CpM^+-induced hexa-alkylation, hexa-allylation or hexabenzylation of C_6Me_6 consists of a series of deprotonations and C-C bond formation sequences. The first step is the deprotonation of the yellow salt of the 18-electron organo-iron cation giving rise to a deep-red 18-electron cyclohexadienyl intermediate, as shown in Scheme 1.3. Regeneration of the aromatic structure of the ligand is achieved by the alkylation, which is indicated by the yellow colour of the solution. This repetitive sequence continues until the steric limitation is reached. The beauty of this exquisite reaction is apparent visually from the "oscillating" colour changes that occur between yellow and red.

The concept of functionalizing polymethylated benzene transition-metal complexes, using MCp^+ (where M = Fe or Ru), has facilitated the synthesis of specifically polybranched cores with various topologies. The building of such molecular architectures has been achieved by single, double and triple branching as shown in Equations 1.18, 1.19 and 1.20, respectively.

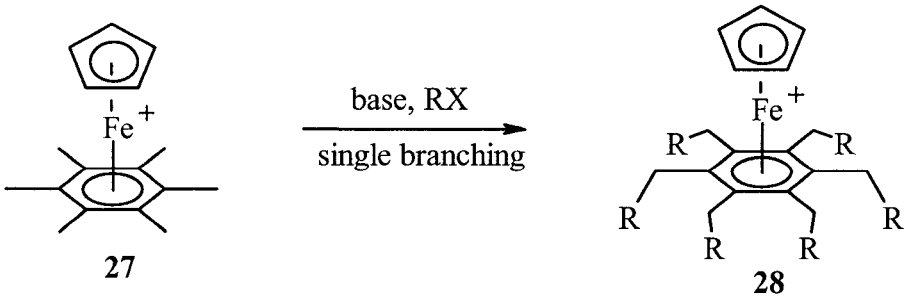

27 28 **1.18**

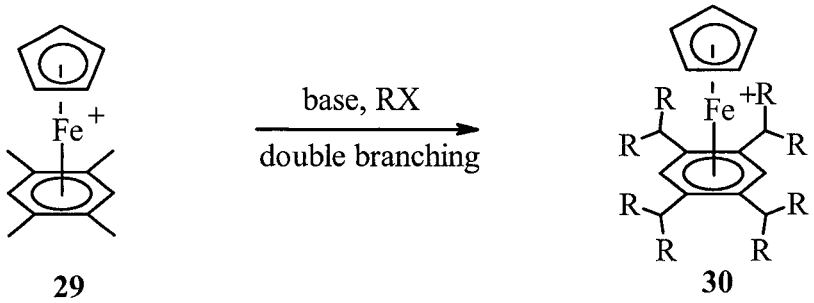

29 30 **1.19**

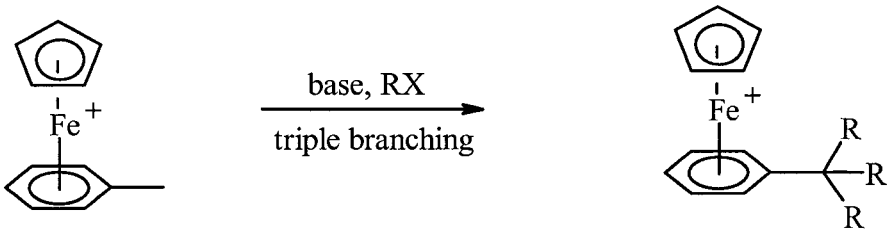

31 32 **1.20**

Single branching of $[CpFe(C_6Me_6)][PF_6]$ with allyl bromide gives rise to a hexa-allylated $CpFe^+$ complex. In this case, $[CpFe(C_6Me_6)][PF_6]$ behaves as a reservoir of six protons since six allyl groups are introduced.[57] Double branching is achieved for 18-electron $CpFe^+$ complexes when each methyl group has only one methyl and one hydrogen neighbour on the benzene ring as seen with *o*-xylene and durene.[57] Triple branching is seen when [(mesitylene)FeCp][PF_6] is treated with an excess of MeI and potassium *tert*-butoxide affording $(1,3,5\text{-}C_6H_3(t\text{-}Bu)_3FeCp][PF_6]$.[56a]

The degree of branching follows the steric rule, which correlates the number of hydrogen atoms replaced on each methyl with the number of vicinal methyl groups on the

benzene ring. That is, only one hydrogen is replaced on a methyl having two vicinal methyl neighbours; two hydrogen atoms are replaced on a methyl having only one vicinal methyl and all three hydrogen atoms are replaced on a methyl having no neighbouring methyl groups.[56] These one-pot syntheses are extremely advantageous for the preparation of dendritic cores, and eliminate the tedious isolation-purification-repetition procedure common to dendrimer chemistry.[57]

1.6 Haptotropic Rearrangements

Haptotropic rearrangements have been classified as those occurring in systems where an ML_n unit alters its connectivity (i.e. hapticity number) to some ligand with multicoordinate site possibilities.[58] One can envisage two types of haptotropic rearrangements: (1) those cases where the metal remains coordinated to the same ring, but exhibits ring slippage, and (2) those cases where the metal moiety moves between adjacent rings in a multi-fused ring system, and are referred to as inter-ring metal migrations. Haptotropic shifts in polyene-ML_n complexes are known, and a schematic representation of such a haptotropic rearrangement is depicted in Figure 1.2.

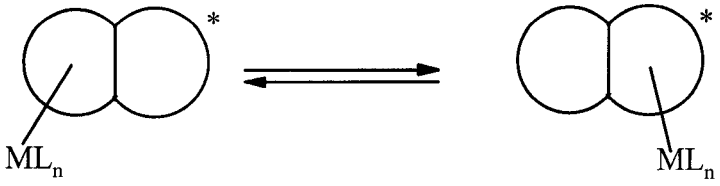

Figure 1.2: Inter-ring metal migrations of a polyene-ML_n.

1.6.1 Ring Slippage

The former process involves geometrical rearrangements of π ligand complexes as a result of an increase in the metal electron count, as a consequence of ligand addition

or electrochemical reduction.[59] This process was first observed by Basolo *et al.* upon investigating the effects of phosphine addition to indenyl manganese tricarbonyl complexes, $(\eta^5\text{-}C_9H_7)Mn(CO)_3$.[60] An enormous increase in the reaction rate was seen for the indenyl complexes relative to the analogous cyclopentadienyl (Cp) complexes and was termed the indenyl effect. For instance, the ligand substitution of $(\eta^5$-indenyl$)Rh(CO)_2$ proceeds at a rate 10^8 times faster than that for the corresponding η^5-cyclopentadienyl system.[61] This rate enhancement has been explained by invoking the development of aromatic character in the six-membered ring in the η^3-intermediate, which would lower the activation energy for the process (Equation 1.21).

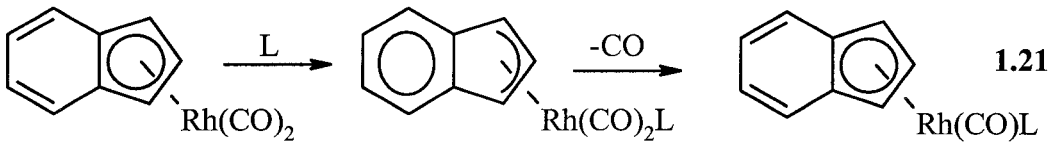

1.21

1.6.2 Inter-ring Haptotropic Rearrangements

π-Complexes of transition metals with polycyclic aromatic hydrocarbons in which many sites of coordination are available, typically display lability, and inter-ring haptotropic rearrangements are frequently observed in such molecules. Although indenyl (C_9H_7) is the most studied of such ligands, this phenomenon has been observed in other systems with extended π systems, for example, fluorenyl ($C_{13}H_9$), cyclopenta[*def*]phenanthrenyl ($C_{15}H_9$) and 1-hydronaphthalenyl ($C_{10}H_9$). Thus deprotonation of $(\eta^6$-indene$)ML_n$ complexes, where ML_n = $Cr(CO)_3$, $Mo(CO)_3$, $(C_9H_7)Fe^+$, $(C_5Me_5)Rh^{2+}$, $(C_5Me_5)Ir^{2+}$, or $(C_2H_4)_2Rh^+$ causes the metal fragment to migrate from the

six-membered ring to the five-membered ring (Figure 1.3). Upon protonation, the process is reversed, and hence it is termed a haptotropic shift.

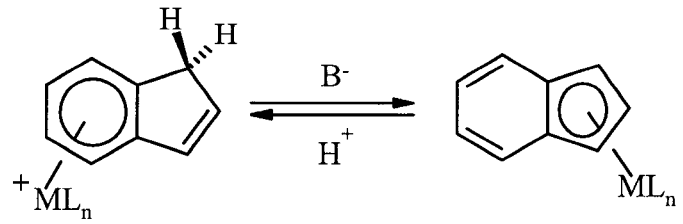

Figure 1.3: Inter-ring haptotropic shifts.

1.7 Buckminsterfullerene, C_{60}

The discovery of Buckminsterfullerene, C_{60}, **33**, has opened many avenues of new chemistry. The 1996 Nobel Prize was awarded to Kroto, Smalley and Curl for the identification of **33**, in 1985, by laser vaporization of graphite.[62] C_{60} is a part of the fullerene family, defined as all carbon molecules with C_{20+2m} composition, consisting of twelve pentagons and *m* hexagons forming hollow closed nets.[63] C_{60} consists of 20 hexagons and 12 pentagons. Its outstanding impact on research led to its nomination as "Molecule of the Year" in 1991. Recently, there has been renewed interest in the area of aromatic hydrocarbons with curved surfaces. The theoretical dismantling of **33** into different fragments has provided chemists with serious synthetic challenges. Retrosynthetic analysis of C_{60} leads to a series of polycyclic aromatic hydrocarbons, which will be further discussed (section 1.7.1).

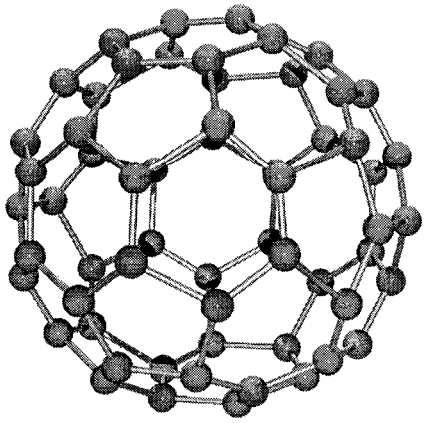

Figure 1.4: Pictorial representation of C_{60}, **33**.

The first fullerene skeleton to be synthesized was dibenzo[*ghi,mno*]fluoranthene, given the trivial name "corannulene", **34**, by Lawton and Barth in 1966. Corannulene represents the polar cap of buckminsterfullerene, C_{60}. This involved a remarkable, but very tedious, 17-step procedure starting from 3-carbomethoxy-4*H*-cyclopenta[*def*]-phenanthrene and employing classical organic transformations that ultimately furnished **34** in 0.14 % yield.[64] This synthetic achievement involved an initial build-up of the entire carbon framework with minimal saturation, and the final step required aromatization by dehydrogenation. It was not until 1991 that Scott and co-workers reported a more convenient way to **34**, starting from simple fluoranthene precursors, by using flash vacuum pyrolysis (FVP) techniques.[65] Since then Siegel[66] and Zimmerman[67] have also developed methods for the production of **34**; however, even these syntheses required a pyrolysis step, and led to low yields of approximately 15 and 18 %, respectively. Scheme 1.4 illustrates the precursors that furnished corannulene. The successful synthesis of corannulene in useful quantities has raised the possibility of the building of other

convex/curved molecular surfaces based on carbon lattices, such as C_{60}. Thus, one major area of interest is the identification and the assembly of smaller fragments upon which one can build.

Flash vacuum pyrolysis (FVP) technique involves passing the compound through a hot quartz tube (800 - 1300 °C) under vacuum (10^{-4} - 1 torr).[68] This process allows the formation of highly strained carbon-carbon bonds that exist in highly curved-bowl like molecules, although yields are invariably low. FVP reactions that furnish buckyball and buckybowls are highly dependent on the temperature and the applied vacuum.

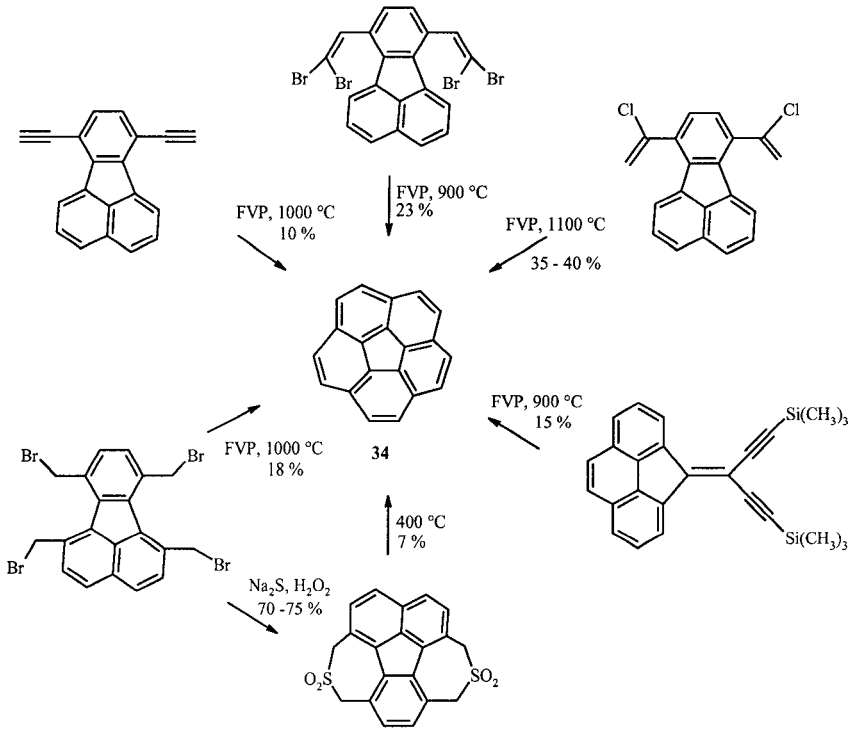

Scheme 1.4: Synthetic routes to corannulene, **34**, the polar cap of C_{60}.[68]

Very recently, a practical, large-scale synthesis of corannulene and related bowl-shaped aromatics was reported. The method involves heating 1,2,5,6-tetrabromo-corannulene under reflux for 1 h in aqueous dioxane containing small quantities of

NaOH. Further treatment with *n*-butyllithium in THF at -78 °C, followed by quenching with dilute HCl, furnished corannulene in 50 - 55 % for the combined two steps.[69]

1.7.1 Fragments of C_{60}

Mehta and co-workers have been working on synthetic strategies towards C_{60}. It has been demonstrated that C_{60} can be theoretically fragmented by essentially three routes that maintain the C_5, C_3, or C_2 symmetry (Scheme 1.5).[70]

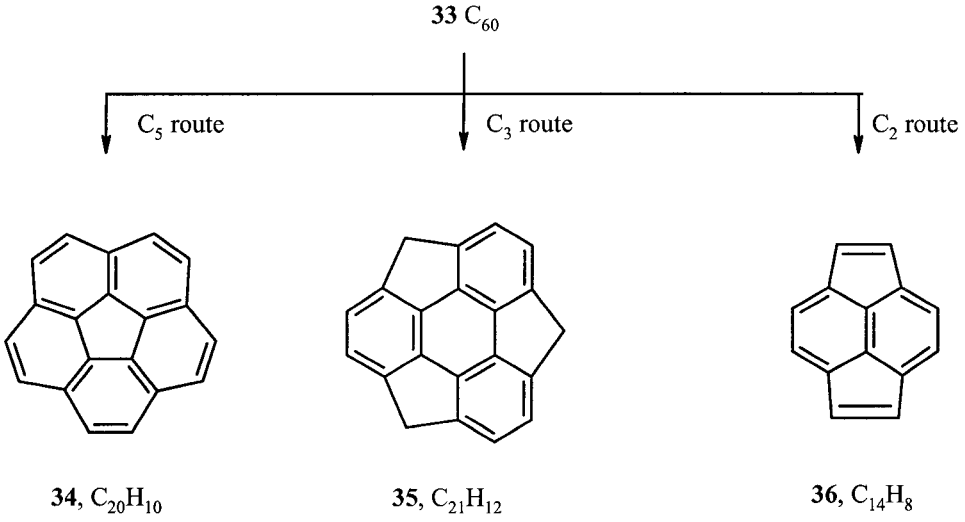

Scheme 1.5: Retrosynthetic dissection of C_{60} retaining C_5, C_3 and C_2 symmetry.

The skeletal fragments at the end of the dismantling process, which retain the three types of symmetry, are corannulene, **34**, sumanene, **35**, and pyracylene, **36**. Of these three substructures, **34** and **36** are well-established synthetically and have also been studied in terms of their build-up to C_{60}.[66,71] However, sumanene still remains to be synthesized, and hence it has attracted attention not only as a potential route to **33** but also for its own intrinsic interest. Sumanene, $C_{21}H_{12}$, in comparison to corannulene, $C_{20}H_{10}$, has just one extra carbon but two additional pentagonal rings, which create

greater strain and curvature within the molecule. This apparent strain is emphasized by theoretical calculations of the bowl-depths of **34** and **35** as being 0.80 and 1.15 Å respectively.[72] The degree of curvature in **35** has presented a synthetic challenge, since it is likely that the synthesis of C_{60} will involve the intermediacy of some highly strained molecules. The trivial name sumanene is derived from the Hindu and Sanskrit word "suman" meaning flower, since the shape of **35** is reminiscent of a flower. [73]

1.7.2 Synthesis of C_{60} Fragments

The closest approach thus far to a synthesis of sumanene is the hexacyclic system **38** obtained in low yield by subjecting the symmetrical tri(bromomethyl)triphenylene, **37**, to FVP.[73] The doubly-bridged compound **38** was isolated from **37**, which has three-fold symmetry, and FVP was employed with the aim of closing the third five-membered ring, but to no avail. The structure of **38** was confirmed by X-ray crystallography.

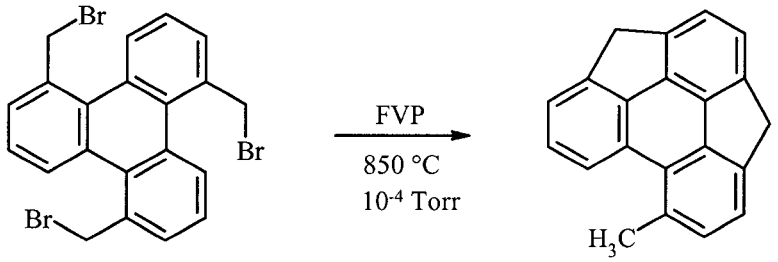

37 **38** **1.22**

Along the same lines, an alternative approach to **35** commenced with a terphenyl derivative, **39**, which, under pyrolytic conditions, yielded the demethylated monobridged **40**, and the dimethano-bridged **41** (Equation 1.23).[74] It is apparent that there is a great deal of strain to surmount when closing all three of the five-membered rings in the final step in the synthesis of sumanene.

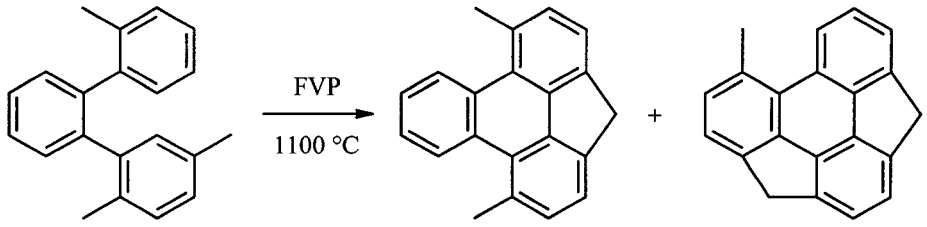

1.23

39 **40 (4 %)** **41 (<1 %)**

Dehmlow and Kelle also attempted to generate a sumanene-like compound starting from a trindane derivative. Dimerization of ketone **42** furnished **43**, which failed to yield **44**.[75]

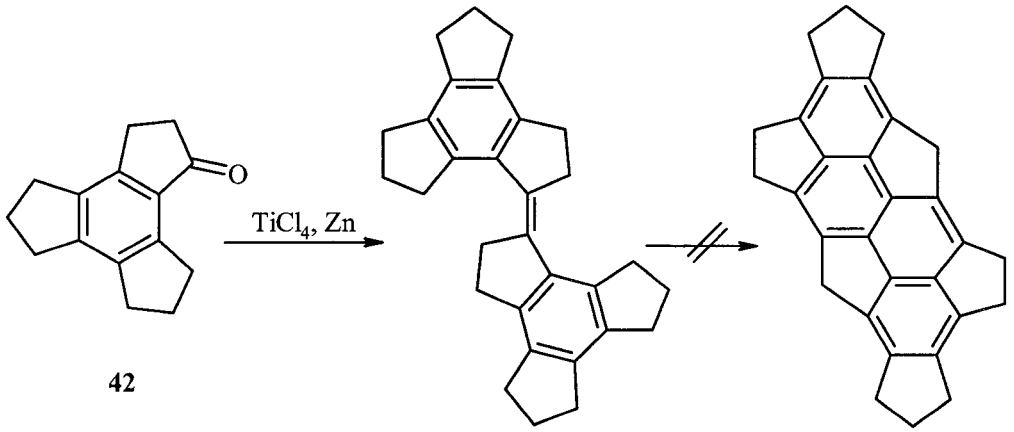

1.24

42 **43** **44**

1.7.3 Alternative Synthetic Routes to C_{60}

Based on molecular structure calculations, it has been established that one critical feature required towards the build-up to C_{60} from skeletal fragments is a significant degree of curvature.[70] It has also been suggested that there is the possibility of the dimerization of two halves to furnish **33**, each being $C_{30}H_{12}$. Rabideau and co-workers reported the first synthesis of a semibuckminsterfullerene, $C_{30}H_{12}$, **45**.[76,77] Semibuckminsterfullerenes consist of 30 sp^2 carbon frameworks (fused five- and six-

membered rings) that may be a part of C_{60} surface and have bowl-shaped geometries.[76b] However, **45** does not represent a symmetrical half of buckyball; the most synthetically desirable intermediate for the production of C_{60} is **46**. Both **45**[76b] (5 %) and **46**[76c] (10 - 15 %) were synthesized by FVP methods, but in such extremely low yields as to preclude further investigation of their chemistry.

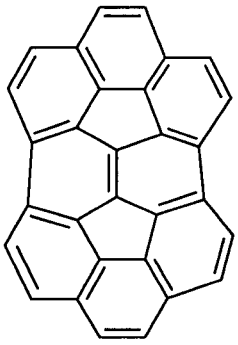

45

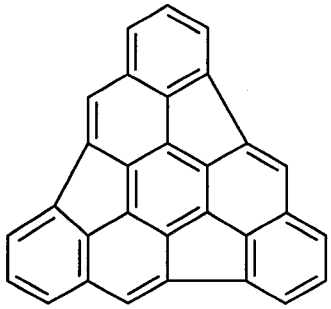

46

Conversely, Sbrogio and co-workers have also attempted to synthesize $C_{30}H_{12}$ and, because of the low yields obtained by Rabideau, an alternative method is still of considerable interest. The potential precursor that they reported was 5,10,15-tris-(dichloromethylene)truxene, **49** from truxenone.

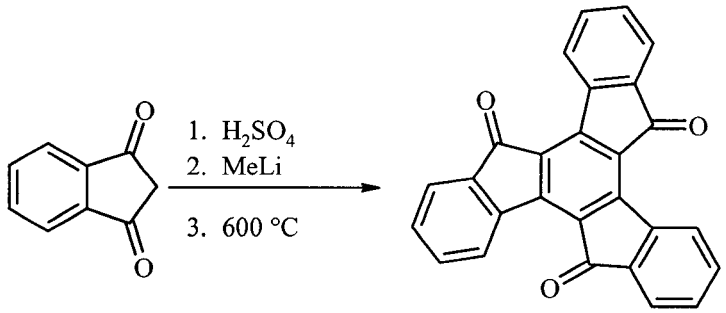

47 **48** (90 %)

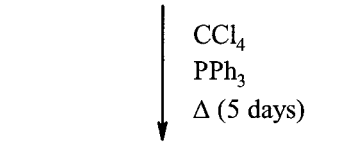

1.25

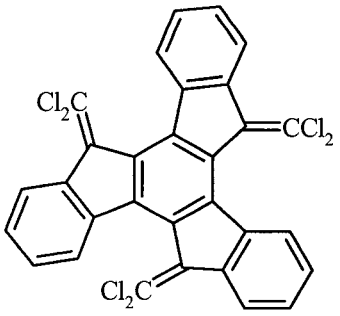

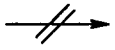

33

49 (17 %)

Recently, Imamura and co-workers have synthesized the first bowl-shaped heteroaromatic, namely triphenyleno[1,12-*bcd*:4,5-*b'c'd'*:8,9-*b"c"d"*]trithiophene, **50**, trithiasumanene.[78] An elegant route was used to prepare **50**, once again using flash-vacuum pyrolytic methods. The X-ray structure of **50** revealed that it adopts the expected bowl-shaped molecular structure; however, owing to the presence of the larger sulfur atoms, it is slightly shallower than that of corannulene, **34**.

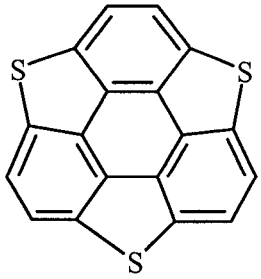

50

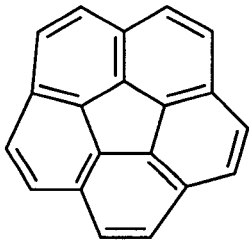

34

Chapman and Loguerico have attempted the preparation of **33** via the triketone precursor **51**, which was itself synthesized from truxenone **52**. However, crystallographic studies of **52** revealed that the triketone is a severely distorted non-planar molecule, thus it is not susceptible to further cyclizations to furnish fullerene fragments.

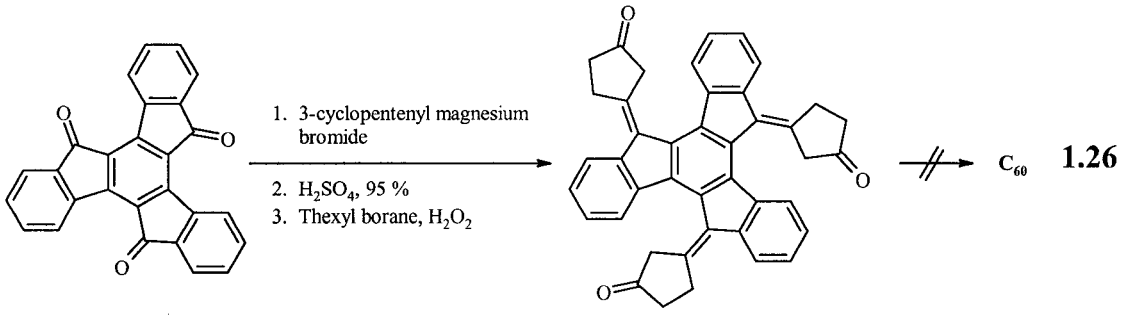

1.26

51 **52**

Fabré and Rassat have reported that the acid-catalyzed trimerization of trindanone, **53**, furnished the dimer $C_{30}H_{30}O$, **54**, and the trimeric compound $C_{48}H_{48}$, **55**, in 5 % yield.[79] However, the characterization of **55** rests purely on mass spectrometric evidence, and this reaction merits further investigation.

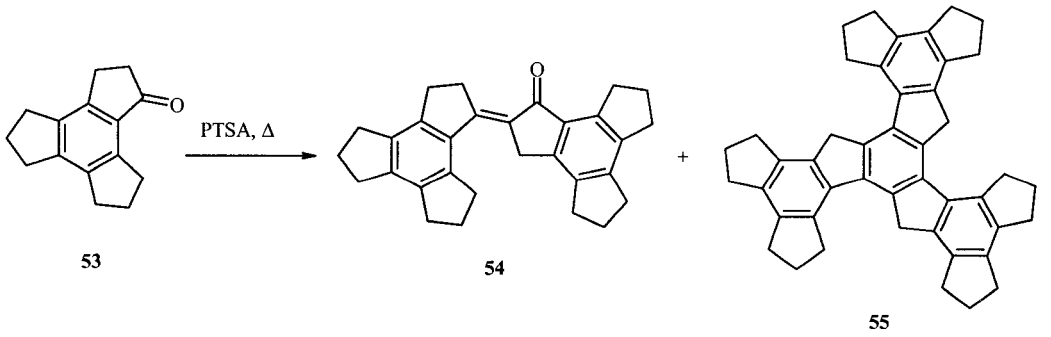

53 54 55 **1.27**

Recently, Scott has described a rational synthesis of buckministerfullerene *via* a 12-step route. However, this new method afforded C_{60} in approximately 1 % yield. The route commences with 1-bromo-4-chlorobenzene which is transformed to a propeller-shaped chlorinated hydrocarbon ($C_{60}H_{27}Cl_3$) by employing classical organic reactions. The flash-vacuum pyrolysis at 1 100 °C of the chlorinated species, $C_{60}H_{27}Cl_3$, **56**, results in the loss of the chlorine and hydrogen atoms, and the formation of fifteen new carbon-carbon bonds to give C_{60}.[80]

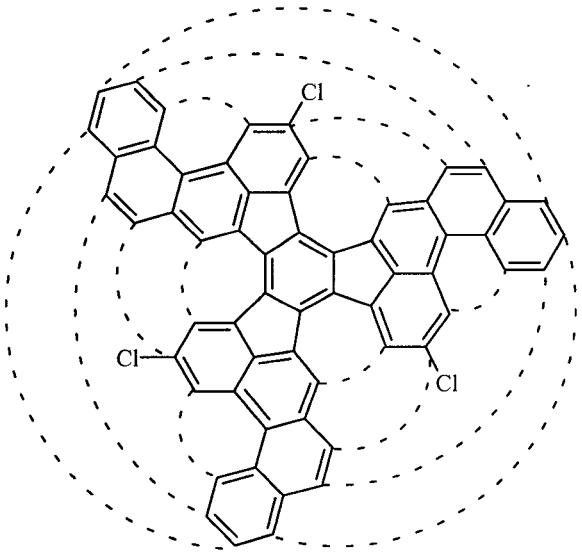

56

1.7.4 An Organometallic Route to Sumanene

A classical total synthesis of C_{60} has been a synthetic challenge, thus the search for an efficient method is still an ongoing process. To date, sumanene, **35**, has not yet been successfully synthesized. However, a potential precursor, **38**, has been synthesized in which the six-membered rings are in place and the final step involves the formation of the five-membered rings.

To overcome the degree of strain in the synthesis of sumanene, the trindane ligand has been identified as a pivotal precursor in which derivatization of the benzylic positions would allow the build up of the six-membered rings. Commencing with tris(cyclopentano)benzene, $C_{15}H_{18}$, **57**, it could alleviate the difficulty encountered by other approaches that involve forming the highly strained five-membered rings in the ultimate step.

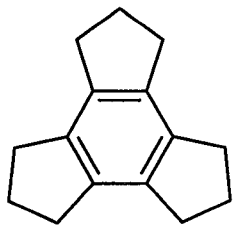

57

An organometallic route to sumanene that did not involve FVP was of great interest and was suggested by McGlinchey *et al.*[81] This proposed route commenced with the synthesis of tris(cyclopentano)benzene, also referred to as trindane, which was then added to the metal fragment of interest. Trindane is commonly prepared by acid-catalyzed condensation of three molecules of cyclopentanone.[82] In 1964, the crystal structure of **57** was determined.[83] Since then, an alternative and less harsh method has

been suggested for the synthesis of tri- and hexa-substitituted benzenes that obviates the need to use strong acids and high temperatures. The milder conditions involve treatment of the respective ketone with one equivalent of tetrachlorosilane in ethanol at room temperature, giving rise to reasonably good yields of the triannulated benzenes (65 % for **57**).[84]

A series of organometallic complexes, **58**, was prepared by coordination of the metal fragments ($Cr(CO)_3$, $Mo(CO)_3$, $Mn(CO)_3^+$ or $Fe(C_5H_5)^+$) to the central aromatic ring of trindane. X-ray crystallographic data were reported for **58a** and revealed that the five-membered ring of trindane adopted an envelope conformation such that the methylene groups bend towards the metal fragment. Previous to this work, the only example of an organometallic compound that contained trindane was in a series of cationic complexes of general formula $^{99m}Tc(arene)_2^+$ where the arene was C_6H_6, C_6Me_6, C_6Et_6, indane or trindane.[85] Only trace quantities of these compounds were obtained and no spectroscopic or analytical data pertaining to the trindane complex were reported.

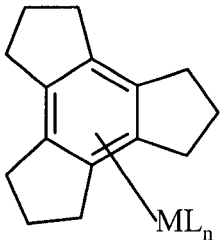

58a $ML_n = Cr(CO)_3$
58b $ML_n = Mo(CO)_3$
58c $ML_n = Mn(CO)_3^+$
58d $ML_n = Fe(C_5H_5)^+$

1.8 Objectives of the Thesis:

The preparation of strained structures, in particular buckyballs and buckybowls, has continued to be a challenge to chemists for the past three decades. One particularly

fascinating target is sumanene, a substructure of C_{60} which has yet to be synthesized. Generally, the synthesis of buckyballs and buckybowls involve common organic transformations and flash vacuum pyrolysis. Our approach to this problem was to attach an organometallic fragment to the organic substrate in hopes of deprotonating the six *exo*-benzylic positions of the ligand. Tri(cyclopentano)benzene, commonly referred to as trindane, was the organic substrate that was coordinated to the $Mn(CO)_3^+$, organometallic unit. The attempted deprotonation and alkylation at the *exo*-benzylic positions of [(η^6-trindane)$Mn(CO)_3$][BF_4] paralleled the methodology employed by Astruc.[56,57] Thus, one of the main objectives of the thesis was to investigate the reactivity of [(η^6-trindane)$Mn(CO)_3$][BF_4] and potassium *tert*-butoxide in the presence of alkylating and donor ligands. Factors that may affect the deprotonation of the benzylic positions were also considered, including altering the substituents of the $Mn(CO)_3$ unit and changing the metal itself. The results of these studies are presented in Chapter Two.

The novel and unexpected products that arose from the aforementioned reaction led to a subsequent objective, which was to investigate the generality of this reaction. Thus, other (arene)$Mn(CO)_3^+$ systems were treated with potassium *tert*-butoxide to examine the possibility of invoking haptotropic shifts. Arenes selected were bicyclic and tricyclic substrates that contained 5-, 6- or 7-membered rings attached to the arene. The synthesis, characterization and reactivity of these systems are presented in Chapter Three.

The stereodynamics of conformationally flexible complexes of the type (HEB)ML_n, where HEB = hexaethylbenzene and ML_n is an organometallic fragment, has been debated in the past and is an emerging area in many different fields. Although the

dynamics of this class of compounds have been examined for various organometallic fragments, none have incorporated manganese as the metal. Chapter Four includes the synthesis, characterization and molecular dynamics of hexaethylbenzene manganese complexes.

Previous studies have experimentally examined the migration of metal fragments, such as $Fe(C_5H_5)$, $Mn(CO)_3$ or $Cr(CO)_3$, across polycyclic surfaces. However, there is a lack of a definitive rationale for the inter-ring haptotropic rearrangements that occur in these systems. Chapter Five contains preliminary theoretical investigations at the extended Hückel level of inter-ring haptotropic shifts in polycyclic transition metal systems. Energy hypersurfaces for these processes have been obtained and are discussed.

CHAPTER TWO

Manganese Complexes of Trindane

2.1 Introduction

Figure 2.1 illustrates the sumanene fragment contained within C_{60}. As part of the continuing interest to synthesize one of the unknown skeletal fragments of C_{60}, sumanene, the following organometallic approach, proposed by McGlinchey *et al.*, eliminates the use of FVP, as depicted in Scheme 2.1.[81] The proposed route commenced with the synthesis of tris(cyclopentano)benzene, **57**, also referred to as trindane, which was coordinated to a metal fragment of interest.

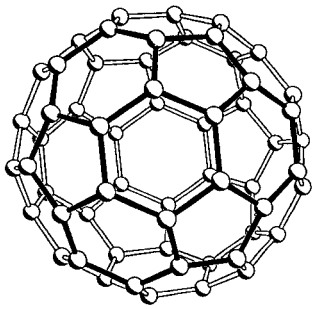

Figure 2.1: Sumanene a substructure of C_{60}.

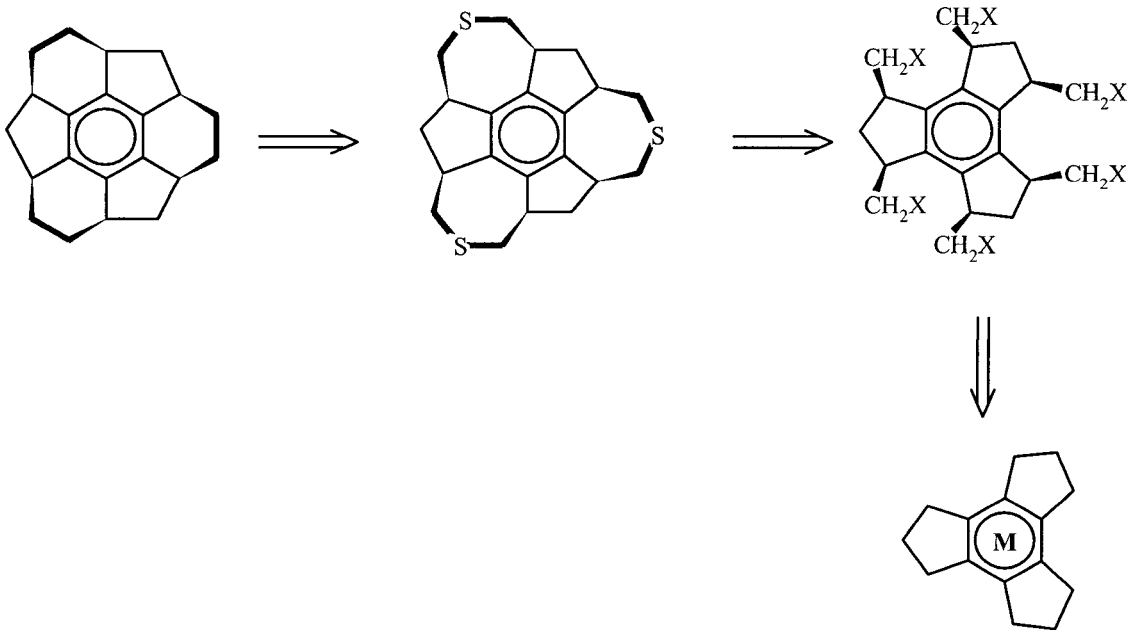

Scheme 2.1: Proposed retrosynthetic route to the sumanene skeleton.

2.1.1 Trindane

Very little chemistry of the trindane molecule has been reported in the literature since its synthesis in 1897.[82] Trindane is commonly prepared by acid-catalyzed condensation of three molecules of cyclopentanone,[82] and was characterized by X-ray crystallography in 1964.[83] Other synthetic routes to **57** have been described in the literature. These syntheses involve the trimerization of cyclopentanone utilizing two equivalents of $SiCl_4$ in ethanol at room temperature (65 %),[84] or by refluxing the ketone with two equivalents of $TiCl_4$ in toluene (39 %).[86] Furthermore, treatment of cyclopentanone with aqueous ammonium chloride at 250 °C also furnished **57** in 23 % yield.[87]

The hexabromo derivative, **59**, of trindane was prepared by Katz and Slusarek[88] (Equation 2.1). They continued with the debromination of **59** that furnished the dihydro-

1*H*-trindene, **60**. Lynch and co-workers later deprotonated **60** with a base producing the trindenide ligand, which was complexed to various organometallic moieties.[89] One distinct characteristic of the trindenyl ligand is its ability to coordinate three metal fragments (such as $Mn(CO)_3$ or $Re(CO)_3$) through the cyclopentadienyl rings, placing two metals in close proximity.

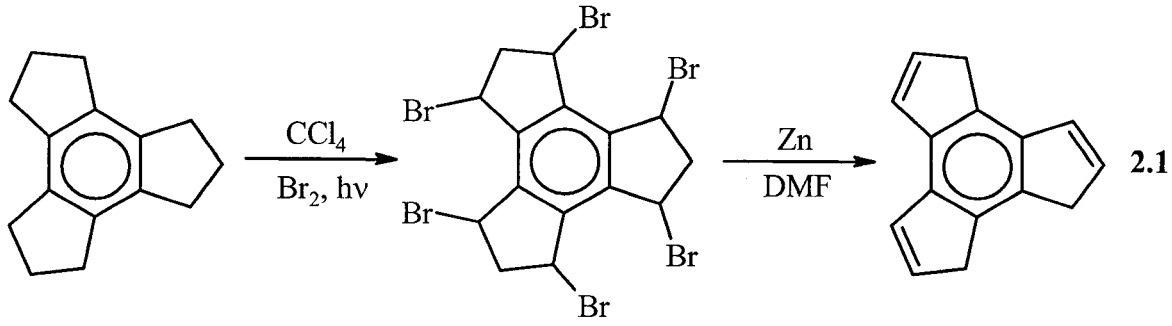

2.1

57 **59** (76 %) **60** (43 %)

A one step transformation of trindane has been used to synthesize **61** by oxidation of the benzene ring with a Ru(VIII) molecule generated *in situ* (Equation 2.2).[90] The structure of the unanticipated carbohydrate-like product was established by X-ray crystallography.

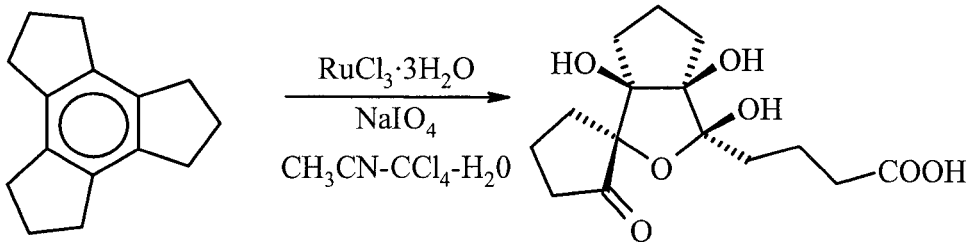

2.2

57 **61** (15 %)

Furthermore, ozonolysis of **57** resulted in the formation of bicyclo(10.3.0)pentadec-1(12)ene-2,6,7,11-tetrone, **62** ($C_{15}H_{18}O_4$), and its aldol product, 12-hydroxy-16-oxatetracyclo(10.3.1.0.^{1,5}0^{7,11})hexadec-7(11)ene-2,6-dione, **63** ($C_{15}H_{18}O_4$), as depicted in

Equation 2.3. The retention of the C_{15} periphery resembles some natural products such as ginkgolides. Ranganathan and co-workers have demonstrated that cleavage of the π-bonds *endo* to the cyclopentane ring of trindane provides a synthetic route to complex natural products from a rather simple molecule, trindane.[91]

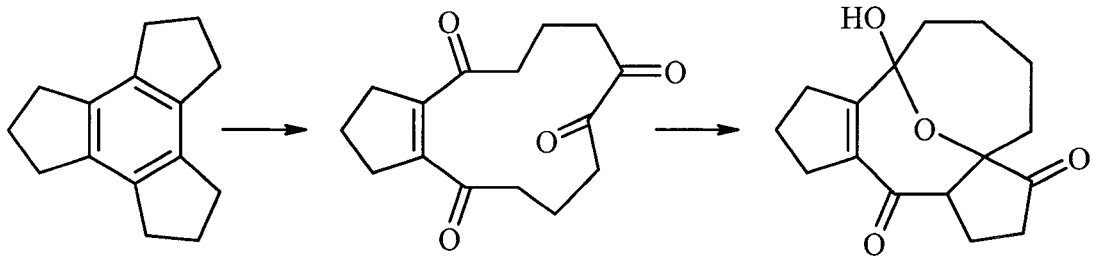

2.3

57 **62** **63**

Very recently, the trindane motif has been investigated in terms of its potential for the construction of artificial receptors. The approach involves the trindane skeleton, along with employing metal carbonyl chemistry to control the stereochemistry (Scheme 2.2). The hexacarboxylate **65** was prepared from 1,3,5-tris(bromomethyl)-2,4,6-tris(chloromethyl)benzene, **64**. The hexaester **65** was isolated in an 80 % yield, when **64** was treated with sodium enolate of diethyl malonate in ethanol.[92] A previous method afforded **65** in a 64 % yield, starting from hexakis(bromomethyl)benzene.[93] Saponification of **65**, followed by decarbonylation and subsequent Fischer esterification of **66** in ethanol, afforded the tricarboxylic ester **68** in a 90 % yield. Benzylation of **68** furnished **70**, but in a very low yield (21 %). The stereoselectivity of the alkylation step was improved by complexing a metal moiety to one face of the trindane skeleton. Hence, treatment of **68** with $Cr(CO)_6$ or $Mo(CO)_6$ furnished the trindane-coordinated metal tricarbonyl complexes, **69**, which were reacted with LDA and benzyl bromide giving rise

to the all-*syn* isomer **70** (68 %).[92] Thus, Choi and co-workers[92] have elegantly demonstrated the utility of coordinating a metal carbonyl moiety to an organic substrate so that the ML_n unit behaves as a steric barrier, which results in the electrophile attacking the *exo* face of the trindane derivative.

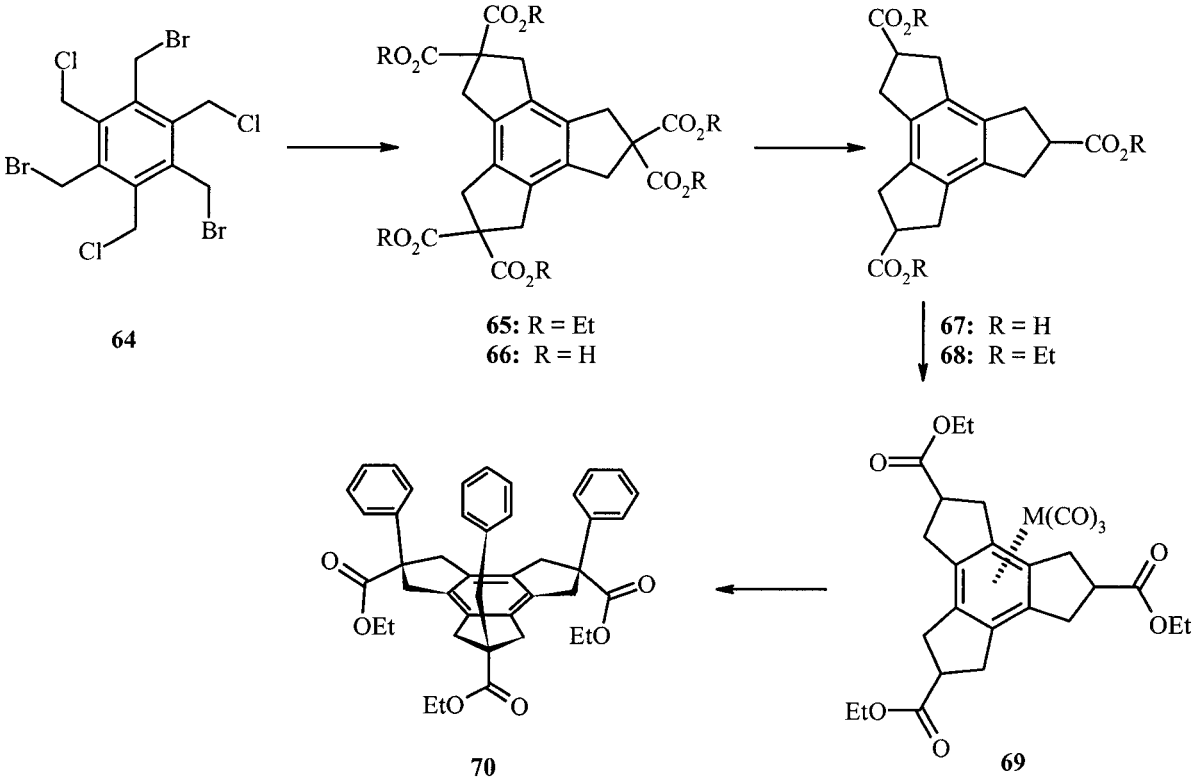

Scheme 2.2: C_{3v}-symmetric tripodal scaffold.

Other known trindane complexes include those mentioned in Chapter 1 (for further details refer to Section 1.7.4). As previously described, the trindane series of organometallic complexes involves complexation of various metal fragments, including $Cr(CO)_3$, $Mo(CO)_3$, $Mn(CO)_3^+$, or $Fe(C_5H_5)^+$, to the central aromatic ring of trindane. As part of our continuing interest in trindane functionalization by means of transition metal complexes, the focus will be on the reactivity of cationic arene manganese complexes,

which are known to be more reactive than the analogous chromium complexes. In order to gain insight into the influence on trindane when bound to a positively charged manganese atom, we chose to attempt to deprotonate the benzylic positions of π-coordinated trindane.

The acidity of the benzylic hydrogen atoms in such systems has been attributed to a combination of the electron-withdrawing effect of the metal and the resonance stabilization of the conjugate base.[48b] It has also been suggested that the $Mn(CO)_3^+$ fragment is more effective than either $FeCp^+$ and $Cr(CO)_3$, and is at the top of the list of electrophilic metal centers in terms of enhancing the acidity of benzylic hydrogen atoms.[34] From the series of trindane complexes listed below, the manganese trindane system was thought to be the ideal candidate for satisfying both the electronic and steric requirements. Accordingly, the $Mn(CO)_3^+$ group serves as an activating agent by enhancing the acidity at the benzylic positions and in addition should act as a stereodirecting group by blocking one π-face of the arene ligand. Therefore in principle, the *exo*-configuration of the benzylic positions should be favoured.

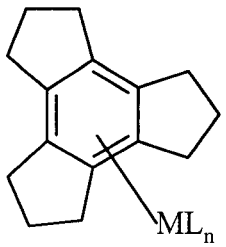

58a $ML_n = Cr(CO)_3$
58b $ML_n = Mo(CO)_3$
58c $ML_n = Mn(CO)_3^+$
58d $ML_n = Fe(C_5H_5)^+$

The attempted deprotonations, followed by alkylation of the *exo*-benzylic positions of the ligand, employed the Astruc methodology[56], which allows the possibility

of synthesizing hexa-functionalized transition-metal-arene complexes in one step (refer to section 1.5.1 for further details).

2.1.2. Cationic Arene Manganese Complexes

Eyman has demonstrated that [(hexamethylbenzene)$Mn(CO)_3^+$][45] and [(hexamethylbenzene)$Mn(CO)_2PR_3^+$][94] complexes undergo abstraction of a benzylic hydrogen affording the corresponding cyclohexadienyl compound that reacts with electrophiles to functionalize the benzylic sites. (η^5-$C_6Me_5(CH_2)$)$Mn(CO)_2PR_3$ complexes were treated with a variety of electrophiles such as CH_3I, I_2, $C_6H_5C(O)Cl$, $Mn(CO)_5Br$ and $CpFe(CO)_2I$.[94] Analogous to the work done by Astruc *et al*,[56] multiple alkylations were achieved by treatment of (η^6-C_6Me_6)$Mn(CO)_2PMe_3$ in the presence of KH with an excess of CH_3I.[94] The reaction was allowed to proceed for 24 h with a minimal quantity of KH (~ 1 equivalent) resulting in a mixture of products with a maximum incorporation of three methyl groups, as determined by mass spectrometry.

In this chapter, we shall investigate and discuss the reaction of [(η^6-trindane)-$Mn(CO)_3$][BF_4] and potassium *tert*-butoxide (*t*-BuOK) with allyl bromide or methyl iodide in the expectation that all six *exo*-benzylic positions would be alkylated. The unexpected products that arose from the aforementioned reactions are reported, and subsequently led to exploration of the reactions of [(η^6-trindane)$Mn(CO)_3$][BF_4] and potassium *tert*-butoxide with donor ligands such as trimethyl phosphite and triphenylphosphine. The syntheses of other organometallic trindane complexes are also described. Much of the material in this chapter has been published in preliminary form in the American Chemical Journal *Organometallics*; a full paper is in preparation.[95]

2.2 Results and Discussion

2.2.1 Synthetic and Spectroscopic Aspects

Attempts to deprotonate the six *exo*-benzylic positions of [(η^6-trindane)-$Mn(CO)_3$][BF_4] were adapted from a similar synthetic technique utilized in the preparation of (η^6-C_6Et_6)$Fe(C_5H_5)^+$ from (η^6-C_6Me_6)$Fe(C_5H_5)^+$.[56] When [(η^6-trindane)-$Mn(CO)_3$][BF_4] and an excess of potassium *tert*-butoxide (*t*-BuOK) were mixed as dry solids and then treated with allyl bromide in THF, a deep red crystalline compound was isolated. After chromatographic purification on silica, the product was identified as [(η^6-trindane)$Mn(CO)_2Br$, **71**, in a 17 % yield.[95] Utilizing the same procedure, [(η^6-trindane)$Mn(CO)_3$][BF_4] was treated with *t*-BuOK and methyl iodide and yielded the analogous [(η^6-trindane)$Mn(CO)_2I$ compound, **73**.[95] The compounds are air-sensitive in solution and decompose over several hours, even when stored under nitrogen. However, compounds **71** and **73** are more stable in the solid form, but still undergo decomposition at a somewhat slower rate. The iodide complex, **73**, was found to be slightly more air-sensitive than **71**. Another viable preparative route to the halide compounds that was employed, parallels the synthetic methodology disclosed by Eyman *et al.* for the synthesis of (η^6-arene)$Mn(CO)_2X$, where arene = C_6H_6, C_6Me_6, or C_6HMe_5 and X = Br, Cl, or I.[47b,96] In this rather facile and convenient route, photolysis, or treatment of the tricarbonyl precursor with trimethylamine N-oxide (Me_3NO), in the presence of a tetrabutylammonium halide yields the corresponding (η^6-arene)$Mn(CO)_2X$. In fact, the latter approach, but using tetrabutylammonium bromide, allowed the preparation of (η^6-

trindane)$Mn(CO)_2Br$ in excellent yield (93 %), which enabled further investigation of its reactivity.

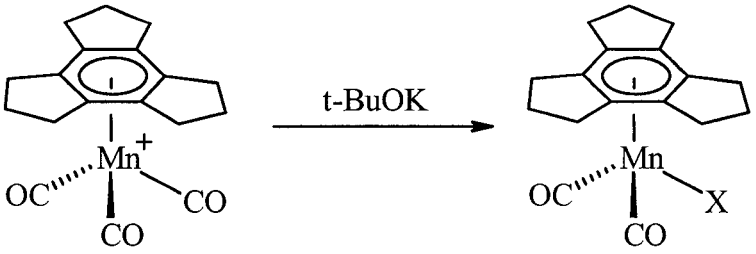

58c

71: X = Br (in THF and allyl bromide)
72: X = Cl (in THF and CD_2Cl_2)
73: X = I (in THF and methyl iodide)

Scheme 2.3: The synthesis of trindane manganese dicarbonyl halide complexes.

The compounds were characterized by NMR, mass spectrometry and infrared spectroscopy, and the structures of **71** and **73** were confirmed by X-ray crystallography.[95] The formation of compounds **71**, **72** and **73** was readily monitored by the use of infrared spectroscopy. In a neutral or anionic molecule, a decrease in the carbonyl stretching frequency is a result of the increased back-donation of electron density from the filled metal d-orbital into the π^* orbital of the CO group; this weakens the C-O bond and provides a probe for the characterization of metal carbonyl complexes. Conversely, a net donation of electron density from the CO group to the metal center results in a stronger C-O bond and thus, a higher ν_{CO} value. Evidently, if the complex is positively charged or contains strongly electron-withdrawing ligands, back-bonding decreases resulting in a stronger C-O bond, and a corresponding higher CO stretching frequency. Typically, M-C-O groups in arene manganese carbonyl complexes have stretching frequencies that lie in the range 2085 - 1900 cm^{-1} for cationic species, and 2030 - 1850 cm^{-1} for neutral

molecules. Overall, infrared spectroscopy is the most widely used technique for the characterization of metal carbonyl complexes, but it cannot be the sole criterion used to identify the product.

The starting material, [(η^6-trindane)Mn(CO)$_3$][BF$_4$], **58c**, has two carbonyl stretches at 2056 and 1997 cm^{-1}. The infrared carbonyl stretching frequencies of complexes **72**, X = Cl, (1980, 1931 cm^{-1}), **71**, X = Br, (1971, 1927 cm^{-1}), and **73**, X = I, (1973, 1926 cm^{-1}) are shifted to lower values as a result of the transformation from a cationic to a neutral species, attributed to an increase of electron density on the manganese atom. The range of carbonyl absorptions in the infrared for the η^6-coordinated trindane complexes are similar to the (η^6-C$_6$Me$_6$)Mn(CO)$_2$X complexes: 1972, 1920 cm^{-1}; 1971, 1921 cm^{-1}; and 1968, 1920 cm^{-1}; where X = Cl, Br and I, respectively.[47b] The potassium *tert*-butoxide method of generating an arene manganese dicarbonyl halide complex was extended to the (HMB)Mn(CO)$_3^+$ and (HEB)Mn(CO)$_3^+$ systems, where HMB = hexamethylbenzene and HEB = hexaethylbenzene. In the former case, treatment of (HMB)Mn(CO)$_3^+$ and *t*-BuOK with CH$_3$I in THF furnished the previously reported (HMB)Mn(CO)$_2$I compound, identified by its mass spectrum and by its carbonyl stretches at 1970 and 1924 cm^{-1} (in CDCl$_3$, lit. values:[47b] ν_{CO} = 1968 and 1920 cm^{-1} in acetone). Previous methods of preparing (HMB)Mn(CO)$_2$I involved photolysis or the use of trimethylamine N-oxide (Me$_3$NO). Similarly, treatment of (HEB)Mn(CO)$_3^+$ and *t*-BuOK with CH$_3$I in THF yielded the (HEB)Mn(CO)$_2$I compound, also identified by its carbonyl infrared absorptions at 1971 and 1927 cm^{-1} (in CDCl$_3$).

Attempts to verify the trindane products utilizing common chemical techniques of analysis, such as elemental analysis and mass spectrometry were inconclusive, which encouraged X-ray crystallographic studies of both **71** and **73** in order to unambiguously establish the identity and structures of these compounds. The mass spectra of **71** showed no parent ions, but displayed ions consistent with decomposition of the compound, similar to the results found for the hexamethylbenzene analogue, $(HMB)Mn(CO)_2X$ where X = Br or Cl.[97] However, the mass spectrum of **73** displayed ions at *m/z* 380 and 253 corresponding to $[M-2CO]^+$ and $[M-2CO-I]^+$, respectively, (which is similar to the behaviour of the analogous $(HMB)Mn(CO)_2I$ compound).

2.2.1.2 X-ray Crystallography

The structures of compounds **71** and **73** were determined by the use of suitable single crystals mounted on a glass fiber. Crystallographic collection and refinement parameters, and bond lengths and angles, may be found in the Appendix. The X-ray crystal structures of **71** and **73** are shown in Figures 2.2 and 2.3, and Figure 2.4, respectively. Compound **71** crystallized in the monoclinic space group $P2_1/c$, while compound **73** crystallized in the orthorhombic space group P*bca*. The manganese centres of two crystallographically characterized compounds, **71** and **73**, exhibit pseudo-octahedral geometry, whereby the trindane ligand occupies three coordination sites and the carbonyl ligands and the halogen atom occupy the other three coordination sites. Both structures display the classical "piano stool" geometry with an η^6-coordinated trindane, and the two carbonyl ligands and the halogen atom occupy the "legs" of this structure.

The geometries of structures **71** and **73** are reminiscent of the previously reported $(\eta^6\text{-}C_6Me_6)Mn(CO)_2Cl$, whereby the tripod is staggered with respect to the arene carbons. The cyclopentene rings in **71** (and **73**) adopt envelope conformations whereby the "wingtip" methylene groups [i.e. C(8), C(11), C(14) for both **71** and **73**] are folded *endo* with respect to the plane of the central six-membered ring, and compare favourably with the previously reported $(\eta^6\text{-trindane})Cr(CO)_3$ and $(\eta^6\text{-trindane})RuCl_2[P(OMe_3)]$.[81,98] This type of bending has been observed in other arene complexes, such as the following chloro-bridged arene diruthenium complexes: $[(\mu\text{-}Cl_3)\{(\eta^6\text{-arene})Ru\}_2][BF_4]$, where arene = C_6H_6 and C_6H_5Me.[99] Bending of the arene substituents (H or CH_3 groups) toward the metal by 6° has been attributed to the increased overlap between certain benzene and metal orbitals, decreasing the overall energy of the system. Extended Hückel molecular orbital calculations were used to examine the bonding interactions between the arene fragments and the metal atoms, and revealed that a 6° bend is required in order to optimize the overlap between the $(\mu\text{-}Cl_3)Ru_2$ fragments and the arenes.[99] Moreover, the crystal structure of uncomplexed trindane, **57**, revealed some disorder in these regions of the molecule.[83] In view of that, these principles may be extended to the trindane complexes whereby the bending of the wingtip CH_2 groups towards the metal atom allows better overlap of the orbitals in each fragment.

In addition, the structures of **71** and **73** may be compared with the known [tris(cyclohexeno)benzene]ML_n where ML_n = $Cr(CO)_3$, **74**, or $Mn(CO)_3^+$, **75**, whereby the $M(CO)_3$ unit displays the typical staggered orientation and the peripheral rings exhibit the "half-boat" conformation.[100]

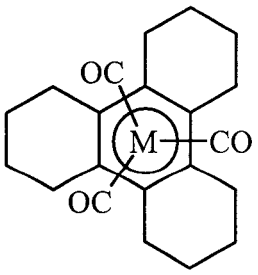

74: M = Cr
75: M = Mn^+

Other structural features of interest in compounds **71** and **73** are that the central ring is slightly folded such that the arene carbons C(1) and C(2), trans to the halogen atom, are slightly closer to the manganese atom than are the other four carbons [i.e. C(3), C(4), C(5), C(6)]. This folding of the ring parallels that of the known (η^6-C_6Me_6)$Mn(CO)_2Cl$. The manganese atoms in **71** and **73** are located 1.677 Å and 1.678 Å below the six-membered ring centroid, slightly closer than is found in (η^6-C_6Me_6)$Mn(CO)_2Cl$ (1.706 (3) Å). The Mn-C (CO) bond lengths range from 1.781 (8) to 1.802 (10) Å, which are typical of Mn-CO distances. All C-C-C angles in the arene ring are ~ 120 °, and the Mn-C-O angles are slightly less than 180 °. The Mn-to-arene-C distances range from 2.133 (7) to 2.230 (4) Å, and the C-C bond distances range from 1.401 (6) to 1.433 (10) Å for the aromatic carbons.

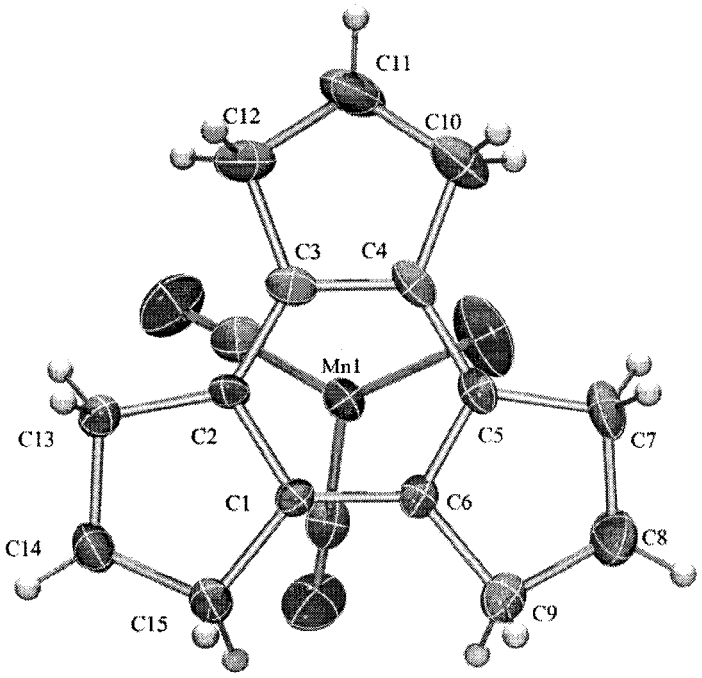

Figure 2.2: The X-ray structure of [(η^6-trindane)Mn(CO)$_2$Br, **71**, showing the staggered orientation of the tripodal manganese moiety. Thermal ellipsoids are shown at the 30 % probability level.

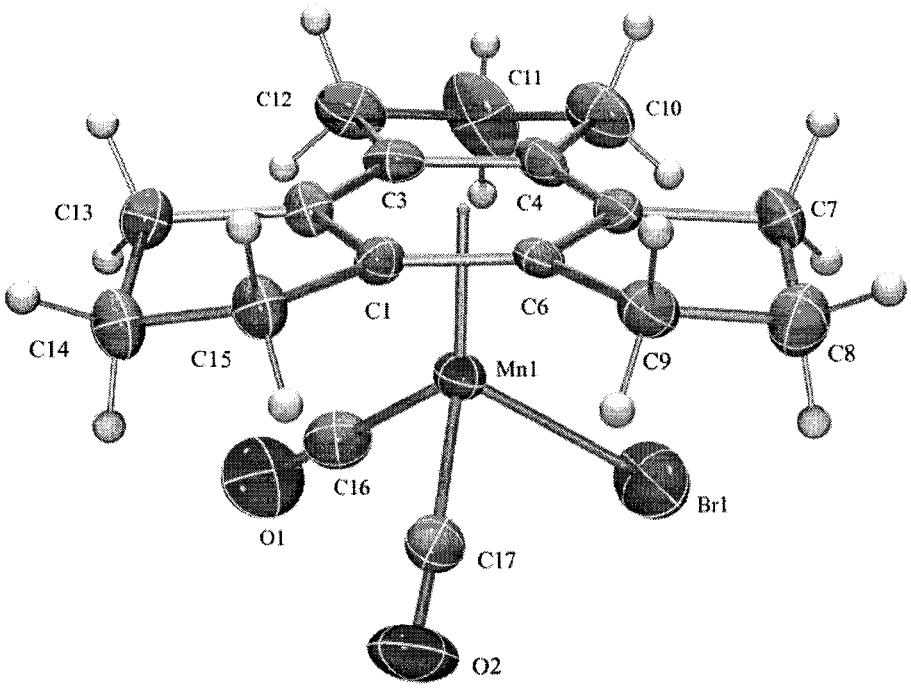

Figure 2.3: X-ray structure of [(η^6-trindane)Mn(CO)$_2$Br, **71**, illustrating the envelope conformation of the peripheral rings. Thermal ellipsoids are shown at the 30 % probability level.

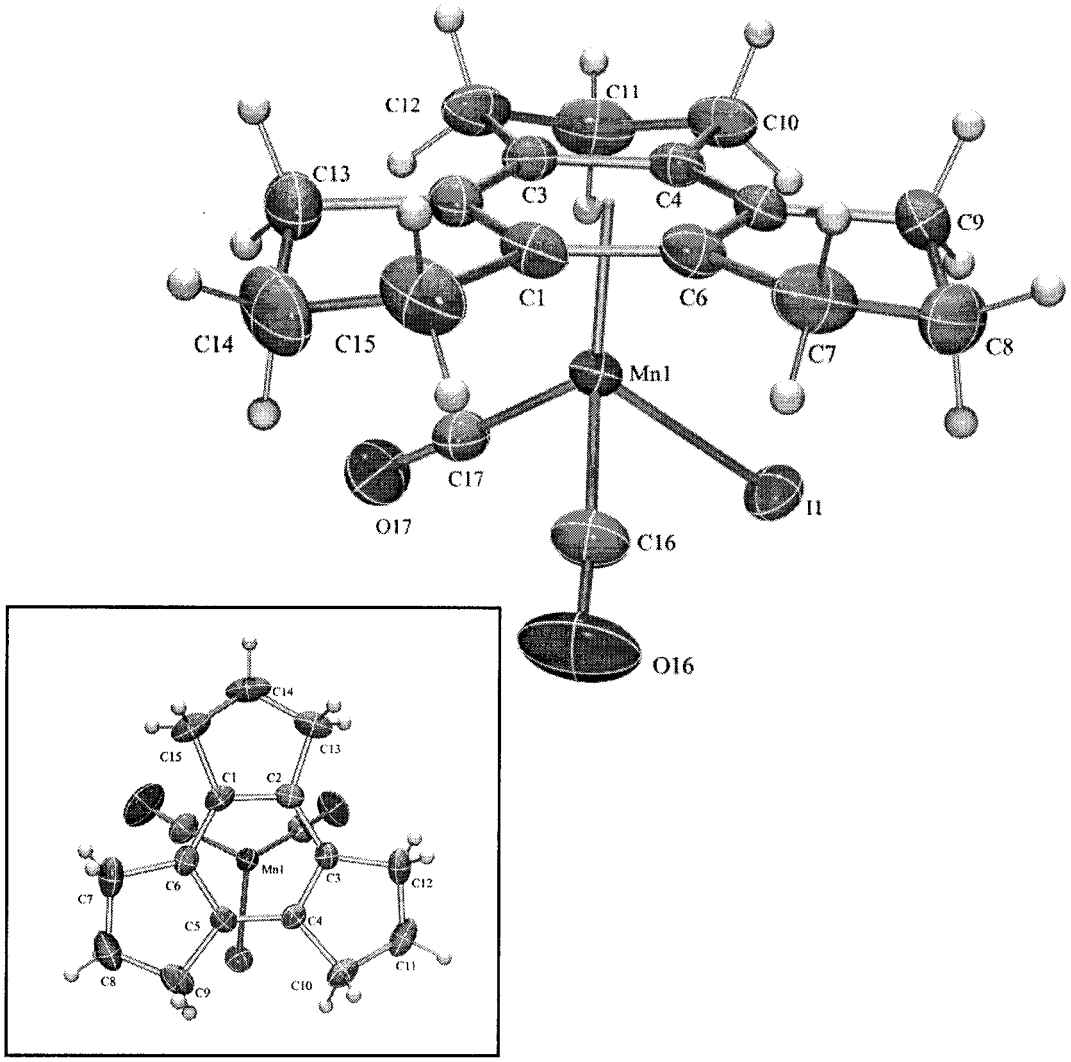

Figure 2.4: The X-ray structure of [(η^6-trindane)Mn(CO)$_2$I, **73**, showing the envelope conformation of the peripheral rings. Thermal ellipsoids are shown at the 30 % probability level; the inset figure illustrates the staggered orientation of the tripodal manganese moiety.

2.2.1.3 Mechanistic Aspects

The results of the above reactions are particularly surprising because it has been well established that conversion of $(\eta^6\text{-}C_6Me_6)Mn(CO)_3^+$ into $(\eta^6\text{-}C_6Me_6)Mn(CO)_2X$ requires either photolysis or use of trimethylamine N-oxide to induce loss of a carbonyl ligand. It has been reported that $(\eta^6\text{-}C_6Me_6)Mn(CO)_2H$ furnishes $(\eta^6\text{-}C_6Me_6)Mn(CO)_2Cl$ in the presence of CCl_4 or $CHCl_3$, but not in CH_2Cl_2.[47b] Consequently, investigations were undertaken to detect the intermediacy of $(\eta^6\text{-trindane})Mn(CO)_2H$.

The synthesis of the hydride manganese compound, $(\eta^6\text{-}C_6Me_6)Mn(CO)_2H$, first reported by Eyman and co-workers in 1984, has since been modified, leading to a more convenient and efficient synthetic route.[47b,101] Treatment of $(\eta^6\text{-}C_6Me_6)Mn(CO)_2I$ with *t*-butyllithium furnished the thermally stable $(\eta^6\text{-}C_6Me_6)Mn(CO)_2H$, **76**. It has been proposed that the hydride is formed by β-hydride elimination of isobutene, $(CH_3)C{=}CH_2$ from the presumed *tert*-butyl intermediate. Indeed, β-hydride elimination of alkyls or alkoxides is a common pathway to many metal hydrides.[102] It has been suggested that the formation of **76** is facilitated by the slippage of the η^6-arene to produce the η^4-arene, a 16-electron analogue, which would have an empty metal orbital required for β-hydride elimination.[47b,101] A correlation may be drawn with the work of Walker and Mawby in 1973, on the reactions of cationic complexes $[(arene)Mn(CO)]^+$, (where the arene is benzene, mesitylene or hexamethylbenzene) with methoxide in methanol to form unstable methyl esters, $(arene)Mn(CO)_2CO_2Me$.[35] These compounds were characterized solely by infrared and ^1H NMR spectroscopy, and their rapid decomposition prevented

complete characterization. However, Angelici and Blacik have reported similar compounds that supported their existence.[50]

Since that time, numerous other organometallic esters have been fully characterized, including through the use of X-ray crystallography.[103] One may propose that a reaction between **58c** and *t*-BuOK could generate the *t*-butyl ester **77** which readily eliminates both isobutene and carbon dioxide *via* a favorable six-membered transition state to yield (η^6-trindane)$Mn(CO)_2H$, **78**, as depicted in Scheme 2.4.[95] Treatment of **58c** with *t*-BuOK in CD_2Cl_2 furnished (η^6-trindane)$Mn(CO)_2Cl$, suggesting that **78** is more reactive than (η^6-C_6Me_6)$Mn(CO)_2H$ toward alkyl halides.

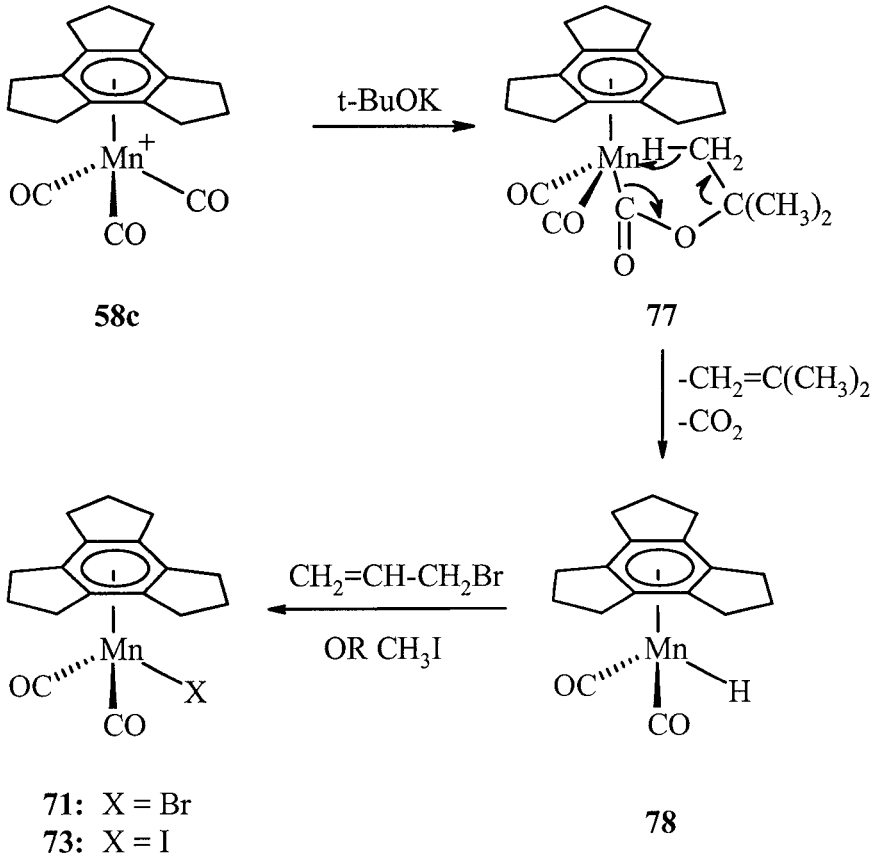

58c **77**

71: X = Br
73: X = I

78

Scheme 2.4: The proposed mechanism for the formation of compounds, **71** and **73**.

Numerous attempts to synthesize **78** by treatment of (η^6-trindane)$Mn(CO)_2Br$, **71**, with $Bu_4N^+BH_4^-$ or to detect the hydride signal by NMR spectroscopy at low temperature were unsuccessful. As part of continuing efforts to synthesize the hydride, (η^6-trindane)$Mn(CO)_2H$, studies were extended to the $[(\eta^6\text{-HEB})Mn(CO)_3][BF_4]$ compound, where HEB = hexaethylbenzene. Hexaethylbenzene, **79**, may be thought of as an "unrestricted" trindane. In hexaethylbenzene, the wingtip CH_2 groups are untethered but are attached to a terminal CH_3 group and hence are free to rotate. While, in trindane, these CH_2 groups are tethered together by another CH_2 linker. Thus, in principle one can envision the possibility of isolating the corresponding hexaethylbenzene manganese dicarbonyl hydride, whereby the ethyl groups act as "arms" on the arene possibly providing protection to the hydride by surrounding the tripodal fragment, and therefore enhancing the thermal stability. However, when $[(\eta^6\text{-HEB})Mn(CO)_3][BF_4]$ was treated with *t*-BuOK, all attempts at detecting or isolating the hydride were unsuccessful; only decomposed products were recovered.

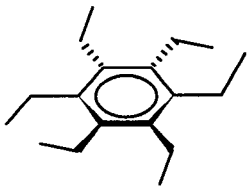

79

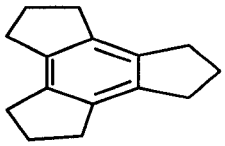

57

(HEB)$Mn(CO)_2Br$ was synthesized in hopes of preparing the corresponding hydride by using the borohydride approach established by Eyman *et al.*[104] Unfortunately, (HEB)$Mn(CO)_2Br$ was rather unstable in solution, readily decomposing to the hexaethylbenzene ligand, thus preventing further investigations of its reactivity.

However, having synthesized the hexaethylbenzene manganese compounds, this prompted an examination of their dynamics. They were investigated by low temperature NMR spectroscopy in order to probe the rotation of the ethyl groups since *proximal* and *distal* ethyl environments are readily differentiable in the ^{1}H and ^{13}C regimes (the dynamics of these molecules are fully explored in Chapter 4).

2.2.2 Synthesis, Characterization and Crystallographic Aspects of [(η^5-$C_{15}H_{15}$)-$Mn(CO)_2L$], where L = CO, PPh_3 or $P(OMe)_3$.

As a result of the unsuccessful attempts to isolate the above-mentioned hydride, another approach was chosen to intercept the purported hydride **78** either as (η^6-trindane)Mn(CO)(PR_3)H or as the formyl complex (η^6-trindane)Mn(CO)(HCO)(PR_3). Hence, the reactions of [(η^6-trindane)$Mn(CO)_3$][BF_4] and potassium *tert*-butoxide with donor ligands such as $P(OMe)_3$ and PPh_3 were examined. When [(η^6-trindane)$Mn(CO)_3$][BF_4] and potassium *tert*-butoxide were treated with trimethyl phosphite in THF and stirred at 40 °C for 20 h, and after chromatographic purification on silica, two yellow crystalline solids, **80** and **81**, were furnished (Scheme 2.5).[95] Along with infrared spectroscopic, mass spectrometric and elemental analysis data, the compounds were also examined by ^{1}H, ^{13}C and ^{31}P NMR spectroscopic techniques. The ^{1}H and ^{13}C NMR spectra of **80** and **81** revealed that the three-fold symmetry of the trindane ligand had been broken. The ^{1}H NMR spectrum of trindane is very straightforward, displaying a triplet for the benzylic protons and a quintet for the central methylene groups. Incorporation of a π-complexed organometallic moiety (such as $Mn(CO)_3^+$, $Cr(CO)_3$) renders the faces of the trindane ligand inequivalent, hence giving

rise to four ^{1}H NMR environments.[81] ^{31}P NMR spectroscopy was used as a probe to identify the products, in which the spectrum of compound **81** exhibited a singlet at 211.6 ppm (c.f. free $P(OMe)_3$ resonates at 141.6 ppm), whereas compound **80** did not contain phosphorus. Mass spectrometric data exhibited parent peaks at *m/z* 334 and 430, respectively, indicative of a molecular formula of $(C_{15}H_{15})Mn(CO)_2L$, where L = CO for **80** and L = $P(OMe)_3$ for **81**. Hence, the data for the products indicated in each case the formation of an η^5-indenyl complex in which the manganese has migrated from the central 6-membered ring to the peripheral 5-membered ring with concomitant loss of three hydrogen atoms from the latter ring.

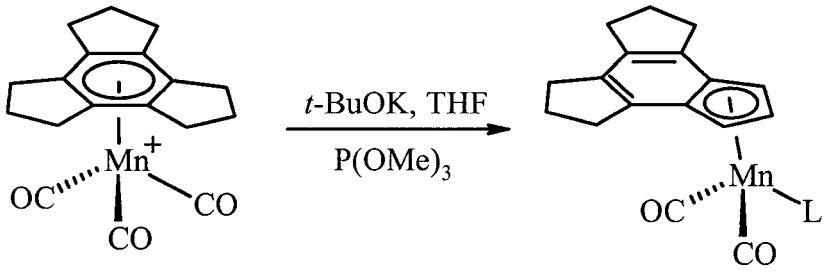

58c

80: L = CO
81: L = $P(OMe)_3$

Scheme 2.5: The synthesis of $(\eta^5\text{-}C_{15}H_{15})Mn(CO)_2L$ complexes, where L = CO or $P(OMe)_3$.

The formation of compounds **80** and **81** were readily monitored by the use of infrared spectroscopy. Compound **80** has two carbonyl bands at 2016 and 1934 cm^{-1}, while compound **81** displayed carbonyl absorptions at 1944 and 1876 cm^{-1}. Analogies can be drawn from the infrared spectra of related compounds. Comparing **80** and **81**: $(\eta^5\text{-}C_5H_5)Mn(CO)_3$ has ν_{CO} absorptions at 2025 and 1938 cm^{-1}, and $(\eta^5\text{-}C_5H_5)$-$Mn(CO)_2P(OMe)_3$ has ν_{CO} stretches at 1948 and 1884 cm^{-1}, respectively.[36d]

2.2.2.1 Structural Aspects

Subsequently, to complement the spectroscopic techniques, crystalline samples of compounds $(\eta^5\text{-}C_{15}H_{15})Mn(CO)_2L$, where L = CO, **80**, or $P(OMe)_3$, **81**, were characterized by X-ray crystallography. The resulting structures are depicted in Figures 2.5 and 2.6, respectively.

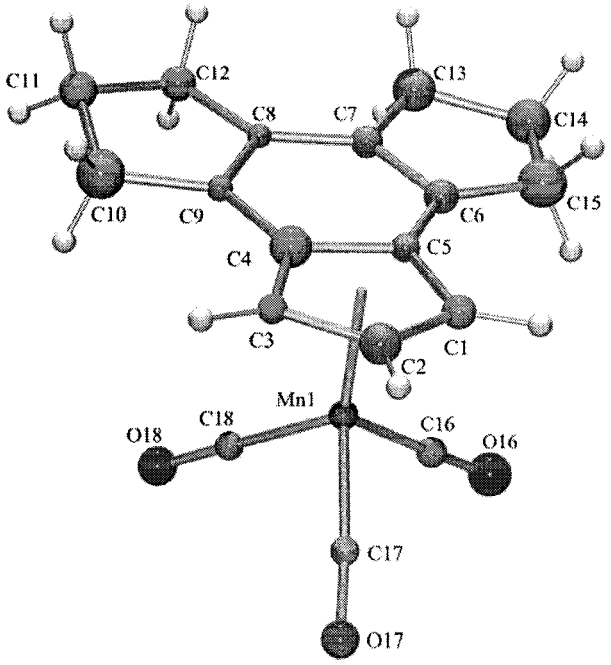

Figure 2.5: The crystallographically determined structure of the rearranged product, $(\eta^5\text{-}C_{15}H_{15})Mn(CO)_3$, **80**, showing the atomic numbering scheme.

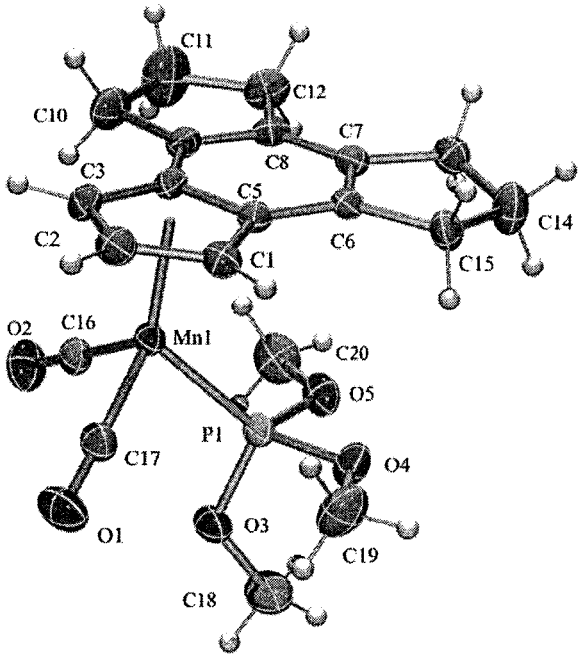

Figure 2.6: The X-ray structure of $(\eta^5\text{-}C_{15}H_{15})Mn(CO)_2[P(OMe)_3]$, **81**, showing the atomic numbering scheme. Thermal ellipsoids are shown at the 30 % probability level.

The structures of compounds **80** and **81** were determined by the use of suitable single crystals mounted on glass fibers. Crystallographic collection and refinement parameters, and bond lengths and angles are presented in the Appendix. Compound **80** crystallized in the monoclinic space group C*2/c*, while compound **81** crystallized in the monoclinic space group P$2_1/c$. Both crystal structures, **80** and **81**, confirmed that the $Mn(CO)_3$ fragment had migrated from the six-membered ring to the five-membered ring furnishing an indenyl type complex *via* the loss of three hydrogen atoms. Although the poor quality of crystal **81** led to weak diffraction, the connectivity of the structure was verified by data obtained during a single crystal X-ray diffraction study.

The manganese centers possess a pseudo-octahedral environment with the trindane ligand occupying three coordination sites. As depicted in Figures 2.5 and 2.6, the molecule also has a "piano stool" structure with an η^5-coordinated arene. In the latter structure, the "legs" consist of the two carbonyl ligands and a phosphite ligand, which are oriented in a slightly staggered conformation relative to the arene carbons. The Mn-CO bonds bisect the C(2)-C(3) and C(3)-C(4) bonds of the arene ring and the phosphite ligand bisects the C(4)-C(5) bond of the arene ring in compound **81**. The manganese atom in **81** lies 1.797 Å below the five-membered ring centroid. The Mn-C (CO) bond lengths are 1.760 (3) and 1.768 (2) in **81** Å which are typical bond distances for Mn-CO complexes. All C-C-C angles in the cyclopentadienyl ring are ~ 107 °, and the Mn-C-O angles are slightly less than 180 °. The Mn-to-cyclopentadienyl-carbon distances range from 2.114 (2) to 2.235 (2) Å, and the C-C bond distances range from 1.399 (3) to 1.442 (3) Å for the Cp carbons. The crystal structures of **80** and **81** may be compared to that of **82**, (η^5-cyclopenta[*def*]phenanthrenyl)$Mn(CO)_3$.[105] The Mn-C(Cp) distances of **81** is similar to **82** which ranges from 2.202 to 2.121 Å. The distances between sp^2 olefinic carbons in **81** are C(6)-C(7) (1.366 (3) Å) and C8-C9 (1.362 Å), which are analogous to **82**, 1.385 (4) - 1.374 (4) Å.

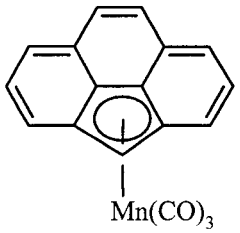

82

As an extension of this work and as an attempt to examine the generality of this rearrangement, the corresponding reaction of $(\eta^6\text{-trindane})Mn(CO)_3^+$ and *t*-BuOK in the presence of triphenylphosphine furnished two products, **80** and **83**.[95] The latter, a yellow crystalline solid, was identified as $(\eta^5\text{-}C_{15}H_{15})Mn(CO)_2PPh_3$. Infrared spectroscopic data of **83** revealed two infrared stretches at 1929 and 1862 cm^{-1}, which is comparable to that of the $(\eta^5\text{-indenyl})Mn(CO)_2(PPh_3)$ compound with carbonyl absorptions at 1931 and 1863 cm^{-1};[106] $(\eta^5\text{-}C_5H_5)Mn(CO)_2(PPh_3)$, ν_{CO} = 1931, 1863 cm^{-1};[106] and the analogous $P(OMe)_3$ compound **81**. ^{31}P NMR spectrum revealed a singlet at 94.3 ppm for the complexed PPh_3 ligand, while the phosphorus signal for the uncomplexed PPh_3 ligand appears at -5.1 ppm.

In addition, the reactions of $(\eta^6\text{-indane})Mn(CO)_3^+$, **84**, and *t*-BuOK in the presence of triphenylphosphine, **85**, or trimethyl phosphite, **86**, furnished the previously reported $(\eta^5\text{-indenyl})Mn(CO)_2L$ complexes, where L = PPh_3 and $P(OMe)_3$ (Scheme 2.6).[107] These complexes were characterized by using infrared and NMR spectroscopy and mass spectrometry.

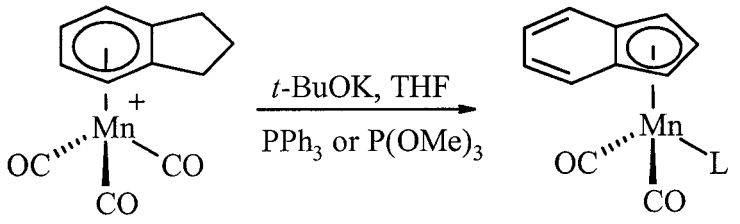

84

85: L = PPh_3
86: L = $P(OMe)_3$

Scheme 2.6: Preparation of indenyl manganese complexes.

2.2.2.3 Mechanistic Aspects

The proposed mechanism for formation of the rearranged product, (**80**, **81** or **83**) depicted in Scheme 2.7, suggests that, in the absence of an alkyl halide, the initially generated (η^6-trindane)$Mn(CO)_2H$, **78**, undergoes a hydrogen migration from an *endo*-benzyl site onto the metal, to produce a cyclohexadienyl complex, **87**, which loses dihydrogen furnishing **88**. A second *endo*-benzyl hydrogen migration gives rise to an isoindene framework, **89**, with a subsequent final hydrogen migration yielding **90**. Loss of dihydrogen and incorporation of either a carbonyl ligand or a phosphite or a phosphine ligand furnishes compounds **80**, **81** and **83**, respectively.[95]

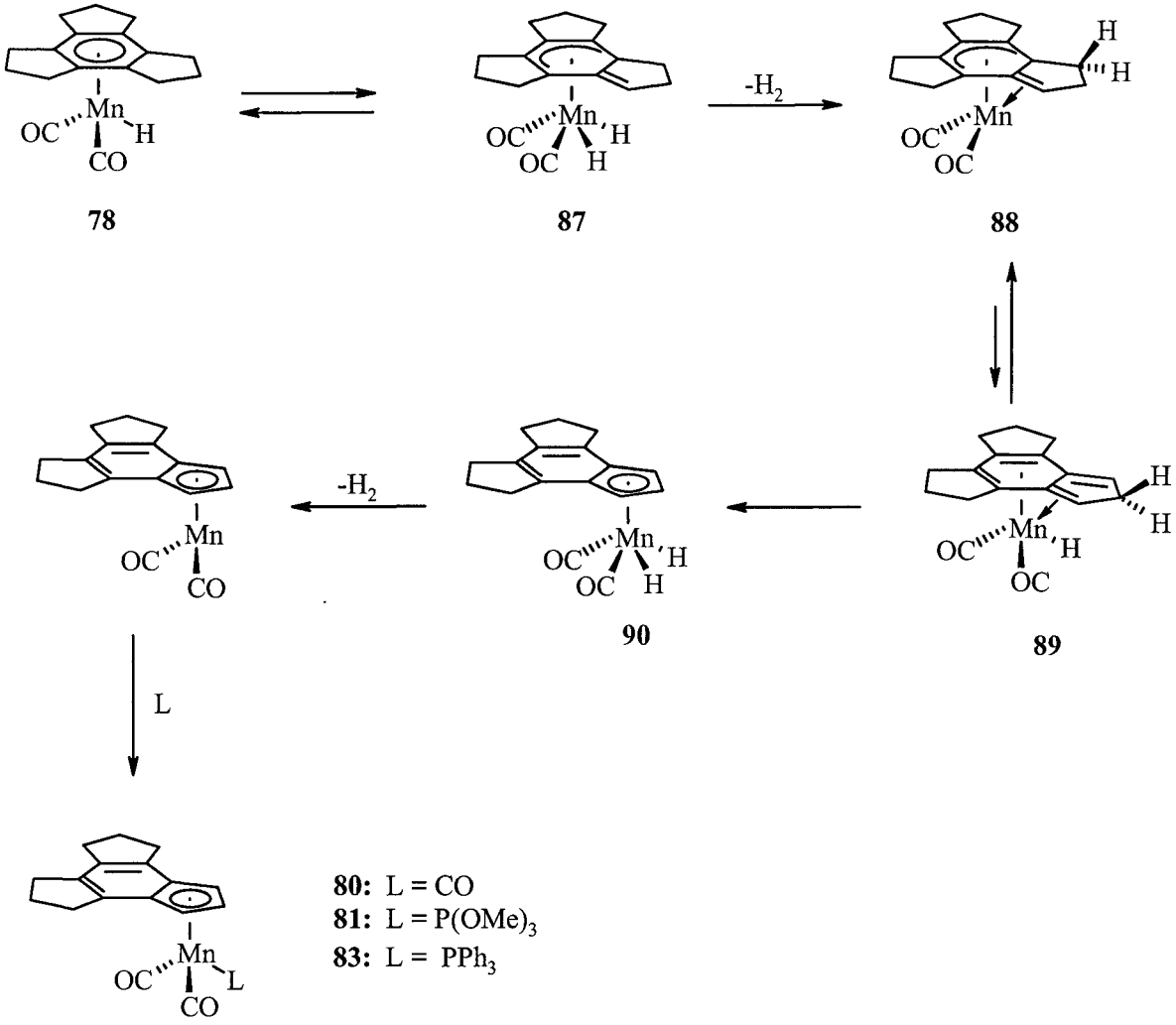

Scheme 2.7: A mechanistic rationale for the formation of the rearranged products (**80**, **81** and **83**).

Such intermediates have also been invoked in the η^6 to η^5 haptotropic shifts observed for (fluorenyl)ML_n or (cyclopenta[*def*]phenanthrenyl)ML_n systems, where ML_n = $Mn(CO)_3$ (Scheme 2.8).[108]

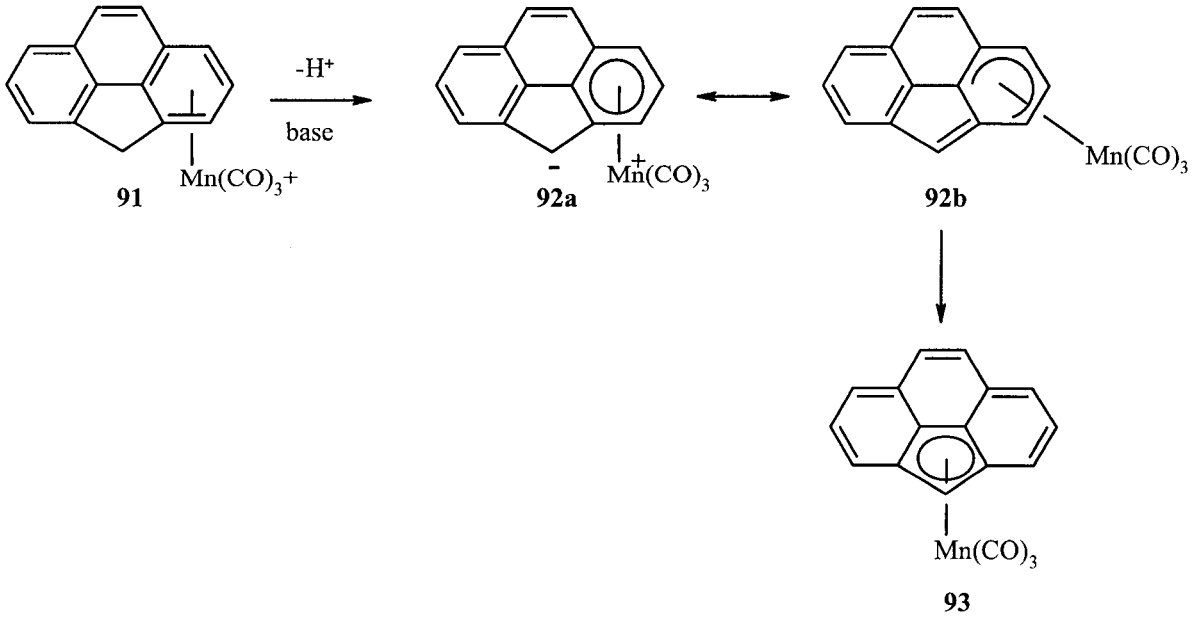

Scheme 2.8: Haptotropic shifts in organometallic complexes of 4*H*-cyclopenta[*def*] phenanthrene.

Furthermore, a report by Ustynyuk and co-workers[109] supports the proposed mechanistic pathway for the formation of **80**, **81** and **83**. They demonstrated that upon warming, (σ-methyl)(η^5-indenyl)tricarbonylchromium, **94**, rearranges to the η^6-(1-endo-methylindene)tricarbonylchromium, **95**, which isomerizes to the thermodynamically favored C(3)-methyl isomer, **97** (Scheme 2.9). This type of rearrangement is known to occur in transition metal complexes whereby the incoming reagent initially adds to the metal atom and then migrates into the π-ligand to one of the carbon atoms. This is referred to as a "ricochet" inter-ring haptotropic rearrangement reaction.[110] In this case, the methyl group is delivered onto the five-membered ring and the tricarbonyl moiety migrates to the six-membered ring. Density functional theory (DFT) calculations were used to examine the mechanistic aspects of the rearrangements, revealing that the

conversion of **94** to **97** proceeds *via* an isoindene intermediate, **96**, whereby the chromium is bonded to the diene portion of the six-membered ring and one double bond of the cyclopentadiene ring. These findings provide some justification for the proposed intermediates **88** and **89** depicted in Scheme 2.8.

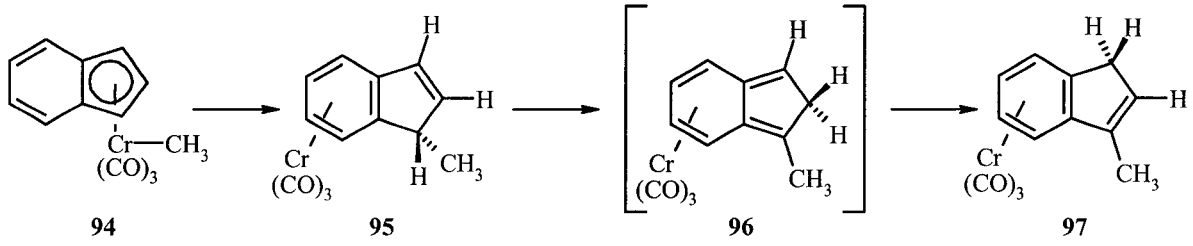

94 **95** **96** **97**

Scheme 2.9: "Ricochet" inter-ring haptotropic rearrangement of **94**.

2.2.3 Synthesis and Characterization of Other Trindane Metal Complexes

With the goal of selectively deprotonating only the *exo*-benzylic positions, an approach was chosen to replace one (or more) of the carbonyl groups on the manganese tricarbonyl moiety with more sterically demanding ligands. However, there can be a downside to this approach, because phosphine ligands also have the electronic effect of increasing the electron density on the manganese atom, and may thus decrease the acidity of the benzylic hydrogen atoms. This electronic effect is made evident by the carbonyl stretches, which are shifted to lower wavenumbers. Thus, treatment of [(η^6-trindane)-$Mn(CO)_3$][BF_4] with trimethyl phosphite and trimethylamine N-oxide furnished a yellow crystalline solid, [(η^6-trindane)$Mn(CO)\{P(OMe)_3\}_2$][BF_4], **98**, which, after chromatographic separation, was characterized by NMR, MS, IR and X-ray crystallography (Scheme 2.10).

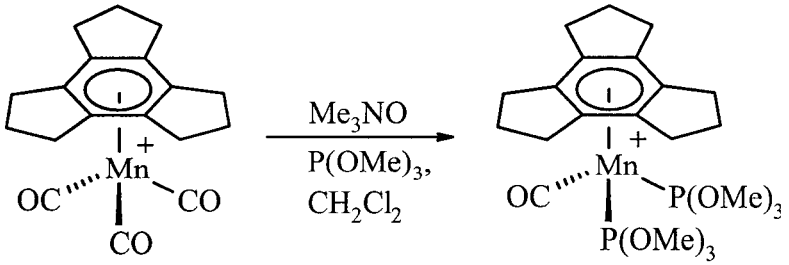

58c **98**

Scheme 2.10: Synthesis of compound **98**.

Preparation of compound **98** was accomplished by a similar method to that used for the (η^6-arene)$Mn(CO)_2X$, halide derivatives[47b] and other phosphine or phosphite substituted complexes, [(η^6-arene)$Mn(CO)L_2$][PF_6].[96,111,112] The infrared spectrum displayed a single carbonyl stretch at 1911 cm^{-1}, indicative of high electron density on the metal atom, similar to that of [(η^6-C_6Me_6)$Mn(CO)\{P(OMe)_3\}_2$][PF_6].[112] The ^1H NMR spectrum displayed a pseudo triplet at 3.38 ppm ($^3J_{H\text{-}P}$ = 5.0 Hz) corresponding to the splitting of the $P(OMe)_3$ methyl groups by two magnetically non-equivalent phosphorus nuclei, confirming the presence of two trimethyl phosphite ligands coordinated to the manganese metal. The ^{31}P NMR spectrum displayed a singlet at 185.5 ppm. Compound **98** was synthesized as part of an ongoing interest in investigating arene functionalization by utilizing transition metal complexes, in particular cationic manganese complexes. Replacing two carbonyl ligands with phosphite ligands would hopefully provide insight into the influence of the nature (steric and electronic) of the ligands surrounding the manganese atom. However, because of the very low yield (11 %) of **98**, deprotonation or other further reactions of this system were not viable. The low yield is not a surprising result, and is accord with the preparation of other analogous compounds such as [(η^6-

toluene)Mn(CO){P(OEt)$_3$}$_2$][PF$_6$][113] (27% from the corresponding cation, or 48 % from the monosubstituted phosphite compound) and [(η^6-C$_6$Me$_6$)Mn(CO){P(OMe)$_3$}$_2$][PF$_6$][112] (46 %). No substitution of the carbonyl groups with triphenylphosphine (PPh$_3$) occurred when [(η^6-toluene)Mn(CO)$_3$][PF$_6$] was treated with Me$_3$NO and PPh$_3$.

The structure of compound **98** was determined by X-ray crystallography of a single crystal mounted on a glass fibre and is depicted in Figure 2.7. Crystallographic collection and refinement parameters, and bond lengths and angles, are listed in the Appendix. Compound **98** crystallized in a triclinic space group $P\bar{1}$ and it compares favorably with the other trindane complexes previously reported,[81] and with those described above. Compound **98** exhibits the well-known piano stool conformation typical of half-sandwich complexes possessing two trimethyl phosphite ligands and a carbonyl ligand in a staggered conformation relative to the carbon atoms of the arene ring. The manganese atom is located 1.724 Å below the arene centroid, similar to the other trindane manganese complexes. The Mn-C (arene) bond lengths range from 2.194 (4) to 2.237 (3) Å. The Mn-C (CO) and two Mn-P bond lengths are 1.772 (4), 2.1996 (12) and 2.2174 (14) Å, respectively. The Mn-C-O angle is slightly less than 180 °, being 173.9 (4) °. To the best of our knowledge, the only other crystallographically characterized disubstituted phosphite arene manganese complex known is the [(η^6-toluene)Mn(CO){P(OEt)$_3$}$_2$][PF$_6$][113]; as well, there is a bis-chelated ditertiaryphosphine compound, [(η^6-C$_6$H$_6$)Mn(CO)(η^2-PPh$_2$C$_3$H$_6$PPh$_2$][PF$_6$] ·2CH$_3$CN.[49]

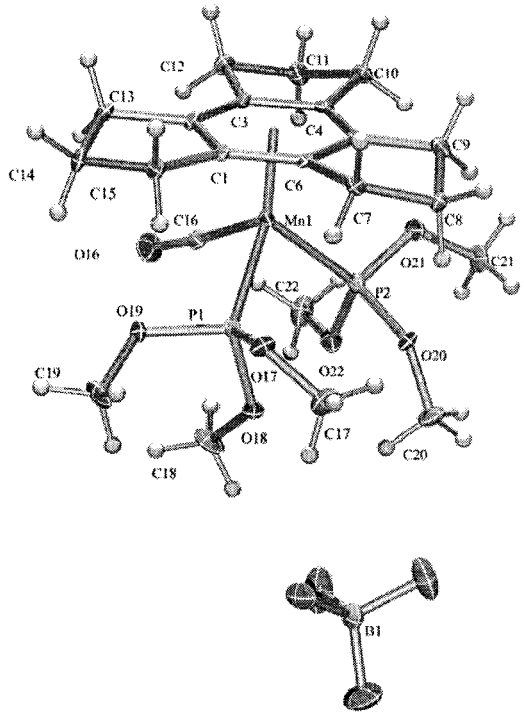

Figure 2.7: The crystallographically determined structure of [(η^6-trindane) Mn(CO){P(OMe)$_3$}$_2$][BF_4], **98**, showing the atomic numbering scheme. Thermal ellipsoids are shown at the 30 % probability level.

The molecules pack in a head-to-head fashion whereby the trindane ligands and the carbonyl tripods, respectively, are stacked on top of each other (Figure 2.8).

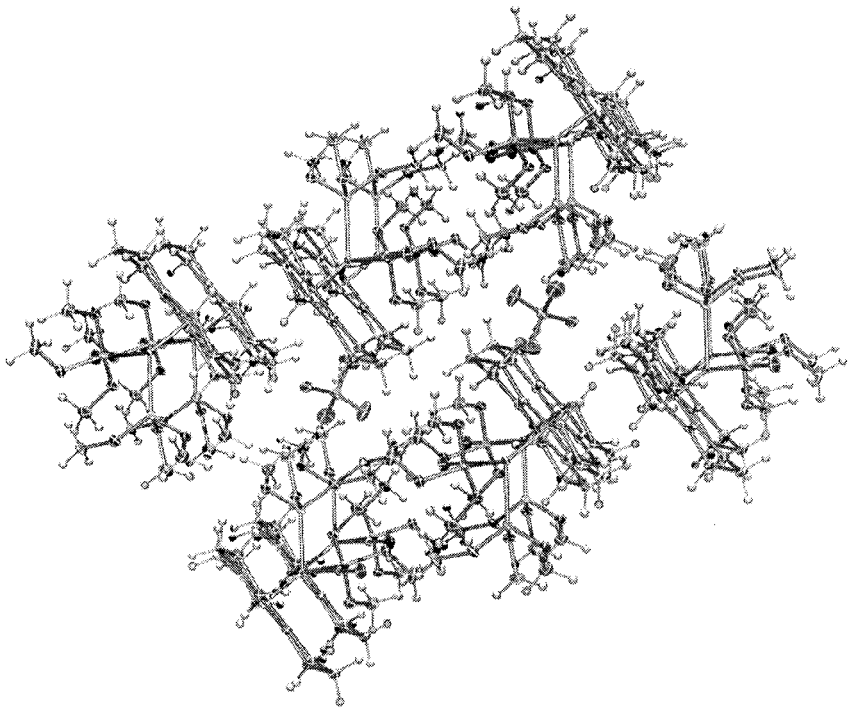

Figure 2.8: The crystal packing of molecules **98**.

The space-filling representation in Figure 2.9 emphasizes the degree of molecular crowding imposed by the trimethyl phosphite ligands of the tripod. Increasing the bulk of the tripodal substituents appears to enhance the steric volume of the organometallic portion of the molecule and, in principle, should prevent deprotonation of the *endo*-benzylic positions. This should allow for the selective deprotonation and functionalization of the six *exo*-benzylic positions of the trindane ligand.

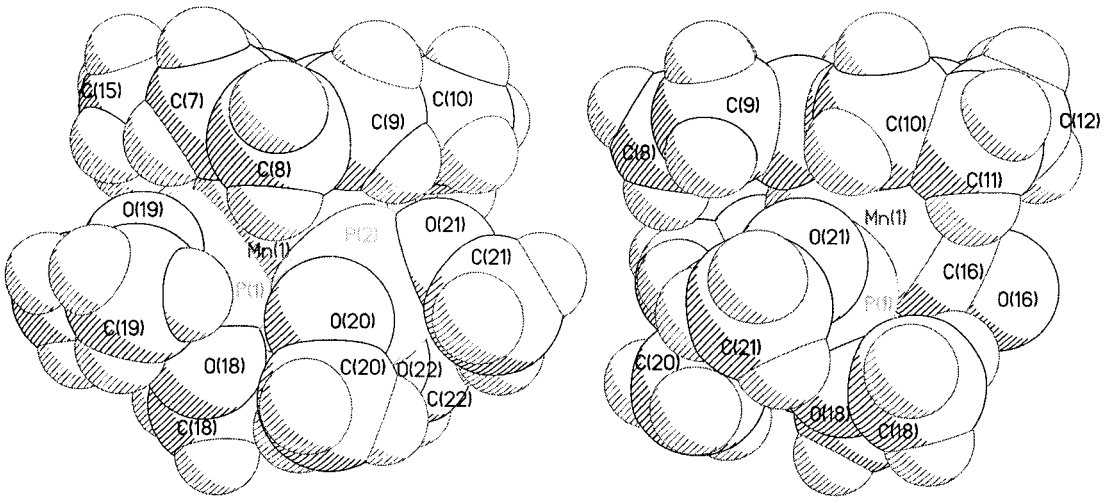

a **b**

Figure 2.9: Crystallographic space-filling view of **98**, accentuating the degree of crowding induced by the tripodal fragment. View (**a**) shows the two trimethyl phosphite ligands and view (**b**) looks along the carbonyl and trimethyl phosphite ligands.

Since it had been suggested that the rearrangement of **58c** to **80** involved the intermediacy of the unstable hydride (η^6-trindane)$Mn(CO)_2H$, it was considered worthwhile to attempt to prepare the corresponding rhenium hydride in the hope that it might be isolable. Hence, the preparation of [(η^6-trindane)$Re(CO)_3$][PF_6], **99**, the rhenium analogue of **58c**, was attempted (Scheme 2.11). The syntheses of several [(η^6-arene)$Re(CO)_3$][PF_6], have been described using well-established methods.[48a] However, the reported poor yield (25 % for toluene, 49 % for p-xylene) and poor reproducibility has been attributed to the rhenium salts reacting with water during the workup. Hence, time spent in the aqueous phase must be minimized. The low yield (~2 %) of **99** prevented further examination of its reactivity. The pattern displayed in the electrospray mass spectrometry is distinctive and diagnostic of the rhenium isotope pattern revealing peaks at *m/z* 467 and 469 corresponding to the molecular ions possessing ^{185}Re and ^{187}Re,

respectively. The ^{1}H NMR data revealed four chemical environments characteristic of trindane metal carbonyl complexes.

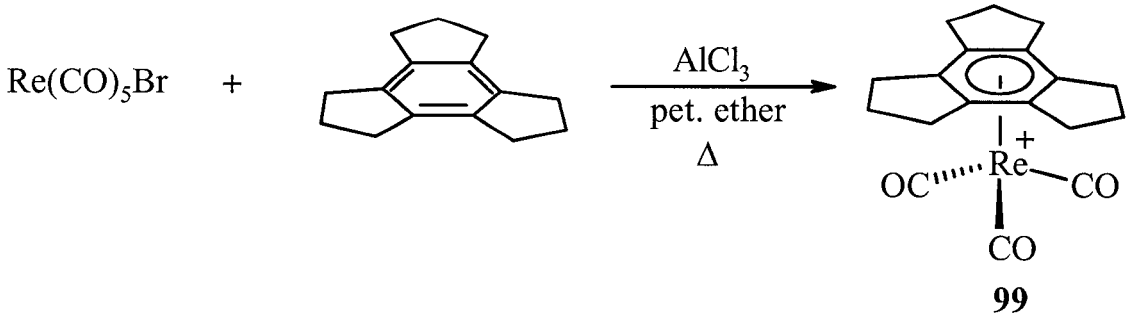

99

Scheme 2.11: Synthetic route to compound **99**.

2.2.4 Activation and Perfunctionalization of [(η^6-trindane)FeCp][PF_6] Complexes

Given the ease of successive activation and perfunctionalization that has been demonstrated for arenes π-complexed to $CpFe^+$ for the construction of organometallic stars and dendrimers,[57] the preparation of similar complexes in which the arene is trindane seemed feasible. Previous studies have shown that when [(η^6-trindane)FeCp][PF_6], **58d**, was treated with potassium *tert*-butoxide in DMSO-d_6 all twelve benzylic protons had been replaced by deuterons, which was verified by ^{13}C NMR spectroscopy and mass spectrometric data.[81] Also, when (η^6-trindane)$Cr(CO)_3$, **58a**, was treated under the same conditions, mass spectrometric data illustrated that multiple deuterium atoms had been incorporated at the benzylic sites (0 - 12).[81] It has been shown that the acidity of benzylic hydrogen is greater when the organometallic unit bound to the organic substrate is a cation rather than a neutral species. In addition, the reaction of **58d** with potassium *tert*-butoxide and DMSO-d_6 appeared to be cleaner in comparison to that

of **58a**. Similar results were reported when $[(\eta^6\text{-}C_6Me_6)FeCp][PF_6]$ was treated with a 20-fold excess of allyl bromide and KOH in dimethoxymethane (DME) furnishing the corresponding dodeca-allylated complex.[57] The product was characterized by ^1H and ^{13}C NMR spectroscopy and mass spectrometry. Hence, preliminary synthetic efforts were directed at the preparation of the dodecamethylated iron analogue, **100**.

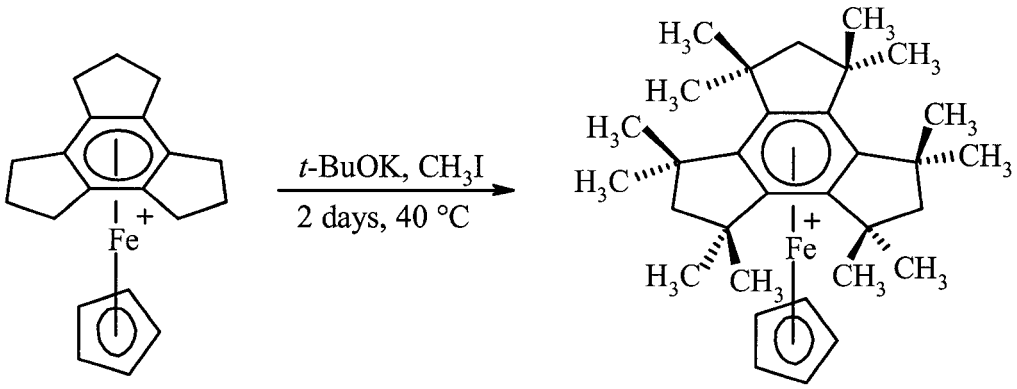

58d **100**

Scheme 2.12: Proposed synthetic route to the dodecamethylated trindane iron complex, **100**.

In a typical experiment, the trindane cyclopentadienyl iron complex and potassium *tert*-butoxide were stirred for 3 h at 40 °C under an inert atmosphere, and was followed by the addition of THF and alkylating reagent. The development of a red colour indicated the formation of a cyclohexadienyl intermediate that eventually disappeared and was noted by a cream/beige coloured solution.

The methylation of **58d** proceeded on a large scale using a 240-fold excess of methyl iodide (CH_3I) and potassium *tert*-butoxide (*t*-BuOK) in THF at 40 °C over 2 days yielding a mixture of products. After chromatographic purification on alumina, three orange solids were isolated and appeared to be unique products. However, mass

spectrometric data revealed three signals at *m/z* 459, 473 and 487, corresponding to the incorporation of 10, 11 and 12 methyl groups, respectively. It is uncertain, if the mass spectrum represents the fragmentation pattern of compound **100** or a mixture of compounds, in which the number of methyl groups at the benzylic positions differ. ^{1}H and ^{13}C NMR data was also inconclusive. Recrystallization from hexanes/acetone mixture furnished orange crystals on which X-ray crystallographic data has been collected; however a disorder with the methylated trindane ligand impedes a solution of the structure. Attempts to resolve a satisfactorily refined crystal structure are ongoing. Despite numerous attempts to synthesize compound **100** and the collection of two sets of data by X-ray crystallography, a definite assignment of the compound cannot be ascertained.

In a similar fashion, **58d** and *t*-BuOK were treated with allyl bromide (CH_2=$CHCH_2Br$) in THF and allowed to stir for 4 days at 40 °C under nitrogen. Despite difficulties encountered with separation of the mixture, chromatographic separation on alumina yielded two yellow components. Mass spectrometric data and NMR spectroscopy seem to reveal a mixture of components. According to the mass spectra, signals consistent to the incorporation of 12 allyl groups are apparent from the *m/z* of 799, followed by consecutive losses of multiples of 40 to a *m/z* of 319, which corresponds to the starting material, **58d**. Attempts to isolate a single crystal suitable for X-ray crystallographic study were hindered since the compounds were oily substances.

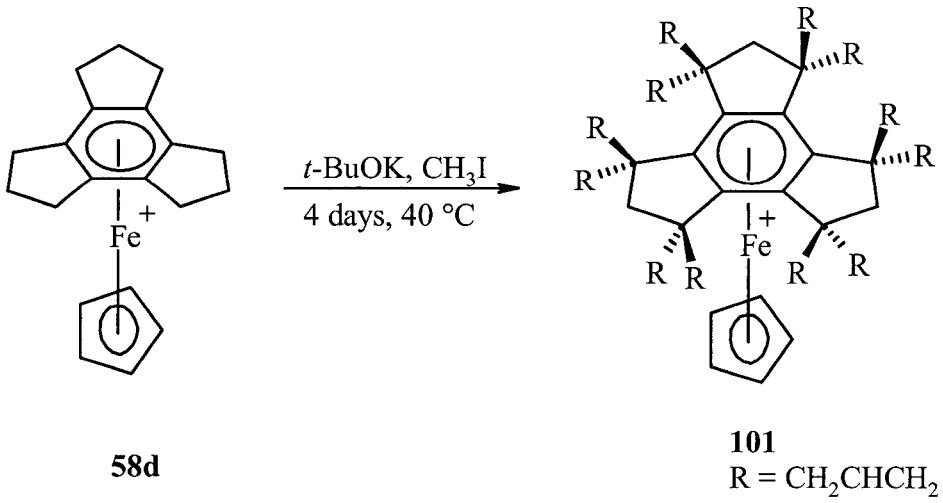

58d

101
R = CH_2CHCH_2

Scheme 2.13: Proposed synthetic route to the dodeca-allylated trindane iron complex, **101**.

2.3 Conclusion

To summarize, a series of previously unknown trindane manganese dicarbonyl halide complexes were synthesized and characterized spectroscopically using infrared and NMR spectroscopy, and mass spectrometry. X-ray crystallographic studies confirmed the identity of the products (**71** and **73**). In an attempt to deprotonate the six *exo*-benzylic sites of $[(\eta^6\text{-trindane})Mn(CO)_3][BF_4]$, a novel and rather facile rearrangement has been established. The reactivity of trindane manganese tricarbonyl and potassium *tert*-butoxide in the presence of donor ligands resulted in a haptotropic shift of the manganese tricarbonyl moiety from the central six-membered ring to the five-membered ring of the trindane ligand. The corresponding products were characterized by a variety of techniques (IR, NMR and MS), and the η^5-indenyl-type structure was verified by X-ray crystallography. Despite the absence of conclusive experimental data for the formation of the hydride, it was possible to rationalize its intermediacy based on

other analogous systems that have been presented in literature.[47b,101] Moreover, a series of other novel trindane complexes have been synthesized, and thus the organometallic chemistry of trindane has been greatly expanded.

CHAPTER THREE

Haptotropic Shifts of Manganese Tricarbonyl Moieties in Bi- and Tricyclic Arenes Possessing Five-, Six- and Seven-Membered Rings

3.1 Introduction

In continuation of previous studies presented in Chapter 2 on the reactivity of trindane manganese complexes, it was decided to investigate systems in which a manganese tricarbonyl moiety is coordinated to bicyclic or tricylic arenes containing six- and seven-membered rings. It has been demonstrated that the treatment of [(η^6-trindane)$Mn(CO)_3$][BF_4], **58c**, and potassium *tert*-buoxide (*t*-BuOK) with trimethyl phosphite in THF and stirring at 40 °C for 20 h, yielded two products, **80** and **81** after chromatographic separation.[95] The infrared, NMR and mass spectrometric data indicated the formation of η^5-indenyl complexes whereby the manganese had undergone a haptotropic shift from the central arene onto a five-membered ring with concomitant loss of three hydrogen atoms (Scheme 3.1). The structures of both **80** and **81** have been confirmed by X-ray crystallography.

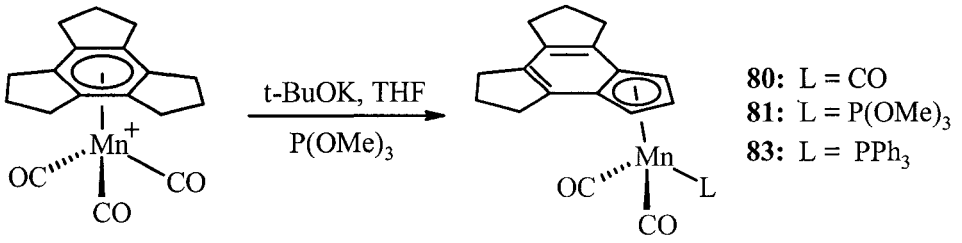

58c

Scheme 3.1: Synthetic route to the unexpected compounds **80**, **81** and **83** which have undergone a haptotropic shift of the tripodal manganese fragment.

The initial objective was to determine whether the reactions of [(η^6-trindane)$Mn(CO)_3$][BF_4], **58c**, with *t*-BuOK are restricted to indenyl-type complexes or whether they can be extended to systems with other sized rings attached to the arene. The second objective was to determine the factors that allow the haptotropic shift to occur in the trindane system. Hence, investigations into the effects of potassium *tert*-butoxide on manganese tricarbonyl moieties in bi- and tricyclic arenes possessing five- (indane), six- (tetralin, *i.e.* 1,2,3,4-tetrahydronaphthalene, $C_{10}H_{12}$) and seven-membered rings (dibenzosuberane, *i.e.* 10,11-dihydro-5H-dibenzo[*a,d*]cycloheptene, $C_{15}H_{14}$) were initiated.

3.2 Results and Discussion

3.2.1 Synthesis

The first step in this project was to synthesize the organometallic compounds to be studied by coordinating the manganese tricarbonyl moiety to the arenes of interest, utilizing the method pioneered by Pauson *et al.*[23] Two compounds, [(η^6-indane) $Mn(CO)_3$][BF_4], **84**, (50 % yield) and [(η^6-dibenzosuberane)$Mn(CO)_3$][BF_4], **102**, (10 % yield) were synthesized using this technique which involved treating $Mn(CO)_5Br$ with $AgBF_4$ in CH_2Cl_2 under argon or nitrogen with the exclusion of light. After heating to reflux for 30 min, the solution was treated with the arene and heating continued for 16 h. The reactive intermediate [$Mn(CO)_5^+$] (which is generated *in situ*) is formed by halide abstraction from $Mn(CO)_5Br$, ultimately giving rise to [(η^6-arene)$Mn(CO)_3$]$^+$. A more detailed discussion on the preparation, characterization and structural features of [(η^6-dibenzosuberane)$Mn(CO)_3$][BF_4], **102**, is given below (section 3.2.1.1). Conversely, the

[(η^6-tetralin)Mn(CO)$_3$][PF$_6$] compound, **103**, was prepared in a 80 % yield as described in the literature by heating Mn(CO)$_5$Br and the arene in the presence of AlCl$_3$.[114] The advantage of using the Mn(CO)$_5^+$ fragment is that the metal has a sixteen-electron configuration with a vacant coordination site, and can be easily coordinated to an arene; facile loss of two of the carbonyl ligands leads to formation of (arene)Mn(CO)$_3^+$ complexes under mild conditions.

As previously stated in other chapters, it is known that the benzylic hydrogen atoms of cyclic π-polyene ligands coordinated to electrophilic transition metal moieties, especially those that contain carbonyl groups and/or cationic metal fragments, are moderately acidic. It has been clearly demonstrated that when the manganese tricarbonyl moiety is coordinated to an arene, it will result in superior electrophilic activation compared to that of the chromium and ruthenium analogues.[34,115] The manganese tricarbonyl fragment can be readily coordinated to a wide range of aromatic molecules including benzenes, hydroquinones, indoles, benzothiophenes and aromatic steroids.[8,26,32]

3.2.1.1 Synthesis of the Tricyclic System, [(η^6-dibenzosuberane)Mn(CO)$_3$][BF$_4$]

The ligand dibenzosuberane, **105**, was prepared in a 77 % yield utilizing a known synthetic methodology for the reduction of diaryl ketones to diaryl methylene derivatives. The protocol involved treating dibenzosuberone, **104**, with a mixture of hypophosphorous acid and a catalytic amount of iodine in refluxing acetic acid (Scheme 3.2).[116] This reduction reaction provides a convenient and high yielding route to diaryl methylene

compounds and supersedes the traditional processes such as the Wolff-Kishner[117] and Clemmensen[118] reductions for the aforementioned conversions.

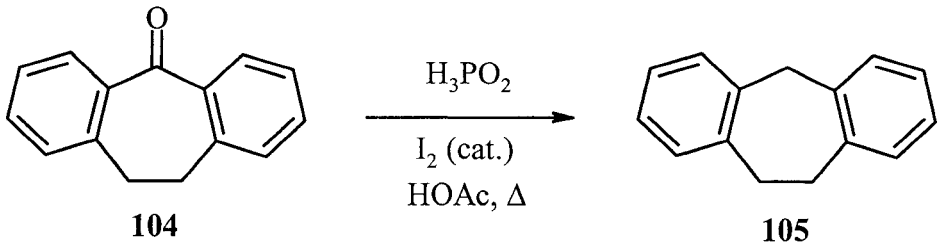

104 **105**

Scheme 3.2: Reduction of a diaryl ketone, dibenzosuberone to its corresponding diaryl methylene compound, dibenzosuberane.

π-Complexation of this organic ligand with a manganese tricarbonyl fragment resulted in the tripodal fragment being attached to a terminal six-membered ring (Scheme 3.3). The only other known complex of this type is (η^6-dibenzosuberane)$Cr(CO)_3$.[119]

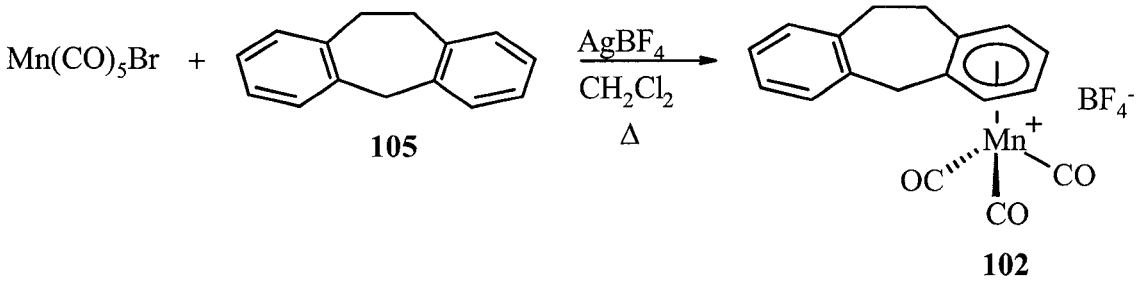

105 **102**

Scheme 3.3: Synthetic protocol for the preparation of the dibenzosuberane manganese tricarbonyl complex, **102**.

Compound **102** was characterized by ^1H and ^{13}C NMR along with standard two-dimensional NMR techniques. Electrospray mass spectrometry revealed a parent peak at *m/z* of 333 followed by peaks at *m/z* 277 and 249, corresponding to the loss of two and three carbonyl ligands, respectively. The infrared spectrum of **102** revealed two carbonyl stretches at 2065 and 2014 cm^{-1}, values typical of $[(arene)Mn(CO)_3]^+$ systems.[120]

The structure of compound **102** was determined by a single crystal X-ray diffraction study, and appears in Figure 3.1. Crystallographic collection and refinement parameters, and bond lengths and angles are listed in the Appendix.

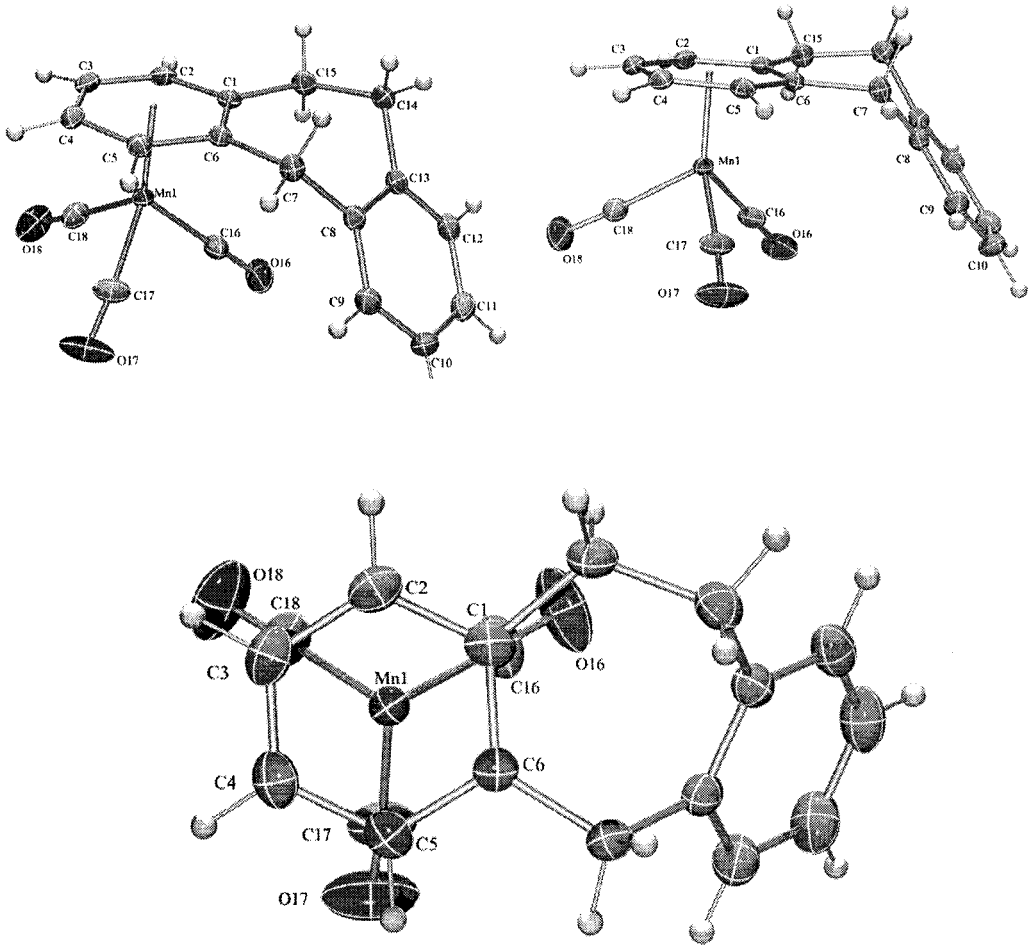

Figure 3.1: Three views of the crystallographically determined structure of [(η^6-dibenzosuberane)$Mn(CO)_3$][BF_4], **102**, depicting (a) the atomic numbering scheme, (b) the arcing of the molecule and (c) the slightly eclipsed orientation of the tripodal $Mn(CO)_3^+$ unit (shown with 30 % thermal ellipsoids).

Compound **102** crystallized in the monoclinic space group $P2_1/n$. Comparison of **102** with several chromium analogues reveals some distinct similarities and differences. Complexation of the manganese tricarbonyl unit occurs on the concave face or *endo* side of the molecule, in contrast to the corresponding, previously reported chromium compound **106**, (η^6-dibenzosuberane)$Cr(CO)_3$ and (η^6-dibenzosuberone)$Cr(CO)_3$, **107** (Figure 3.2).[119] However, the manganese complex **102** complexes in a similar fashion to (η^6-dibenzosuberol)$Cr(CO)_3$, **108**, (also referred to as (10,11-dihydro-5H-dibenzo[*a,d*] cyclohepten-5-ol)$Cr(CO)_3$) in which the tricarbonyl unit is likewise located on the concave (*endo*) face.[119] This is thought to be a result of the packing of the molecule, **102**, and the presence of the BF_4^- counter-ion. It is common for polycyclic molecules that are π-complexed to metal fragments to arc/fold away from the organometallic fragment. Such examples include α- and β- chromium complexes of methyl *O*-methyl-podocarpate,[121] as well as ruthenium and chromium derivatives of estradiol and estrone.[122]

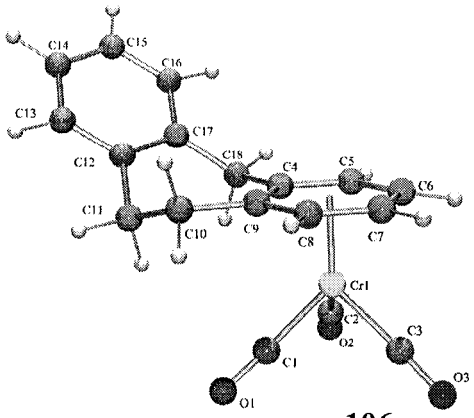

106

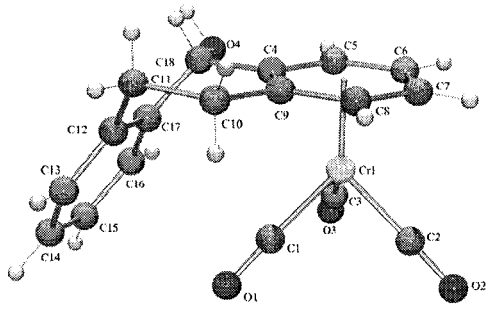

108

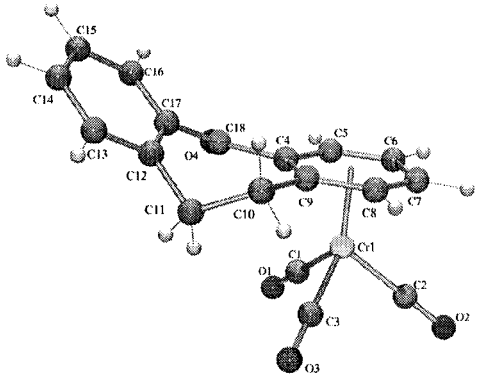

107

Figure 3.2: The X-ray structures of (η^6-dibenzosuberane)$Cr(CO)_3$, **106**, (η^6-dibenzosuberone)$Cr(CO)_3$, **107**, (η^6-dibenzosuberol)$Cr(CO)_3$, **108**.[119] Thermal ellipsoids are shown at the 30 % probability level.

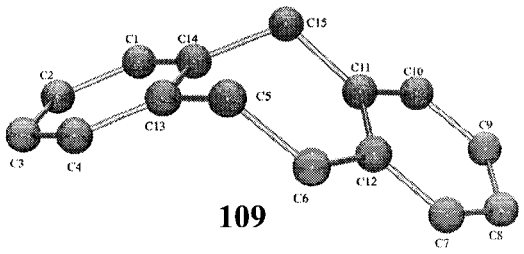

109

Figure 3.3: X-ray structure of dibenzosuberane (10,11-Dihydro-5H-dibenzo[*a,d*]cycloheptene), **109**, showing the atomic numbering scheme.[123] Thermal ellipsoids are shown at the 30 % probability level.

The free organic ligand represented in Figure 3.3 demonstrates that the molecule is not planar but rather is severely arced. The interplanar angle between the two arene rings is 123°.[123]

Other crystallographically characterized molecules that contain the dibenzosuberane framework are compounds **110** and **111**.[124] The former compound, **110**, is formed by the incorporation of a diarylcarbene ligand into an organomanganese complex, $(\eta^5\text{-}C_5H_5)Mn(CO)_2(THF)$ by a diazoalkane route, while the η^2-ketene complex, **111**, arises from treatment of the metal carbene **110** with carbon monoxide at high pressures.

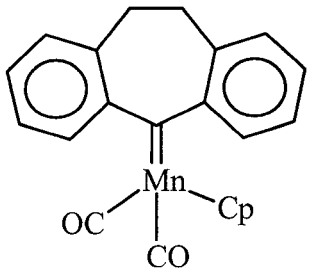

110

$Cp = C_5H_5$

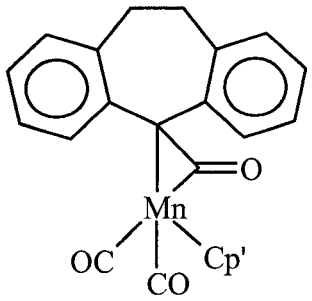

111

$Cp' = C_5H_4(CH_3)$

The structure of compound **102** shows that the benzene rings are almost planar with a deviation from the least-squares planes of 0.009 Å for the coordinated arene and 0.007 Å for the uncoordinated arene. The interplanar angle between the two external six-membered rings is 51.34 (0.10) °. The manganese tripod is coordinated to the arene ring in an η^6 fashion whereby the manganese atom is located 1.688 Å below the six-

membered ring centroid. The Mn to the arene-C distances range from 2.169 (3) to 2.252 (3) Å. The Mn-C(CO) bond lengths range from 1.807 (3) to 1.824 (3) Å, and are typical of Mn-CO distances, and the Mn-C-O angles are slightly less than 180 °. The carbonyl groups of the $Mn(CO)_3$ unit adopt a conformation whereby they are almost eclipsed.

It is also informative to look at the packing of the molecule in the unit cell (Figure 3.4). The molecules of **102** are arranged in layers of cations and anions.

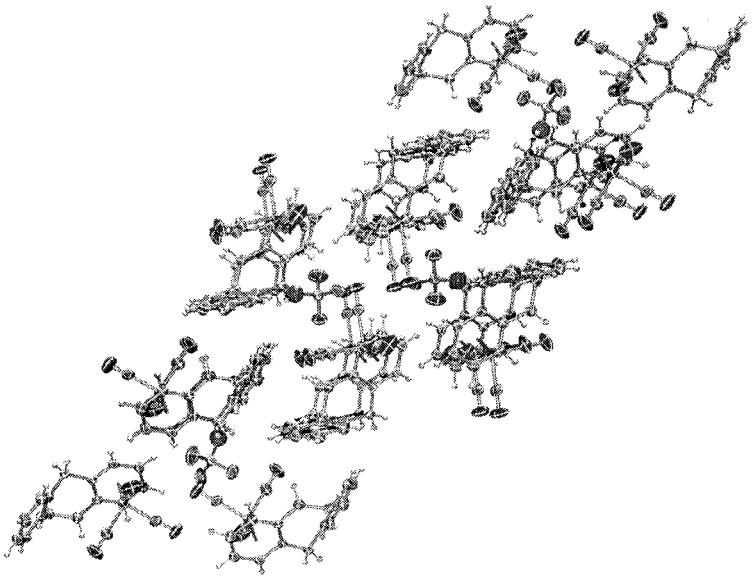

Figure 3.4: The crystal packing of molecules **102**.

The second and final step for this project involved probing the generality of the haptotropic shift that occurred with $[(\eta^6\text{-trindane})Mn(CO)_3][BF_4]$. Hence, the respective arene manganese complexes (**84**, **102** and **103**) were treated with potassium *tert*-butoxide in the presence of a donor ligand, such as trimethyl phosphite, $P(OMe)_3$. The viability of

haptotropic shifts of manganese tricarbonyl moieties in bi- and tricyclic systems comprising five-, six- and seven-membered rings are presented herein.

3.2.2 Reactivity Studies

3.2.2.1 Bicyclic System Containing a Five-Membered Ring

To reiterate what was described in Chapter 2 for the purpose of further comparison, the reactions of $[(\eta^6\text{-indane})Mn(CO)_3][BF_4]$ and *t*-BuOK gave rise to the known compound $(\eta^5\text{-indenyl})Mn(CO)_2L$,[107] where L = PPh_3, $P(OMe)_3$ (Scheme 3.4). This result is consistent with that found in the trindane system in that the manganese unit migrates from the six- to the five-membered ring. Since indane is a substructure of trindane, this result is not surprising.

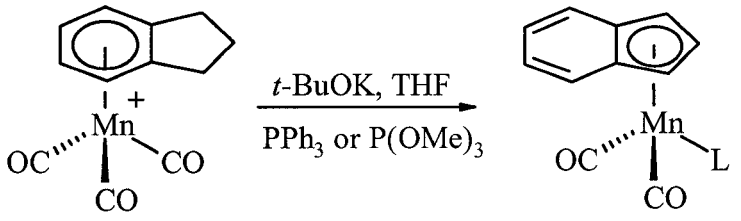

84

85: L = PPh_3
86: L = $P(OMe)_3$

Scheme 3.4: The synthetic route to the η^5-indenyl manganese complexes **85** and **86**.

3.2.2.2 Bicylic System Containing a Six-Membered Ring

The tetralin manganese tricarbonyl cation, $[(\eta^6\text{-tetralin})Mn(CO)_3][PF_6]$, **103**, was selected as the ideal candidate for probing the reactivity of a bicyclic system possessing a six-membered ring conjoined to an arene. The choice seemed sensible as its synthetic methodology had already been established.[114] Since the original synthesis of the tetralin manganese tricarbonyl cation in 1984, there has been only one report on its reactivity.[30a]

In this 1995 report, Lee and co-workers investigated the reactivity of **103** with nucleophiles and found that nucleophilic addition afforded α-position adducts, except when **103** was treated with MeMgBr in THF at 0 °C.[114] This latter reagent yielded two products in a 5.2 : 1 ratio: the α-position adduct, **112a** and the acyl compound, **112b** (Scheme 3.5). Along with common spectroscopic techniques, compound **112b** was also characterized by a single crystal X-ray diffraction study, and was the first reported structure of an (arene)manganese acyl compound.[114]

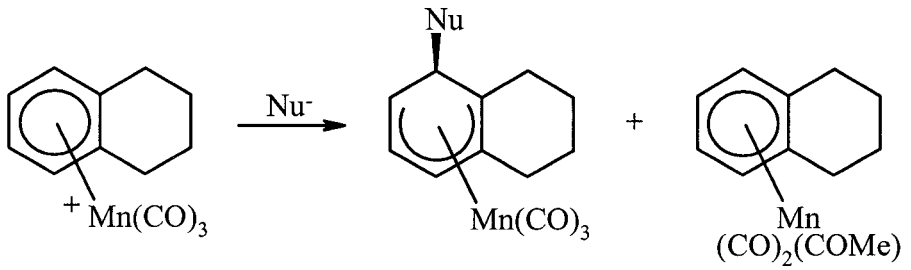

103 **112a:** Nu = H **112b**
113: Nu = Me
114: Nu = Ph
115: Nu = $P(O)(OMe)_2$
116: Nu = CH_2CN

Scheme 3.5: Reactions of **103** with nucleophiles.

The possibility of invoking a haptotropic rearrangement in a bicyclic system seemed like an attractive option. However, treatment of $[(\eta^6\text{-tetralin})Mn(CO)_3][PF_6]$, **103**, with *t*-BuOK and $P(OMe)_3$ in THF yielded, after chromatographic separation by use of a chromatotron, several products in very low yields. Despite several attempts at careful purification, not enough material was isolated to allow for characterization. As a result of the complexity of the reaction involving $[(\eta^6\text{-tetralin})Mn(CO)_3][PF_6]$ with *t*-

BuOK and $P(OMe)_3$ in THF, it was decided to investigate the effects of each reagent separately to help clarify their roles in the overall reaction (Scheme 3.8).

The addition of $P(OMe)_3$ in THF to $[(\eta^6\text{-tetralin})Mn(CO)_3][PF_6]$ yielded a yellow crystalline solid that was identified by ^1H, ^{13}C and ^{31}P NMR and mass spectrometry as $[(\eta^6\text{-tetralin})Mn(CO)_2P(OMe)_3][PF_6]$, **117**; the assignment was verified by a single crystal X-ray diffraction study. The infrared spectrum revealed two carbonyl stretches at 2008 and 1961 cm^{-1}. Compound **117** exhibited ^{31}P NMR resonances for each of the phosphorus atoms, P(1) $\{P(OMe)_3\}$ and P(2) $\{PF_6\}$. When the solution was exposed to light, the sole product was compound **117**. However, protecting the solution from light resulted in no reaction, and only starting materials were isolated. Both reactions were monitored by *in situ* IR spectroscopy. The formation of **117** is not surprising since the replacement of a carbonyl by a phosphine or halide in $[(C_6Me_6)Mn(CO)_3]^+$ requires either photolysis or use of Me_3NO.[34,47,125]

A comparison may be made with structure **117** to that of the analogous acyl derivative, $[(\eta^6\text{-tetralin})Mn(CO)_2(C(O)Me)]$, **112b**.[114] Compound **117** crystallized in the orthorhombic space group P*nma*. The structure of **117** appears in Figure 3.5, while crystallographic data and refinement parameters, and bond lengths and angles are collected in the Appendix. The anion was disordered, in that two orientations were found for the PF_6^- anion. There is also a disorder among atoms, C(7a) and C(7), in which there exits two twisted half-chair conformations. This allows the molecule to lie on a crystallographic plane, a mirror plane, thus only half of the molecule was solved and the other half of the molecule was generated by the mirror plane. The manganese atom is

located 1.679 Å below the plane of the arene ring. The Mn-C(arene) distances range from 2.179(2) to 2.207(2) Å similar to those previously found in compound **112b**. The benzene ring displayed no deviation from planarity. The Mn-C-O angles are essentially linear, and the carbonyl groups of the $Mn(CO)_3$ group are staggered and there is some ring slippage relative to the benzene fragment of the tetralin ring. That is, the manganese atom is not connected centrally to the arene ring but is displaced towards the C(2) position whereby the Mn-C(arene) bond distances are found to be Mn-C(1/1a) 2.183 (2) Å, Mn-C(2/2a) 2.179 (2) Å, Mn-C(3/3a) 2.207 (2) Å. The essentially staggered orientation of the tripodal manganese unit in **117** is typical of such polycyclic manganese complexes (Figure 3.5, inset).[26,95] The cyclohexene ring adopts a twisted half-chair conformation, with one of the homobenzylic ring carbon atoms lying below, and the other lying above, the molecular plane defined by the arene ring.

Other X-ray structures are known in which the tetralin fragment is bound to a $Cr(CO)_3$ moiety.[126] Volk *et al.* reported the synthesis and characterization of a variety of (η^6-tetralin)$Cr(CO)_3$ complexes, along with investigations of their benzylic deprotonations, and the regioselectivity of these reactions (Scheme 3.6). Both single crystal X-ray diffraction and NMR spectroscopic studies aided in the assignment of the *exo*- and *endo*-benzylic hydrogen atoms of complexes (**120** and **122**) allowing for the regioselectivity of the deprotonation/alkylation to be determined. A typical reaction involved dissolving the complex in a solvent mixture consisting of THF/HMPA in a 10:1 ratio (HMPA = hexamethyl phosphoric triamide), followed by the addition of 1.5 - 3 equivalents of *n*-butylithium (*n*-BuLi).[126] The formation of the anion intermediate was

evident by the development of a red solution. The anion was further treated with D_2O, methyl iodide or acetyl chloride furnishing the respective deuterated, alkylated or acylated products. The data revealed that in the case of two competing *exo* hydrogen atoms having comparable steric environments, it is not necessarily the *exo*-benzylic hydrogen atom that adopts a pseudoaxial position that is preferentially abstracted.[126] It was concluded that the conformation of the chromium tricarbonyl tripod may influence the regioselectivity of benzylic deprotonation in chiral (arene)$Cr(CO)_3$ complexes.[126]

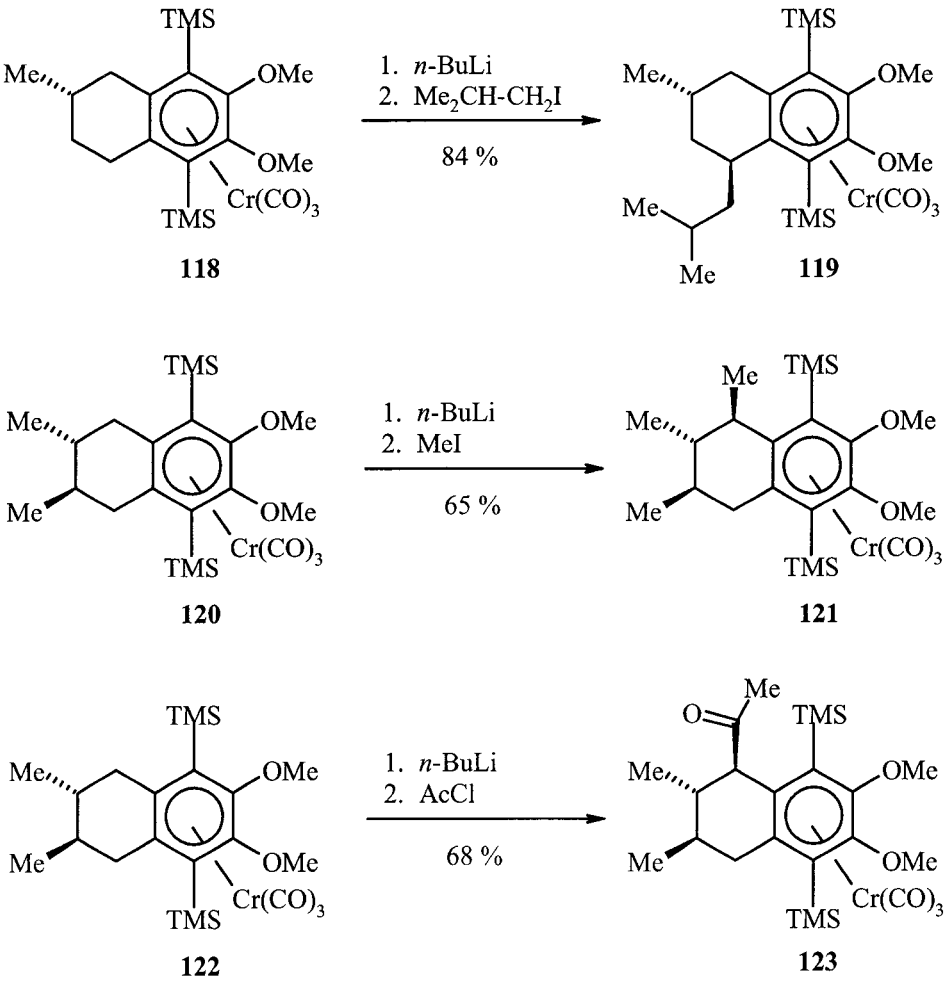

Scheme 3.6: Benzylic deprotonations and alkylations of functionalized tetralin tricarbonyl chromium complexes.

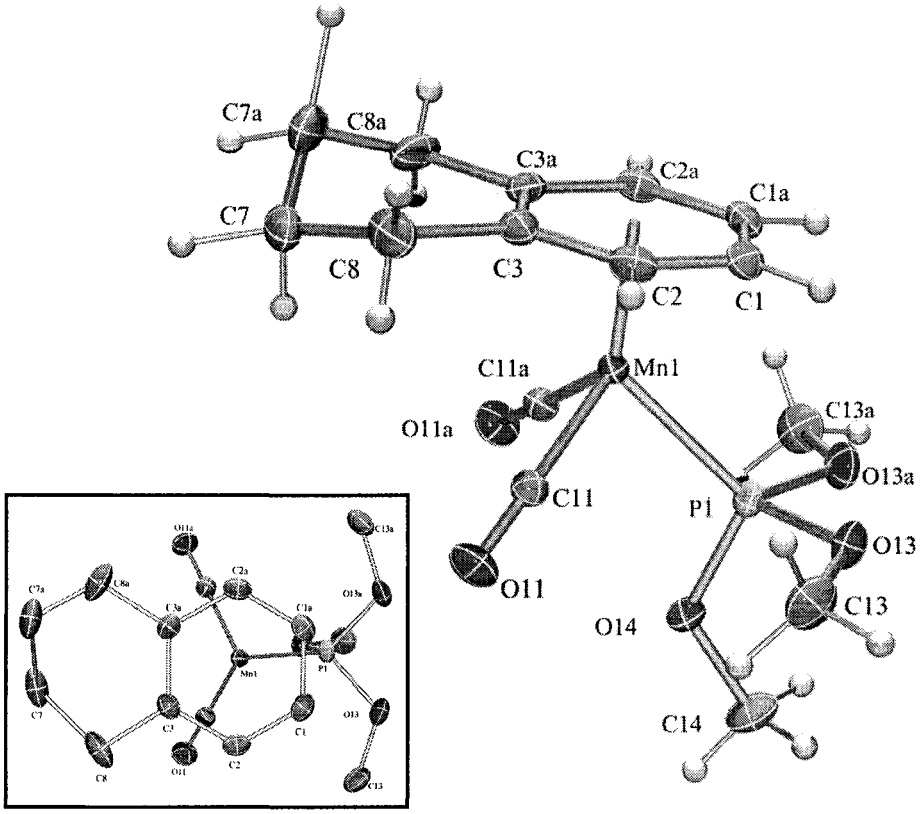

Figure 3.5: X-ray structure of $[(\eta^6\text{-tetralin})Mn(CO)_2P(OMe)_3][PF_6]$, **117**, showing the atomic numbering scheme (thermal ellipsoids are shown at the 30 % probability level); the inset figure illustrates the staggered orientation of the tripodal manganese fragment (Hydrogen atoms are omitted for clarity).

Treatment of $[(\eta^6\text{-tetralin})Mn(CO)_3][PF_6]$, **103**, with potassium *tert*-butoxide in THF afforded a yellow-orange oil. From infrared and mass spectrometric data, this substance has been tentatively assigned as compound **124**. Carbonyl absorptions are seen at 2007 and 1927 cm^{-1} (neat) in the infrared spectrum, which are indicative of a cyclohexadienyl compound (cf. 2004 - 1913 cm^{-1}).[114] Chemical ionization data revealed a $[M+1]^+$ peak at *m/z* value of 403 followed by a loss of 131 corresponding to $C_{10}H_{11}$. Subsequent loss of two and three carbonyl groups, and a manganese atom followed. The ^1H and ^{13}C NMR spectra exhibit many peaks, and the assignments are currently

incomplete. Despite several attempts at crystallization, attempts to isolate a single crystal suitable for X-ray crystallography have so far been unsuccessful.

In the absence of crystallographic evidence, the identity of compound **124** must remain tentative. However given the data presented in the literature on tetralin systems, it is still possible to suggest how **124** might have arisen. [114,126] The proposed mechanism for the formation of **124** is depicted in Scheme 3.7. In the presence of excess potassium *tert*-butoxide, deprotonation at the benzylic site would generate the anion, **103a**, which nucleophilically adds to another molecule of $(tetralin)Mn(CO)_3^+$. Subsequent loss of the metal fragment furnishes **124**.

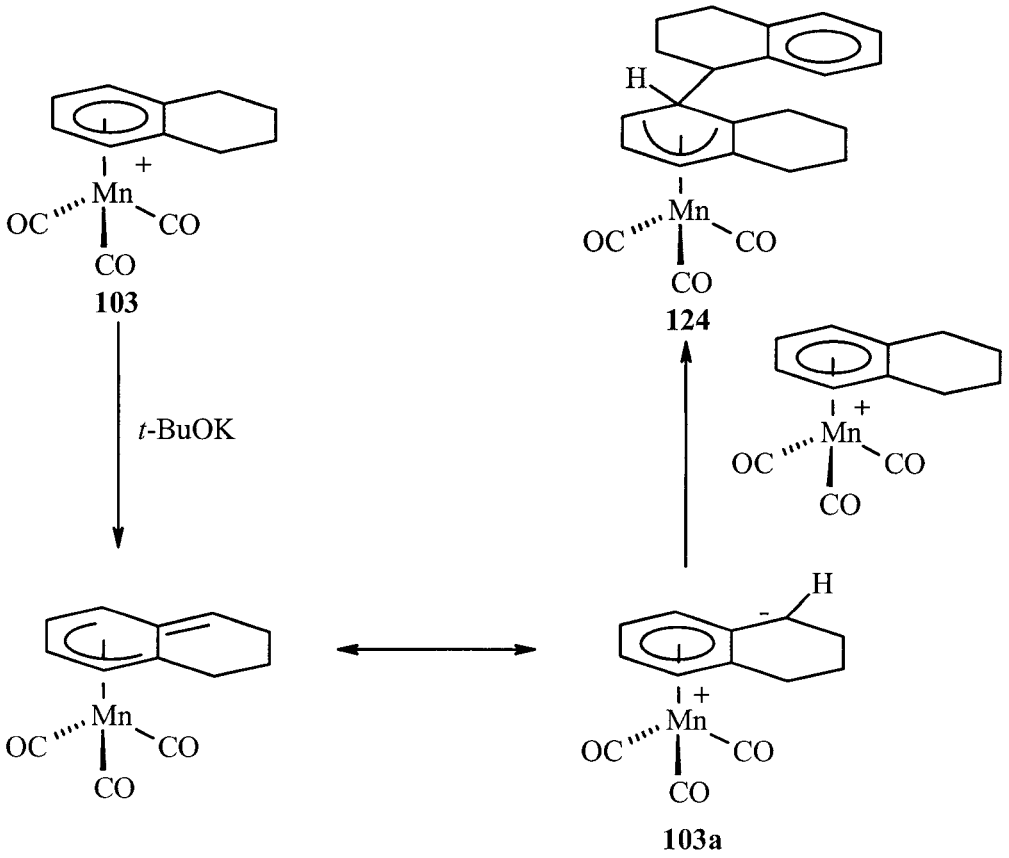

Scheme 3.7: A proposed mechanistic rationale for the formation of **124**.

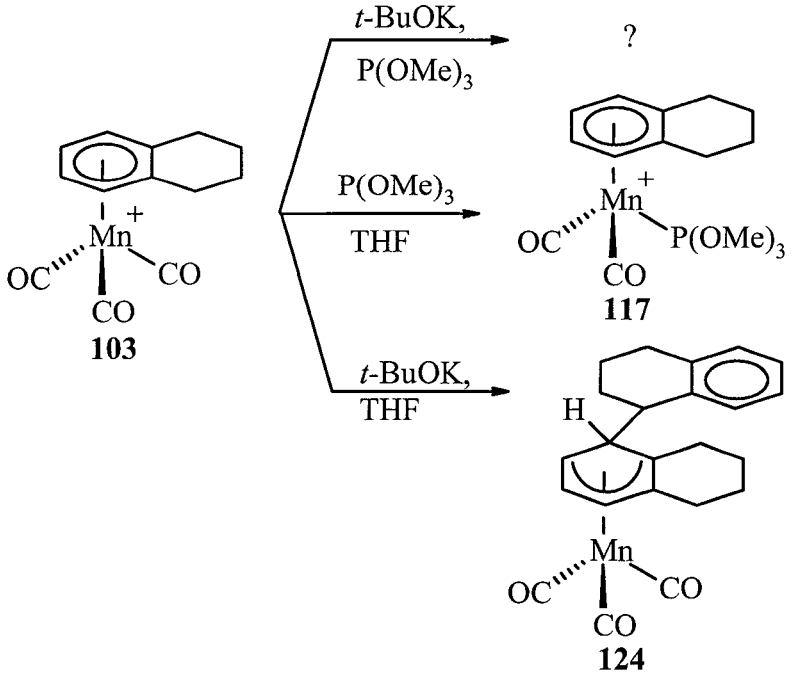

Scheme 3.8: Reactions involving the tetralin manganese tricarbonyl complex, **103**.

3.2.2.3 Tricyclic System Containing a Seven-Membered Ring

Having synthesized and fully characterized the necessary tricarbonyl manganese complex, **102**, its reactivity with potassium *tert*-butoxide was probed. Treatment of [(η^6-dibenzosuberane)$Mn(CO)_3$][BF_4], **102**, and *t*-BuOK with $P(OMe)_3$ in THF yielded, after chromatographic separation, a mixture of products in very low yields insufficient for characterization. Consequently, as was done in the [(η^6-tetralin)$Mn(CO)_3$][PF_6] case, each reagent was treated separately with [(η^6-dibenzosuberane)$Mn(CO)_3$][BF_4] (Scheme 3.13). Treatment of **102** with *t*-BuOK in THF gave (η^5-$C_{15}H_{13}$)$Mn(CO)_3$, **125**, an orange powder, as the major product after chromatographic separation. Compound **125** was characterized by X-ray crystallography as an η^5-complex in which deprotonation of the

benzylic proton had occurred resulting in generation of a double bond in the central seven-membered ring (Scheme 3.9).

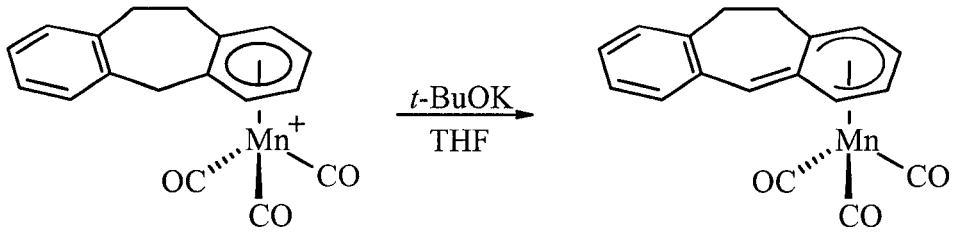

102 **125**

Scheme 3.9: Treatment of **102** with potassium *tert*-butoxide furnishing the cyclohexadienyl complex, **125**.

This is reminiscent of the behaviour of (η^5-cyclopentadienyl)(η^5-fluorenyl)iron which was generated from the reaction of potassium *tert*-butoxide with the cationic precursor $[Fe(C_5H_5)(C_{13}H_{10})][PF_6]$ in toluene.[127] Deprotonation of the (η^6-fluorenyl)-tricarbonylmanganese or (cyclopentadienyl)iron cations, **126** or **127**, respectively, yielded species in which the metal moiety was still attached to the six-membered ring (Scheme 3.10).[127,128] These neutral molecules can be represented either as zwitterions, as in **128a**, or possessing a formal double bond, as in **128b**. The X-ray structures of the (η^5-fluorene)M, where M = $Mn(CO)_3$ and FeCp, confirmed the presence of the η^5-cyclohexadienyl ring and a double bond in the central ring.[129,130] Upon heating, the manganese tricarbonyl moiety eventually migrates onto the central five-membered ring, **129**. Despite initial claims, it is now evident that migration to produce the ferrocenyl analogue **129** does not occur.

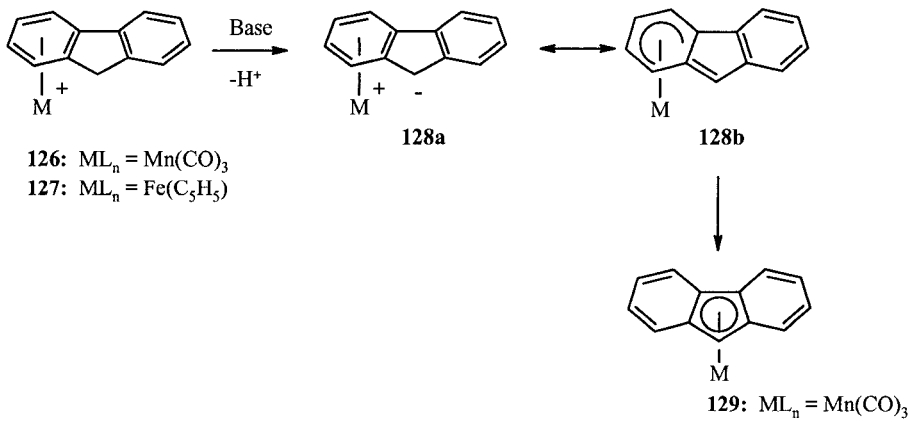

Scheme 3.10: Haptotropic shifts in the (η^5-fluorenyl)ML_n system.

Similar results were obtained upon deprotonation of [(η^6-8,9-dihydro-4H-cyclopenta[*def*]phenanthrene)$Mn(CO)_3$][PF_6], **130**, which occurs in a stepwise fashion.[108c] The initially generated neutral molecule **131** is relatively stable, and has been unequivocally identified by ^1H and ^{13}C NMR and mass spectrometry. Subsequently, mild theromolysis of **131** brings about a haptotropic shift yielding **132**, whereby the $Mn(CO)_3$ fragment is η^5 bonded to the five-membered ring (Scheme 3.11).[108c]

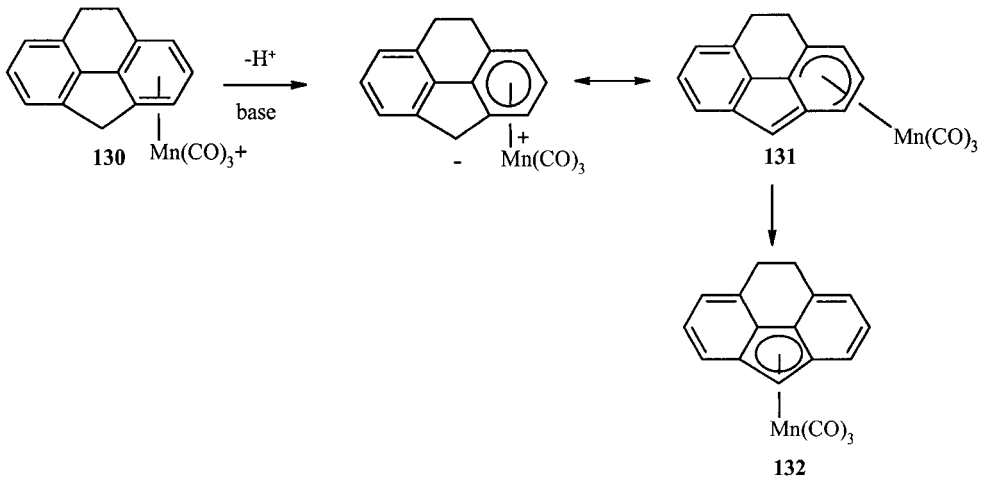

Scheme 3.11: Haptotropic shifts in the (4,5-dihydrocyclopenta[*def*]phenanthrenyl)-$Mn(CO)_3$ complex.

Furthermore, deprotonation of **133** with Proton Sponge (1,8-bis(dimethylamino)naphthalene) or $KOCMe_3$ furnished two isomers **134a** and **134b** of the $[Ru(C_5Me_5)(\eta^5\text{-fluoradenyl})$ as depicted in Scheme 3.12.[131] The isomer ratio depends on reaction conditions; for instance, one equivalence of Proton Sponge in CD_2Cl_2 yielded a **134a/134b** ratio of 20 : 1 while excess *t*-BuOK in THF gave rise to a **134a/134b** in a 1.7 : 1 ratio. Protonation of **134** with trifluoromethanesulfonic acid in CH_2Cl_2 afforded **135**. The structures of **133** and **135** were established by X-ray crystallography, confirming the *exo* (convex) and *endo* (convave) coordination of the $[Ru(C_5Me_5)]^+$ fragment to the inner arene ring.[131]

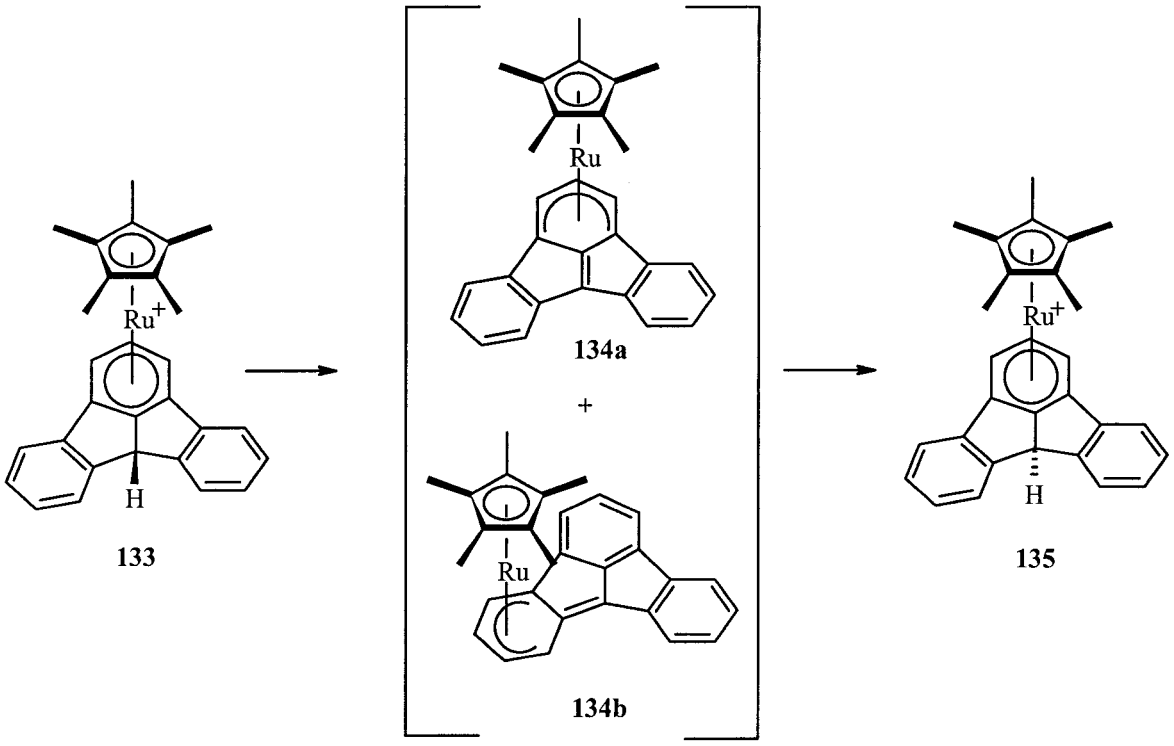

Scheme 3.12: Deprotonation studies of *exo*-$[Ru(C_5Me_5)(\eta^6\text{-fluoradene})][CF_3SO_3]$, **133**.

The infrared spectrum of the starting material, [(η^6-dibenzosuberane)-$Mn(CO)_3$][BF_4], exhibits carbonyl stretches at 2065 and 2014 cm^{-1}, typical of [(arene)$Mn(CO)_3$]$^+$ complexes.[120] Upon deprotonation by potassium *tert*-butoxide, the carbonyl stretches are significantly lowered. This had also been reported for the fluorenyl-manganese tricarbonyl compound, [(η^6-$C_{13}H_{10}$)$Mn(CO)_3$][PF_6] that, when treated with potassium *tert*-butoxide or other bases (such as sodium methoxide or triethylamine), gave rise to ($C_{13}H_9$)$Mn(CO)_3$.[127] The infrared spectrum of the deprotonated product revealed carbonyl stretches that were lowered by ~30 cm^{-1}.

The structure of compound **125** was determined by X-ray crystallography; it crystallizes in the monoclinic space group *C2*. Crystallographic data and refinement parameters are collected in the Appendix. The manganese tripod is coordinated in an η^5-fashion to one of the outer six-membered rings, such that the manganese is located 1.718 Å below the ring (Figure 3.6). The Mn-C(CO) bond lengths range from 1.798 (6) to 1.805 (5) Å, and are typical of Mn-CO distances. The Mn-C-O angles are slightly less than 180 °.

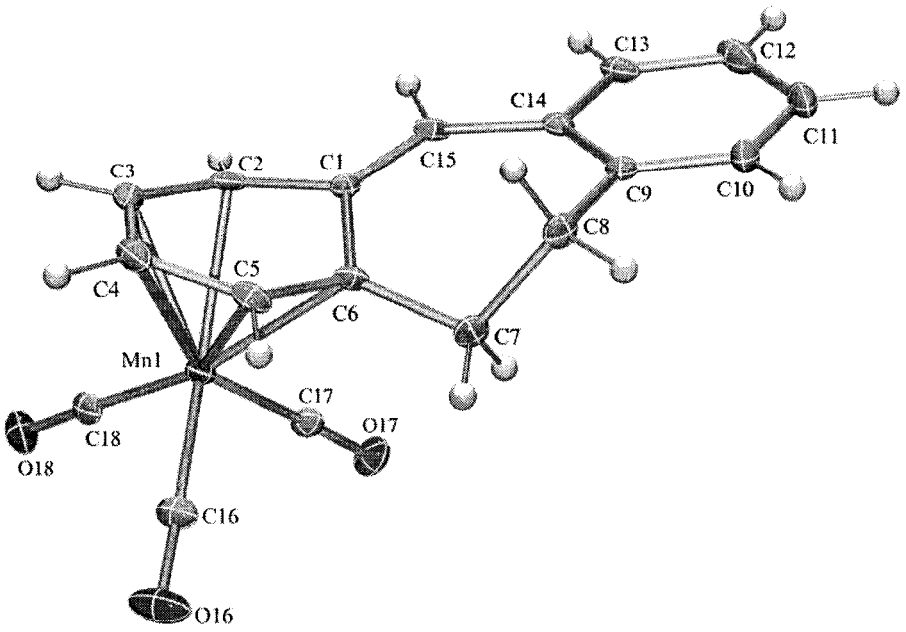

Figure 3.6: The X-ray structure of $(\eta^5\text{-}C_{15}H_{13})Mn(CO)_3$, **125**, showing the atomic numbering scheme. Thermal ellipsoids are shown at the 30 % probability level.

Compound **125** can be compared to the dienyl complex, **136**, generated from the nucleophilic addition of $LiCH_2C(O)CCH_3$ to [(β-estradiol 3,17-dimethyl ether)$Mn(CO)_3$][BF_4],[8] and also to the dimanganese complex **137**. The manganese-dienyl carbon bond distances in **125** range from 2.126 (5) to 2.287 (5) Å, characteristic for cyclohexadienyl manganese complexes (average for compound **136** was 2.193 (4) Å). The C(1)-C(15) bond length of 1.358 (6) Å is significantly shorter than C(1)-C(6) (1.468 (6) Å), indicative of a double bond. As well, this double bond is similar to one found for **137** (1.344 (11) Å).[132] The mean carbon-carbon distances of the cyclohexadienyl ring averaged 1.407 Å. Distortion from planarity of the cyclohexadienyl ring is typical of organometallic complexes. For instance, the dihedral angle in $(\eta^5\text{-}C_6H_7)Mn(CO)_3$ is

43°;[133] the corresponding angles are 41 ° for [{η^5-$(C_2H_5O_2C)_2CHC_6H_6$}$Mn(CO)_3$], 47.5 ° for *endo*-(η^5-C_6Me_6H)$Mn(CO)_2P(OMe)_3$,[134] 47.4 ° for *endo*-($\eta^5C_6Me_6H$)Mn(CO)-{$P(OMe)_3$}$_2$,[134] 40.2 ° for **136**,[8] 30.1 ° for **137**,[132] 36.0 (2) ° for **138**[135] and 33.4 (3) ° for **139**.[136] The related dihedral angle for compound **125** is 30.71 (0.47) ° (*i.e.* the intersection of planes: C(2)-C(3)-C(4)-C(5)-C(6) and C(2)-C(1)-C(6). The cyclohexadienyl unit exhibits a deviation from planarity of 0.002 Å.

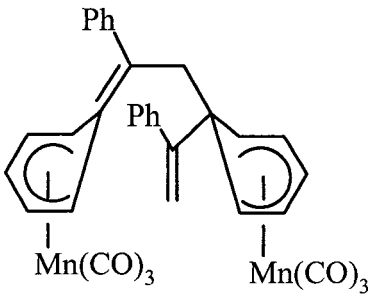

137

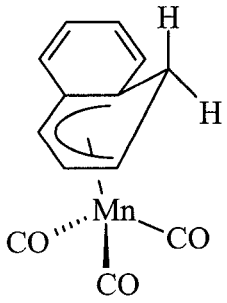

138

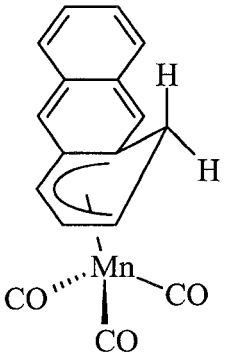

139

It is also instructive to examine the crystal packing of the molecules in the unit cell, which is shown below (Figure 3.7). The molecules of **125** are arranged in a head to head fashion, in which the carbonyl tripods and the arene rings respectively, are stacked on top of each other.

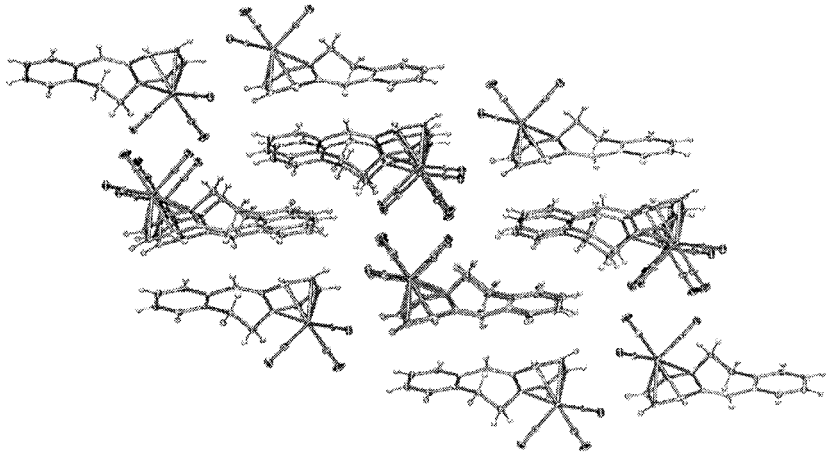

Figure 3.7: The crystal packing of molecules **125**.

The reaction of **102** with $P(OMe)_3$ in THF in the absence of light revealed that no reaction had occurred, since only starting materials were recovered. This is not surprising, since the replacement of carbonyl groups in arene manganese complexes usually requires photolysis or treatment with Me_3NO, as stated above.[34,47,125] Substitution of a carbonyl group by a trimethylphosphite ligand was not of interest, therefore, the reaction was not further pursued with Me_3NO or an exposure to light.

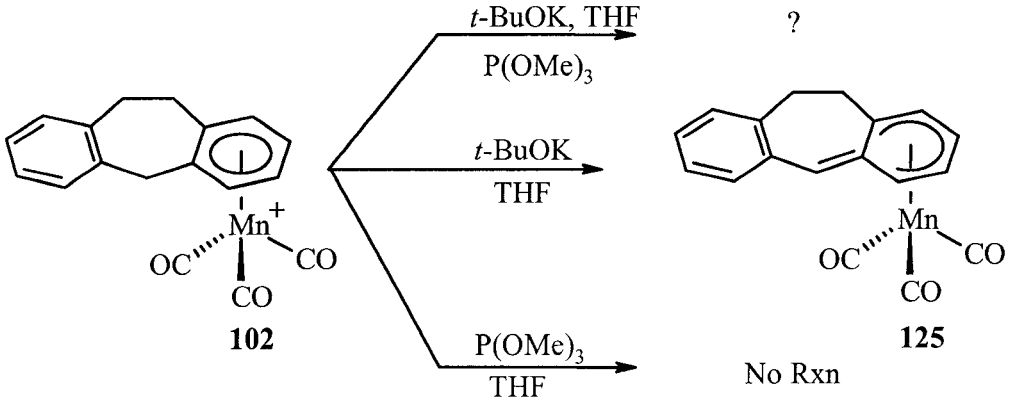

Scheme 3.13: Reactions with dibenzosuberane tricarbonyl manganese, **102**.

Haptotropic shifts of a π-bonded metal atom from a six-membered to a five-membered ring are known for several systems, including indenyl, fluorenyl and other polycyclic aromatic complexes. One such example involves the (cyclopenta[*def*]phenanthrenyl)ML_n complexes, **140** and **141**, where deprotonation at the benzylic position allows a haptotropic migration to occur readily.[108c]

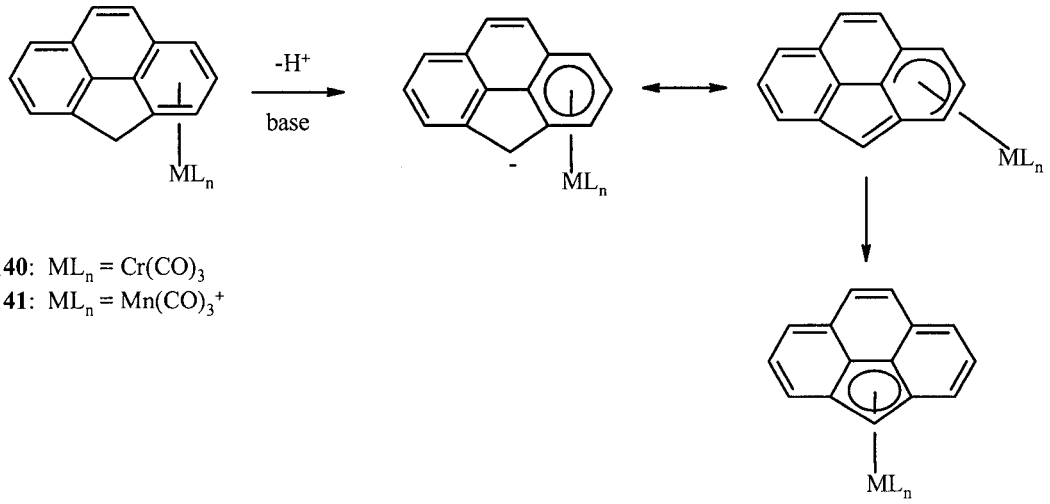

140: $ML_n = Cr(CO)_3$
141: $ML_n = Mn(CO)_3^+$

142: $ML_n = Cr(CO)_3^-$
143: $ML_n = Mn(CO)_3$

Scheme 3.14: Haptotropic shifts in the (cyclopenta[*def*]phenanthrenyl)ML_n systems.

3.2.3 Generality of the System

One must now ask the following crucial question: *Why does the dehydrogenation/haptotropic migration process occur in the trindane (or indane) $Mn(CO)_3$ cationic complexes but not for the tetralin or dibenzosuberane systems?* The hapticity changes exemplified by the dibenzosuberane system are not unusual and parallel the fluorenyl[127,128] and cyclopenta[*def*]phenanthrenyl[108c] systems. As well, the reactivity of (tetralin)$Mn(CO)_3^+$ with potassium *tert*-butoxide is comparable to other

tetralin systems that exhibited either deprotonation of the benzylic position[126] or nucleophilic additions.[114] What remains to be determined is under what conditions of the migration of the manganese tripodal fragment from the six- to five-membered ring in the trindane or indane systems are brought about. Scheme 3.15 depicts the systems that are of focus in this section.

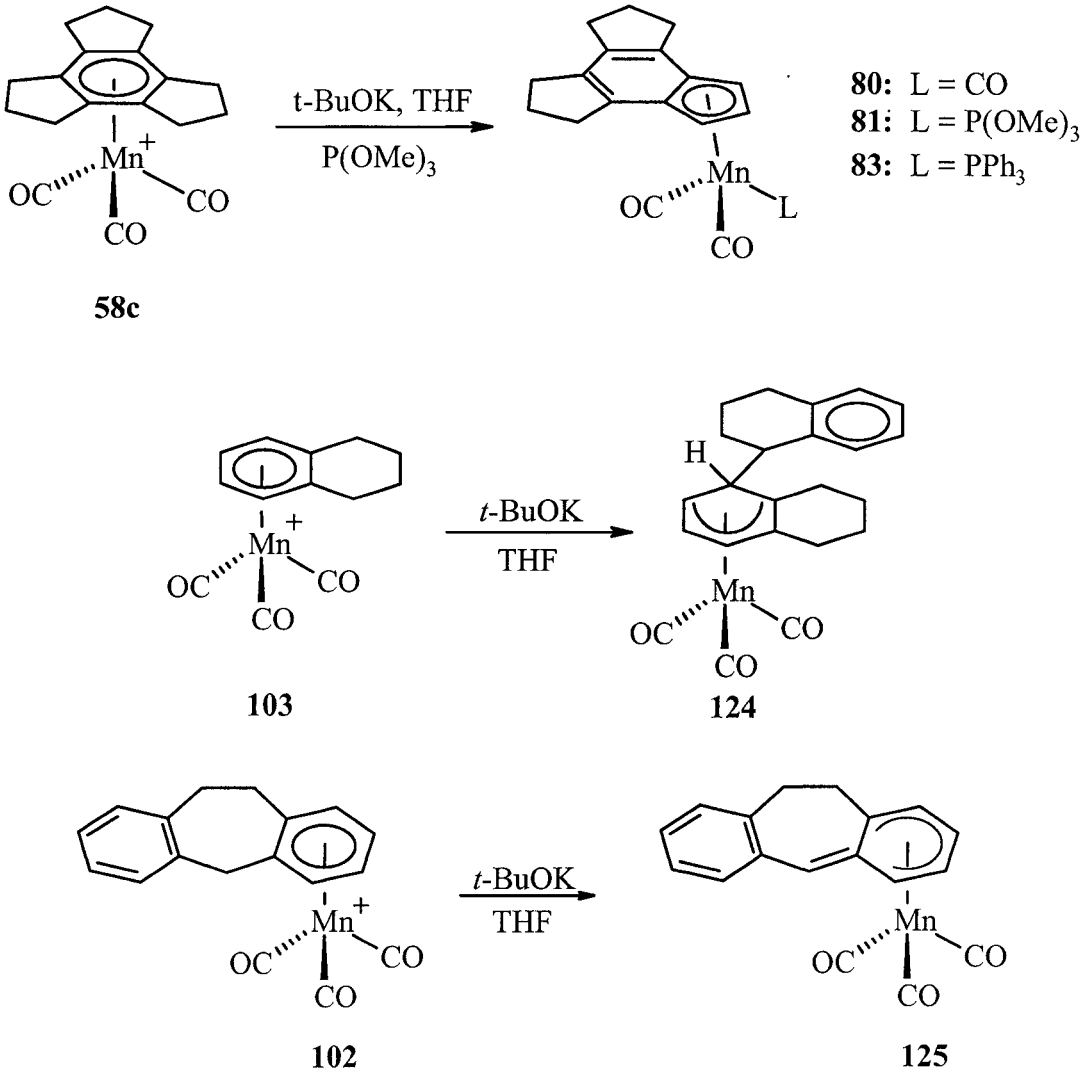

Scheme 3.15: An overview of the reactivity of the three systems, **58c**, **102** and **103**, with potassium *tert*-butoxide.

Firstly, the factors that have already been established for haptotropic shifts, either inter-ring haptotropic rearrangements or ring slippage, will be outlined (refer to Chapter 1 section 1.6 for a description of these processes). Haptotropic shifts are usually a result of either electronic or steric effects and sometimes a combination of both. For instance, the addition of a ligand to a system may result in the occupation of antibonding orbitals, which is unfavorable. Therefore, the driving force for the molecule to undergo a haptotropic shift is to relieve the antibonding character of the ortibals, common in the case of ring slippage (as in the indenyl systems).[137] The ability of organometallic units to migrate across the surface of polycyclic systems may be elucidated in terms of the interactions between the frontier orbitals of the ML_n moiety and of the π-organic system.[108c,137] Theoretical studies performed by Albright, Hoffman and co-workers have demonstrated that haptotropic rearrangements of the metal moiety over an organic surface between six- and five-membered rings does not take place *via* the least-motion pathway, but rather by the non-least-motion pathway.[137] Along the same lines, the $Mn(CO)_3^+$ and $Cr(CO)_3$ complexes of cyclopenta[*def*]phenanthrene revealed rather facile haptotropic η^6 to η^5 rearrangements, as depicted in Scheme 3.14. The migration has been suggested to proceed *via* a naphthalene-type transition state (**144**), the 10π aromatic character of **144** would be expected to lower the activation barrier for this process.[59,108c,138] This process parallels that of the indenyl effect where the key factors are the ability of the metal to undergo ring slippage into an η^3-transition state, and the development of aromatic character in the six-membered ring during this process.

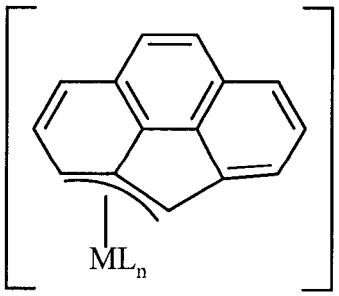

144

Furthermore when the double bond in cyclopenta[*def*]phenanthrene is selectively hydrogenated, the migration of the organometallic unit from **130** to **132** through **131** is rather slow (Scheme 3.11) and is attributed to the loss of the 10π system.[108c] As previously mentioned, the intermediates in this migration process are isolated and clearly identified by spectroscopic methods. EHMO calculations performed on the cyclopenta[*def*]phenanthrenyl)$Mn(CO)_3$ system revealed a rate determining step of ~18 kcal mol^{-1} to intermediate **144**.[108c] Also, the final product, **143**, was calculated to be ~16 kcal mol^{-1} which is more favorable than the η^6 compound, **141** (Scheme 3.14).[108c]

When considering the indane and trindane systems, a discussion of the structure of the trindane compounds can provide insight into the mechanism haptotropic rearrangements. Table 3.1 lists the bond distances of the *exo*- and *endo*-benzylic hydrogen atoms to the manganese atom. These values are of particular interest, since it is thought that the dehydrogenation/haptotropic shift process is initiated by an agostic interaction (as in molecule **145**) leading to formation of a dihydride (or a dihydrogen complex), and ultimately giving rise to the rearranged products, **80**, **81**, and **83**, as shown in Scheme 3.16.

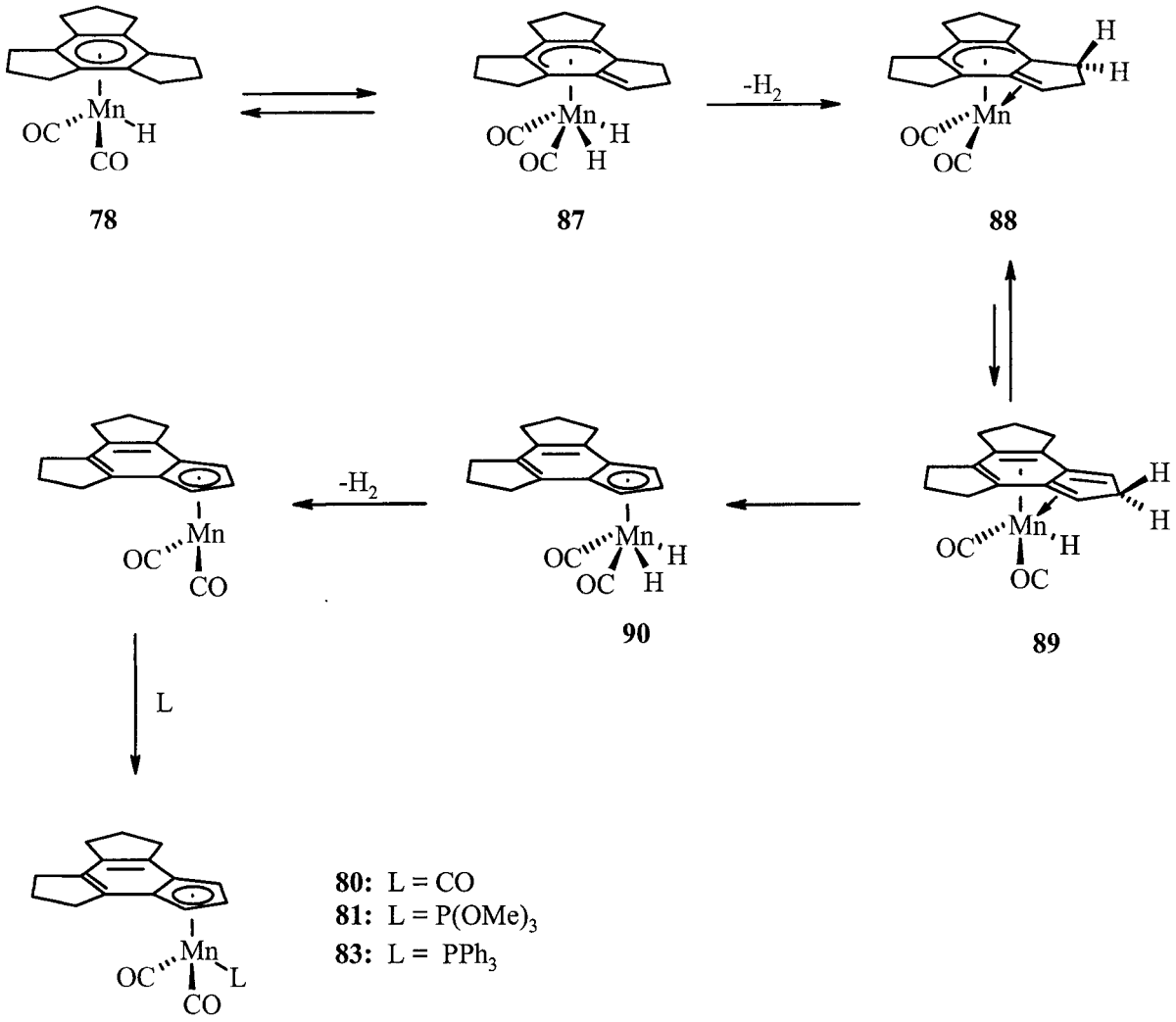

Scheme 3.16: Proposed mechanism for the generation of the rearranged products, **80**, **81** and **83**.

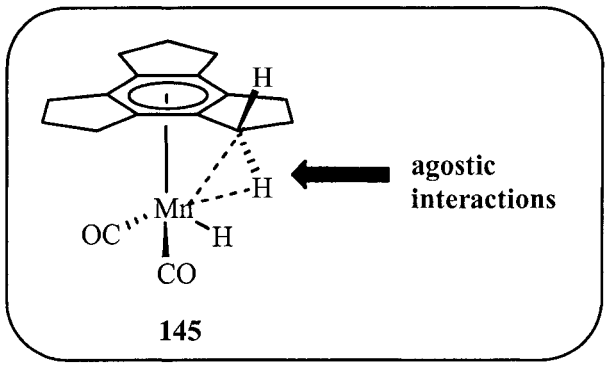

Agostic interactions have been invoked in other manganese complexes. For instance, the isomerizations of the η^5-naphthalenyl, $[(\eta^5\text{-}C_{10}H_9)Mn(CO)_3]$, **138**, and η^5-anthracenyl, $[(\eta^5\text{-}C_{14}H_{11})Mn(CO)_3]$, **139**, complexes have been proposed to occur through agostic and σ donation interactions while maintaining an 18-electron configuration.[135,136] The energy of activation for the metal-mediated 1,4-hydride migration was determined by simulations of the dynamic ^1H NMR spectra, that is, from the magnetization transfer experiments of compounds **138** and **139,** to be ~ 26.4 and ~ 14.6 kcal mol^{-1}, respectively. Crystallographic studies of **138** and **139** allowed the determination of crucial structural parameters, such as the $Mn\cdots H_{endo}$ distances, by locating and refining the positions of the hydrogen atoms, which aided in the determination of the migration mechanism. The $Mn\cdots H_{endo}$ distances in the naphthalenyl and anthracenyl complexes, **138** and **139**, are 3.23 (1) Å and 3.13 (1) Å, respectively.[135] Veauthier and co-workers proposed a mechanism for the 1,4-hydride shift; a migration step in which increased interaction of the hydride with the metal center is synchronous with de-ligation of the carbon atoms carrying the aromatic substituent as depicted in Scheme 3.17.[136] The key aspect of this fluxional process shown in Scheme 3.17, is that it has been suggested to occur through a least-motion pathway by the movement of a hydrogen atom around the system.

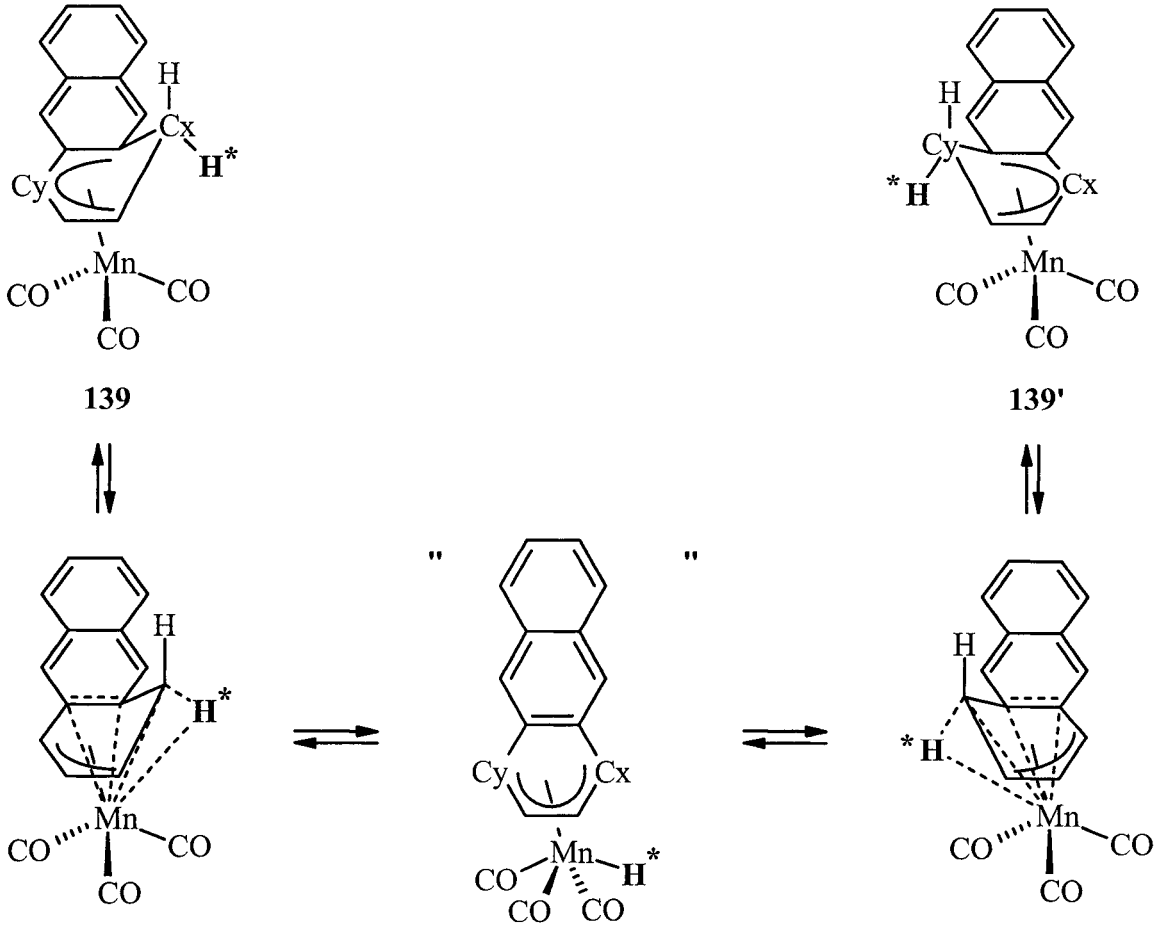

Scheme 3.17: The low-energy metal-mediated 1,4-hydride migration in the (anthracenyl)$Mn(CO)_3$ complex.

The separation between the manganese atom and the *endo* hydrogen atoms for compounds **71**, **73**, **124** and **125** were determined and are listed in Table 3.1. The Mn···H_{endo} distances for **71** and **73** are slightly longer (~ 0.3 and 0.4 Å) than those of **138** and **139** (cf. 3.23 and 3.13 Å). As presented in Chapter 2 (section 2.2.2.3), Ustynyuk and co-workers[109] have performed DFT calculations that support the mechanism proposed for the formation of compounds **80**, **81** and **83**. The calculations reveal that a metal hydride

may arise from a number of transformations, one that may involve an apparent agostic bond between the chromium and C-H.[109] A characteristic agostic interaction involves the elongation of the C-H bond and a decrease in the Cr-C distance between the chromium and one of the C-H bonds from the five-membered ring, in the case of the (σ-methyl)(η^5-indenyl)tricarbonylchromium compound. For an agostic interaction to occur in (trindane)$Mn(CO)_2H$, **78**, the separation between the manganese and *endo* hydrogen should not exceed the sum of the covalent radii of the two atoms, that is 1.72 Å.

It was thought that the distance between the hydrogen atoms of the Mn-H and the C-H_{endo} were vital and would provide mechanistic insight into the migration that occurs in the trindane system. However, since the (trindane)$Mn(CO)_2H$ was not isolable, an analogy was drawn with the corresponding (HMB)$Mn(CO)_2H$, where HMB = hexamethylbenzene. In order to determine the H···H distance between the Mn-H and C-H_{endo} hydrogen atoms in the trindane system, the value of the Mn-H distance was taken from the (HMB)$Mn(CO)_2H$ crystal structure. Extrapolating the (HMB)$Mn(CO)_2H$ data onto the crystal structures of (trindane)$Mn(CO)_2Br$, **71**, and (trindane)$Mn(CO)_2I$, **73**, allowed us to estimate the $H_{hydride}$···H_{endo} distance. The mean $H_{hydride}$···H_{endo} distances for **71** and **73** were found to be 2.673 and 2.692 Å, respectively. The following distances were taken from the crystallographic data of (HMB)$Mn(CO)_2H$: Mn-H = 1.367 Å, Mn-C(arene centroid) = 2.571 Å and C(centroid)-H = 1.664 Å. The $H_{hydride}$···H_{endo} distance in (HMB)$Mn(CO)_2H$ was found to be 2.657 Å, similar to that of the trindane systems.

The observation of the migration of the manganese moiety from the six-membered ring to the five-membered ring may be attributed to the possibility that the η^5

complex is thermodynamically more stable. In terms of electronic effects, the manganese atom becomes a neutral species and the bond distances of the manganese atom to the ligated ring are slightly shorter (refer to Table 3.2). Moreover, and this may well be a crucial factor, the entropy increase associated with the formation of two moles of hydrogen will undoubtedly lead to a favorable change in the free energy. The cleavage and formation of carbon-hydrogen and metal-hydrogen bonds, along with the associated bond energies are fundamental for the understanding and reasoning of organometallic reaction mechanisms. The bond energies are as follows: BE(H-H) = 436 kJ mol^{-1}, BE(C-H) = 413 kJ mol^{-1}, BE(Mn-H)[139] = 2881 kJ mol^{-1} (calculated value) and BE (Mn-CO)[140] = 159 kJ mol^{-1}. Thus, cleavage of three C-H bonds and one Mn-H bond has an energy cost of approximately 1527 kJ mol^{-1} of which only 1031 kJ mol^{-1} are recovered as one Mn-CO and two H-H bonds. Since the reaction occurs readily, one must assume that the overall free energy change is controlled by stronger bonding of the manganese to the five-membered ring, and of course, by the favorable increase in entropy.

Another factor that can affect the ease of deprotonation of a particular *exo*-benzylic site is the molecular conformation. The ideal case would be when the *exo*-benzylic hydrogen adopts an axial orientation, since it is known that the base attacks on the *exo* side of the molecule. Volk *et al.* has suggested that both the conformation of the benzylic hydrogen atoms and the conformation of the metal tripod ($Cr(CO)_3$) influences the site of deprotonation (Scheme 3.18).[126] The role of the $Cr(CO)_3$ moiety is apparent when there are two competing benzylic positions, and deprotonation occurs preferentially where the adjacent aryl center bears the greater positive partial charge.[126] This argument

is analogous to the regioselectivity of kinetically controlled nucleophilic additions to (arene)$Cr(CO)_3$ complexes, whereby the $Cr(CO)_3$ tripod is influential. The assumption that is implied with these charge-controlled reactions is that the positive charge induced on the arene carbon atoms by the eclipsing carbonyl ligand of the $Cr(CO)_3$ tripod are preferentially attacked by a nucleophile.[126] The findings presented by Volk *et al.* are consistent with the benzylic proton that is abstracted, in that it is eclipsed by a carbonyl ligand in the crystalline state. However, caution must be ascertained since one can never unequivocally conclude a preferred conformation in solution from a crystal structure.[126]

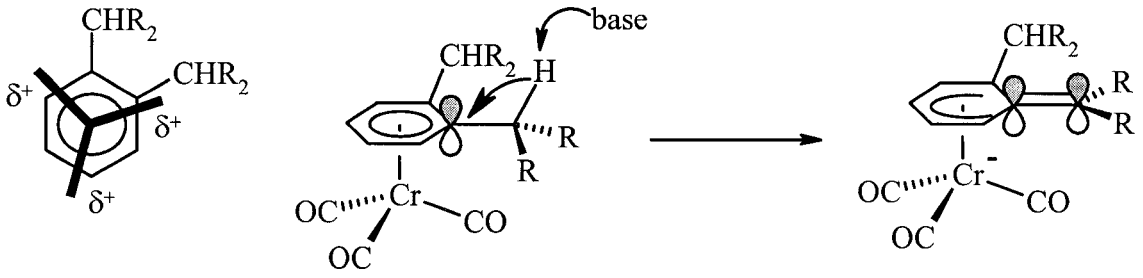

Scheme 3.18: Rationalization of the stereoelectronic effects that establish which benzylic hydrogen atom is abstracted in a $Cr(CO)_3$ system.

In the case of the dibenzosuberane system, **102**, migration of the manganese unit to the seven-membered ring might not be feasible in terms of stereoelectronic features. Examining the crystal structure of **102**, there are two possible benzylic positions that could be abstracted, C(7) and C(15), and only C(7) has an *exo*-hydrogen in the ideal pseudoaxial position. According to Volk and co-workers, if there are two competing benzylic positions, as in **102**, then the favorable site of deprotonation would be C(15), since that carbon atom is eclipsed with the Mn-CO bond based on the solid state structure. However, the hydrogen that is actually abstracted is the one on C(7),

presumably the *exo*-hydrogen. As previously mentioned, the preferred conformation in the solid state does not necessary reflect its conformation in solution.

Overall, the coordination of the organic ligand following a haptotropic shift in a particular system, is generally a consequence of the electronic factors (disrupting the aromaticity, weakening of M-C bonds of the organic ligand) and the different van der Waals inter-ligand interactions as demonstrated for the $[(\eta^5\text{-}C_5H_5)M(CO)_3]$ systems, where M = $Mn(CO)_3$ and $Re(CO)_3$.[59]

Table 3.1: Metal-hydrogen distances of compounds **71**, **73**, **124** and **125**.

Compound	**Mn-H distance**		**Length of Mn-H (Å)**	
	endo	***exo***	***endo***	***exo***
$(\eta^6\text{-}C_{15}H_{18})Mn(CO)_2Br$, **71**	Mn1-H7b	Mn1-H7a	3.583	4.199
	Mn1-H9a	Mn1-H9b	3.512	4.168
	Mn1-H10a	Mn1-H10b	3.530	4.183
	Mn1-H12b	Mn1-H12a	3.528	4.182
	Mn1-H13a	Mn1-H13b	3.482	4.111
	Mn1-H15b	Mn1-H15a	3.480	4.094
	average		**3.519**	**4.156**
$(\eta^6\text{-}C_{15}H_{18})Mn(CO)_2I$, **73**	Mn1-H7a	Mn1-H7b	3.544	4.177
	Mn1-H9b	Mn1-H9a	3.574	4.196
	Mn1-H10a	Mn1-H10b	3.531	4.170
	Mn1-H12b	Mn1-H12a	3.522	4.159
	Mn1-H13a	Mn1-H13b	3.498	4.121
	Mn1-H15b	Mn1-H15a	3.493	4.120
	average		**3.527**	**4.157**
$[(\eta^6\text{-}C_{10}H_{12})Mn(CO)_2\{P(OMe)_3\}][PF_6]$, **124**	Mn1-H8b	Mn1-H8a	3.426	3.947
$[(\eta^6\text{-}C_{15}H_{14})Mn(CO)_3\}][BF_6]$, **125**	Mn1-H7b	Mn1-H7a	3.707	4.213
	Mn1-H15b	Mn1-H15a	3.440	4.119
	Average		**3.574**	**4.166**

Table 3.2: Selected bond lengths for compounds **71**, **73**, **80**, **81**, **102**, **125**, **138** and **139**.

	71	**73**	**80**	**81**	**102**	**125**	**138**[135]	**139**[136]
Mn-C	1.784 (8)	1.792	1.77 (2)	1.760 (3)	1.807(3)	1.798 (6)	1.785 (3)	1.790 (5)
	1.802 (10)	1.792	1.78 (2)	1.768 (2)	1.819(3)	1.801 (5)	1.807 (3)	1.779 (6)
			1.83 (2)		1.824 (3)	1.805 (5)	1.808 (3)	1.728 (6)
mean	**1.793**	**1.792**	**1.79**	**1.764**	**1.817**	**1.801**	**1.800**	**1.766**
C-O	1.119 (9)	1.154	1.18 (2)	1.162 (3)	1.136 (4)	1.141 (6)	1.149 (4)	1.133 (6)
	1.143 (8)	1.146	1.15 (2)	1.161 (3)	1.137 (4)	1.158 (6)	1.146 (4)	1.145 (6)
			1.17 (2)		1.132 (4)	1.143 (6)	1.150 (4)	1.167 (6)
mean	**1.131**	**1.150**	**1.17**	**1.162**	**1.135**	**1.147**	**1.148**	**1.148**
Mn-C	2.133 (7)	2.205 (5)	2.15 (2)	2.147 (2)	2.252 (3)	2.262 (5)	2.183 (3)	2.155 (5)
	2.157 (7)	2.148 (5)	2.15 (2)	2.114 (2)	2.185(3)	2.157 (5)	2.129 (3)	2.095 (5)
	2.203 (6)	2.154 (5)	2.19 (2)	2.125 (2)	2.179 (3)	2.126 (5)	2.121 (3)	2.095 (5)
	2.210 (6)	2.198 (4)	2.24 (2)	2.214 (2)	2.178 (3)	2.153 (5)	2.260 (3)	2.296 (5)
	2.223 (7)	2.205 (4)	2.25 (2)	2.235 (2)	2.169 (3)	2.287 (5)	2.395 (3)	2.485 (5)
	2.220 (7)	2.230(4)			2.232 (3)			
mean	**2.191**	**2.190**	**2.17**	**2.167**	**2.199**	**2.197**	**2.218**	**2.225**
Mn-X/L	2.477 (2)	2.6756 (8)		2.1673 (6)				
C=C			1.41 (3)	1.362 (3)				1.371
			1.44 (3)	1.366 (3)				1.381

3.3 Conclusions

Polycyclic systems and their coordination to organometallic fragments are of interest with respect to understanding the role that each substrate plays when they are united. Deprotonation of polycyclic organometallic complexes has been shown to initiate migration of the metal unit across the carbon framework, resulting in an inter-ring haptotropic rearrangement.

In the course of determining the generality of the haptotropic rearrangements that occur with the trindane and indane manganese tricarbonyl systems, but not with other polycyclic manganese tricarbonyl complexes, the following compounds, **117**, **124** and **125** were generated. Crystallographic data were obtained for compounds **124** and **125**, which were derived from the polycyclic arene manganese tricarbonyl compounds, **103** and **102**, respectively. As well, the structure of **102** was established by X-ray crystallographic studies.

While a mechanism has been proposed in an attempt to rationalize the formation of indenyl-type complexes, **80**, **81** and **83**, from the trindane manganese tricarbonyl compound, **58c**, this system seems to be unique in comparison to the other polycyclic systems probed in this chapter. As stated above, there are several factors that determine whether a compound will undergo a haptotropic shift. The effect of potassium *tert*-butoxide on other polycyclic manganese systems is still of considerable interest, and further developments in this area are still needed to help establish a greater understanding of the trindane system.

CHAPTER FOUR

Dynamics of Hexaethylbenzene Manganese Complexes

4.1 Introduction

Hexaethylbenzene (HEB) and other persubstituted benzenes are prevalent in the literature by reason of their applications in supramolecular chemistry. Persubstituted benzenes have been shown to be excellent building blocks for numerous host molecules and supramolecular systems.[141] Along with their application to the aforementioned areas, functionalized benzene cores have also been of interest as ligands in organometallic complexes and as candidates for analyses of their dynamic behaviour.[142] The continuing interest in hexaethylbenzene systems have led us to focus our attention on the syntheses and dynamics on arene manganese complexes since, to the best of our knowledge, there have not been any investigations into the dynamics of these complexes. A brief synopsis of organometallic hexaethylbenzene complexes and their dynamics is presented.

The alkyl groups in hexaethylbenzene (HEB), **79**, occupy positions alternating above and below the benzene plane, giving rise to D_{3d} symmetry.[143,144] Other compounds in the class of hexaalkylbenzenes include those where the alkyl group is cyclopropyl,[145] trimethylsilylmethyl,[146] bromomethyl,[147] neopentyl[148] and benzyl.[149] Ligation of hexaethylbenzene to various metal fragments ML_n has been performed, where ML_n is $Cr(CO)_3$, **136**;[143c] $Cr(CO)_2(CS)$, **137**;[150] $Mo(CO)_3$, **138**;[143a] $Mo(CO)_3Cl^+$, **139**;[151] and $Fe(C_5H_5)^+$, **140**.[56a,152] The dynamic behaviour of symmetrically hexasubstituted benzenes and other 1,3,5-substituted-2,4,6-triethylbenzene compounds along with their

organometallic derivatives has been of interest for the past decade, as will be discussed below.

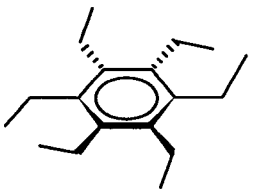

79

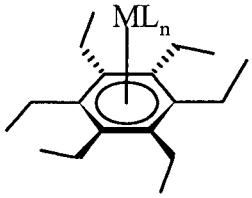

136: $ML_n = Cr(CO)_3$
138: $ML_n = Mo(CO)_3$
141: $ML_n = W(CO)_3$
137: $ML_n = Cr(CO)_2(CS)$
142: $ML_n = Cr(CO)_2(NO)^+$
143: $ML_n = Cr(CO)(CS)(NO)^+$
144: $ML_n = Cr(CO)_2(PPh_3)$
145: $ML_n = Cr(CO)_2(PEt_3)$

Temperature-dependent NMR studies provide a convenient method for determining the rotational barriers (i.e. the dynamic behaviour) of the ethyl substituents on the arene ring and/or the rotation of the tripod around the metal-arene bond in the organometallic systems. The rotation of either carbon-carbon or metal-carbon bonds of stereochemically non-rigid systems are often appealing in terms of determining the energy required for the rearrangement. Dynamic NMR techniques are a common method for determining the free energy of activation ($\Delta G^{\neq}$) at the coalescence point, when the two exchanging peaks combine so there is just one broad resonance. An estimate of the free energy of activation at the coalescence point, $\Delta G_c^{\neq}$, and temperature, T_c, may be obtained from Equation 4.1:

$$\Delta G^{\neq}/RT_c = 22.96 + ln\,(T_c/\Delta\nu) \qquad (4.1)$$

In equation 4.1, $\Delta\nu$ denotes the frequency difference (in Hz) for two equally populated sites and R is the ideal gas constant (1.987 cal K^{-1} mol^{-1}). The free energy of activation, $\Delta G^{\neq}$, is commonly expressed as kilocalories per mole (kcal mol^{-1}). The barrier to rotation

for the C_{aryl}-$C_{methylene}$ bond was determined for various persubstituted benzene derivatives ($\Delta G^{\neq}$ ~ 11-12 kcal mol^{-1}).[153]

Complexation of hexaethylbenzene to organometallic moieties has invoked controversy regarding the orientation of the ethyl groups.[154,155,158] With the aid of X-ray crystallographic studies, Hunter and co-workers established that the ethyl groups in HEB were found to alternate above and below the plane of the arene ring.[143a,c] Also, X-ray data reveals that the coordination of HEB to the organometallic tripods, $Cr(CO)_3$ and $Mo(CO)_3$, are oriented eclipsed with respect to the *distal* ethyl groups, hence minimizing any steric interactions with the *proximal* ethyl groups.[156] The overall symmetry of the complexed molecule, $(HEB)M(CO)_3$, is C_{3v} and thus the *proximal* and *distal* methyl, methylene, and arene carbons are rendered magnetically non-equivalent. A splitting of each of the three sets of arene carbons into two equally intense lines is seen in the low-temperature ^{13}C NMR spectrum.[156,158a]

Energy calculations performed by Mislow on the conformers of HEB showed that the 1,3,5-*distal*-2,4,6-*proximal* (**A**) isomer was favored. The highest energy conformer was that with all six ethyl groups facing up (**B**), in which the molecule possesses C_{6v} symmetry.[143a] Ligating the latter with an organometallic unit places all the ethyl groups *distal* with respect to the metal.

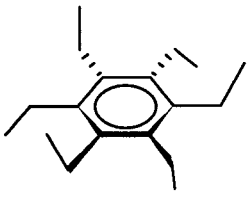

A

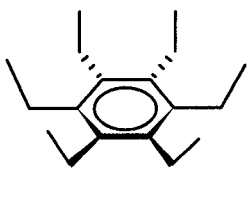

B

The barrier towards tripodal rotation has been determined either by altering the substituents on the arene ring or changing the fragments of the tripod. In the former case, incorporation of an acetyl group, **146**, breaks the threefold symmetry such that at low temperatures the tripodal rotation was slowed as evidenced in the ^{13}C NMR spectra by the splitting of the carbonyl environments into a 2:1 ratio.[157] NMR and X-ray crystallographic studies of **146** revealed the alternating proximal-distal pattern. The barrier to tripodal rotation for **146** was determined to be 9.5 ± 0.5 kcal mol^{-1}.[157] Conversely, the cationic species $[(HEB)Cr(CO)(CS)(NO)][BF_4]$, **143**, in which the symmetry of the molecule was lowered by altering the substitutents on the tripod was also probed by low-temperature NMR spectroscopy. The low-temperature ^{13}C NMR spectrum of **143** displayed six methyl, six methylene and six aromatic ring carbon environments.[158] The compound was characterized by X-ray crystallography and was shown to adopt the 1,3,5-*distal*-2,4,6-*proximal* conformation. The data for **143** revealed uncorrelated tripodal and ethyl rotations with barriers of ~ 9.5 and 11.5 kcal mol^{-1}, respectively.[158]

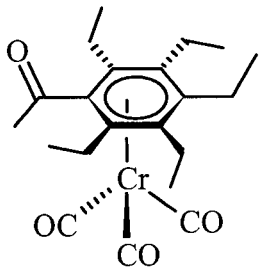

146

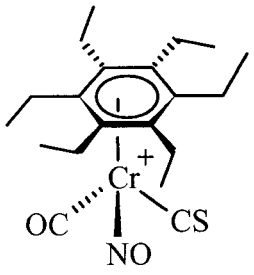

143

In this chapter, we will deal with the synthesis of the novel compounds: [(η^6-HEB)$Mn(CO)_3$][BF_4], **147**, (HEB = hexaethylbenzene) and (η^6-HEB)$Mn(CO)_2Br$, **148**. Since (η^6-C_6Me_6)$Mn(CO)_2H$ is known,[47b] it was thought that the analogous (HEB)$Mn(CO)_2H$ complex might be isolable from the reaction of (HEB)$Mn(CO)_3^+$ and *t*-BuOK (as discussed in Chapter 2, section 2.2.1.3), and that the Mn-H bond might be to some extent protected by the alternating *proximal* and *distal* ethyl substituents. An alternative route to (HEB)$Mn(CO)_2H$ was attempted by reaction of (HEB)$Mn(CO)_2Br$ with sodium borohydride, but was unsuccessful. In furtherance of our interest in arene manganese complexes, the dynamic stereochemistry and structural features of hexaethylbenzene manganese complexes were investigated.

The dynamics of (HEB)$Mn(CO)_3^+$ and of (HEB)$Mn(CO)_2Br$ were investigated by low-temperature NMR in order to probe the rotation of the ethyl groups since the *proximal* and *distal* ethyl environments are readily differentiable in the ^1H and ^{13}C regimes. Such data allow the barrier toward ethyl rotation to be calculated. A comparison will be made with the analogous (HEB)$Cr(CO)_3$ compound investigated by our group,[158] and by Mislow and Hunter[143a,c] several years ago.

4.2 Results and Discussion

[(HEB)$Mn(CO)_3$][BF_4], **147**, was prepared utilizing the synthetic methodology disclosed by Pauson and co-workers[23] which involves heating $BrMn(CO)_5$ and $AgBF_4$ for 3 h in CH_2Cl_2; subsequently, upon addition of hexaethylbenzene in CH_2Cl_2, heating was continued for 18 h. The pale yellow crystalline solid was isolated in an astonishingly high 79 % yield; previous attempts to isolate the compound in our laboratory harvested

only minute quantities.[159] The compound was characterized by common spectroscopic methods including infrared, NMR and MS. Mass spectrometric data revealed the typical pattern for arene metal carbonyl complexes, that is, the loss of one, two and three carbonyl groups evident from the *m/z* signals at 357, 329 and 301, respectively. The infrared spectrum displays two carbonyl stretching frequencies at 2058 and 1996 cm^{-1}.

(HEB)$Mn(CO)_2Br$, **148**, a deep red-purple solid, was prepared by treatment of (HEB)$Mn(CO)_3^+$ with trimethylamine N-oxide (Me_3NO) in the presence of tetrabutylammonium bromide. This synthetic methodology is a favorable approach for the synthesis of (arene)$Mn(CO)_2X$ complexes, where X is a halogen atom (Cl, Br or I) (for a more detailed discussion refer to Chapter 2, section 2.2.1).[47b,96] The compound is extremely air-sensitive in solution and decomposes over several hours, even when stored under nitrogen. The formation of compound **148** was monitored by infrared spectroscopy; the spectrum displayed two carbonyl absorptions at 1974 and 1927 cm^{-1}. The chemical ionization spectrum revealed the $[M+1]^+$ peak minus the bromine atom at an *m/z* value of 358, followed by the loss of one and two carbonyl groups at *m/z* 357 and 329, respectively. Furthermore, the loss of the manganese atom followed, giving rise to a peak at *m/z* 246, corresponding to the hexaethylbenzene ligand.

Having successfully prepared the desired hexaethylbenzene complexes, [(HEB)$Mn(CO)_3$][BF_4] and (HEB)$Mn(CO)_2Br$, the molecular dynamics of these compounds were probed by utilizing low-temperature NMR spectroscopy.

The 500 MHz ^1H NMR spectrum of [(η^6-HEB)$Mn(CO)_3$][BF_4], **147**, in CD_2Cl_2 displayed singlets at 2.68 and 1.41 ppm for the methylene and methyl resonances,

respectively (Figure 4.1). At 173 K (the minimum lowest temperature possible before the solvent freezes), both the methyl and methylene signals are broadened, however, a splitting is observed only for the methylene protons at 2.56 and 2.45 ppm (Figure 4.1). The 125 MHz ^{13}C NMR spectrum of **147** in CD_2Cl_2 displayed four signals at room temperature, corresponding to the methyl, methylene, arene and carbonyl carbons. Broadening of the methyl, methylene and arene carbons is seen below 281 K and decoalescence is complete at 203 K, when each of the three signals has split into two. The low temperature ^{13}C NMR spectra of **147** in CD_2Cl_2 revealed the presence of the two ethyl environments, confirming the three-fold symmetry of the complex. The ^{13}C NMR spectrum of **147** displayed singlets for the methyl (17.1 ppm), methylene (22.6 ppm) and arene (120.3 ppm) carbons at 298 K. Lowering the temperature to 203 K revealed the expected splitting of the methyl (13.6 and 20.0 ppm), the methylene (19.7 and 23.2 ppm) and the aromatic (113.6 and 124.0 ppm) carbons into two equally intense resonances as depicted in Figure 4.2. This is indicative of slowed interconversion of the two ethyl group environments, and yielded a barrier of ~11.5 kcal mol^{-1}, which falls in the normal range for such ethyl rotations. The analogous chromium, (HEB)$Cr(CO)_3$; molybdenum, (HEB)$Mo(CO)_3$; and tungsten, (HEB)$W(CO)_3$ complexes behave similarly, whereby the variable-temperature ^{13}C NMR studies revealed the alternating *proximal-distal* arrangement of the ethyl groups.[143a,143c,154] Therefore, complex **147** possesses idealized C_{3v} symmetry whereby the hexaethylbenzene ligand adopts the 1,3,5-*distal*-2,4,6-*proximal* conformation. By analogy to related NMR spectroscopic data, the [(η^6-

HEB)Mn(CO)$_3$][BF$_4$] complex exhibits the geometrical *proximal-distal* pattern, and hence an X-ray investigation was not warranted.

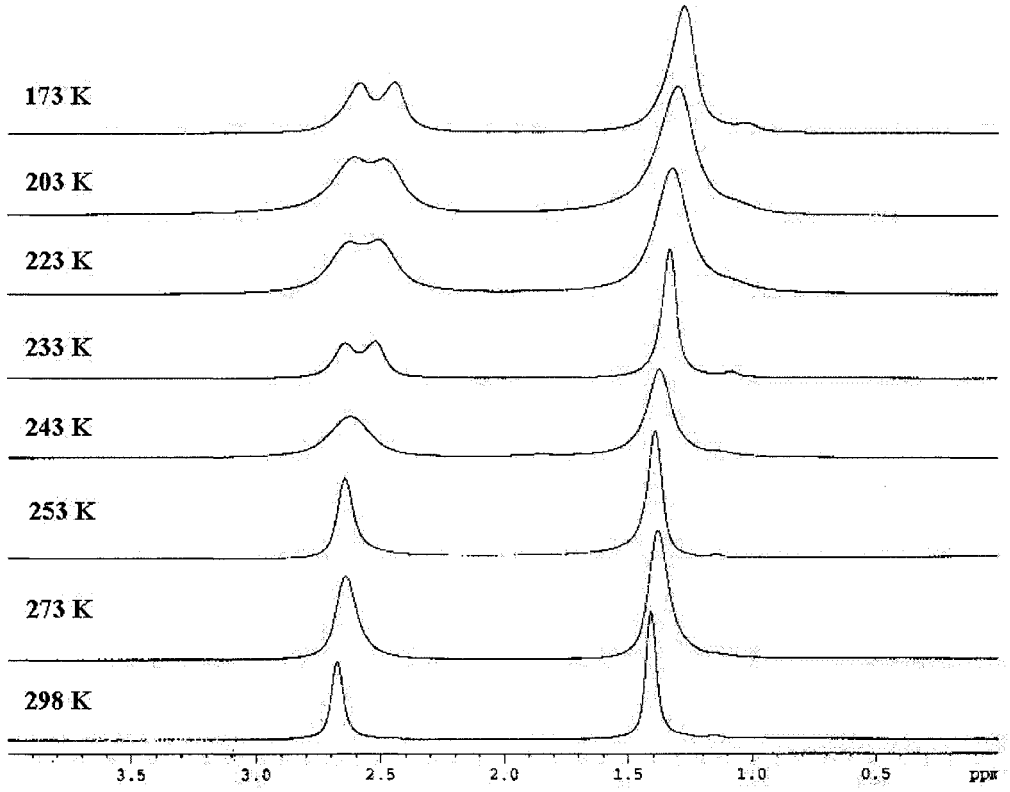

Figure 4.1: Variable-temperature 500 MHz ^{1}H NMR spectra of [(η^6-HEB)Mn(CO)$_3$][BF$_4$], **147**, in CD_2Cl_2 illustrating the two equally populated ethyl environments.

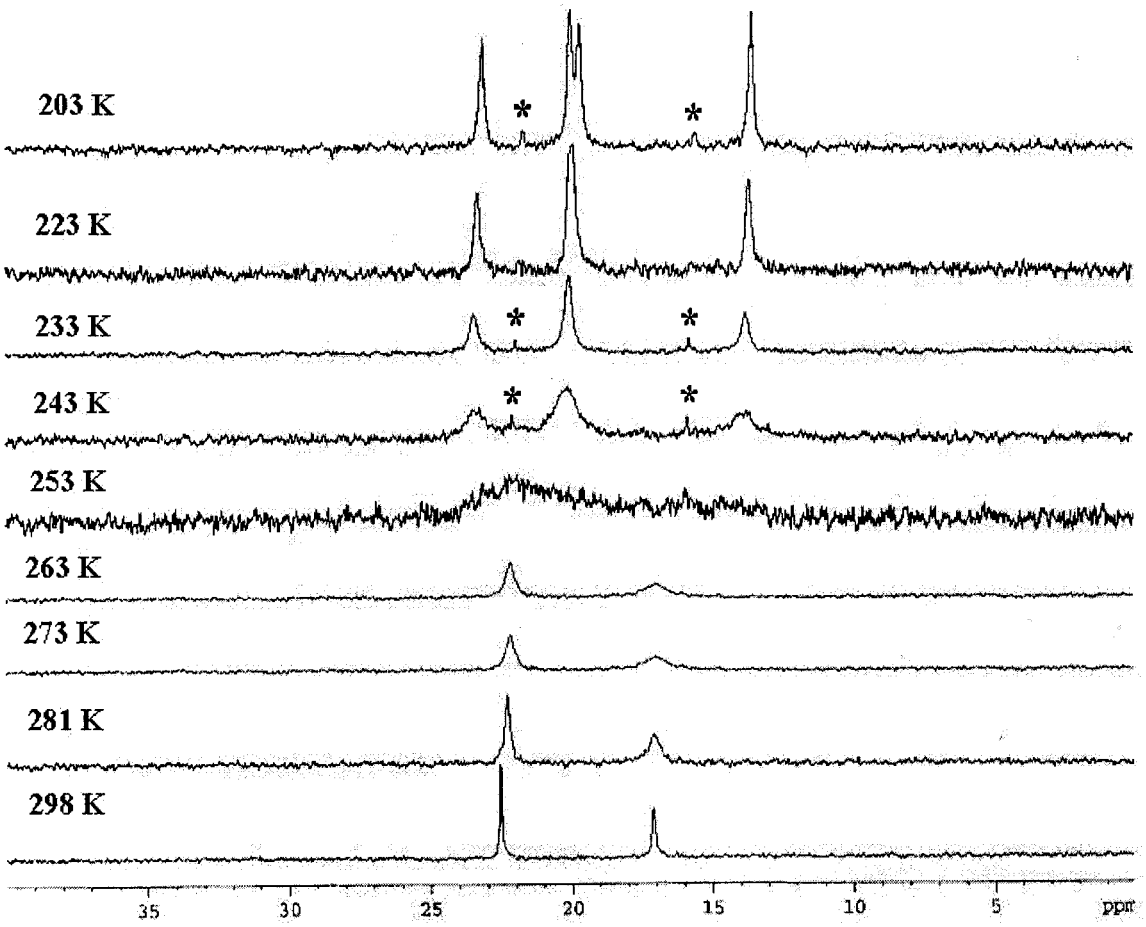

Figure 4.2: Variable-temperature 125 MHz ^{13}C NMR spectra of [(η^6-HEB)Mn(CO)$_3$][BF$_4$], **147**, in CD_2Cl_2 illustrating the splitting of the methyl and methylene carbons. The small peaks marked with an asterisk are hexaethylbenzene resonances.

Upon replacing one of the carbonyl groups with a bromine atom, one would anticipate similar behaviour to that previously exhibited by the (HEB)Cr(CO)$_2$CS, **137**, complex, which adopts the 1,3,5-*distal*-2,4,6-*proximal* conformation.[158] That is, at low temperatures the ^{13}C NMR spectrum would be expected to display a 2:1:2:1 pattern for each of the ring carbon, methylene and methyl environments, as seen for **137**. However, this was not the case for **148**, suggesting that the ethyl groups are perhaps not in the

1,3,5-*distal*-2,4,6-*proximal* arrangement. The 500 MHz ^{13}C NMR revealed no broadening of peaks. However, lowering the temperature gave rise to signals in the methyl and methylene region. There was no definite change in the spectra from 281 K to 223 K, thus the aforementioned signals in the 10 - 25 ppm region may be attributed to the decomposition of **148** to the hexaethylbenzene ligand.

We chose to carry out a crystallographic characterization to determine the orientations of the ethyl groups, at least in the solid state. However, attempts at growing crystals suitable for single X-ray studies were seriously hampered as a result of the tendency of the compound to decompose in solution. After several efforts, a crystal was grown under N_2 from an acetone/pentane solution, and the data were collected at 173 K. To our surprise, and inconsistent with NMR investigations, the X-ray crystallographic studies revealed that the manganese tripodal fragment was coordinated in an η^6-fashion to the hexaethylbenzene ligand that exhibited the favoured 1,3,5-*distal*-2,4,6-*proximal* arrangement.

These data suggest that (HEB)$Mn(CO)_2Br$ behaves differently in solution and in the solid state. Since all previously known 1,3,5-*distal*-2,4,6-*proximal* (HEB)ML_n systems exhibit restricted rotation of the ethyl groups at low temperature,[158a] one must assume that the major conformer in solution is not the same as was found in the solid state. Other examples of HEB complexes exhibiting variable conformational behaviour include (HEB)$Fe(C_5H_5)^+$ which has been crystallographically characterized as both the 1,2,3,5-*distal*-4,6-*proximal* isomer (with a PF_6^- counter-ion)[56a] and as the penta-*distal* structure (with a BPh_4^- counter-ion)[152b] In the particular case of (HEB)$Fe(C_5H_5)^+$, the

existence of several coexisting rotamers is detectable through the observation of multiple cyclopentadienyl resonances in the low-temperature ^{13}C NMR spectrum.[154]

The X-ray crystal structure of **148** is depicted in Figure 4.3. Crystallographic collection and refinement parameters, and bond lengths and angles are presented in the Appendix. Compound **148** crystallized in the monoclinic space group $P2_1/n$. The manganese centre of the crystallographically characterized compound exhibited pseudo-octahedral geometry whereby the hexaethylbenzene ligand adopts the alternating geometrical 1,3,5-*distal*-2,4,6-*proximal* pattern of the ethyl groups, and the carbonyl and bromine ligands eclipse the *distal* ethyl substituents. The manganese atom is located 1.682 Å below the six-membered ring centroid, and is comparable to other manganese systems such as (HMB)$Mn(CO)_2Cl$[47b,96] and (trindane)$Mn(CO)_2Br$.[95] There is disorder between one of the carbonyl groups and a bromine atom in the crystal structure, where the occupancies of each atom are split. The Mn-C(CO) bond lengths are 1.878 (6), 1.456 (37) and 1.618 (9) Å, which are typical of Mn-CO distances. The Mn-Br distance is 2.506 (2) and 2.584 (3) Å, analogous to that found in the (η^6-trindane)$Mn(CO)_2Br$ compound (2.477 (2) Å). Overall, the geometric features found in the crystal structure of **148** parallel those of other previously reported (hexaethylbenzene)ML_n complexes, where ML_n = $Cr(CO)_3$, $Cr(CO)_2(CS)$, $Cr(CO)_2(NO)^+$ and $Mo(CO)_3$. The average C_{arene}-$C_{methylene}$-C_{methyl} bond angles were determined to be 115.5 ° and 111.7 ° for the *proximal* and *distal* ethyl groups, respectively. As mentioned above, the organometallic tripod is oriented such that the carbonyl ligands lie beneath the *distal* ethyls groups, hence minimizing any steric interactions with the *proximal* ethyl groups. The arene ring is

planar and the Mn atom is symmetrically bonded to the arene. The crystal packing diagram for **148** reveals that the arene rings stack above each other and packs in a fashion as to minimize the contacts between the distal ethyl groups as depicted in Figure 4.4.

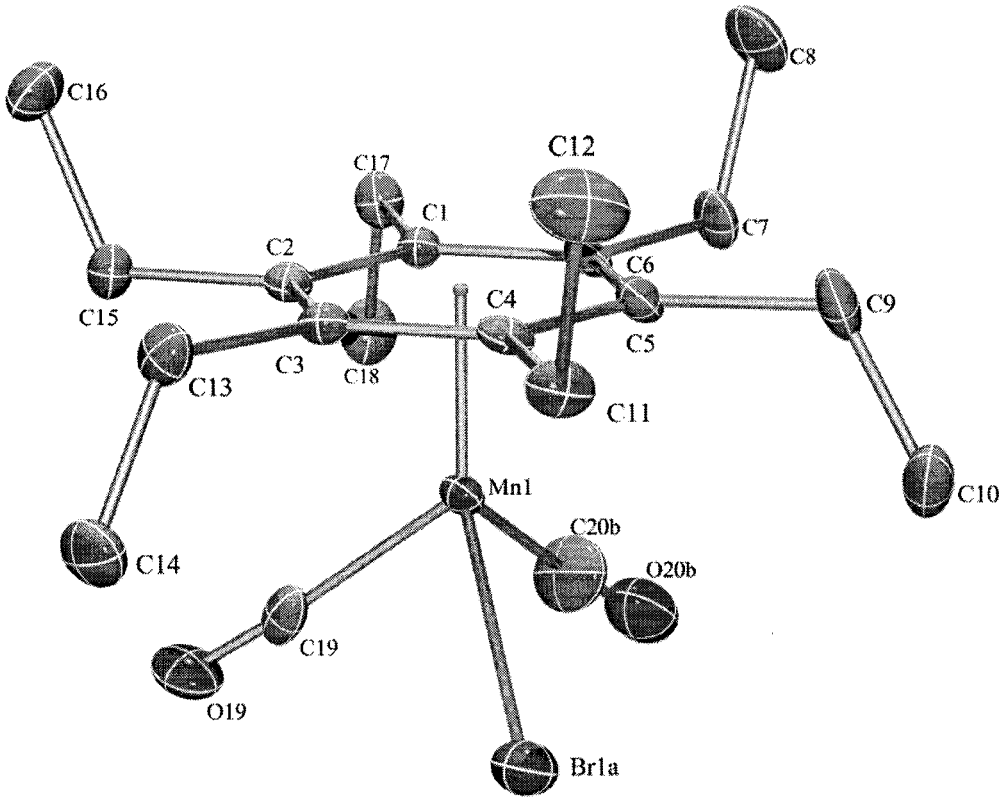

Figure 4.3: The X-ray structure of (HEB)Mn(CO)$_2$Br, **148**, illustrating the alternating geometrical *proximal* and *distal* arrangement of the ethyl groups. Thermal ellipsoids are shown at the 30 % probability level (Hydrogen atoms are omitted for clarity).

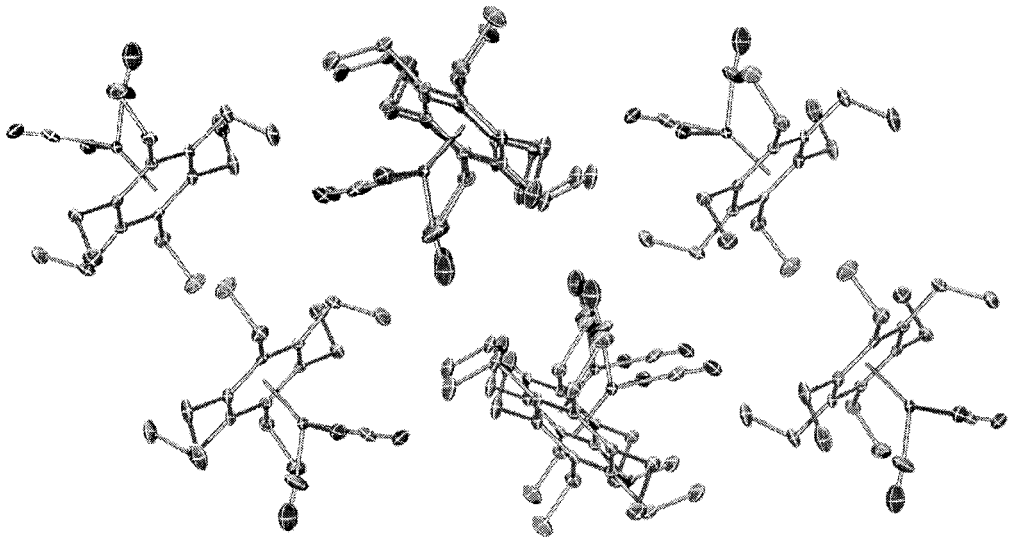

Figure 4.4: Crystal packing diagram for **148**. Hydrogen atoms are omitted for clarity.

4.3 Conclusions

The dynamic behaviour of the hexaethylbenzene manganese complexes presented herein extends this class of hexasubstituted organometallic complexes already examined. The barrier ($\Delta G^{\neq}$) for ethyl rotation for **147** was determined to be ~ 11.5 kcal mol^{-1}, which is in agreement with values previously reported for similar hexaethylbenzene systems. As well, crystallographic data were obtained for **148**, which exhibited analogous geometrical features common to 1,3,5-*distal*-2,4,6-*proximal* transition metal complexes. The synthesis of hexaethylbenzene manganese complexes, **147** and **148**, could potentially play a role in the flourishing field of supramolecular chemistry, as well as, in the design of other stereochemically non-rigid architectures. Opening the avenue of applying dynamics to organometallic manganese complexes leaves the function that manganese imparts still remains to be explored. The significance that the benzene

platform has taken in the field of supramolecular chemistry and other areas, along with the ease of preparation of persubstituted benzene manganese complexes, establishes manganese as a potentially ideal candidate for continued examination.

CHAPTER FIVE

Migrations of Organometallic Units Across Polycyclic Surfaces

5.1 Introduction

Dynamic molecular processes in organometallic complexes have gained renewed interest with their application in catalysis and in studying the reactivity of organometallic compounds. In particular, two processes are of interest: sigmatropic and haptotropic rearrangements of either σ-bonded elements or π-bonded metal moieties. Respectively, both are prompted by the rich variety of polycyclic platforms available today. Although the capacities of these transformations are influenced by the topological properties of the interacting orbitals, the same organic substrate does not necessarily support both sigmatropic and haptotropic migrations with equal facility.

Albright, Hoffmann *et al.*[160] presented the first theoretical approach describing the major regularities of inter-ring haptotropic shifts. This field has been most recently reviewed by Oprunenko.[161] Disregarding competing intermolecular dissociative pathways, it has been shown that as ML_n fragments traverse the faces of π systems, direct migration across the common bond between fused rings is typically a symmetry disallowed process (cf. sigmatropic shifts) and a circuitous minimum energy route is followed.[160] However, persistent uncertainties in the nature of transition states and intermediates make it difficult to distill kinetic and thermodynamic effects. Three bicyclic examples (naphthalene, indene and pentalene) demonstrate these claims and provide the necessary design for polycyclic models.

The migrations of a metal fragment over the two six-membered rings in appropriately substituted naphthalenes (as well as acenaphthenes or biphenylenes) have been the subject of a number of experimental studies.[162] For the unlabeled (η^6-$C_{10}H_8$)$Cr(CO)_3$ **149**, the potential energy landscape (at the EHMO level of approximation) features both a transition state and η^3-allylic-type local minimum (**150b**) lying 27 and 21 kcal mol^{-1}, respectively, above the ground state (Scheme 5.1).[160] This contrasts with the DFT-predicted lowest energy η^6-to-η^6 degenerate rearrangement, which proceeds via a C_s-symmetric trimethylenemethane-type first order saddle point (ΔE = 30.4 kcal mol^{-1}) only.[163]

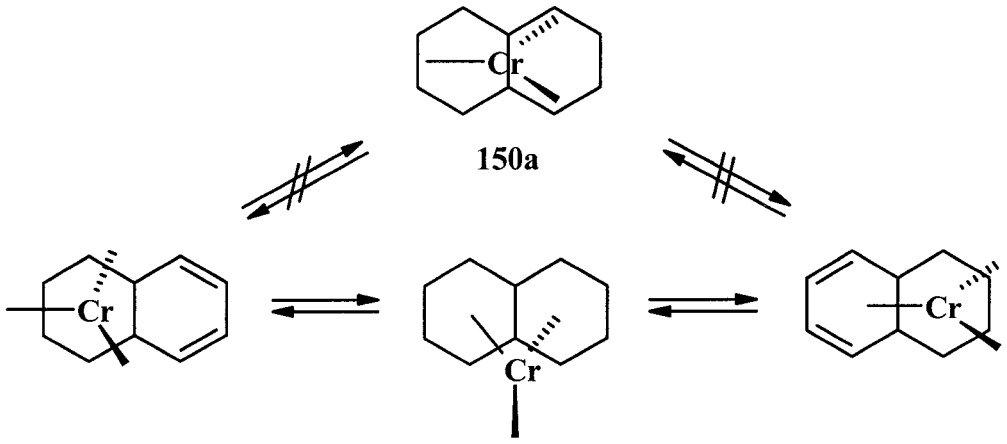

Scheme 5.1: η^6-to-η^6 migratory pathway of a $Cr(CO)_3$ unit in naphthalene.

There also exists a considerable amount of experimental data concerning η^6-to-η^5 interconversions in indenyl-ML_n complexes[164] and fluorenyl analogues.[165] In the asymmetric ligand, the pH-dependent rearrangement between the pentahapto (favoured) and hexahapto isomers involves a non-least motion path and coordinatively unsaturated η^3-allylic-type minimum, as demonstrated for the (indenyl)$Fe(C_5H_5)$ system **151 - 153**

(Scheme 5.2a).[160] Benzannulation of the indenyl scaffold destroys the 5-6 ring internal plane of symmetry and the non-degenerate η^6-to-η^5 exchange proceeds through one of two peripherally bound η^3 minima (pathways A or B, see Scheme 5.2b).[160] Reversibility and isomer distribution aside, deprotonation of an [(η^6-fluorene)ML_n] species, **126** or **127**, where ML_n = $Mn(CO)_3^+$ or $Fe(C_5H_5)^+$, has yielded isolable zwitterionic intermediates, **128a**, which are perhaps better described as having an η^5-bonded metal, and an exocyclic double bond, **128b**, before undergoing migration to **129**.[165]

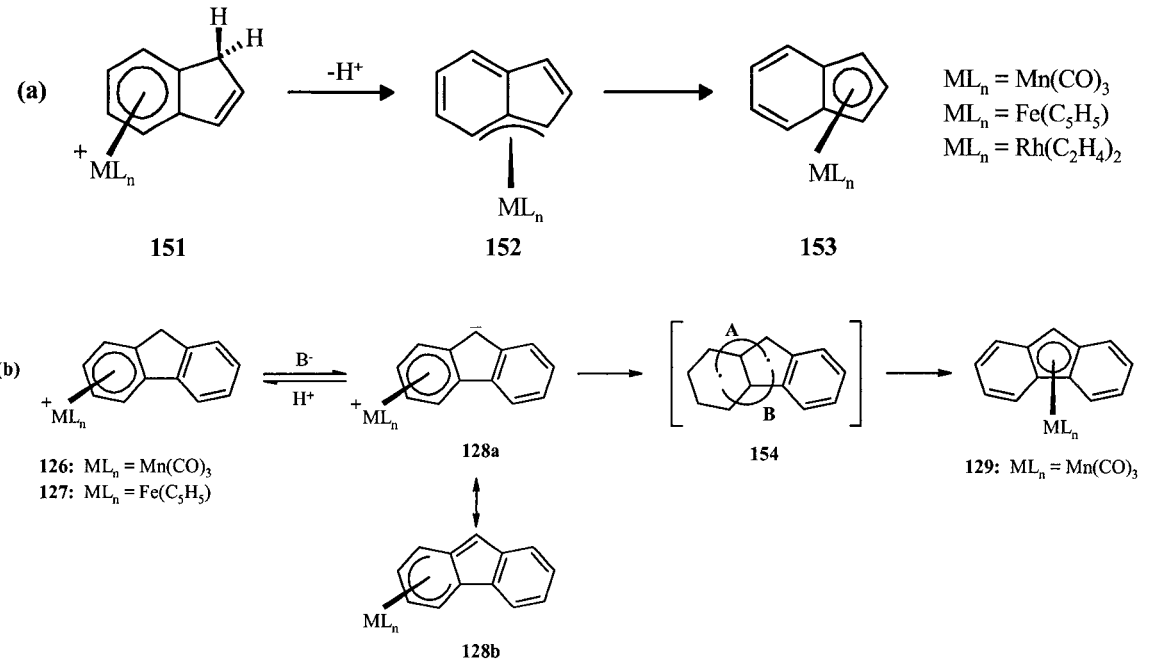

Schemes 5.2: η^6-to-η^5 haptotropic shift in the (a) indenyl and (b) fluorenyl systems, (**151 - 153**) and (**126 - 129**), respectively.

A π-manifold for η^5-to-η^5 haptotropic rearrangements is provided by the third bicyclic example, pentalene. Theoretical (EHMO level) considerations of the (pentalene)$Fe(C_5H_5)$ system in both its cationic and anionic forms (**155** and **156**, respectively) identified two distinct bonding topologies.[160] In the former case, one of the

primary frontier metal-ligand orbital overlaps is maintained during a least-motion transit; the calculated trajectory takes the FeCp moiety only 0.6 Å away from the midpoint of the central carbon-carbon bond (Scheme 5.3a). The addition of two electrons, as in **156**, results in the loss of both iron-pentalene bonding interactions and renders the least-motion pathway highly unfavourable. Instead, the migration route is extended to the carbocyclic periphery via an η^3-intermediate **157**, as depicted in Scheme 5.3b. To generalize, Albright, Hoffmann *et al.* advanced an electron-counting rule such that when the total number of electrons supplied by the polycyclic ligand and the metal equals $4q$ + 2, where q = 2, 3, …, then haptotropic shifts passing directly under the common bond are forbidden. On the other hand, when this sum equals $4q$, the process is "partially allowed".[160] That is when the ML_n unit moves across the internal carbon-carbon bond, some of the valence orbital interactions are maintained between the metal fragment and the bicyclic polyene.

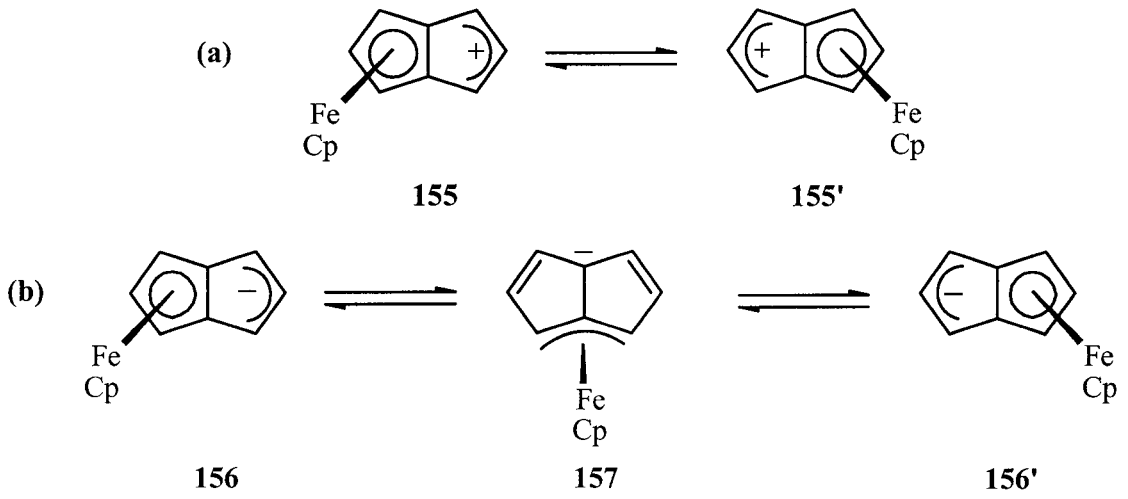

Schemes 5.3: η^5-to-η^5 haptotropic rearrangement of FeCp in the (a) cationic and (b) anionic forms of pentalene.

5.1.1 An Aromaticity Argument

Although attempts to intercept an η^3-structure analogous to **152** have not yet succeeded,[166] there is indirect support for such an intermediate / transition state in fused polycyclic systems. Deprotonation of (η^6-cyclopenta[*def*]phenanthrene)$Mn(CO)_3^+$, **141**, yields the corresponding (η^5-cyclopenta[*def*]phenanthrenyl)$Mn(CO)_3$, **142**, even at -40 °C.[108c] In contrast, deprotonation of the analogous (η^6-8,9-dihydrocyclopenta[*def*]phenanthrene)$Mn(CO)_3^+$, **130**, furnishes **131**, in which the manganese maintains its attachment to the external six-membered ring (comparable to the fluorenyl complexes, **128**). Complex **131** does not undergo a haptotropic shift to generate the centrally-bonded (η^5-cyclopenta[*def*]phenanthrenyl)$Mn(CO)_3$, **132**, even when left at room temperature for 72 h; the rearrangement occurs only when the molecule is heated in hexane at 60 °C for an hour. This result was interpreted in terms of maintaining the 10π-naphthalene-type aromatic character in **144** (as shown in Scheme 5.4a) that is not available to the dihydro analogue.[108c]

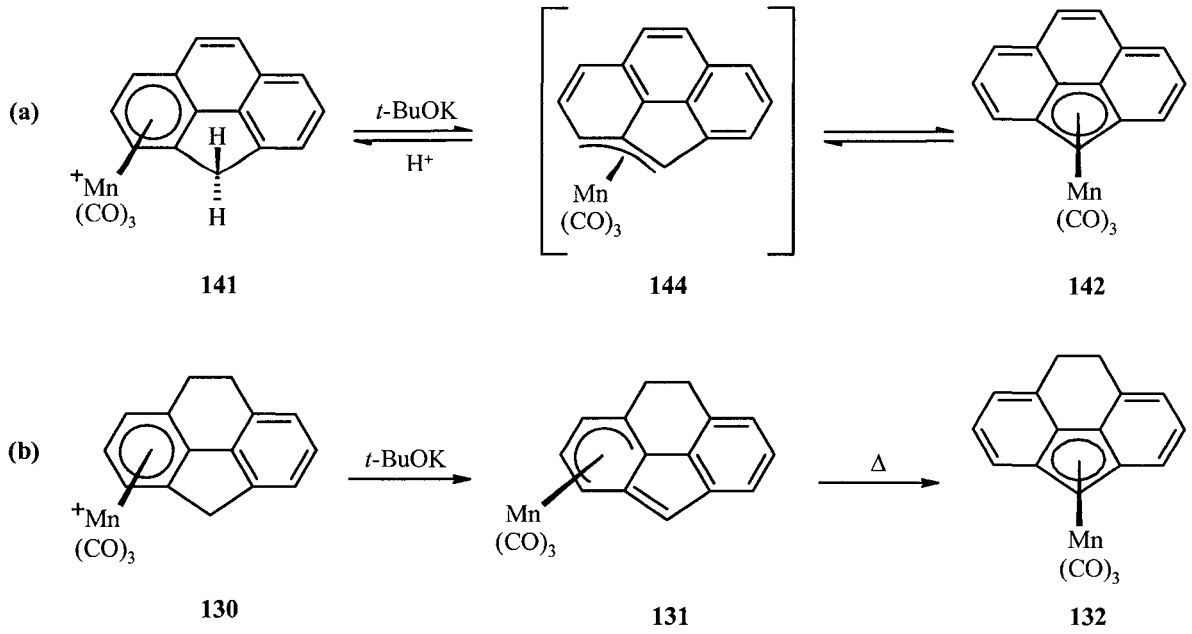

Scheme 5.4: The facility of haptotropic shifts in (a) (cyclopenta[*def*]phenanthrenyl)ML_n complexes **141** - **142** is diminished in (b) its dihydro analogue, **130** - **132**.

In this chaper, we will examine other multicyclic systems containing the pentalene, indene and/or naphthalene substructures that present potentially competitive pathways for η^5-to-η^5, η^6-to-η^5/η^5-to-η^6 and η^6-to-η^6 inter-ring haptotropic rearrangements. Theoretical studies of these processes, even at the extended Hückel level, may help to clarify general regularities associated with the nature and magnitude of the activation energies that need to be overcome. Organometallic derivatives of the four fused polycyclic ligands, **157** - **160** exhibit very different dynamic behaviour and thus have been selected as challenging candidates for a qualitative mechanistic survey using potential energy surfaces (PES). The material in this chapter has been submitted for publication in the American Chemical Journal *Organometallics*.[167]

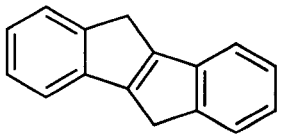

157

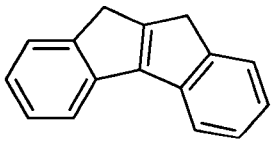

158

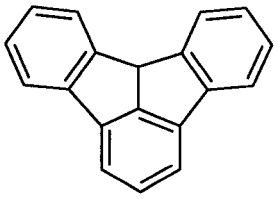

159

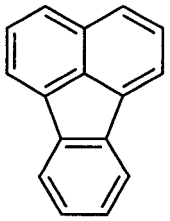

160

5.2 Results and Discussion

5.2.1 *Anti-* and *syn*-dibenzpentalene complexes

Despite previous attempts at synthesizing benzannulated versions of pentalene,[168] the first and only experimental evidence for an η^5-to-η^5 haptotropic rearrangement was provided by Ustynuk's laboratory in 1990.[169] The chromium and manganese tricarbonyl complexes of the isomeric ligands, 5,10-dihydroindeno[2,1-*a*]indene and 9,10-dihydroindeno[1,2-*a*]indene, **157** and **158**, which are more trivially named as derivatives of *anti-* and *syn*-dibenzpentalene, respectively, were prepared and their dynamic properties analyzed. The anionic complex $[(\eta^6\text{-}anti\text{-dibenzpentalenyl})Cr(CO)_3]^{1-}$, **161**, rearranges readily and irreversibly into its η^5 isomer, **162a**, whereas the di-anionic complex $[(\eta^5\text{-}anti\text{-dibenzpentalenyl})Cr(CO)_3]^{2-}$, **163a**, does not interconvert with its pentahapto derivative **164a** (Scheme 5.5). Likewise, the corresponding mono-anionic manganese tricarbonyl complex, $[(\eta^5\text{-}anti\text{-dibenzpentalenyl})Mn(CO)_3]^{1-}$, **163b**, fails to undergo η^5-to-η^5 interconversion. This is in complete contrast to the fluxional behavior of the isomeric species, $[(\eta^5\text{-}syn\text{-dibenzpentalenyl})Mn(CO)_3]^{1-}$, **165a**, which exhibits rapid η^5-to-η^5 interconversion with **166a**, even at -40 °C (Scheme 5.6); NMR lineshape analyses yielded an activation energy barrier of approximately 15 kcal mol^{-1}.

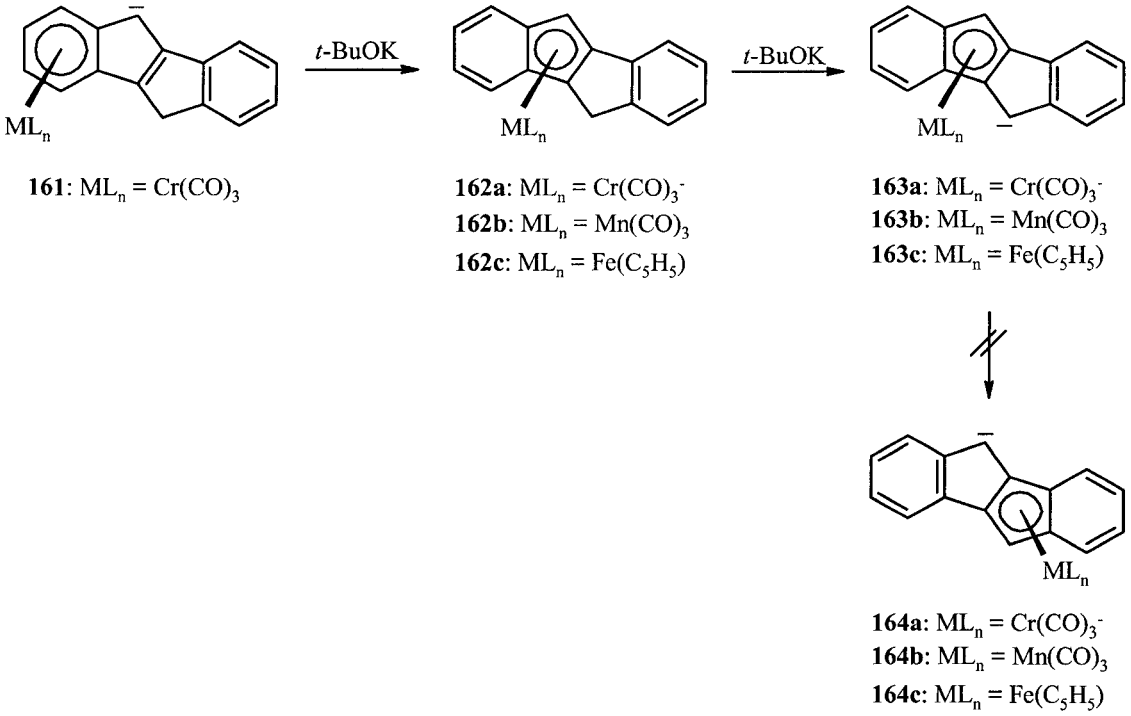

161: $ML_n = Cr(CO)_3$

162a: $ML_n = Cr(CO)_3^-$
162b: $ML_n = Mn(CO)_3$
162c: $ML_n = Fe(C_5H_5)$

163a: $ML_n = Cr(CO)_3^-$
163b: $ML_n = Mn(CO)_3$
163c: $ML_n = Fe(C_5H_5)$

164a: $ML_n = Cr(CO)_3^-$
164b: $ML_n = Mn(CO)_3$
164c: $ML_n = Fe(C_5H_5)$

Schemes 5.5: η^6-to-η^5 rearrangements in organometallic complexes (**161** - **164c**) of 5,10-dihydroindeno[2,1-a]indene, **157**.

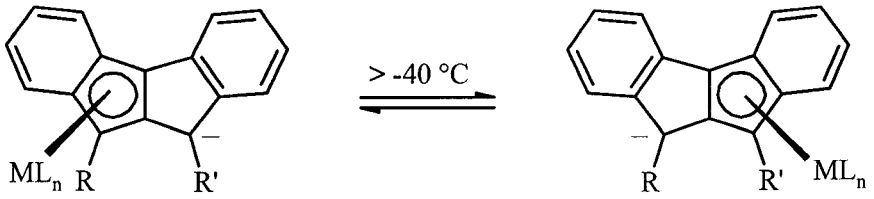

165a: $ML_n = Mn(CO)_3$
R = Me, R' = H;
R = Me, R' = Ph

165b: $ML_n = Fe(C_5H_5)$
R = R' = H

166a: $ML_n = Mn(CO)_3$
R = Me, R' = H;
R = Me, R' = Ph

166b: $ML_n = Fe(C_5H_5)$
R = R' = H

Scheme 5.6: η^5-to-η^5 interconversion within metal π complexes (**165a** - **166b**) of 9,10-dihydroindeno[2,1-a]indene, **158**.

The very different dynamic behaviour of the complexes derived from *anti*- and *syn*-dibenzpentalenes, **157** and **158**, has been tentatively rationalized in terms of the

symmetries of the pentalene frontier orbitals,[169] but no simple picture emerged. In **157**, the ligand has a two-fold axis, whereas in **158** there is a mirror plane bisecting the bond shared by the two five-membered rings. Clearly, it is not a question of the number of electrons supplied by the ligand and the metal totaling $4q + 2$ in one instance, and $4q$ in the other, since these molecules are isomeric.

These fascinating results prompted us to calculate potential energy surfaces for the migration of an ML_n unit across the anionic forms of **157** and **158**. Initially, the organometallic fragment selected was $(C_5H_5)Fe^+$, which is isolobal to $Mn(CO)_3^+$ but does not require that one take account of the different orientation of the tripod at each point since rotation about the metal-Cp axis has a very low barrier.[170] Following the method used previously[160] for $[(pentalene)FeCp]^+$, the iron was held at a constant distance of 1.59 Å from the plane of each dibenzpentalenyl ligand, and allowed to move across the polycyclic framework in steps of 0.1 Å to generate the potential energy surfaces (PES) shown as Figures 5.1 and 5.2.

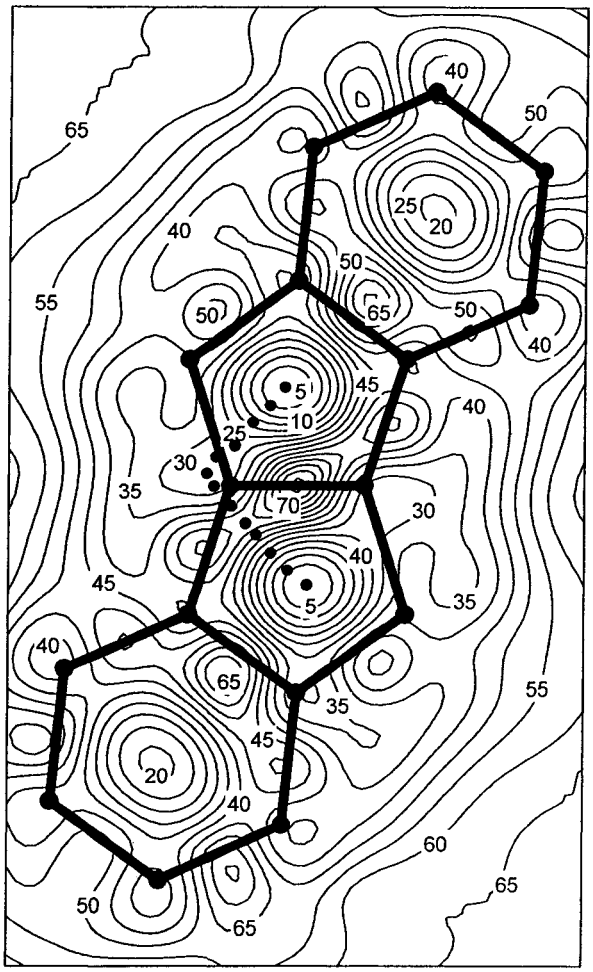

Figure 5.1: Potential energy hypersurface (EHMO-calculated) for the migration of an $Fe(C_5H_5)$ fragment over the *anti*-dibenzpentalene substrate, **157**. Solid contour lines are incremented at 5 kcal mol^{-1}, whereas the reaction path is superimposed as a dashed line.

In viewing the PES for the *anti* isomer **157** (Figure 5.1), the most obvious result is the greatly disfavored (72 kcal mol^{-1}) least-motion pathway directly across the common bond between the five-membered rings (see **163c** → **164c** in Scheme 5.5). Moreover, the alternative route that bypasses the center of this bond still requires that the migrating group surmount a barrier of 45 kcal mol^{-1} and, as mentioned previously,[169] this η^5-to-η^5 shift is not observed experimentally for the manganese and chromium complexes shown in Scheme 5.5. Interestingly, the η^6-to-η^5 haptotropic shift, **161** → **162a**, does proceed irreversibly, and the PES indicates why this should be so. When the CpFe moiety is initially bonded to the six-membered ring it must – and experimentally does in the case of **161** – traverse a barrier of 33 kcal mol^{-1} before attaining the metallocenyl-type structure (cf. **162a**). However, the reverse process starts from the η^5 isomer that is 18 kcal mol^{-1} more stable than the η^6-bonded structure, (cf. **161**), and so raises the barrier to 51 kcal mol^{-1}, and renders the η^5-to-η^6 haptotropic shift both thermodynamically and kinetically non-viable. These values should be compared with the corresponding results for the (indenyl)FeCp system for which the η^5 geometry was calculated to be favored over the η^6 structure by about 19 kcal mol^{-1}, and the η^6-to-η^5 barrier was estimated as 35 kcal mol^{-1}

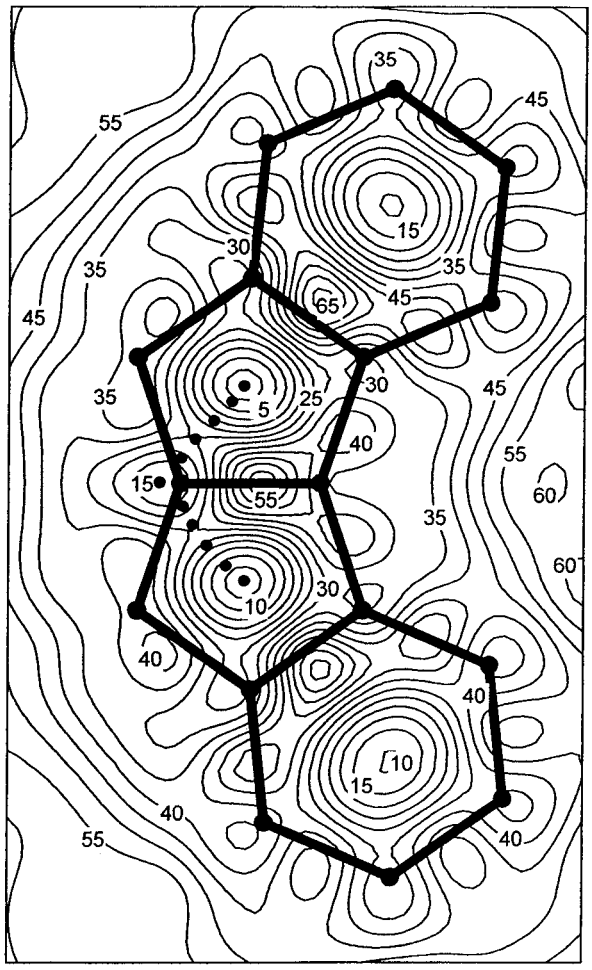

Figure 5.2: Potential energy hypersurface (EHMO-calculated) for the migration of an $Fe(C_5H_5)$ fragment over the *syn*-dibenzpentalene framework, **158**. Solid contour lines are incremented at 5 kcal mol^{-1}, whereas the reaction path is superimposed as a dashed line.

As illustrated in Figure 5.2, the situation is completely different for the corresponding *syn* isomer **158**, for which the η^5-to-η^5 haptotropic shift process occurs readily with an experimental barrier for the manganese complex, **165**, of approximately 15 kcal mol^{-1}.[169] The potential energy surface for [(*syn*-η^5-dibenzpentalenyl)FeCp]$^{1-}$ reveals a relatively low energy pathway by which the organometallic fragment can migrate between the five-membered rings. The favored trajectory takes the iron atom almost directly underneath a ring junction carbon to yield an intermediate structure only 10.1 kcal mol^{-1} less stable than the η^5 minimum; the highest point on this route is approximately 25 kcal mol^{-1} above the ground state, which is about half of that required in the *anti*-analogue **162c**.

As noted previously,[160] such calculations are rather sensitive to the Fe-ligand plane distance, which was set initially at 1.59 Å. Optimization of this value at the η^5 and η^4 minima, and at the top of the barrier, gave distances of 1.66 Å, 1.64 Å and 1.77 Å, respectively, which leaves the η^4 geometry 10.6 kcal mol^{-1} above the η^5 minimum, but lowers the migration barrier to 20.6 kcal mol^{-1}. It should be emphasized that, since vibronic analyses were not performed, the 'transition states' discussed here are merely the highest points along the favored EHMO-calculated trajectories, and no claims are made beyond that.

One can relate these calculations and the experimental observations on the dibenzpentalenyl complexes back to our previous discussion concerning (cyclopenta[*def*]phenanthrenyl)$Mn(CO)_3$, **142**, and its dihydro analogues, **131** and **132**. In the former system, one could invoke the aromatic character of the intermediate (and/or

transition state), **144**, which lowers the activation energy for the migration process, somewhat analogous to Basolo's famous "indenyl effect" for ligand displacements in (indenyl)$Rh(CO)_2$ versus (cyclopentadienyl)$Rh(CO)_2$ complexes.[171] In [(*syn*-dibenzpentalenyl)FeCp]$^{1-}$, **165b/166b**, the intermediate (and possibly even the transition state) possesses two 6π aromatic rings while the metal is essentially in an (η^4-trimethylenemethane)ML_n local environment.

For comparative purposes, Figure 5.3 depicts the calculated trajectory for the η^5-to-η^5 haptotropic shift in [(*syn*-dibenzpentalene)$Mn(CO)_3$]$^{1-}$, **165a (R = R′ = H)**, and yields an activation energy barrier of 14 kcal mol^{-1}. The tripod orientation was taken into account by rotating the metal fragment in 10 ° steps over a range of 120 ° at each point of the hydrocarbon surface. It is noticeable how the favored orientation of the tripod changes during the migration such that at the "trimethylenemethane structure" the manganese is essentially in an octahedral environment as would be anticipated for a d^6 $[Mn(CO)_3]^+$ fragment.[172] As in the iron derivative, the η^6-to-η^5 and η^5-to-η^6 routes are more energetically demanding, with estimated barriers of 26 and 41 kcal mol^{-1}, respectively.

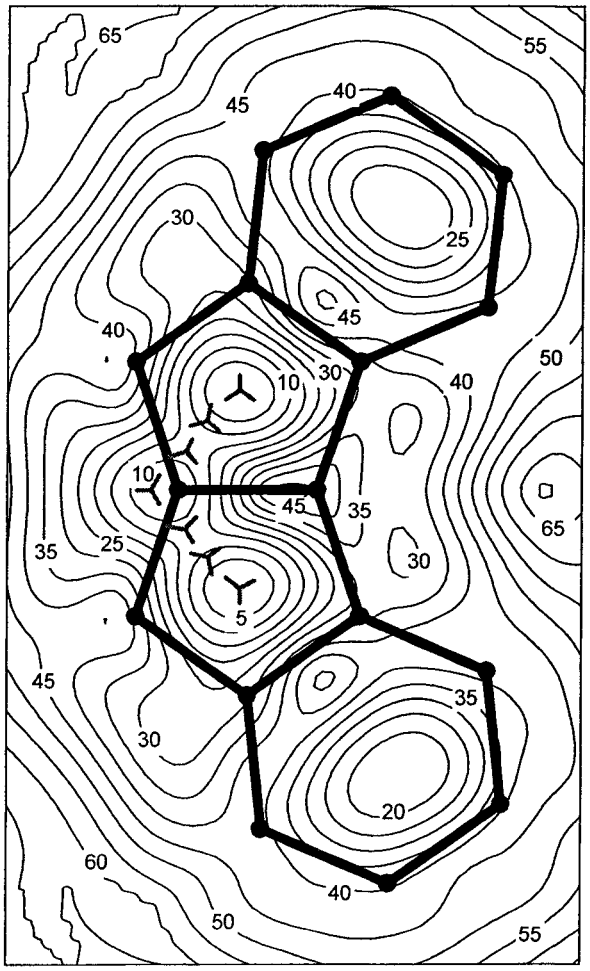

Figure 5.3: Potential energy hypersurface (EHMO-calculated) for the migration of an $Mn(CO)_3$ moiety over the *syn*-dibenzpentalene framework, **158**. Solid contour lines are incremented at 5 kcal mol^{-1}, whereas the minimum energy trajectories with corresponding orientations of the tripod are depicted as (⅄) symbols.

5.2.2 Fluoradenyl-metal complexes

The fluoradenyl ligand **159** may be regarded as a tribenzpentalenyl system derived by incorporation of a third ring onto the *syn*-dibenzpentalenyl framework. Until recently, there was only a single report describing an attempt to detect a rearrangement in this system whereby (η^6-fluoradene)$Cr(CO)_3$ **167** (for which endo- vs. exo-stereochemistry was not determined) apparently does not undergo an η^6-to-η^5 haptotropic shift to give **169** (Scheme 5.7).[173] This stabilization was originally rationalized on the basis of charge delocalization in the two five- and unique six-membered rings.[161] Apart from this, the viability of an η^5-to-η^5 shift in such a hydrocarbon has yet to be established (experimentally or computationally). As a result, the PES for the migration of a $CpFe^+$ unit across the surface of the tetracyclic framework of the fluoradenyl anion was generated and is depicted in Figure 5.4.

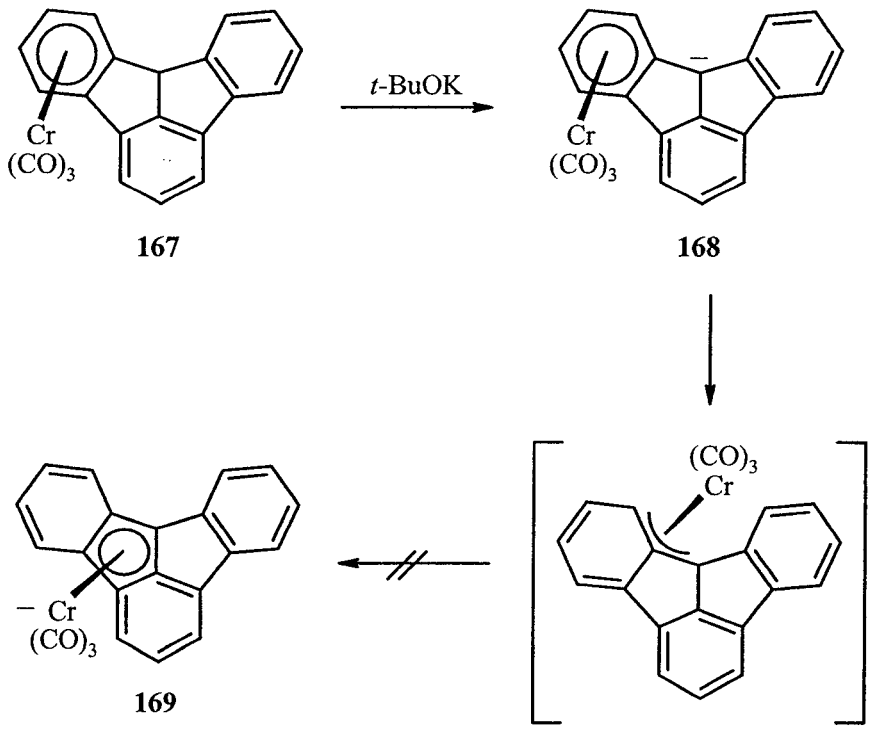

Scheme 5.7: η^6-to-η^5 migration of a chromium tripod over the fluoradenyl framework.

It is noticeable that while the favored site of attachment of the iron fragment in (fluoradenyl)FeCp is to a five-membered ring, **170**, the fluoradenyl η^6-isomers are only destabilized to the tune of 5.4 and 6.2 kcal mol^{-1} for the two peripheral rings, **171**, and for the unique ring, **172a/b**, respectively. When the Fe-ligand distance is optimised at 1.62 Å for the η^5 structure, **170**, and at 1.59 Å for the η^6 isomers **171** and **172b**, respectively, the metallocene-type molecule, **170**, is further stabilized, but only by a trivial amount, 0.16 kcal mol^{-1} (EHMO prediction). As usual, the least-motion pathways for all the η^6-to-η^5 and η^5-to-η^5 haptotropic shifts are strongly disfavored, with barriers ranging from approximately 50 kcal mol^{-1} for the former to about 42 kcal mol^{-1} for the latter.

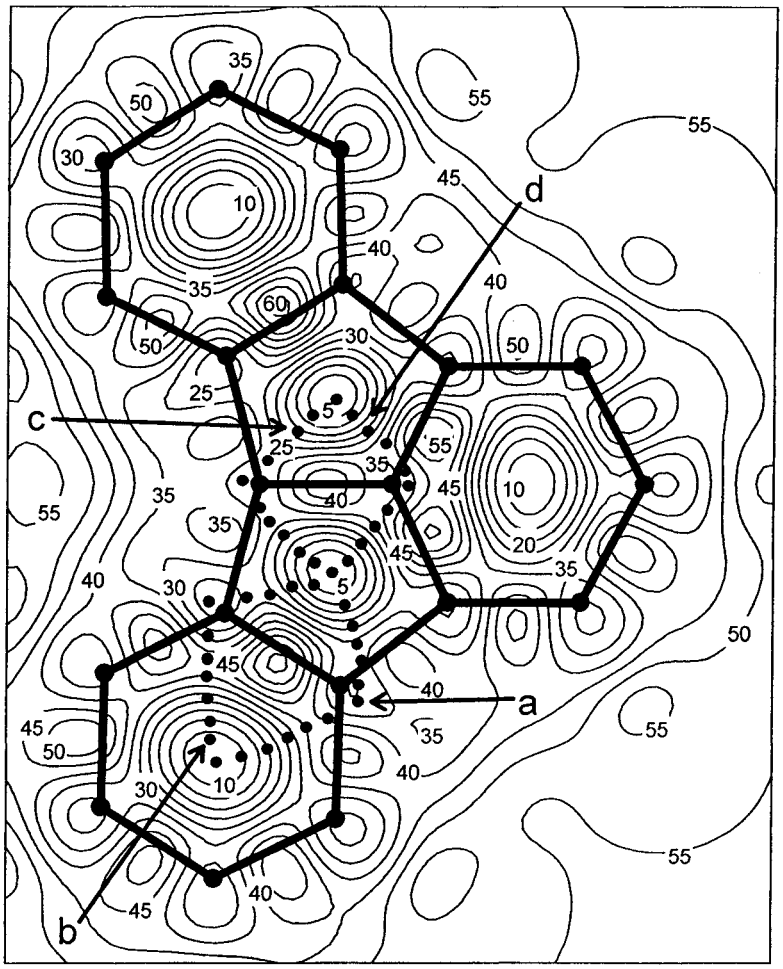

Figure 5.4: Potential energy hypersurface (EHMO-calculated) for the migration of an $Fe(C_5H_5)$ fragment over the fluoradene substrate, **159**. Solid contour lines are incremented at 5 kcal mol^{-1}, whereas the plausible reaction paths (*a* through *d*) are superimposed as dashed lines.

More importantly are the trajectories that precede via η^3 or η^4 structures, as indicated by pathways *a* through *d* in Figure 5.5. The η^6-to-η^5 exocyclic routes labeled *a* and *b* pass over barriers of 37 and 35 kcal mol^{-1}, respectively, before reaching the corresponding η^4 structures, which lie 22 and 29 kcal mol^{-1}, respectively, above the ferrocene-type ground state (**170**). These values are not markedly different from those calculated and observed in related systems,[174] and suggest that such a process should be experimentally observable. The η^5-to-η^5 migration via route *c* has a calculated minimum barrier of approximately 28 kcal mol^{-1}, a value slightly below that calculated for the corresponding pathway via the "bay region" in [(*syn*-dibenzpentalenyl)FeCp]$^{1-}$, but noticeably higher than the favored route as indicated in Figures 5.1 and 5.2. By comparison, any pathway proceeding via an η^3 or η^4 geometry at the central carbon (path *d*) is strongly disfavored with a barrier approaching 40 kcal mol^{-1}; a CpFe fragment at such a site would prefer to move into the unique six-membered ring where it could bind in a pentahapto fashion, as in structure **172**.

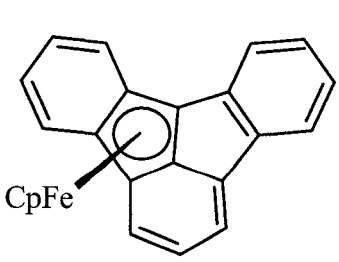

170

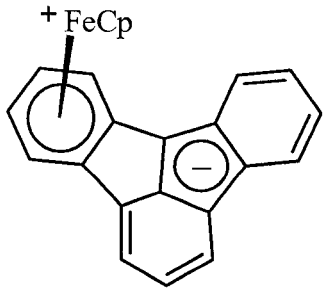

171

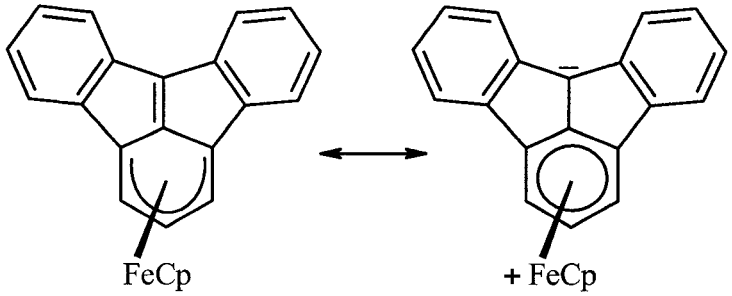

172a **172b**

A 2000 report by Selegue *et al.*[175] describes the synthesis and crystallographic characterization of the related *exo*- and *endo*-(η^6-fluoradene)Ru(C_5Me_5)$^+$ cations, **133** and **135**. Deprotonation of the *exo* complex yielded a 20:1 ratio of two η^5 isomers, **134a** and **134b**, which correspond to the secondary minima **172** and **171**, respectively, calculated for the iron analogue (Scheme 5.8). Earlier attempts to generate an η^5 isomer directly by treatment of fluoradene **159** with $M_2(CO)_{10}$ (M = Re or Mn) resulted in the η^1 rhenium complex, **173,** as confirmed by X-ray diffraction analysis, while quantitative formation of the (η^5-fluoradenyl)$Mn(CO)_3$, **174**, was less unequivocally established by spectral methods.[176] That η^6-to-η^5 slippage, as in **134a** or **134b**, takes preference over the formation of a metallocenic structure (cf. **170**) is not too surprising; the former

pentahapto bonding mode disrupts the aromaticity of one rather than two of the six-membered rings and should therefore be thermodynamically favored.

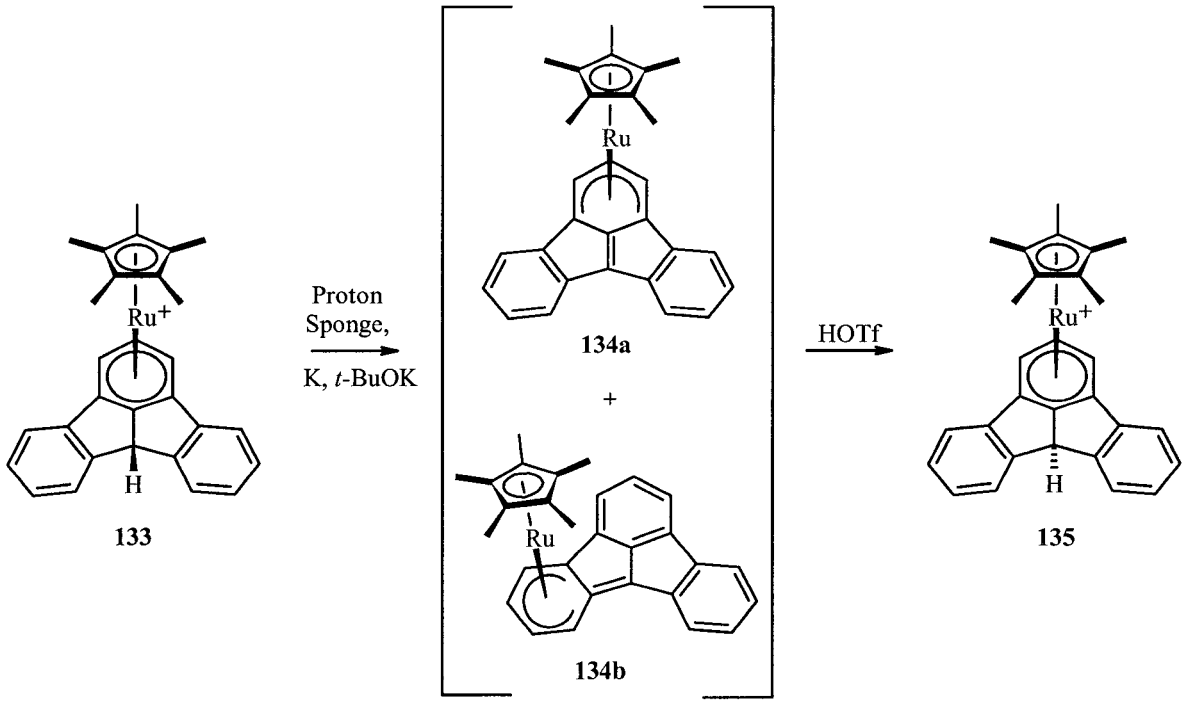

Scheme 5.8: *Exo*-to-*endo* inversion of the $(\eta^6$-fluoradene$)Ru(C_5Me_5)^+$ cations, **133** and **135**.

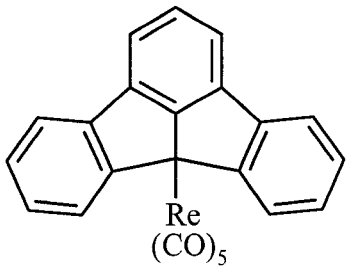

173

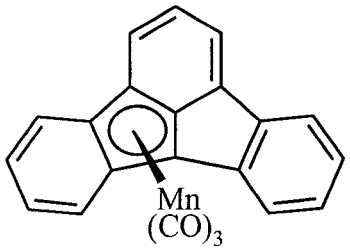

174

5.2.3 Fluoranthene-metal complexes

In 2002, Oprunenko *et al.*[177] demonstrated that, in the fluoranthene system **160**, a tricarbonylchromium fragment originally bonded to a ring in the naphthalene unit, **175a** undergoes a thermally-induced, irreversible intramolecular rearrangement (32.6 kcal mol^{-1}) so as to allow the chromium access to the unique six-membered ring, as in **176a** (Scheme 5.9). This parallels an earlier report by Elschenbroich[178] whereby analogous behaviour was observed in the sandwich compound bis(fluoranthene)chromium. In the absence of appropriate labels, dynamic NMR evidence for chromium migration between the two six-membered rings of the naphthalene moiety in **175a** (cf. enantiomers **175a'**) has yet to be established.[161,177]

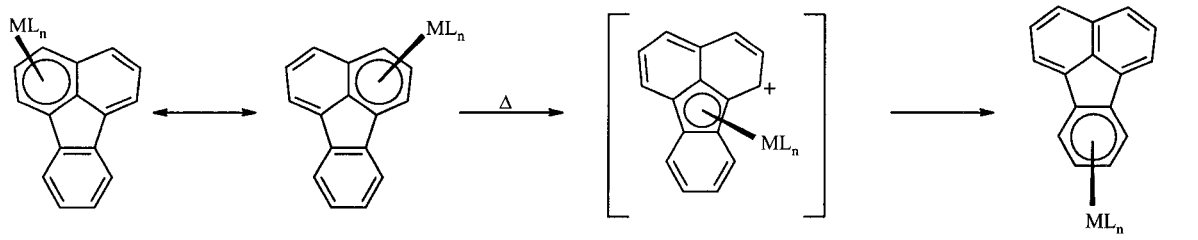

175a': $ML_n = Cr(CO)_3$ **175a**: $ML_n = Cr(CO)_3$ **177**: $ML_n = Fe(C_5H_5)$ **176a**: $ML_n = Cr(CO)_3$

175b': $ML_n = Fe(C_5H_5)^+$ **175b**: $ML_n = Fe(C_5H_5)^+$ **176b**: $ML_n = Fe(C_5H_5)^+$

Scheme 5.9: η^6-to-η^6 haptotropic rearrangement routes available to the (fluoranthene)ML_n complexes **175a** and **175b**.

In this tetracyclic system, the favored site of attachment for a CpFe moiety is also in the single six-membered ring, **176b**, which lies 3.3 kcal mol^{-1} below **175b**, and 9 kcal mol^{-1} below isomer **177**, in which the metal is bonded to the central five-membered ring. The EHMO-calculated lowest energy trajectory (Figure 5.5) takes the metal over a 32 kcal/mol barrier to an η^4 geometry, beneath a carbon common to the central ring and

the naphthyl ring. An excursion via the η^5 site, **177**, could then continue to a second η^4 structure before reaching the global minimum at **176b**. However, the lack of a pathway involving one or more transition states possessing evident aromatic character results in high barriers such that the overall η^6-to-η^6 haptotropic shift occurs only at elevated temperatures. A barrier of 32 kcal mol^{-1} is estimated for the degenerate 'naphthalene' type η^6-to-η^6 rearrangement (**175b** → **175b'**), but this process was not reported as being experimentally observable.[177]

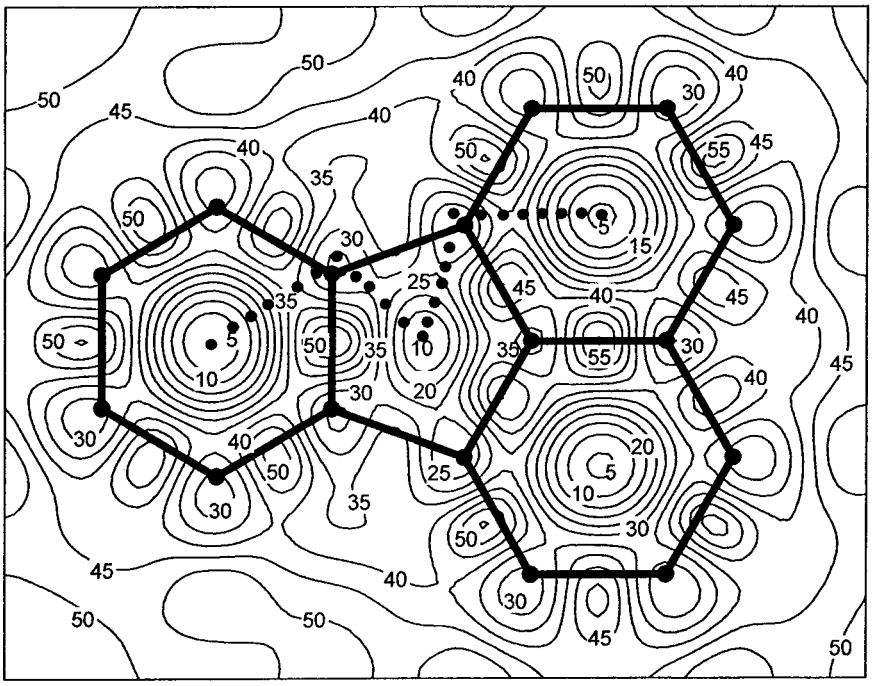

Figure 5.5 Potential energy hypersurface (EHMO-calculated) for the migration of an $Fe(C_5H_5)$ fragment over the fluoranthene framework, **160**. Solid contour lines are incremented at 5 kcal mol^{-1}, whereas the reaction path is superimposed as a dashed line.

This result contrasts markedly with the corresponding (cyclopenta-[*l*]phenanthrenyl)FeCp system, **178**, where positioning the iron on the central six-membered ring is strongly disfavored by approximately 40 kcal mol^{-1}.[179] Given the dibenzindenyl framework, the η^5-to-η^6 shift is hindered by the need to sacrifice the aromatic character of the peripheral six-membered rings (see Figure 5.6).

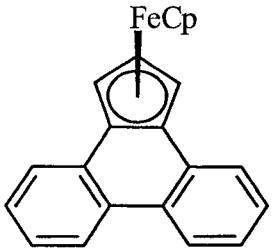

178

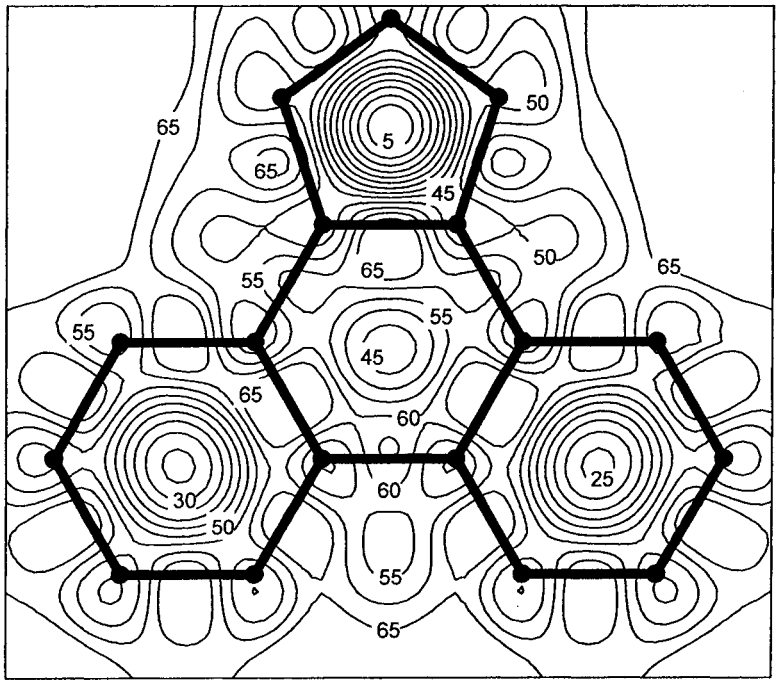

Figure 5.6: Potential energy hypersurface (EHMO-calculated) for the migration of an $Fe(C_5H_5)$ fragment within the (cyclopenta[*l*]phenanthrenyl)FeCp system, **178**. Solid contour lines are incremented at 5 kcal mol^{-1}.

5.3 Conclusion

These patterns of haptotropic shifts, which are controlled by the interactions of the ML_n fragment with the π-manifold of the ligand, may be profitably compared with the sigmatropic migrations of R_3M groups (M = Si, Ge or Sn) or of $(C_5H_5)(CO)_2Fe$ across similar polycyclic frameworks.[180,181] Beyond orbital considerations, the energy requirements of both types of rearrangements can be correlated with the *aromatic character of the transition state and/or intermediates.*

For example, the barriers to [1,5]-suprafacial silatropic shifts in the indenyl system **179** (> 25 kcal mol^{-1}) are dramatically reduced upon mono- and dibenzannulation (cf. **180** and **181a**), which allows for the isoindene intermediates (and their accompanying transition states) to retain an increasing degree of aromaticity.[182] In fact, the isoindene derived from cyclopenta[*l*]phenanthrene (**181a**) is sufficiently long-lived as to undergo a Diels-Alder dimerization with its progenitor.[183]

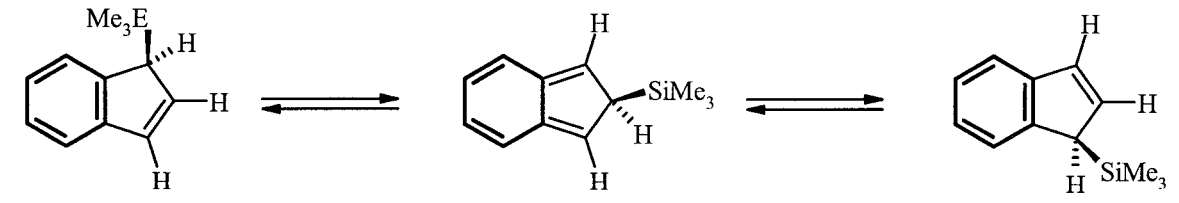

179

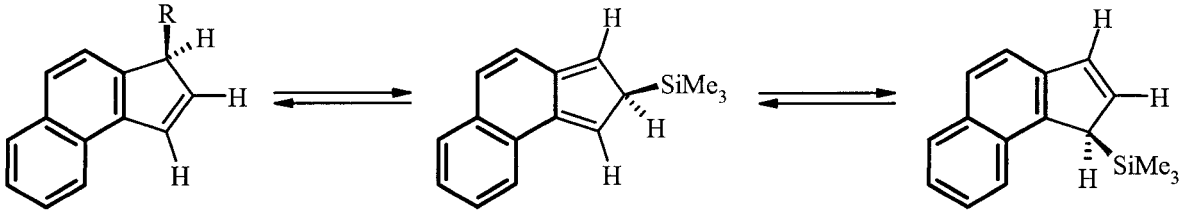

180

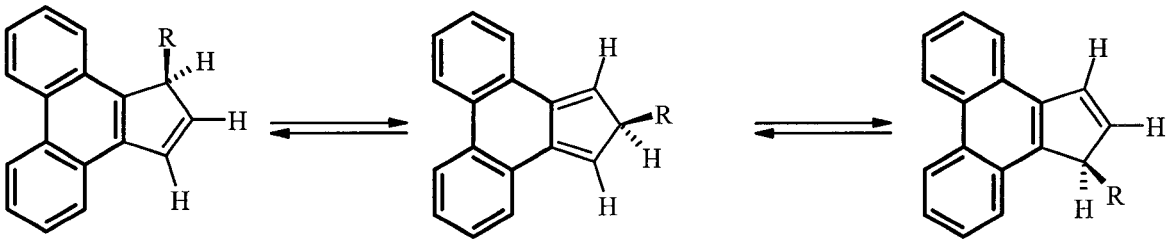

181a, b **182a, b**

a: R = $SiMe_3$
b: R = H

Metal π-complexes of fused polycycles may present a variety of competing reaction pathways for (η^5-to-η^5, η^6-to-η^5/η^5-to-η^6 and η^6-to-η^6) haptotropic shifts, as demonstrated by the five cases examined herein. For these processes, the transition state (or intermediate) is generally of the η^3 or η^4 type such that cyclic π electron delocalization can be maintained as the ML_n traverses a circuitous route on the molecular periphery. To this end, indenyl (**151**) and fluorenyl (**126**, **127**) skeletons are suitable substrates for η^6-to-η^5 migrations haptotropic shifts; the further fusion of benzene rings, as in **178**, diminishes the aromatic stabilization of certain isomeric forms and thus limits

the migratory possibilities. These kinetic and thermodynamic trends are not easily differentiated from or related to the structure of the organic ligand, providing merit to the EHMO approximation of the energy landscape. The application of more rigorous quantum-mechanical methods to the study of haptotropic transformations will enhance both the accuracy of mechanistic details, particularly the nature of saddle points, and the predictive aspects of this electronic structure and bonding argument.

CHAPTER SIX

Conclusions and Future Work

6.1 Concluding Remarks

Since the first reported account of organometallic trindane complexes,[81,98] the reactivity of these complexes has been unexplored. It has now been established that [(η^6-trindane)$Mn(CO)_3$][BF_4], **58c**, reacts with potassium *tert*-butoxide and either allyl bromide, deuterated methylene chloride or methyl iodide, affording the corresponding halide complexes, (η^6-trindane)$Mn(CO)_2X$, where X = Br, Cl and I, respectively. In contrast, **58c** and potassium *tert*-butoxide react in the presence of donor ligands to generate (η^5-$C_{15}H_{15}$)$Mn(CO)_2L$, where L = CO, $P(OMe)_3$ and PPh_3, in which the metal has migrated from the central ring onto a peripheral ring that has lost three hydrogen atoms. A mechanistic pathway has been proposed in which the initially formed [(η^6-trindane)$Mn(CO)_2(CO_2Bu^t)$ suffers loss of CO_2 and isobutene to yield the hydride (η^6-trindane)$Mn(CO)_2H$, which in turn undergoes three successive C-H insertions with concomitant loss of two moles of dihydrogen.

This novel and rather facile rearrangement prompted its exploration with other (arene)$Mn(CO)_3^+$ systems, where the arene is bicyclic or tricyclic and possesses attached 5-, 6- or 7-membered rings. Therefore, we utilized similar conditions, that is treating the respective (arene)$Mn(CO)_3^+$ with potassium *tert*-butoxide in the presence of trimethyl phosphite. The corresponding indane compound, [(η^6-indane)$Mn(CO)_3$][BF_4] behaved similarly to the trindane system, furnishing the known indenyl manganese complexes. The [(η^6-dibenzosuberane)$Mn(CO)_3$][BF_4] paralleled the chemistry of the fluorenyl and

cyclopenta[*def*]phenanthrenyl systems, whereby abstraction of the benzylic proton resulted in the formation of a double bond in the central seven-membered ring. The bicyclic [(η^6-tetralin)$Mn(CO)_3$][PF_6] complex exhibited different behaviour from all the other systems. It appears from preliminary data that [(η^6-tetralin)$Mn(CO)_3$][PF_6] undergoes deprotonation at a benzylic position followed by nucleophilic addition and loss of a manganese unit from another tetralin manganese tricarbonyl complex. A rationale was provided that took into account previous theoretical investigations, crystallographic data and electronic factors.

Since the chemistry of the (η^6-trindane)$Mn(CO)_3^+$ seems to be unique from other polycyclic systems, it warrants further investigations. One possibility would be to treat the cation with other bases to see if similar results are obtained.

One of the initial goals of this thesis remains of interest, that being the proposed organometallic route to sumanene. Trindane, a potential synthetic precursor to sumanene that contains a central six-membered ring fused to three cyclopentene rings, could ideally alleviate the difficulty encountered by other synthetic methodologies where the final step involves the formation of the five-membered rings of sumanene. Perhaps this may be achieved utilizing the (η^6-trindane)$FeCp^+$, **58d**, complex which underwent deprotonation of the benzylic positions followed by alkylation. This was apparent from the deuterium exchange studies as well as with attempts to replace the benzylic protons for allyl or methyl groups. However, this methodology for deprotonation/alkylation needs to be perfected before extending its synthetic viability towards sumanene. Alkylation at only the benzylic *exo* positions seems to be a challenge. One may consider altering the

organometallic moiety substituents to increase sterics and possibly prevent substitution at the *endo* benzylic sites. In the case of compound, **58d**, the Cp (C_5H_5) ring may be substituted for Cp* (C_5Me_5). Also, one must be wary that the Cp* ring may also undergo a substitution.[57] However, altering the substituents affects the electronics of the metal. Attempts to change the substituents and the metal of the (η^6-trindane)$Mn(CO)_3^+$ complex to (η^6-trindane)$Mn(CO)_2\{P(OMe)_3\}_2^+$ and (η^6-trindane)$Re(CO)_3^+$, respectively, afforded the products in very low yields; insufficient amounts prevented further study.

The persubstituted hexaethylbenzene (HEB) ligand is similar to that of trindane in that the benzene core is hexasubstituted, however, in the latter the substituents are tethered together. For this reason, the HEB ligand seemed like an ideal candidate for the synthesis of the hydride (HEB)$Mn(CO)_2H$, since attempts to isolate the corresponding trindane analogue, (η^6-trindane)$Mn(CO)_2H$, were unsuccessful. Despite all efforts towards isolating any of the manganese hydride compounds, the HEB complexes were also of interest for their dynamics and stereochemical features. The following HEB compounds were synthesized and probed by low-temperature NMR spectroscopy: (HEB)$Mn(CO)_3^+$, **147** and (HEB)$Mn(CO)_2Br$, **148**. NMR data for **147** displayed typical signals corresponding to the 1,3,5-*distal*-2,4,6-*proximal* arrangement of the ethyl groups. The data for **148** suggests that its behaviour in the solution and in the solid state differs. Crystallographic data revealed that the ethyl groups exhibit the 1,3,5-*distal*-2,4,6-*proximal* conformation, although the corresponding ^{13}C NMR spectrum did not display the expected 2:1:2:1 pattern.

Haptotropic shifts of ML_n fragments, such as $(C_5H_5)Fe$, $Mn(CO)_3$ or $Cr(CO)_3$, across polycyclic carbon frameworks generally follow a "non-least motion" trajectory. Haptotropic shifts over the indenyl and fluorenyl skeletons have been suggested to proceed via an exocyclic η^3-transition state of low-energy, which possess 6π-aromatic character.

The potential energy surfaces for the organometallic derivatives of dibenzpentalene (*anti*-**157**, *syn*-**158**), fluoradene (**159**), and fluroranthene (**160**) suggest that aromaticity in the transition state plays an important role in determining the migration barrier. Thus, we have seen that haptotropic shifts over bicyclic and polycyclic skeletons are reasonably facile when cyclic π electron delocalization can be maintained as the metal unit traverses a circuitous route on the molecular periphery. Despite the level of computation, a qualitative and a simple perspective was presented. Ultimately, the EHMO approximation has provided fundamental details of the energy landscape, expanding the pioneering arguments advanced for haptotropic rearrangements in bicyclic systems. The application of more rigorous quantum-mechanical methods to the characterization of saddle points will eliminate discrepancies and invoke the potential to forecast transition states and/or intermediates. It is expected that detailed knowledge of reaction mechanisms will enable the prediction of new transformations within specifically designed templates.

CHAPTER SEVEN

Experimental Data

7.1 General

All reactions were carried out under an atmosphere of nitrogen in oven-dried glassware (oven temperature = 110 °C). All solvents were dried and distilled by standard procedures.[184] Unless otherwise stated, reagents were obtained from Aldrich Chemicals Company and used as received. Dimanganese decacarbonyl was purchased from Strem Chemical, Inc. and deuterated NMR solvents were obtained from Cambridge Isotope Laboratories. Column chromatography was performed with 230 - 400 mesh silica gel. Silica gel, TLC grade 7749 with gypsum binder and fluorescent indicator was used for the chromatroton plates. Radial chromatography was performed using a Chromatotron (7942T, Harrison Research, Inc.), with silica-coated plates (thickness: 1 mm, 2 mm or 4 mm). The ^{1}H, ^{13}C and ^{31} P NMR spectral data were acquired using the Bruker Avance-500, Avance-300 or Avance-200 spectrometer and the field strength is specified in each spectrum. In all cases, NMR data were obtained from samples dissolved in deuterated solvents. ^{1}H and ^{13}C NMR chemical shifts are given relative to residual proton or ^{13}C solvent signal. ^{31}P NMR spectra were recorded in proton-decoupled mode, externally referenced relative to 85% H_3PO_4 in D_2O. In certain cases, proton COSY 2-D NMR and ^{1}H-^{13}C 2-D HSQC NMR experiments were used to aid in the assignment of chemical shifts. Melting and decomposition points were measured in open glass plates using a Fischer-Johns melting point apparatus, and are not corrected. Infrared spectra were

recorded on a Bio-Rad FTS-40 single beam spectrometer using KBr pellets or NaCl windows. *In situ* infrared spectra were recorded on an ASI Applied Systems ReactIR 1000 with a SiComp probe. Mass spectrometric data were obtained on a Finnigan EI/CI mass spectrometer system, using direct electron impact and chemical ionization methods. The positive ion electrospray mass spectra were obtained on a Micromass Quattro LC triple quadrupole mass spectrometer. Microanalyses were performed by Guelph Chemical Laboratories (Guelph, Ontario).

7.2 X-ray Crystal Structure Determinations

X-ray crystallographic data were collected from single crystal samples, which were mounted on a glass fiber. Data were collected using a P4 Bruker diffractometer, equipped with a Bruker SMART 1K charge coupled device (CCD) area detector, using the program SMART,[185] and a rotating anode, using graphite-monochromated Mo-K_α radiation (λ = 0.71073 Å). The crystal-to-detector distance was 4.987 cm, and the data collection was carried out in 512 x 512 pixel mode, utilizing 2 x 2 pixel binning. The initial unit cell parameters were determined by a least-squares fit of the angular settings of the strong reflections, collected by a 12 ° scan in 40 frames over three different sections of reciprocal space (160 frames in total). A hemisphere of data was collected with high redundancy, to better than 0.8 Å resolution at 153 K. Upon completion of the data collection, the first 40 frames were recollected in order to improve the decay correction analyses. Processing was carried out using the program SAINT,[186] which applied Lorentz and polarization corrections to the three-dimensionally integrated diffraction spots. The program SADABS,[187] was utilized for the scaling of the diffraction

data, the application of a decay correction and an empirical absorption correction based on redundant reflections for the data set. The structure was solved by using the direct-methods procedure in the Bruker SHELXTL program library,[188] and refined by full-matrix least squares methods on F^2 with anisotropic thermal parameters for all non-hydrogen atoms. Hydrogen atoms were added as fixed contributors at calculated positions, with isotropic thermal parameters based on the carbon atom to which they were bonded for structures **71**, **73**, **80**, **81**, **98**, **102**, **125** and **148**. For structure **117**, all hyrogen atoms were found and added from the difference map, and allowed to refine isotropically except for hydrogen atoms, H(7A), H(7AB) and H(7AC), which were added as fixed contributors at calculated positions, with isotropic thermal parameters based on the carbon atom to which they were bonded.

The final structure of **73** was based on a disorder model in which the $Mn(CO)_2I$ tripod could exist in two conformations. The occupancy of the two conformations was allowed to refine as a free variable (final ratio of approximately 88 : 12). The carbonyl group, C(17A)-O(17A), of the minor component could not be refined anisotropically as a result of the partial overlap with the electron density from the iodine atom and hence was refined isotropically. The planarity of the cyclopentadienyl ring [i.e. C(1), C(2), C(3), C(4) and C(5)] in structure **80** was fixed. Also, the lack of intensity from the diffraction of the sample prevented the refinement of carbon atoms, C(16) and C(17), corresponding to the carbonyl groups anisotropically and was therefore refined isotropically due to the poor quality of the crystal. In the case of $[(\eta^6\text{-tetralin})Mn(CO)_2P(OMe)_3][PF_6]$, **117**, the molecule lies on a crystallographic plane, a mirror plane, in which only half of the

molecule was refined and the other half of the molecule was generated by the mirror plane. This is a result of the disorder between C(7a) and C(7), in which there exits two twisted half-chair conformations. Also, the anion was disordered, in that two orientations were found for the PF_6 anion (final ratio of approximately 90 : 10). The minor component of the PF_6 anion was refined isotropically. The structure of **148** exhibited a disorder between one of the carbonyl groups and a bromine atom and hence, the occupancy of the two conformations was allowed to refine as a free variable (final ratio of approximately 70 : 30).

7.3 Molecular Orbital Calculations

Calculations were performed via the extended Hückel method using weighted H_{ij}'s;[189] orbital drawings were obtained by the use of the program CACAO.[190] The following distances were used: Fe-Cp = 1.59 Å, Mn-CO = 2.16 Å and C-O = 1.16 Å. To generate the energy hypersurface, $Fe(C_5H_5)$ or $Mn(CO)_3$ coordinates were incremented in units of 0.1 Å. Orbital parameters were taken from reference 161.

7.4 Syntheses and Characterization of Compounds

Preparation of Trindane, 57. Trindane was prepared as described in literature.[82] To a solution of cyclopentanone (16 mL, 0.18 mol) and dry ethanol (18 mL), H_2SO_4 (8 mL) was added dropwise, followed by heating the solution under reflux for 18 h. The dark green solution was poured over ice (70 g) and extracted with diethyl ether (4 X 30 mL), followed by neutralization with sodium bicarbonate, washing with water and drying over $MgSO_4$. The solution was filtered and the solvent was removed by rotary evaporation.

Distilling off cyclopentanone under vacuum and collecting white crystals purified the compound. ^{1}H NMR (200 MHz, $CDCl_3$): δ 2.84 (t, 12H, CH_2), 2.11 (q, 6H, CH_2); ^{13}C NMR (50MHz, $CDCl_3$): δ 137.6 (aromatic C), 31.2 (CH_2), 25.5 (CH_2).

[(η^6-Trindane)Mn(CO)$_3$][BF$_4$], 58c. This compound was prepared utlizing the method described by McGlinchey and co-workers.[81] A mixture of $Mn(CO)_5Br$ (2.75 g, 10 mmol) and $AgBF_4$ (1.95 g, 10 mmol) in dry CH_2Cl_2 (50 mL) was heated to a reflux for 3 h under nitrogen and then cooled to room temperature. To the reaction mixture a solution of trindane was added, and continued heating for an additional 18 h. After cooling, the filtrate was passed through Celite and concentrated to approximately one-third its volume under reduced pressure, and excess hexane (50 mL) was added. The resulting orange-yellow solid was filtered and dried in *vacuo* to give **58c** (1.912 g, 4.520 mmol; 55 %). IR and ^{1}H NMR was consistent with literature reported values. ^{1}H NMR (200 MHz, $CDCl_3$): δ 3.17 (m, 6H, CH_2), 2.73 (m, 6H, CH_2), 2.89 (m, 3H, CH_2), 1.89 (m, 3H, CH_2); ^{13}C NMR (50 MHz, $CDCl_3$): δ 217.3 (Mn-CO), 117.3 (aromatic C), 29.9 (benzylic CH_2), 24.2 (wingtip CH_2); IR (KBr pellet): υ_{CO} 2056 (s), 1997 (s) cm^{-1}.

(η^6-trindane)Mn(CO)$_2$Br, 71. A 3-neck round bottom flask equipped with a stir bar was charged with [(η^6-trindane)Mn(CO)$_3$][BF$_4$] (0.500 g, 1.182 mmol) and *t*-BuOK (1.33 g, 11.8 mmol) and stirred under vacuum for 3 h at 40 °C. A solution of THF (25 mL) containing allyl bromide (1.02 mL, 11.8 mmol) was added *via* cannula under N_2, which produced a green solution. The solution was maintained at 40 °C under N_2, which eventually turned brownish-orange. After 20.5 h, the solvent was removed under reduced

pressure and the residue, pinkish-red in colour was dissolved in CH_2Cl_2. Not all of the residue was soluble in CH_2Cl_2, therefore, the solution was filtered and extracted with H_2O (3 x 10 mL). The organic layers were combined, dried with Na_2SO_4 and filtered. The solvent was removed by rotary evaporation and dried in *vacuo* to give **2** as a dark red powder (0.077 g, 0.198 mmol; 16.7 %), 128-130 °C (dec). ^{1}H NMR (200 MHz, CD_2Cl_2): δ 2.76 (br, 12H, benzylic CH_2), 2.04 (br, 6H, wingtip CH_2); ^{13}C NMR (50 MHz, CD_2Cl_2): δ 110.3 (aromatic C), 30.1 (benzylic CH_2), 24.1 (wingtip CH_2); IR (NaCl windows, $CDCl_3$): υ_{CO} 1971(s), 1927 (s) cm^{-1}. As a result of the instability of the compound in solution, no ^{13}C chemical shift for Mn-CO was seen in the spectrum. Even when the NMR tube was flamed sealed, decomposition peaks corresponding to free trindane were apparent. Anal. Calcd for $C_{17}H_{18}MnBrO_2$: C, 52.47; H, 4.66. Found: C, 52.04; H, 4.92. The mass spectra showed no parent ions but displayed ions consistent with decomposition of the compound similar results were found for the hexamethylbenzene compound.[47b] MS (DEI, m/z (%)); 198 (100, $[C_{15}H_{18}]^+$), 115 (4.8, $[C_9H_7]^+$). A sample suitable for structural determination by single-crystal X-ray diffraction (0.06 x 0.08 x 0.24 mm^3) was obtained by crystallization from dichloromethane by slow evaporation under an atmosphere of nitrogen at room temperature.

Alternative synthesis to (η^6-trindane)Mn(CO)$_2$Br, 71. The synthesis of compound **2** is based on a similar synthetic method previously described in literature.[47b,96] Compounds [(η^6-Trindane)Mn(CO)$_3$][BF_4] (0.501 g, 1.18 mmol), Me_3NO (0.107 g, 1.29 mmol) and (*n*-Bu)$_4$NBr (0.566 g, 1.433 mmol) were combined in a 2-neck round bottom. The

system was evacuated and flushed with N_2 (three times) followed by the addition of CH_2Cl_2 (25 mL). The resulting red solution was left to stir under N_2 for ~2 h, after which the solvent was removed under reduced pressure. The crude product was separated by chromatography on a silica gel column (eluent hexane/acetone 50/50) affording **2** (0.425 g, 1.092 mmol, 93 %). **NOTE:** Trimethylamine *N*-oxide hydrate ($Me_3NO{\cdot}2H_2O$) was dehydrated by azeotroping the water from a toluene solution. Tetra-*n*-butylammonium bromide was purchased from Aldrich Chemical Co. and used as received.

(η^6-trindane)Mn(CO)$_2$I, 73. A 3-neck round bottom flask equipped with a stir bar was charged with [(η^6-trindane)Mn(CO)$_3$][BF_4] (0.513 g, 1.182 mmol) and *t*-BuOK (2.65 g, 23.6 mmol) and stirred under vacuum for 3 h at 40 °C. A solution of THF (25 mL) containing methyl iodide (1.47 mL, 23.6 mmol) was added by syringe under N_2, which produced a purple solution that disappeared and turned yellow-cream. This colour change persisted until all of the methyl iodide/THF solution added, as well; the reaction flask became hot through the addition. The solution was maintained at 40 °C under N_2, the solution remained orangish-cream in colour. After 20.5 h, the solvent was removed under reduced pressure and the residue, pinkish-red in colour was dissolved in CH_2Cl_2. Not all of the residue was soluble in CH_2Cl_2, therefore, the solution was filtered and extracted with H_2O (3 x 10 mL). The organic layers were combined, dried with Na_2SO_4, filtered and washed with diethyl ether. The solvent was removed under reduced pressure and dried in *vacuo*. The compound was purified by radial chromatography (chromatotron,

eluent hexane/CH_2Cl_2 20/80) giving rise to two products: (η^6-trindane)$Mn(CO)_2I$, **73**, and (η^5-$C_{15}H_{15}$)$Mn(CO)_3$, **80**.

Compound **73**: ^1H NMR (500 MHz, $CDCl_3$): δ 2.80 (m, 12H, benzylic CH_2), 2.09 (b, 6H, wingtip CH_2);^{13}C NMR (125 MHz, $CDCl_3$): δ 108.8 (aromatic C), 30.1 (benzylic CH_2), 23.7 (wingtip CH_2). As a result of the instability of the compound in solution, no ^{13}C chemical shift for Mn-CO was seen in the spectrum. IR (NaCl windows, $CDCl_3$): υ_{CO} 1973 (s), 1926 (s) cm^{-1}; MS (DEI, m/z (%)): 380 (40, $[M-2CO]^+$), 253 (10, $[M-2CO-I]^+$), 198 (100, $[C_{15}H_{18}]^+$). A sample suitable for structural determination by single-crystal X-ray diffraction (0.14 x 0.28 x 0.33 mm^3) was obtained by crystallization from dichloromethane by slow evaporation under an atmosphere of nitrogen at room temperature.

(η^5-$C_{15}H_{15}$)$Mn(CO)_2[P(OMe)_3]$, 81. A 3-neck round bottom flask equipped with a condenser and stir bar was charged with [(η^6-trindane)$Mn(CO)_3$][BF_4] (0.500 g, 1.182 mmol) and *t*-BuOK (2.65 g, 23.6 mmol) and stirred under vacuum for 3 h at 40 °C. A solution of THF (30 mL) containing $P(OMe)_3$ (2.78 mL, 23.6 mmol) was added dropwise under N_2, which produced a red solution that eventually turned orangish-brown. After 20.5 h, the solvent was removed under reduced pressure and the residue, brownish-beige in colour was dissolved in CH_2Cl_2. Not all of the residue was soluble in CH_2Cl_2, therefore, the solution was filtered and extracted with H_2O (2 x 10 mL). The organic layers were combined, dried with $MgSO_4$ and filtered. The solvent was removed by rotary evaporation and chromatographed on a silica gel column (eluent hexane/CH_2Cl_2

70/30) giving rise to two fractions; (η^5-$C_{15}H_{15}$)$Mn(CO)_2[P(OMe)_3]$, **81** (0.055 g, 0.130 mmol; 11 %), mp 124-126 °C, and (η^5-$C_{15}H_{15}$)$Mn(CO)_3$, **80** (0.080 g, 0.240 mmol; 20%), mp 87-90 °C.

Compound **81:** ^{1}H NMR (500 MHz, $CDCl_3$): δ 4.84 (m, 3H, CH), 3.38 (d, $^3J_{H-P}$ = 11.7 Hz, 9H, OCH_3), 3.04 (m, 2H, benzylic CH_2), 2.92 (m, 2H, benzylic CH_2), 2.84 (m, 2H, benzylic CH_2), 2.75 (m, 2H, benzylic CH_2), 2.16 (m, 4H, wingtip CH_2); ^{13}C NMR (125 MHz, $CDCl_3$): δ 137.9 (C6/C9 or C7/C8, C=C), 135.8 (C6/C9 or C7/C8, C=C), 100.9 (C4/C5), 87.0 (C2, CH), 68.7 (C1/C3, CH), 51.1 (OCH_3), 32.2 (benzylic CH_2), 31.8 (benzylic CH_2), 24.6 (wingtip CH_2); IR (NaCl windows, $CDCl_3$): υ_{CO} 1944 (s), 1876 (s) cm^{-1}; ^{31}P NMR (81.04 MHz, $CDCl_3$): δ 211.6 (s); MS (DEI, m/z (%)): 430 (11, $[M]^+$), 374 (100, $[M\text{-}2CO]^+$), 281(21, $[M\text{-}2CO\text{-}(OMe)_3]^+$), 251 (51, $[M\text{-}2CO\text{-}(OMe)_3\text{-}P]^+$), 195 (44, $[(C_{15}H_{15})]^+$). Anal. Calcd for $C_{20}H_{24}MnO_5P$: C, 55.82; H, 5.62. Found: C, 55.45; H, 5.96. A yellow crystalline sample (0.08 x 0.33 x 0.35 mm^3) suitable for structural determination by single-crystal X-ray diffraction studies was grown from deuterated chloroform by slow evaporation under an atmosphere of nitrogen at low temperatures.

Compound **80:** ^{1}H NMR (200 MHz, $CDCl_3$): δ 5.03 (d, 2H, CH), 4.94 (t, 1H, CH), 2.93 (m, 4H, benzylic CH_2), 2.79 (m, 4H, benzylic CH_2), 2.13 (m, 4H, wingtip CH_2); ^{13}C NMR (50 MHz, $CDCl_3$): δ 225.4 (Mn-CO), 139.4 (C6/C9 or C7/C8, C=C) 135.2 (C6/C9 or C7/C8, C=C), 101.1 (C4/C5), 87.4 (C2, CH), 69.7 (C1/C3, CH), 32.1 (benzylic CH_2), 25.5 (wingtip CH_2), 32.1 (benzylic CH_2). The instability of the compound in solution is apparent from the presence of signals in the ^{13}C NMR spectrum, which correspond to the trindane ligand (δ 137.7 (aromatic CH), 31.7 (CH_2) and 25.5 (CH_2)). IR (NaCl windows,

$CDCl_3$): υ_{CO} 2016 (s), 1934 (s) cm^{-1}; MS (DEI, m/z (%)): 334 (13, $[M]^+$), 306 (3, $[M-CO]^+$), 278 (15, $[M-2CO)]^+$), 250 (90, $[M-3CO]^+$), 195 (100, $[C_{15}H_{15}]^+$), 115 (7, $[C_9H_7]^+$). A yellow crystalline sample (0.04 x 0.22 x 0.42 mm^3) suitable for structural determination by single-crystal X-ray diffraction studies was grown from deuterated chloroform by slow evaporation under an atmosphere of nitrogen at low temperatures.

(η^5-$C_{15}H_{15}$)Mn(CO)$_2$[PPh$_3$], 83. A 3-neck round bottom flask equipped with a condenser and stir bar was charged with [(η^6-trindane)Mn(CO)$_3$][BF_4] (0.500 g, 1.182 mmol) and *t*-BuOK (2.65 g, 23.6 mmol) and stirred under vacuum for 3 h at 40 °C. A solution of THF (30 mL) containing PPh_3 (619 g, 23.6 mmol) was added dropwise under N_2, which produced a brown solution that eventually turned orange. After 20.5 h, the solvent was removed under reduced pressure and the residue, dark green-black in colour was dissolved in CH_2Cl_2. The solution was extracted with H_2O (3 x 10 mL). The organic layers were combined, dried with $MgSO_4$ and filtered. The solvent was removed by rotary evaporation and the mixture was purified using a chromatotron (eluent hexane/CH_2Cl_2 90/10) giving rise to three fractions; (η^5-$C_{15}H_{15}$)Mn(CO)$_3$, PPh_3, and (η^5-$C_{15}H_{15}$)Mn(CO)$_2$[PPh_3], **83**, (0.060g, 0.1056 mmol; 9 %), 179-180 °C (dec). Compound **83**: ^{1}H NMR (500 MHz, $CDCl_3$): δ 7.31 (m, 15H, aromatic CH), 4.60 (d, 2H, CH), 4.47 (m, 1H, CH), 2.51 (m, 8H, benzylic CH_2), 2.08 (m, 4H, wingtip CH_2); ^{13}C NMR (125 MHz, $CDCl_3$): δ 138.1, 137.8, 136.1, 133.1 (J_{C-P} = 10.4 Hz), 129.5, 128.1 (J_{C-P} = 9.3 Hz), 100.7 (C4/C5), 89.0 (C2, CH), 70.7 (C1/C3, CH), 32.3 (benzylic CH_2), 32.0 (benzylic CH_2), 24.6 (wingtip CH_2); ^{31}P NMR (81.04 MHz, $CDCl_3$): δ 94.3; IR (NaCl windows,

$CDCl_3$): υ_{CO} 1929 (s), 1862 (s) cm^{-1}; MS (DEI, m/z (%)): 569 (100, $[M+1]^+$), 512 (58.3, $[M-2CO]^+$), 195 (62.5, $[C_{15}H_{15}]^+$); MS (CI, NH_3, m/z (%)): 569 (100, $[M+1]^+$), 512 (58, $[M-2CO]^+$), 195 (63, $[C_{15}H_{15}]^+$).

[(η^6-indane)Mn(CO)$_3$][BF$_4$], 84. A mixture of $Mn(CO)_5Br$ (1.08 g, 4.029 mmol) and $AgBF_4$ (0.78 g, 4.029 mmol) in dry CH_2Cl_2 (40 mL) was heated to reflux for 3 h under nitrogen, and then cooled to room temperature. To the reaction mixture, a solution of indane (0.493 mL, 4.029 mmol) in dry CH_2Cl_2 (10 mL) was added, and heating was continued for an additional 18 h. After cooling and filtration, the filtrate was passed through Celite and concentrated to approximately one-third its volume under pressure, and excess hexane (80 mL) was added. The resulting yellow solid was filtered and dried *in vacuo* to furnish **84**, (0.658 g, 1.918 mmol, 50 %). ^1H NMR (200 MHz, CD_2Cl_2): δ 6.53 (m, 4H, aromatic), 3.03 (m, 4H, benzylic CH_2), 2.44 (m, 1H, wingtip CH_2), 2.10 (m, 1H, wingtip CH_2); ^{13}C NMR (50 MHz, CD_2Cl_2): δ 227.2 (Mn-CO), 99.3 (aromatic C), 98.2 (aromatic C), 32.2 (benzylic CH_2), 23.7 (wingtip CH_2); IR (NaCl windows, $CDCl_3$): υ_{CO} 2065 (s), 2008 (s) cm^{-1}; MS (Positive ESI, m/z (%)): 258 (M+1, 24 % of $[M]^+$), 257 (100, $[M]^+$), 229 (5.3, $[M-CO]^+$), 201 (2.7, $[M-2CO]^+$), 173 (1.9, $[M-3CO]^+$). Anal. Calcd $C_{12}H_{10}O_3MnBF_4$: C, 41.90; H, 2.93. Found C, 41.69; H, 2.76.

[(η^5-indenyl)Mn(CO)$_2$PPh$_3$], 85. A 3-neck round-bottom flask equipped with a condenser and stir bar was charged with [(η^6-indane)Mn(CO)$_3$][BF$_4$] (0.106 g, 0.3089 mmol) and *t*-BuOK (0.693 g, 6.178 mmol) and stirred under vacuum for 3 h at 40 °C. A solution of THF (35 mL) containing PPh_3 (1.620 g, 6.178 mmol) was added dropwise

under N_2, and produced a reddish-orange solution. After ~22 h, the solvent was removed under reduced pressure and the residue, brown in colour was dissolved in CH_2Cl_2 and filtered. The orange solution was extracted with H_2O (3 x 10 mL). The organic layers were combined, dried with $MgSO_4$ and filtered. The solvent was removed by rotary evaporation and give rise to **85** (0.017 g, 0.0348 mmol, 11 %). ^1H NMR (300 MHz, CD_2Cl_2): δ 7.09 (m, 19H, aromatic C and CH=CH), 4.65 (m, 3H, Cp); ^{13}C NMR (75 MHz, $CDCl_3$): δ 232.8 (Mn-CO), 133.7, 133.5, 130.1, 128.6, 128.5, 126.1, 125.9, 90.1 (Cp), 72.9 (Cp); ^{31}P NMR (81.05 MHz, CD_2Cl_2): δ 92.4 (s); IR (NaCl windows, $CDCl_3$): ν_{CO} 1934 (s), 1866 (s) cm^{-1}; MS (DEI, *m/z* (%)): 488 (6 $[M]^+$), 432 (92, $[M-2CO]^+$), 377 (1, $[M-2CO-Mn]^+$), 115 (100, $[C_9H_7]^+$).

(η^5-indenyl)Mn(CO)$_2$[P(OMe)$_3$] , 86. A 3-neck round-bottom flask equipped with a condenser and stir bar was charged with [(η^6-indane)Mn(CO)$_3$][BF_4] (0.500 g, 1.457 mmol) and *t*-BuOK (3.27g, 29.0 mmol) and stirred under vacuum for 3 h at 40 °C. A solution of THF (30 mL) containing $P(OMe)_3$ (619 g, 23.6 mmol) was added dropwise under N_2, and produced a reddish-orange solution. After ~22 h, the solvent was removed under reduced pressure and the residue, red in colour, was dissolved in CH_2Cl_2 and filtered. The yellow solution was extracted with H_2O (3 x 10 mL). The organic layers were combined, dried with $MgSO_4$ and filtered. The solvent was removed by rotary evaporation and yielded **86** (0.001 g, 2.857 mmol, 2%). ^1H NMR (200 MHz, $CDCl_3$): δ 7.40 (m, 2H, CH=CH), 7.02 (m, 2H, CH=CH), 4.97 (m, 2H, CH), 4.83 (m, 1H, CH), 3.42 (d, 9H, $^3J_{C-P}$ = 11.7 Hz, OCH_3); ^{31}P NMR (81.05 MHz, CD_2Cl_2): δ 211.4 (s). IR (NaCl

windows, $CDCl_3$): ν_{CO} 1950 (s), 1881 (s) cm^{-1}. MS (DEI, *m/z* (%)): 350 (12, $[M]^+$), 322 (5, $[M\text{-}CO]^+$), 294 (100, $[M\text{-}2CO]^+$), 170 (29, $[C_9H_7Mn]^+$), 115 (41, $[C_9H_7]^+$).

[(η^6-trindane)Mn(CO){P(OMe)$_3$}$_2$][BF$_4$], 98. [(η^6-trindane)Mn(CO)$_3$][BF_4] (0.463 g, 1.095 mmol) and Me_3NO (0.173 g, 2.307 mmol) were stirred in CH_2Cl_2 (55 mL) under N_2. To the yellow solution was added $P(OMe)_3$ (0.20 mL, 1.696 mmol) which resulted in the solution turning red instantaneously. The solution was allowed to stir under N_2 for 6 h at room temperature; the solvent was removed under reduced pressure. The compound was purified by chromatographic separation on a silica gel column (eluent CH_2Cl_2/acetone 90/10) giving rise to two fractions. The first was fraction was identified as trindane and the second was compound **98** (0.071 g, 0.115 mmol, 11 %), mp 88-90 °C. Compound **98**: ^1H NMR (300 MHz, CD_2Cl_2): δ 3.71 (t, 18H, $^3J_{P\text{-}H}$ = 5.0 Hz, $P(OMe)_3$), 2.74 (m, 12H, benzylic CH_2), 2.08 (m, 6H, wingtip CH_2); ^{13}C NMR (75 MHz, CD_2Cl_2): δ 111.7 (aromatic C), 54.5 (OCH_3), 30.4 (benzylic CH_2), 23.2 (wingtip CH_2); ^{31}P NMR (121.509 MHz, CD_2Cl_2): δ 185.5 (s); IR (NaCl windows, $CDCl_3$): υ_{CO} 1911 (s) cm^{-1}; MS (Positive ESI, m/z (%)): 529 (100, $[M^+]$), 405 (2.96, $[M\text{-}P(OMe)_3]^+$), 377 (7.69, $[M\text{-}P(OMe)_3\text{-}CO]^+$). A sample suitable for structural determination by single-crystal X-ray diffraction (0.18 x 0.42 x 0.44 mm^3) was obtained by crystallization from dichloromethane by slow evaporation under an atmosphere of nitrogen at room temperature.

[(η^6-trindane)Re(CO)$_3$][PF$_6$], 99. In a 100 mL round bottom, $BrRe(CO)_5$ (0.944 g, 2.324 mmol), trindane (0.765 g, 3.864 mmol), $AlCl_3$ (1.630 g, 12.22 mmol) and

petroleum ether (55 mL) were heated to reflux under nitrogen for 16.5 h. The solution was cooled in an ice-bath followed by addition of an ice-water slush (25 mL). The pet. ether layer was decanted and the remaining H_2O layer was washed with cold ethyl ether followed by the addition of excess NH_4PF_6 in water (5 mL). The resultant white precipitate (0.028 g, 0.0456 mmol, 2 %) was filtered and washed with cold water and methanol. ^1H NMR (500 MHz, CD_2Cl_2): δ 3.38 (m, 6H, benzylic CH_2), 2.95 (m, 6H, benzylic CH_2), 2.44 (m, 3H, wingtip CH_2), 1.91 (m, 3H, wingtip CH_2); ^{13}C NMR (125.773 MHz, CD_2Cl_2): δ 185.7 (Re-CO), 118.7 (aromatic C), 30.4 (benzylic CH_2), 24.7 (wingtip CH_2); IR (KBr pellet): υ_{CO} 2052 (s), 1956 (s) cm^{-1}; IR (NaCl windows, $CDCl_3$): υ_{CO} 2058 (s), 1966 (s) cm^{-1}; MS (Positive ESI, m/z (%)): 469 (100, $[M]^+$).

Attempted synthesis of [(η^6-$(CH_3)_{12}C_{15}H_6$)FeCp][PF_6], 100. [(η^6-$C_{15}H_{18}$)FeCp][PF_6] (0.124 g, 0.267 mmol) and potassium *tert*-butoxide (7.20 g, 64 mmol) were stirred together under vacuum for 3 h, and then an inert atmosphere was maintained. A solution of methyl iodide (3.98 mL, 64 mmol) in freshly distilled THF (60 mL) was introduced by syringe. Upon addition, the solution became deep red in colour and continued to change colour (dark purple to mauve to pink) until the solution remained yellowish-cream in colour. The solution was maintained under nitrogen at 40 °C for 48 h in the dark. The solvent was then removed under vacuum; the beige-brown residue was treated with CH_2Cl_2 and extracted with water. The organic layers were combined, dried with Na_2SO_4, filtered and washed with diethyl ether. The solvent was removed under pressure and dried in *vacuo*. The crude product was chromatographed on a neutral alumina column

(eluent hexane/acetone 90/10) affording three orange products. ^{1}H and ^{13}C NMR appeared of each fraction still appeared to be a mixture of compounds. Similarly positive ESI mass spectrometric data exhibited signals at *m/z* 459, 473 and 487 corresponding to the incorporation of 10, 11 and 12 methyl groups, respectively. Two samples suitable for structural determination by single-crystal X-ray diffraction (0.20 x 0.28 x 0.54 and 0.08 x 0.16 x 0.60 mm^3) were obtained by crystallization from hexanes/acetone mixture; however, the structure has not been satisfactorily refined as a result of a disorder in the trindane fragment.

Attempted synthesis of $[(\eta^6\text{-}(CH_2CHCH_2)_{12}C_{15}H_6)FeCp][PF_6]$, 101. $[(\eta^6\text{-}C_{15}H_{18})FeCp][PF_6]$ (0.233 g, 0.502 mmol) and potassium *tert*-butoxide (13.5 g, 120 mmol) were stirred together under vacuum for 3 h, and then an inert atmosphere was maintained. A solution of allyl bromide (10.43 mL, 120 mmol) in freshly distilled THF (60 mL) was introduced by syringe. Upon addition, the solution became deep red in colour and continued to change colour (pink to violet to mauve) until the solution remained yellowish-cream in colour. The solution was maintained under nitrogen at 40 °C for 72 h in the dark. The solvent was then removed under vacuum; the beige-brown residue was treated with CH_2Cl_2 and extracted with water. The organic layers were combined, dried with Mg_2SO_4, filtered and washed with diethyl ether. The solvent was removed under pressure and dried in *vacuo*. The crude product was chromatographed on a neutral alumina column (eluent hexane) affording two yellow products. ^{1}H and ^{13}C NMR appeared of each fraction still appeared to be a mixture of compounds. Similarly positive ESI mass spectrometric data exhibited signals consistent with the incorporation

of 12 allyl groups at *m/z* 799, followed by consecutive losses of multiples of 40 to a *m/z* of 319 (which corresponds to $[\eta^6\text{-}C_{15}H_{18})FeCp]^+$).

Reduction of Dibenzosuberone, 105. Procedure outlined in literature was followed.[116] In a 100 ml two-neck round bottom equipped with a condenser and a dropping funnel iodine (1.00 g, 4.00 mmol) and acetic acid (50 mL) were stirred under N_2 for ~5 min. Hypophosphorous acid, 50 % aq. (2 mL, 19.3 mmol) was added and the solution was heated to a reflux. A solution of dibenzosuberone and acetic acid (15 mL) was added to the refluxing solution over ~ 45 min. The solution was heated to reflux for an additional 24 h, cooled, diluted with H_2O (150 mL) and extracted with hexanes (4 x 75 mL). The hexane layer was dried with $MgSO_4$, filtered and rotary evaporated yielding yellow crystals of dibenzosuberane (1.784 g. 9.195 mmol, 77 %). ^{1}H NMR (200 MHz, $CDCl_3$): δ 7.32 (m, 8H, aromatic CH), 4.24 (s, 2H, CH_2), 3.29 (s, 4H, CH_2); ^{13}C NMR (50 MHz, $CDCl_3$) : δ 139.2, 138.9, 129.5, 128.9, 126.4, 125.9, 40.8, 32.4; MS (DEI, m/z (%)): 194 (100, $[M^+]$); MS (CI, NH_3, m/z (%)): 212 (100, $[M + NH_3]$), 194 (20.6, $[M^+]$).

$[(\eta^6$-dibenzosuberane)$Mn(CO)_3][BF_4]$, 102. A mixture of $Mn(CO)_5Br$ (1.90 g, 6.92 mmol) and $AgBF_4$ (1.48 g, 7.61 mmol) in dry CH_2Cl_2 (50 mL) was heated to reflux for 3 h under nitrogen and then cooled to room temperature. To the reaction mixture a solution of dibenzosuberane (1.78 g, 9.20 mmol) in dry CH_2Cl_2 (15 mL) was added, and the reaction mixture was heated overnight. After cooling and filtration, the filtrate was passed through Celite and concentrated to approximately one-third its volume under pressure, and excess hexane (100 mL) was added. The resulting yellow solid was filtered

and dried in *vacuo* furnishing **102** (0.301 g, 0.718 mmol, 10 %), mp 218-220 °C. ^{1}H NMR (500 MHz, acetone-d_6): δ 7.38 (d, 1H, $^{3}J_{H-H}$ = 7.3 Hz, H7/H10), 7.31 (m, 2H, H8, H9), 7.25 (t, 1H, $^{3}J_{H-H}$ = 7.1, H7/H10), 7.13 (d, 1H, $^{3}J_{H-H}$ = 6.6 Hz, H1/H4), 6.91 (t, 1H, $^{3}J_{H-H}$ = 6.3 Hz, H2/H3), 6.58 (t, 2H, $^{3}J_{H-H}$ = 6.3 Hz, H1/H3 or H2/H4), 4.48 (d, 1H, $^{3}J_{H-H}$ = 15.5 Hz, H11a/H11b), 4.31 (d, 1H, $^{3}J_{H-H}$ = 15.5 Hz, H11a/H11b), 3.44 (m, 3H, H6a/H6b, H5a/H5b), 3.27 (m, 1H, H6a/H6b, H5a/H5b); ^{13}C NMR (125.773 MHz, acetone-d_6): δ 216.4 (Mn-CO), 139.6 (C12/C15), 138.6 (C12/C15), 130.2 (C8/C9), 129.8 (C7/C10), 129.4 (C8/C9), 128.0 (C7/C10), 123.7 (C14/C15), 118.6 (C14/C15), 105.5 (C1/C4), 103.1 (C2/C3), 100.6 (C2/C3), 97.3 (C2/C3 or C2/C4), 38.4 (C11), 32.1 (C5/C6); IR (NaCl windows, $CDCl_3$): υ_{CO} 2065 (s), 2014 (s) cm^{-1}; MS (Positive ESI, m/z (%)): 333 (100, [M^{+}]), 277 (6.15, [M-2CO]), 249 (17.75, [M-3CO]) . A sample suitable for structural determination by single-crystal X-ray diffraction (0.12 x 0.28 x 0.42 mm^3) was obtained by crystallization from acetone at room temperature.

[(η^6-tetralin)Mn(CO)$_3$][PF$_6$], 103. Prepared as described in literature.[114] $Mn(CO)_5Br$ (1.97 g, 7.16 mmol), $AlCl_3$ (1.91 g, 0.0143 mmol), tetralin (1.88 mL, 0.0138 mmol) and cyclohexane (50 mL) were heated to reflux for 5 h under N_2. The solution was cooled followed by the addition of ice-cold H_2O (40 mL). To the aqueous layer, NH_4PF_6 (2.21 g, 0.0138 mmol) was added forming a yellow precipitate, which was filtered and dried under *vacuo*. The product (2.383 g, 5.73 mmol, 80 %) was recrystallized with a mixture of acetone and diethyl ether followed by gravity filtration. Complete assignment of this compound had not been published prior to this study. ^{1}H NMR (200 MHz, acetone-d_6):

δ 6.84 (s, 4H, CH), 3.13 (m, 4H, CH_2), 2.30 (m, 4H, CH_2); ^{13}C NMR (50 MHz, acetone-d_6): δ 216.9, 119.5, 101.9, 99.8, 28.2, 21.6; IR (NaCl windows, $CDCl_3$): υ_{CO} 2068 (s), 2025(s), 2003(s) cm^{-1}, Lit. values (NaCl): υ_{CO} 2056(s), 2016(s); MS (Positive ESI, m/z (%)): 271 (100, [M^+]), 243 (7.7, [M-CO]), 214 (23.1, [M-2CO]), 187 (7.1, [M-3CO]).

[(η^6-tetralin)Mn(CO)$_2$P(OMe)$_3$][PF$_6$], 117. To a 100 mL schlenk flask equipped with a stir bar was charged with [(η^6-tetralin)Mn(CO)$_3$][PF$_6$] (0.902 g, 2.168 mmol) and evacuated and purged with N_2 three times. A solution of THF (30 mL) containing $P(OMe)_3$ (5.11 mL, 43.4 mmol) was added dropwise under N_2, the solution was yellow in colour. The solution was stirred for 20 h under N_2. The solvent was removed under reduced pressure. The residue was dissolved in CH_2Cl_2 and hexanes, a precipitate formed and it was filtered. The remaining solution was chromatographed on a silica gel column (eluent 100 % hexane) affording **117**, a yellow compound (0.658 g, 1.285 mmol, 59 %), mp 86-88 °C. ^1H NMR (200 MHz, $CDCl_3$): δ 5.94 (m, 4H, aromatic CH), 3.70 (t, 9H, $^3J_{H-P}$ = 11.6 Hz, OCH_3), 2.73 (m, 4H, CH_2), 1.79 (m, 4H, CH_2); ^{13}C NMR (50 MHz, $CDCl_3$): δ 220.3 (d, $^2J_{C-P}$ = 43.2 Hz, Mn-CO), 113.9 (C1/C6), 97.8 (C2/C5 or C3/C4), 96.7 (C2/C5 or C3/C4), 54.1 (d, $^2J_{C-P}$ = 7.3 Hz, OCH_3), 27.5 (C7/C10), 21.1 (C7/C10); ^{31}P NMR (81.04 MHz, $CDCl_3$): δ 182.1(s, $P(OMe)_3$), -167.4 (septet, PF_6); IR (NaCl windows, $CDCl_3$): υ_{CO} 2008 (s), 1961 (s) cm^{-1}; MS (Positive ESI, m/z (%)): 367 (100, [M^+]), 311 (18.7, [M-2CO]). A yellow crystalline sample (0.32 x 0.45 x 0.70 mm^3) suitable for structural determination by single-crystal X-ray diffraction studies was grown

from a mixture of deuterated chloroform by slow evaporation under an atmosphere of nitrogen at room temperature.

(η^5-$C_{20}H_{23}$) Mn(CO_3), 124. To a round bottom flask equipped with a stir bar was charged with [(η^6-tetralin)Mn$(CO)_3$][PF_6] (0.952 g, 2.288 mmol) and *t*-BuOK (5.14 g, 45.8 mmol) and evacuated and purged with N_2 three times. This was followed by the addition of THF (30 mL) under N_2, which produced a dark orange-brown solution. The solution was stirred for 6 h under N_2. The solvent was removed under pressure and the residue was dissolved in methylene chloride. Hexanes was added to the solution and filtered. The solvent was removed by rotary evaporation yielding a yellow-orange compound that was chromatotron (eluent hexane with gradual addition of CH_2Cl_2) furnishing **124** (0.114 g, 0.284 mmol, 12 %). IR (NaCl windows, neat): υ_{CO} 2007 (s), 1927 (s) cm^{-1}; MS (CI, NH_3, m/z (%)): 403 (100, $[M+1]^+$), 271 (57, $[M-C_{10}H_{11}]^+$), 187 (3, $M-C_{10}H_{11}-3CO]^+$, 131 (8, $[C_{10}H_{11}]^+$).

[(η^5-$C_{15}H_{13}$)Mn$(CO)_3$], 125. To a round bottom flask equipped with a stir bar was charged with [(η^6-dibenzosuberane)Mn$(CO)_3$][BF_4] (0.377 g, 0.899 mmol) and *t*-BuOK (2.02 g, 17.99 mmol) and evacuated and purged with N_2 three times. This was followed by the addition of THF (25 mL) under N_2, which produced a dark red-brown-orange solution. The solution was stirred for 4 h under N_2. The solvent was removed under pressure and the residue was dissolved in Et_2O. Water (40 mL) was added to the ether solution and extracted with Et_2O (2 x 10 mL). The organic layers were combined, dried with $MgSO_4$ and filtered. The solvent was removed by rotary evaporation yielding a red-

orange compound that was chromatotron (eluent hexane with gradual addition of CH_2Cl_2) furnishing **125**, an orange powder (0.131 g, 0.395 mmol, 44 %). ^1H NMR (500 MHz, CD_2Cl_2): δ 7.05 (m, 4H, aromatic CH), 5.61 (t, 1H, $^3J_{H-H}$ = 5.1 Hz, CH), 5.18 (t, 1H, $^3J_{H-H}$ = 6.3 Hz, CH), 5.09 (d, 1H, $^3J_{H-H}$ = 5.3 Hz, CH), 4.41 (d, 1H, $^3J_{H-H}$ = 7.3 Hz, CH), 4.10 (s, 1H, CH), 3.23 (m, 2H, CH_2), 2.47 (m, 2H, CH_2); ^{13}C NMR (125 MHz, CD_2Cl_2): δ 222.4 (Mn-CO), 138.7, 133.5, 130.1, 129.5, 126.6, 125.3, 106.7, 100.3, 98.6, 74.8, 74.6, 60.8, 38.0, 36.4, 32.9; IR (NaCl windows, $CDCl_3$): υ_{CO} 2022 (s), 1950 (s) cm^{-1}; MS (DEI, m/z (%)): 332 (2, $[M^+]$), 276 (3.2, $[M-2CO]^+$), 248 (3.2, $[M-3CO]^+$), 193 (100, $[C_{15}H_{13}]^+$). A rod-shaped, orange crystalline sample (0.03 x 0.05 x 0.50 mm^3) suitable for structural determination by single-crystal X-ray diffraction studies was grown from a mixture of methylene chloride and deuterated methylene chloride by slow evaporation under an atmosphere of nitrogen at room temperature.

[(η^6-Hexaethylbenzene)Mn(CO)$_3$][BF$_4$], 147. A mixture of $Mn(CO)_5Br$ (2.48 g, 9.03 mmol) and $AgBF_4$ (1.75 g, 9.03 mmol) in dry CH_2Cl_2 (50 mL) was heated to reflux for 3 h under nitrogen and then cooled to room temperature. To the reaction mixture, a solution of hexaethylbenzene (2.23 g, 9.03 mmol) in dry CH_2Cl_2 (20 mL) was added, and heating was continued for 16 h. After cooling and filtration, the filtrate was passed through Celite and concentrated to approximately one-third its volume under pressure, and excess hexane (100 mL) was added. The resulting orange-yellow solid was filtered and dried in *vacuo* furnishing **147** (3.34 g, 7.08 mmol, 79 %), 266 °C (dec). ^1H NMR (500 MHz, CD_2Cl_2): δ 1.41 (broad singlet, 12H, CH_2), 2.68 (broad singlet, 18H, CH_3).

At 173 K, a splitting is observed for the methylene protons at 2.56 and 2.45 ppm. ^{13}C NMR (125 MHz, CD_2Cl_2): δ 217.8 (Mn-CO), 120.3 (aromatic C), 22.6 (CH_3), 17.1 (CH_2). At 203 K, the aromatic, methylene and methyl signals are split into two (aromatic 124.0 and 113.6, methylene 23.2 and 19.7, methyl 20.0 and 13.6 ppm). IR (NaCl windows, $CDCl_3$): υ_{CO} 2058 (s), 1996 (s) cm^{-1}; MS (Positive ESI, m/z (%)): 385 (100, $[M]^+$), 386 ([M+1], 24 % of M^+), 357 (0.5, $[M-CO]^+$), 329 (1.2, $[M-2CO]^+$), 301 (0.5, $[M-3CO]^+$).

(η^6-Hexaethylbenzene)Mn(CO)$_2$Br, 148. A mixture of [(η^6-hexaethylbenzene) $Mn(CO)_3][BF_4]$, (0.559 g, 1.187 mmol), Me_3NO (0.089 g, 1.187 mmol) and $(n\text{-}Bu)_4NBr$ (0.462 g, 1.463 mmol) were placed in a two neck round bottom and evacuated. This was followed by the addition of dry CH_2Cl_2 (30 mL), the resulting solution was deep red in colour. The solution was stirred for 2 h under N_2. The solvent was removed under pressure and chromatographed on a silica gel column (eluent hexane/acetone 50/50) giving rise to a red/purple solid, **148** (0.356 g, 0.819 mmol, 69 %), mp 127 - 129 °C. ^1H NMR (500 MHz, CD_2Cl_2): δ 2.67 (s, H), 1.21 (s, 18H); ^{13}C NMR (50.323 MHz, CD_2Cl_2): δ 230.3 (Mn-CO), 112.0 (aromatic C), 22.6 (CH_3), 16.3 (CH_2); IR (NaCl windows, $CDCl_3$): υ_{CO} 1974 (s), 1927 (s) cm^{-1}; MS (DEI, m/z (%)): 357 (1.08, $[M-Br]^+$), 329 (1.62, $[M-Br-CO]^+$), 301 (4.59, $[M-Br-2CO]^+$), 246 (100, $[C_{18}H_{30}]^+$); MS (CI, NH_3, m/z (%)): 357 (1.08, $[M-Br]^+$), 329 (2.16, $[M-Br-CO]^+$), 301 (13.5, $[M-Br-2CO]^+$), 246 (100, $[C_{18}H_{30}]^+$). A sample suitable for structural determination by single-crystal X-ray diffraction (0.25 x 0.32 x 0.55 mm^3) was obtained by crystallization from a mixture of

pentane/acetone by slow evaporation under an atmosphere of nitrogen at room temperature.

8.0 REFERENCES

1. (a) Wilkinson, G.; Rosenblum, M.; Whiting, M. C.; Woodward, R. B. *J. Am. Chem. Soc.* **1952**, *74*, 2125. (b) Miller, S. A.; Tebboth, J. A.; Tremaine, J. F. *J. Chem. Soc* **1952**, 632. (c) Kealy, T. J.; Pauson, P. L. *Nature* **1961**, *168*, 1039.

2. Bochmann, M. *Organometallics 2: Complexes with Transition Metal-Carbon π-bonds*; Oxford University Press: New York, **1994**, p. 1.

3. Crabtree, R. H. *The Organometallic Chemistry Of Transition Metals*; John Wiley & Sons: New York, **1988**, pp. 113-114.

4. (a) Dickson, R. S.; Wilkinson, G. *J. Chem. Soc.* **1964**, 2699. (b) McCleverty, J. A.; Wilkinson, G. *J. Chem. Soc.* **1964**, 4200.

5. (a) Harman, W. D.; Taube, H. *J. Am. Chem. Soc.* **1987**, *109*, 1883. (b) Harman, W. D.; Sekine, M.; Taube, H. *J. Am. Chem. Soc.* **1988**, *110*, 5725. (c) Brooks, B. C.; Gunnoe, T. B.; Harman, W. D. *Coord. Chem. Rev.* **2000**, *206-207*, 3 and references therein.

6. Cotton, F. A. *J. Am. Chem. Soc.* **1968**, *90*, 6230.

7. (a) Fischer, E. O.; Öfele, K.; Essler, H.; Fröhlich, W.; Mortensen, J. P.; Semmlinger, W. *Chem. Ber.* **1958**, *91*, 2763. (b) King, R. B.; Fronzaglia, A. *Inorg. Chem.* **1966**, *5*, 1837.

8. Woo, K.; Carpenter, G. B.; Sweigart, D. A. *Inorg. Chim. Acta* **1994**, *220*, 297.

9. (a) Rodgers, R. D.; Atwood, J. L.; Albright, T. A.; Lee, W. A.; Rausch, M. D. *Organometalics* **1984**, *3*, 263. (b) Elschenbroich, C.; Möckel, R.; Vasil'kov, A.; Metz, B.; Harms, K. *Eur. J. Inorg. Chem.* **1998,** 1392.

10. (a) Fischer, E. O.; Öfele, K.; Essler, H.; Fröhlich, W.; Mortensen, J. P.; Semmlinger, W. *Z. Naturforsch* **1958**, *13b*, 458. (b) Nicholls, B.; Whiting, M. C. J. Chem. Soc. 1959, 551. (c) Natta, G.; Ercoli, R.; Calderazzo, F.; Santambrogio, S. *Chim. Ind. (Milan)* **1958**, *40*, 1003.

11. Fischer, E. O.; Kögler, H. P. *Chem. Ber.* **1957**, *90*, 250.

12. (a) Green, M. L. H.; Pratt, L.; Wilkinson, G. *J. Chem. Soc.* **1960**, 989. (b) Nesmeyanov, A. N.; Vol'kenau, N. A.; Bolesova, I. N. *Tetrahedron Lett.* **1963**, 1725. (c) King, R. B. *Organometal. Syn.* **1965**, *1*, 138.

13. Braga, D.; Dyson, P. J.; Greponi, F.; Johnson, B. F. G. *Chem. Rev.* **1994**, *94*, 1585 and references therein.

14. Top, S.; Jaouen, G. *J. Organomet. Chem.* **1979**, *182*, 381.

15. Fischer, E. O.; Hafner, W. *Z. Anorg. Allg. Chem.* **1956**, *286*, 146.

16. Brown, D. A.; Hughes, F. J. *J. Chem. Soc. A* **1968**, 1519.

17. Bennett, M. A.; Smith, A. K. *J. Chem. Soc., Dalton Trans.* **1974**, 233.

18. Munro, G. A.; Pauson, P. L. *Anorg. Allg. Chem.* **1979**, *458*, 211.

19. (a) McGlinchey, M. J.; Hao, N.; Sayer, B. G.; Tan, T. -S. *J. Organomet. Chem.* **1980**, *194*, 325. (b) Laposa, J. D.; Hao, N.; Sayer, B. G.; McGlinchey, M. J. *J. Organomet. Chem.* **1980**, *195*, 193. (c) Hao, N.; McGlinchey, M. J. *J. Organomet. Chem.* **1978**, *161*, 381. (d) Agarwal, A.; McGlinchey, M. J.; Tan, T. -S. *J. Organomet. Chem.* **1977**, *141*, 85. (e) McGlinchey, M. J.; Tan, T. -S. *J. Am. Chem. Soc.* **1976**, *98*, 2271.

20. (a) Hein, F. *Chem. Ber.* **1919**, *52*, 195. (b) Hein, F. *Chem. Ber.* **1921**, *54*, 1905.

21. (a) Zeiss, H. H.; Herwig, W. *J. Am. Chem. Soc.* **1956**, *78*, 5959. (b) Zeiss, H. H.; Tsutsui, M. *J. Am. Chem. Soc.* **1957**, *79*, 3062.

22. (a) Fischer, E. O.; Hafner, W. *Z. Naturforsch., B* **1955**, *10*, 665. (b) Fischer, E. O.; Seus, D. *Chem. Ber.* **1956**, *89*, 1809. (c) Coffield, T. H.; Sandel, V.; Closson, R. D. *J. Am. Chem. Soc.* **1957**, *79*, 5826.

23. Bhasin, K. K.; Balkeen, W. G.; Pauson, P. L. *J. Organomet. Chem.* **1981**, *204*, C25.

24. (a) Jeong, E.; Chung, Y. K. *J. Organomet. Chem.* **1992**, *434*, 225. (b) Miles, W. H.; Smiley, P. M; Brinkman, H. R. *J. Chem. Soc., Chem. Commun.* **1989**, 1897. (c) Miles, B. H.; Brinkman, H. R. *Tetrahedron Lett.* **1992**, *33*, 589. (d) Krow, G. R.; Miles, W. H.; Smiley, P. M.; Lester, W. S.; Kim, Y. J. *J. Org. Chem.* **1992**, *57*, 4040.

25. Ryan, W. J.; Peterson, P. E.; Cao, Y.; Williard, P. G.; Sweigart, D. A.; Baer, C. D.; Thompson, C. F.; Chung, J. K.; Chung, T. -M. *Inorg. Chim. Acta* **1993**, *211*,1.

26. Woo, K.; Williard, P. G.; Sweigart, D. A.; Duffy, N. W.; Robinson, B. H.; Simpson, J. *J. Organomet. Chem.* **1995**, *487*, 111.

27. (a) Lee, Y. -A.; Chung, Y. K.; Kim, Y.; Jeong, J. H. *Organometallics* **1990**, *9*, 2851. (b) Jeong, E.; Chung, Y. K. *J. Organomet. Chem.* **1992**, *434*, 225. (c) Lee, S. S.; Lee, J. -S.; Chung, Y. K. *Organometallics* **1993**, *12*, 4640. (d) Chaffee, S. C.; Sutton, J. C.; Babbitt, C. S; Maeyer, J. T.; Guy, K. A.; Pike, R. D. *Organometallics* **1998**, *17*, 5586.

28. Rybinskaya, M. I.; Kaganovich, V. S.; Kydinov, A. R. *Izv. Akad. Nauk SSR, Ser. A. Khim* **1984**, 885.

29. Jackson, J. D.; Villa, S. J.; Bacon, D. S.; Pike, R. D. *Organometallics* **1994**, *13*, 3972.

30. Stobart, S. R.; Zaworotko, M. J. *J. Chem. Soc.; Chem. Commun.* **1984**, 1700.

31. Sun, S.; Yeung, L. K.; Sweigart, D. A.; Lee, T. -Y.; Lee, S. S.; Chung, Y. K.; Switzer, S. R.; Pike, R. D. *Organometallics* **1995**, *14*, 2613.

32. Sun, S; Dullaghan, C. A.; Sweigart, D. A. *J. Chem. Soc.; Dalton Trans.* **1996**, 4493.

33. Pape, A. R.; Kaliappan, K. P.; Kündig, E. P. *Chem. Rev.* **2000**, *100,* 2917, and references therein.

34. Kane-Maguire, L. A. P.; Honig, E. D.; Sweigart, D. A. *Chem. Rev.* **1984**, *84*, 525, and references therein.

35. Walker, P. J. C.; Mawby, R. J. *Inorg. Chim. Acta* **1973**, *7*, 621.

36. (a) Winkhaus, G.; Pratt, L.; Wilkinson, G. *J. Chem. Soc.* **1961**, 3807. (b) Jones, D.; Pratt, L.; Wilkinson, G. *J. Chem. Soc.* **1962**, 4458. (c) Jones, D.; Wilkinson, G. *J. Chem. Soc.* **1964**, 2479. (d) Pauson, P. L.; Segal, J. A. *J. Chem. Soc., Dalton Trans.* **1975**, 1683.

37. Churchill, M. R.; Scholer, F. R. *Inorg. Chem.* **1969**, *8*, 1950.

38. Ittel, S. D.; Whitney, J. F.; Chung, Y. K.; Williard, P. G.; Sweigart, D. A. *Organometallics* **1988**, *7*, 1323.

39. (a) Brookhart, M.; Lukacs, A. *J. Am. Chem. Soc.* **1984**, *106*, 4161. (b) Chung, Y. K; Williard, P. G.; Sweigart, D. A. *Organometallics* **1982**, *12*, 224.

40. Roell, B. C.; McDaniel, K. F.; Vaughan, W. S; Macy, T. S. *Organometallics* **1993,** *12*, 224 and ref 18.

41. (a) Breimar, J.; Weidman, T.; Wagner, B.; Beck, W. *Chem. Ber.* **1991**, *124*, 2431. (b) Wieser, M.; Sünkel, K.; Robl, C.; Beck, W. *Chem. Ber.* **1992**, *125*, 1369. (c) Beck, W.; Neimer, B.; Wieser, M. *Angew. Chem.* **1993**, *32*, 923. (d) Bitterwolf, T. E.; Everly, S. C.; Rheingold, A. L.; Yapp, G. J. *J. Organomet. Chem.* **1997**, *531*, 1. (e) Milke, J.; Sünkel, K.; Beck, W. *J. Organomet. Chem.* **1997**, *543*, 39.

42. Renard, C.; Valentic, R.; Rose-Munch, F.; Rose, E. *Organometallics* **1998**, *17,* 1587.

43. Rose, E.; Le Corre-Susanne, C.; Rose-Munch, F.; Renard, C.; Gagliardini, V.; Teldji, F.; Vaissermann, J. *Eur. J. Inorg. Chem.* **1999**, 421.

44. (a) Kim, J. A.; Chung, T. -M.; Chung, Y. K.; Chung, Jung, J. -H.; Lee, S. W. *J. Organomet. Chem.* **1995**, *486*, 211. (b) Niemer, B.; Breimar, J.; Völkel, T.; Wagner, B.; Polburn, K.; Beck, W. *Chem. Ber.* **1991**, *124*, 2237.

45. LaBrush, D. M.; Eyman, D. P.; Baenziger, N. C.; Mallis, L. M. *Organometallics* **1991**, *10*, 1026.

46. Hull, J. W.; Roesselet, K. J.; Gladfelter, W. L. *Organometallics* **1992**, *11*, 3630.

47. (a) Bernhardt, R. J.; Wilmoth, M. A.; Weers, J. J.; LaBrush, D. M.; Eyman, D. P.; Huffman, J. C. *Organometallics* **1986**, *5*, 883. (b) Bernhardt, R. J.; Eyman, D. P. *Organometallics* **1984**, *3*, 1445. and ref 17.

48. (a) Kane-Maguire, L. A. P.; Sweigart, D.A. *Inorg. Chem.* **1979**, *18*, 700. (b) Pike, R. D.; Sweigart, D.A. *Coord.Chem. Rev.* **1999**, *187*, 183.

49. Brown, D. A.; Glass, W. K.; Kreddan, K. M. *J. Organomet. Chem.* **1991**, *418*, 91.

50. Angelici, R. J.; Blacik, L. J. *Inorg. Chem.* **1972**, *11*, 1754.

51. (a) Ryan, W. J.; Peterson, P. E.; Cao, Y.; Willard, P. G.; Sweigart, D. A.; Baer, C. D.; Thompson, C. F.; Chung, Y. K., Chung, T.-M. *Inorg. Chim. Acta* **1993**, *211*, 1. (b) reference 34 and references therein.

52. (a) Pauson, P. L.; Segal, J. A. *J. Chem. Soc., Dalton Trans.* **1975**, 1677. (b) Lee, S.-G.; Kim, J.-A.; Chung, Y. K.; Yoon, T.-S.; Kim, N.; Shin, W.; Kim, J.; Kim,

K. *Organometallics* **1995**, *14*, 1023. (c) Sun, S.; Carpenter, G. B.; Sweigart, D. A. *J. Organomet. Chem.* **1996**, *512*, 257.

53. (a) Lee, C. C.; Gill, U. S.; Sutherland, R. G. *J. Organomet. Chem.* **1981**, *206*, 89. (b) Moinet, C.; Raoult, E. *J. Organomet. Chem.* **1982**, *231*, 245.

54. Heppert, J. A.; Boyle, T. J.; Takusagawa, F. *Organometallics* **1989**, *8*, 461.

55. Jaouen, G.; Top, S.; Laconi, A.; Couterier, D.; Jacques, B. *J. Am. Chem. Soc.* **1984**, **106**, 2207.

56. (a) Hamon, J.-R.; Saillard, J.-Y.; Le Beuze, A.; McGlinchey, M. J.; Astruc, D. *J. Am. Chem. Soc.* **1982**, *104*, 7549. (b) Valério, C.; Alonso, E.; Ruiz, J.; Blais, J.-C.; Astruc, D. *Angew. Chem., Int. Ed.* **1999**, *38*, 1747, and references therein.

57. Astruc, D. *Acc. Chem. Res.* **2000**, *33*, 287, and references therein.

58. Albright, T. A.; Hofmann, P.; Hoffmann, R.; Lillya, C. P.; Dobosh, P. A. *J. Am. Chem. Soc.* **1983**, *105*, 3396.

59. Veiros, L. F. *Organometallics* **2000**, *19*, 5549.

60. Rerek, M. E.; Ji, L.-N.; Basolo, F. *J. Chem. Soc., Chem. Commun.* **1983**, 1208.

61. Basolo, F. *Inorg. Chim. Acta* **1985**, *100*, 33.

62. Kroto, H. W.; Heath, J. R.; O'Brien, S. C.; Curl, R. F.; Smalley, R. E. *Nature* **1985**, *318*, 162.

63. Diederich, F.; Rubin, Y. *Angew. Chem., Int. Ed. Engl.* **1992**, *31*, 1101, and references cited therein.

64. Barth, W. E.; Lawton, R. G. *J. Am. Chem. Soc.* **1966**, *88*, 380.

65. Scott, L. T.; Hashemi, M. M.; Meyer, D. T.; Warren, H. B. *J. Am. Chem. Soc.* **1991**, *113*, 7082.

66. Borchardt, A.; Fuchicello, A.; Kilway, K. V.; Baldridge, K. K.; Siegel, J. S. *J. Am. Chem. Soc.* **1992**, *114*, 1921.

67. Zimmermann, G.; Nuechter, U.; Hagen, S.; Nuechter, M. *Tetrahedron Lett.* **1994**, *35*, 4747.

68. Mehta, G.; Rao, H. S. P. *Tetrahedron* **1998**, *54*, 13325 and references therein.

69. Sygula, A.; Rabideau, P. W. *J. Am. Chem. Soc.* **2000**, *122*, 6323.

70. Sastry, G. N.; Jemmis, E. D.; Mehta, G.; Shah, S. R. *J. Chem. Soc. Perkin Trans. 2* **1993**, 1867.

71. (a) Kroto, H. W.; Allaf, A. W.; Balm, S. P. *Chem. Rev.* **1991**, *91*, 1213. (b) Scott, L. T.; Hashemi, M. M.; Batcher, M. S. *J. Am. Chem. Soc.* **1992**, *114*, 1920. (c) Allemand, P. M.; Koch, A.; Wudl, F.; Rubin, Y.; Diederich, F.; Alvarez, M. M.; Anz, S. T.; Whetten, R. L. *J. Am. Chem. Soc.* **1991**, *113*, 1050. and reference 68.

72. Sastry, G. N.; Jemmis, E. D.; Mehta, G.; Shah, S. R. *J. Chem. Soc., Perkin Trans. 2* **1993**, 1867.

73. Mehta, G.; Shah, S. R.; Ravikumar, K. *J. Chem. Soc., Chem. Commun.* **1993**, 1006.

74. Mehta, G.; Panda, G. unpublished results cited in reference 68.

75. Dehmlow, E. V.; Kelle, T. *Syn. Commun.* **1997**, 2021.

76. (a) Rabideau, P. W.; Sygula, A. *Acc. Chem. Res.* **1996**, *29*, 235. (b) Rabideau, P. W.; Abdourazak, A. H.; Folsom, H. E.; Marcinow, Z.; Sygula, A.; Sygula, R. *J. Am. Chem. Soc.* **1994**, *116*, 7891. (c) Abdourazak, A. H.; Marcinow, Z.; Sygula, A.; Sygula, R.; Rabideau, P. W. *J. Am. Chem. Soc.* **1995**, *117*, 6410.

77. Sbrogiò, F.; Fabris, F.; DeLucchi, O. *Gazz. Chim. Ital.* **1995**, *125*, 623.

78. Imamura, K.; Takimiya, K.; Aso, Y.; Otsubo, T. *Chem. Commun.* **1999**, 1859.

79. Fabre, C.; Rassat, A. *C. R. Acad. Sci. Paris, Serie II* **1989**, *308,* 1223.

80. (a) Dagani, R. *Science* **2002**, *80*, 7. (b) Scott, L. T.; Boorum, M. M.; McMahon, B. J.; Hagen, S.; Mack, J.; Blank, J.; Wegner, H.; deMeijere, A. *Science* **2002**, *295*, 1500.

81. Gupta, H. K.; Lock, P. E. McGlinchey, M. J. *Organometallics* **1997**, *16*, 3628.

82. (a) Mayer, R. *Chem. Ber.* **1956**, *89*, 1443. (b) Petru, F.; Galik, V. *Chem. Listy* **1957**, *51*, 2371. (c) Wallach, O. *Chem. Ber.* **1897**, *30*, 1094.

83. Boyko, E. R.; Vaughan, P. A. *Acta Cryst.* **1964**, *17*, 152.

84. Elmorsy, S. S.; Pelter, A.; Smith, K. *Tetrahedron Lett.* **1991**, *32*, 4175.

85. Wester, D. W.; Coveney, J. R.; Nosco, D. L.; Robbins, M. S.; Dean, R. T. *J. Med. Chem.* **1991**, *34*, 3284.

86. Li, Z.; Sun, W. -H.; Jin, X.; Shao, C. *Synlett* **2001**, *12*, 1947.

87. Kotsuki, H.; Mehta, B. K.; Yanagisawa, K. *Synlett* **2001**, *8*, 1323.

88. Katz, T. J.; Ślusarek, W. *J. Am. Chem. Soc.* **1980**, *102*, 1058.

89. (a) Helventson, M. C.; Lynch, T. J. *J. Organometal. Chem.* **1989**, *359*, C50. (b) Lynch, T. J.; Helvenston, M. C.; Rheingold, A. L.; Staley, D. L. *Organometallics* **1989**, *8*, 1959. (c) Bang, H.; Lynch, T. J.; Basolo, F. *Organometallics* **1992**, *11*, 40. (d) Winter, R.; Pierce, D. T.; Geiger, W. E.; Lynch, T. J. *J. Chem. Soc., Chem. Commun.* **1994**, 1949.

90. Ranganathan, S.; Muraleedharan, K. M.; Bharadwaj, P.; Madhusudanan, K. P. *J. Chem. Soc., Chem. Commum.* **1998**, 2239.

91. Ranganathan, S.; Muraleedharan, K. M.; Rao, C. C.; Vairamani, M.; Karle, I. L. *Org. Lett.* **2001**, *16*, 2447.

92. Choi, H.-J.; Park, Y. S.; Yun, S. H.; Kim, H.-S.; Cho, C. S.; Ko, K.; Ahn, K. H. *Organic Lett.* **2002**, *4*, 795.

93. Holý, P.; Havránek, M.; Pánková, M.; Ridvan, L.; Závada, J. *Tetrahedron* **1997**, *53*, 8195.

94. Moler, J. L.; Eyman, D. P.; Nielson, J. M.; Morken, A. M.; Schauer, S. J.; Snyder, D. N. *Organometallics* **1993**, *12*, 3304.

95. Reginato, N.; McGlinchey, M. J. *Organometallics* **2001**, *20*, 4147.

96. Bernhardt, R. J.; Wilmoth, M. A.; Weers, J. J.; LaBrush, D. M.; Eyman, D. P.; Huffman, J. C. *Organometallics* **1986**, *5*, 883.

97. Bernhardt, R. J.; Eyman, D. P. *Organometallics* **1984**, *3*, 1445.

98. Gupta, H. K.; Lock, P. E.; Hughes, D. W.; McGlinchey, M. J. *Organometallics* **1997**, *16*, 4355.

99. Grepioni, F.; Braga, D.; Dyson, P. J.; Johnson, B. F. G.; Sanderson, F. M.; Calhorda, M. J.; Veiros, L. F. *Organometallics* **1995**, *14*, 121.

100. Gommans, L. H. P.; Main, L.; Nicholson, B., K. *J. Organomet. Chem.* **1988**, *346*, 385.

101. Scholm, P. J.; Morken, A. M.; Eyman, D. P.; Baenziger, N. C.; Schauer, S. J. *Organometallics* **1993**, *12*, 3461.

102. Crabtree, R. H. *The Organometallic Chemistry of the Transition Metals*; John Wiley and Sons, New York, **1994**, p. 187.

103. (a) Albano, V. G.; Bellon, P. L.; Sansomi, M. *Inorg. Chem.* **1969**, *8*, 298. (b) Bellon, P. L.; Manassero, M.; Porta, F.; Sansoni, M. *J. Organomet. Chem.* **1974**, *80*, 139. (c) Gladysz, J. A.; Selover, J. C.; Strouse, C. E. *J. Am. Chem. Soc.* **1978**, *100*, 6766. (d) Selover, J. C.; Vaughn, G. D.; Strouse, C. E.; Gladysz, J. A. *J. Am. Chem. Soc.* **1986**, *108*, 1455. (e) Burk, P. L.: Van Engen, D.; Campo, K. S. *Organometallics* **1984**, *3*, 493. (f) Werner, H.; Hoffman, L.; Zolk, R. *Chem. Ber.* **1987**, *120*, 379. (g) Williams, D. E.; Mandal, S. K.; Gibson, D. H. *Acta Cryst.* **1988**, *44C*, 1738. (h) Mandal, S. K.; Ho, D. M.; Orchin, M. *Polyhedron* **1992**, *11*, 2055.

104. (a) Schlom, P. J.; Morken, A. M.; Eyman, D. P.; Baenziger, N. C.; Schuer, S. J. *Organometallics* **1993**, *12*, 3461. (b) Morken, A. M.; Eyman, D. P.; Wolff, M. A.; Schauer, S. J. *Organometallics* **1993**, *12*, 725.

105. Decken, A.; Britten, J. F.; McGlinchey, M. J. *J. Am. Chem. Soc.* **1993**, *115*, 7275.

106. King, R. B.; Efraty, A. *J. Organomet. Chem.* **1970**, *23*, 527.

107. King, R. B. *J. Organomet. Chem.* **1970**, *23*, 527.

108. (a) Nicholas, L. M.; Kerber, R. C.; Steifel, E. I. *Inorg. Chem.***1971**, *10*, 1519. (b) Treichel, P. M.; Johnson, J. W. *J. Am. Chem. Soc.* **1977**, *99*, 427. (c) Decken, A.; Britten, J. F.; McGlinchey, M. J. *J. Am. Chem. Soc.* **1993**, *115*, 7275. (d) Decken, A.; Rigby, S. S.; Girard, L.; Bain, A. D.; McGlinchey, M. J. *Organometallics* **2000**, *19*, 3127.

109. Trifonova, O. I.; Ochertyanova, E. A.; Akhmedov, N.G.; Roznyatovsky, V. A.; Laikov, D. N.; Ustynyuk, N. A.; Ustynyuk, Y. A. *Inorg. Chim. Acta* **1998**, *280*, 328.

110. (a) Nesmeyanov, A. N,; Ustynyuk, N. A.; Novikova, L. N.; Andrianov, V. G.; Struchkov, Y. T.; Ustynyuk, Y. A.; Oprunenko, Y. F.; Luzikov, Y. N. *J. Organomet. Chem.* **1982**, *226*, 239. (b) Nesmeyanov, A. N.; Ustynyuk, N. A.; Makarova, L. G.; Andre, S.; Ustynyuk, Y. A.; Novikova, L. N.; Luzikov, Y. N. *J. Organomet. Chem.* **1978**, *154*, 45.

111. (a) Brown, D. A.; Glass, W. K.; Kreddan, K. M. *J. Organomet. Chem.* **1991,** *413*, 233. (b) Chung, T. M.; Lee, J. J.; Chung, Y. K.; Jung, I. N. *Organometallics*, **1990**, *9*, 1976. (c) Huang, Y.; Carpenter, G. B.; Sweigart, D. A. Chung, Y. K.; Lee, B. Y. *Organometallics* **1995**, *14*, 1423.

112. Snyder, D. B.; Schauer, S. J.; Eyman, D. P.; Moler, J. L.; Weers, J. J. *J. Am. Chem. Soc.* **1993**, *115*, 6718.

113. Rose-Munch, F.; Susanne, C.; Renard, C.; Rose, E.; Vaissermann, J. *J. Organomet. Chem.* **1996**, *519*, 253.

114. Lee, T.-Y.; Lee S. S.; Chung, Y. K.; Lee, S. W. *J. Organomet. Chem.* **1995**, *486*, 141.

115. (a) Ryan, W. J.; Peterson, P. E.; Cao, Y.; Willard, P. G.; Sweigart, D. A.; Baer, C. D.; Thompson, C. F.; Chung, Y. K., Chung, T.-M. *Inorg. Chim. Acta* **1993**, *211*, 1. (b) Kane-Maguire, L. A. P.; Honig, E. D.; Sweigart, D. A. *Chem. Rev.***1984**, *84*, 525 and references therein.

116. Hicks, L. D.; Han, J. K.; Fry, A. J. *Tet. Lett.* **2000**, *41*, 7817.

117. Todd, D. *Org. React.* **1948**, *4*, 378.

118. Vedejs, E. *Org. React.* **1975**, *22*, 401.

119. Weissensteiner, W.; Hofer, O.; Wagner, U. G. *J. Org. Chem.* **1988**, *53*, 3988.

120. Reference 29 and references therein.

121. (a) Cambie, R. C.; Clark, G. R.; Gourdie, A. C; Rutledge, P. S.; Woodgate, P. D. *J. Organomet. Chem.* **1985**, *297*, 177. (b) Mailvaganam, B.; Perrier, R. E.; Sayer, B. G.; McCarry, B. E.; Bell, R. A.; McGlinchey, M. J. *J. Organomet. Chem.* **1988**, *354*, 325.

122. (a) Vessières, A.; Top, S; Ismail, A. A.; Bulter, I. S.; Louer, M.; Jaouen, G. *Biochemistry* **1988**, *27*, 6659. (b) Moriarty, R. M.; Ku, Y.-Y.; Gill, U. S.; Gilardi, R.; Perrier, R. E.; McGlinchey, M. J. *Organometallics* **1989**, *8*, 960.

123. Reboul, P. J. P.; Cristau, B.; Pèpe, G. *Acta Cryst.* **1981**, *B37*, 394.

124. Herrmann, W. A.; Plank, J.; Kriechbaum, G. W.; Ziegler, M. L.; Pfisterer, H.; Atwood, J. L; Rogers, R. D. *J. Organomet. Chem.* **1984**, *264*, 327.

125. Kane-Maguire, L. A. P.; Honig, E. D.; Sweigart, D. A. *J. Chem., Dalton Trans.* **1996**, 4493.

126. Volk, T.; Bernicke, D.; Bats, J. W.; Schmalz, H.-G. *Eur. J. Inorg. Chem.* **1998**, 1883.

127. Treichel, P. M.; Johnson, J. W. *Inorg. Chem.* **1977**, *16*, 749.

128. Johnson, J. W.; Treichel, P. M. *J. Am. Chem. Soc.* **1977**, *99*, 1427.

129. Johnson, J. W.; Treichel, P. M. *J. Chem. Soc., Chem. Commun.* **1976**, 688.

130. Treichel, P. M.; Fivizzanai, K. P.; Haller, K. J. *Organometallics* **1982**, *1*, 931.

131. Xia, A.; Selegue, J. P.; Carrilo, A.; Brock, C. P. *J. Am. Chem. Soc.* **2000**, *122*, 3973.

132. Son, S. U.; Lee, S. S.; Chung, Y. K. *J. Am. Chem. Soc.* **1997**, *119*, 7711.

133. Churchill, M. R.; Scholer, S. *Inorg. Chem.* **1969**, *8*, 1950.

134. Synder, D. B.; Schauer, S. J.; Eyman, D. P.; Moler, J. L.; Weers, J. J. *J. Am. Chem. Soc.* **1993**, *115*, 6718.

135. Veauthier, J. M.; Chow, A.; Fraenkel, G.; Geib, S. J.; Cooper, N. J. *Organometallics* **2000**, *19*, 3942

136. Veauthier, J. M.; Chow, A.; Fraenkel, G.; Geib, S. J.; Cooper, N. J. *Organometallics* **2000**, *19*, 661.

137. Albright, T. A.; Hofmann, P.; Hoffmann, R.; Lillya, C. P.; Dobosh, P. A. *J. Am. Chem. Soc.* **1983**, *105*, 3396 and references therein.

138. McGlinchey, M. J. *Can. J. Chem.* **2001**, *79*, 1295.

139. Folga, E.; Zeigler, T. *J. Am. Chem. Soc.* **1993**, *115*, 5169.

140. (a) Barckholtz, T. A.; Bursten, B. E. *J. Organomet. Chem.* **2000**, *596*, 212. (b) Smith, G. P. *Polyhedron* **1988**, *7*, 1605.

141. (a) Hennrich, G.; Anslyn, E. V. *Chem. Eur. J.* **2002**, *10*, 2219 and references therein. (b) Hennrich, G.; Lynch, V. M.; Anslyn, E. V. *Chem. Eur. J.* **2002**, *10*, 2274 and references therein.

142. Brydges, S.; Harrington, L. E.; McGlinchey, M. J. *Coord. Chem. Rev.* **2002**, *233-234*, 75.

143. (a) Iverson, D. J.; Hunter, G.; Blount, J. F.; Damewood, J. R., Jr.; Mislow, K. *J. Am. Chem. Soc.* **1981**, *103*, 6073. (b) Hunter, G.; Blount, J. F.; Damewood, J. R., Jr.; Iverson, D. J.; Mislow, K. *Organometallics* **1982**, *1*, 448. (c) Hunter, G.; Iverson, D. J.; Mislow, K.; Blount, J. F. *J. Am. Chem. Soc.* **1980**, *102*, 5942.

144. Pal, H. K.; Guha, A. C. *Z. Kristallogr.* **1935**, *A92*, 392.

145. Bar, I.; Bernstein, J.; Christensen, A. *Tetrahedron* **1977**, *33*, 3177.

146. Bock, H.; Kaim, W. *Chem. Ber.* **1978**, *111*, 3552.

147. Marsau, M. P. *Acta Crystallogr.* **1965**, *18*, 851.

148. (a) Iverson, D. J.; Mislow, K. *Organometallics* **1982**, *1*, 3. (b) Tidwell, T. T. *Tetrahedron* **1978**, *34*, 1855.

149. Frampton, C. S.; Gall, J. H.; MacNicol, D. D. *Acta Crystallogr. Sect. C* **2000**, *56*, e22.

150. McGlinchey, M. J.; Fletcher, J. L.; Sayer, B. G.; Bougeard, P; Faggiani, R.; Lock, C. J.L.; Bain, A. D.; Rodger, C. A.; Kündig, E. P.; Astruc, D., Hamon, J.-P.; LeMaux, P.; Top, S.; Jaouen, G. *J. Chem. Soc., Chem. Commun.* **1983**, *1*, 634.

151. Herrmann, W. A.; Thiel, W. R.; Herdtweck, E. *Polyhedron* **1988**, *7*, 2027,

152. Dubois, R. H.; Zaworotko, M. J.; White, P. S. *J. Organomet. Chem.* **1989**, *362*, 155.

153. Kilway, K. V.; Siegel, J. S. *Tetrahedron* **2001**, *57*, 3615.

154. Hunter, G.; Mislow, K. *J. Chem. Soc., Chem. Commun.* **1984**, 172.

155. McGlinchey, M. J.; Bougeard, P.; Sayer, B. G.; Hofer, R.; Lock, C. J. L. *J. Chem. Soc., Chem. Commun.* **1984**, 789.

156. Maricq. M. M.; Waugh, J. S.; Fletcher, J. L.; McGlinchey, M. J. *J. Am. Chem. Soc.* **1978**, *100*, 6902.

157. Downtown, P. A.; Mailvaganam, B.; Frampton, C. S.; Sayer, B. G. McGlinchey, M. J. *J. Am. Chem. Soc.* **1990**, *112*, 27.

158. (a) McGlinchey, M. J. *Adv. Organometallic Chem.* **1992**, *34*, 285. (b) Mailvaganam, B.; Frampton, C. S.; Top, S.; Sayer, B. G.; McGlinchey, M. J. *J. Am. Chem. Soc.* **1991**, *113*, 1177.

159. Unpublished results from this laboratory.

160. Albright, T. A.; Hofmann, P.; Hoffmann, R.; Lillya, C. P.; Dobosh, P. A. *J. Am. Chem. Soc.* **1983**, *105*, 3396, and references therein.

161. Oprunenko, Y. F. *Russ. Chem. Rev.* **2000**, *69*, 683-704, and references therein.

162. (a) Oprunenko, Y. F.; Malyugina, S. G.; Nesterenko, P.; Mityuk, D.; Malyshev, O. *J. Organomet. Chem.* **2000**, *597*, 42. (b) Afanasova, O. B.; Zubarev, Y. E.; Sharapov, V. A.; Kirillova, N. N.; Gusev, A. I.; Nosova, V. M.; Alekseev, N. V.; Chernyshev, E. A.; Struchkov, Y. T. *Dokl. Akad. Nauk SSSR* **1984**, *279*, 904. (c) Oprunenko, Y. F.; Malyugina, S. G.; Trifonova, O. I.; Babushkina, O. Y.; Pisarevskii, A. P.; Ustynyuk, Y. A.; Ustynyuk, N. A.; Nesterenko, P. N. *Izv. Akad. Nauk SSSR, Ser. Khim.* **1988**, 438. (d) Oprunenko, Y. F.; Malyugina, S. G.; Trifonova, O. I.; Babushkina, O. Y.; Ustynyuk, Y. A.; Nesterenko, P. N.; Ustynyuk, N. A.; Kravtsov, D. N.; Piven', V. A. *Metalloorg. Khim.* **1988**, *1*, 384.

163. (a) Laikov, D. N.; Ustynyuk, Y. A. XVIIIth International Conference on Organometallic Chemistry, Munich, **1998**, Abstract B17. (b) Oprunenko, Y. F.; Akhmedov, N. G.; Laikov, D. N.; Malyugina, S. G.; Mstislavsky, V. I.; Roznyatovsky, V. A.; Ustynyuk, Y. A.; Ustynyuk, N. A. *J. Organomet. Chem.* **1999**, *583*, 136.

164. See, for example: (a) Treichel, P. M.; Johnson, J. W. *J. Organomet. Chem.* **1975**, *88*, 207. (b) Salzer, A.; Täschler, C. *J. Organomet. Chem.* **1984**, *291*, 261. (c) Clark, D. T.; Mlekuz, M.; Sayer, B. G.; McCarry, B. E.; McGlinchey, M. J. *Organometallics* **1987**, *6*, 2201. (d) Veiros, L. F. *J. Organomet. Chem.* **1999**, *587*, 221. (e) Veiros, L. F. *Organometallics* **2000**, *19*, 3127.

165. See, for example: references 127, 128 and 130.

166. Decken, A.; Rigby, S. S; Girard, L.; Bain, A. D.; McGlinchey, M. J. *Organometallics* **1997**, *16*, 1308.

167. Reginato, N.; Brydges, S.; McGlinchey, M. J. Submitted to *Organometallics*.

168. (a) Cais, M.; Modiano, A.; Raveh, A. *J. Am. Chem. Soc.* **1965**, *87*, 5607. (b)) Cais, M.; Modiano, A.; Tirosh, N.; Eisenstadt, A. 8th International Conference on Coordination Chemistry, Vienna, Sept. 7-11, **1963**; Abstracts of Papers, pp. 229-232.

169. Ustynyuk, Y. A.; Trifonova, O. I.; Oprunenko, Y. F.; Mstislavsky, V. I.; Gloriozov, I. P.; Ustynyuk, N. A. *Organometallics* **1990**, *9*, 1707.

170. Bagus, P.; Walgren, U. I.; Almlof, J. *J. Chem. Phys.* **1976**, *64*, 2324.

171. (a) Ji, L-N.; Rerek, M. E.; Basolo, F. *Organometallics* **1984**, *3*, 740. (b) Crabtree, R. H. *The Organometallic Chemistry of the Transition Metals, 2nd Edition*; John Wiley & Sons: New York, 1993, pp. 91-92, and references therein. (c) O'Connor, J. M.; Casey, C. P. *Chem. Rev.* **1987**, *87*, 307.

172. Although (trimethylenemethane)$Mn(CO)_3^+$ has not, to our knowledge, been reported, the analogous (TMM)$Fe(CO)_3$ system does indeed adopt the staggered orientation: Girard, L.; Baird, M. C.; Chetcuti, M. J.; McGlinchey, M. J. *J. Organomet. Chem.* **1994**, *478*, 179, and references therein.

173. Ustynyuk, N. A.; Oprunenko, Y. F.; Malyugina, S. G.; Trifonova, O. I.; Ustynyuk,Y. A. *J. Organomet. Chem.* **1984**, *270*, 185.

174. (a) Nesmeyanov, A. N.; Ustynyuk, N. A.; Makarova, L. G.; Andre, S.; Ustynyuk, Yu. A.; Novikova, L. N.; Luzikov, Yu. N. *J. Organomet. Chem.* **1978**, *154*, 45. (b) White, C.; Thompson, J.; Maitlis, P. M. *J. Chem. Soc., Dalton Trans.* **1977**, 1654.

175. Xia, A.; Selegue, J. P.; Carrillo, A.; K.; Brock, C. P. *J. Am. Chem. Soc.* **2000**, *122*, 3973.

176. Trifonova, O. I.; Ustynyuk, Y. A; Ustynyuk, N. A.; Oprunenko, Y. F.; Batsanov, A. S.; Struchkov, Y. T. *J. Metalloorg. Khim.* **1989**, *2*, 581.

177. Oprunenko,Y. F.; Malyugina, S.; Vasil'kov, A.; Lyssenko, K.; Elschenbroich, C; Harms, K. *J. Organomet. Chem.* **2002**, *641*, 208.

178. Elschenbroich, C;. Möckel, R.; Vasil'kov, A.; Metz, B.; Harms, K. *Eur. J. Inorg. Chem.* **1998**, 1391.

179. Rigby, S. S.; Decken, A.; Bain, A. D.; McGlinchey, M. J. *J. Organometal. Chem.* **2001**, *637-639*, 372.

180. (a) Stradiotto, M.; McGlinchey, M. J. *Coord. Chem. Rev.* **2001**, *219-221*, 311, and references therein. (b) Stradiotto, M.; Rigby, S. S.; Hughes, D. W.; Brook, M. A.; Bain, A. D.; McGlinchey, M. J. *Organometallics* **1996**, *15*, 5645.

181. Stradiotto, M.; Hughes, D. W.; Bain, A. D.; Brook, M. A.; McGlinchey, M. J. *Organometallics* **1997**, *16*, 5563.

182. (a) Rigby, S. S.; Gupta, H. K.; Werstiuk, N. H.; Bain, A. D.; McGlinchey, M. J. *Polyhedron* **1995**, *14*, 2787. (b) Rigby, S. S.; Gupta, H. K.; Werstiuk, N. H.; Bain, A. D.; McGlinchey, M. J. *Inorg. Chim. Acta* **1996**, *251*, 355.

183. Rigby, S. S.; Stradiotto, M.; Brydges, S.; Pole, D. L.; Top, S.; Bain, A. D.; McGlinchey, M. J. *J. Org. Chem.* **1998**, *63*, 3735.

184. *Purification of Laboratory Chemicals, 2nd ed.*, Perrin, D. D.; Armarego, W. L. F.; Perrin, D. R. Eds.; Pergamon: Oxford, 1980.

185. SMART, Version 4.05, Bruker AXS Inc., Madison, WI 53711, **1996**.

186. SAINT, Version 4.05, Bruker AXS Inc., Madison, WI 53711, **1996**.

187. Sheldrick, G.M. SADABS, **1996**.

188. Sheldrick, G. M. SHELXTL, Version 5.03, Bruker AXS Inc., Madison, WI 53711, **1994**.

189. (a) Hoffmann, R. *J. Chem. Phys.* **1963**, *39*, 1397. (b) Hoffmann, R.; Lipscomb, W. N. *J. Chem. Phys.* **1962**, *36*, 2179 (see also p. 3489) (c) Ammeter, J. -H.; Bürgi, H. -B.; Thibeault, J. C.; Hoffmann, R. *J. Am. Chem. Soc.* **1978**, *100*, 3686.

190. (a) CACAO, Version 5.0, 1998. (b) Mealli, C.; Proserpio, D. M. *J. Chem. Ed.* **1990**, *67*, 3399.

APPENDIX

Table A1.1: Crystal data and structure refinement for **71**.
Table A1.2: Atomic coordinates (x 10^4) and equivalent isotropic displacement parameters ($Å^2$ x 10^3) for **71**. U(eq) is defined as one third of the trace of the orthogonalized U^{ij} tensor.
Table A1.3: Bond lengths [Å] and angles [°] for **71**.
Table A1.4: Anisotropic displacement parameters ($Å^2$ x 10^3) for **71**. The anisotropic displacement factor exponent takes the form: $-2\pi^2[h^2a^{*2}U^{11} + ... + 2 h k a^* b^* U^{12}]$.
Table A1.5: Hydrogen coordinates (x 10^4) and isotropic displacement parameters ($Å^2$ x 10^3) for **71**.

Table A2.1: Crystal data and structure refinement for **73**.
Table A2.2: Atomic coordinates (x 10^4) and equivalent isotropic displacement parameters ($Å^2$ x 10^3) for **73**. U(eq) is defined as one third of the trace of the orthogonalized U^{ij} tensor.
Table A2.3: Bond lengths [Å] and angles [°] for **73**.
Table A2.4: Anisotropic displacement parameters ($Å^2$ x 10^3) for **73**. The anisotropic displacement factor exponent takes the form: $-2\pi^2[h^2a^{*2}U^{11} + ... + 2 h k a^* b^* U^{12}]$.
Table A2.5: Hydrogen coordinates (x 10^4) and isotropic displacement parameters ($Å^2$ x 10^3) for **73**.

Table A3.1: Crystal data and structure refinement for **80**.
Table A3.2: Atomic coordinates (x 10^4) and equivalent isotropic displacement parameters ($Å^2$ x 10^3) for **80**. U(eq) is defined as one third of the trace of the orthogonalized U^{ij} tensor.
Table A3.3: Bond lengths [Å] and angles [°] for **80**.
Table A3.4: Hydrogen coordinates (x 10^4) and isotropic displacement parameters ($Å^2$ x 10^3) for **80**.

Table A4.1: Crystal data and structure refinement for **81**.
Table A4.2: Atomic coordinates (x 10^4) and equivalent isotropic displacement parameters ($Å^2$ x 10^3) for **81**. U(eq) is defined as one third of the trace of the orthogonalized U^{ij} tensor.
Table A4.3: Bond lengths [Å] and angles [°] for **81**.
Table A4.4: Anisotropic displacement parameters ($Å^2$ x 10^3)for **81**. The anisotropic displacement factor exponent takes the form: $-2\pi^2[h^2a^{*2}U^{11} + ... + 2 h k a^* b^* U^{12}]$.
Table A4.5: Hydrogen coordinates (x 10^4) and isotropic displacement parameters ($Å^2$ x 10^3) for **81**.

Table A5.1: Crystal data and structure refinement for **98**.
Table A5.2: Atomic coordinates (x 10^4) and equivalent isotropic displacement parameters ($Å^2$ x 10^3) for **98**. U(eq) is defined as one third of the trace of the orthogonalized U^{ij} tensor.
Table A5.3: Bond lengths [Å] and angles [°] for **98**.
Table A5.4: Anisotropic displacement parameters ($Å^2$ x 10^3) for **98**. The anisotropic displacement factor exponent takes the form: $-2\pi^2[h^2a^{*2}U^{11} + ... + 2 h k a^* b^* U^{12}]$.
Table A5.5: Hydrogen coordinates (x 10^4) and isotropic displacement parameters ($Å^2$ x 10^3) for **98**.

Table A6.1: Crystal data and structure refinement for **102**.
Table A6.2: Atomic coordinates (x 10^4) and equivalent isotropic displacement parameters ($Å^2$ x 10^3) for **102**. U(eq) is defined as one third of the trace of the orthogonalized U^{ij} tensor.
Table A6.3: Bond lengths [Å] and angles [°] for **102**.
Table A6.4: Anisotropic displacement parameters ($Å^2$ x 10^3) for **102**. The anisotropic displacement factor exponent takes the form: $-2\pi^2[h^2a^{*2}U^{11} + ... + 2 h k a^* b^* U^{12}]$.
Table A6.5: Hydrogen coordinates (x 10^4) and isotropic displacement parameters ($Å^2$ x 10^3) for **102**.

Table A7.1: Crystal data and structure refinement for **117**.
Table A7.2: Atomic coordinates (x 10^4) and equivalent isotropic displacement parameters ($Å^2$ x 10^3) for **117**. U(eq) is defined as one third of the trace of the orthogonalized U^{ij} tensor.
Table A7.3: Bond lengths [Å] and angles [°] for **117**.
Table A7.4: Anisotropic displacement parameters ($Å^2$ x 10^3) for **117**. The anisotropic displacement factor exponent takes the form: $-2\pi^2[h^2a^{*2}U^{11} + ... + 2 h k a^* b^* U^{12}]$.
Table A7.5: Hydrogen coordinates (x 10^4) and isotropic displacement parameters ($Å^2$ x 10^3) for **117**.

Table A8.1: Crystal data and structure refinement for **125**.
Table A8.2: Atomic coordinates (x 10^4) and equivalent isotropic displacement parameters ($Å^2$ x 10^3) for **125**. U(eq) is defined as one third of the trace of the orthogonalized U^{ij} tensor.
Table A8.3: Bond lengths [Å] and angles [°] for **125**.
Table A8.4: Anisotropic displacement parameters ($Å^2$ x 10^3) for **125**. The anisotropic displacement factor exponent takes the form: $-2\pi^2[h^2a^{*2}U^{11} + ... + 2 h k a^* b^* U^{12}]$.
Table A8.5: Hydrogen coordinates (x 10^4) and isotropic displacement parameters ($Å^2$ x 10^3) for **125**.

Table A9.1: Crystal data and structure refinement for **148**.
Table A9.2: Atomic coordinates (x 10^4) and equivalent isotropic displacement parameters ($Å^2$ x 10^3) for **148**. U(eq) is defined as one third of the trace of the orthogonalized U^{ij} tensor.
Table A9.3: Bond lengths [Å] and angles [°] for **148**.
Table A9.4: Anisotropic displacement parameters ($Å^2$ x 10^3) for **148**. The anisotropic displacement factor exponent takes the form: $-2\pi^2[h^2a^{*2}U^{11} + ... + 2 h k a^* b^* U^{12}]$.
Table A9.5: Hydrogen coordinates (x 10^4) and isotropic displacement parameters ($Å^2$ x 10^3) for **148**.

Table A1.1: Crystal data and structure refinement for **71**.

Empirical formula	$C_{17}H_{18}O_2BrMn$	
Formula weight	389.16	
Temperature	299(2) K	
Wavelength	0.71073 Å	
Crystal system	Monoclinic	
Space group	P2(1)/c	
Unit cell dimensions	a = 9.8049(13) Å	α= 90°.
	b = 8.8852(13) Å	β= 94.825(3)°.
	c = 18.682(3) Å	γ = 90°.
Volume	1621.8(4) $Å^3$	
Z	4	
Density (calculated)	1.594 Mg/m^3	
Absorption coefficient	3.278 mm^{-1}	
F(000)	784	
Crystal size	.06 x .08 x .24 mm^3	
Theta range for data collection	2.08 to 23.25°.	
Index ranges	$-10 \le h \le 10$, $-9 \le k \le 9$, $-20 \le l \le 20$	
Reflections collected	10041	
Independent reflections	2318 [R(int) = 0.0907]	
Refinement method	Full-matrix least-squares on F^2	
Data / restraints / parameters	2318 / 0 / 191	
Goodness-of-fit on F^2	1.075	
Final R indices [I>2sigma(I)]	R1 = 0.0560, wR2 = 0.1326	
R indices (all data)	R1 = 0.1070, wR2 = 0.1582	
Extinction coefficient	0.0000(5)	
Largest diff. peak and hole	0.464 and -0.436 $e.Å^{-3}$	

Table A1.2: Atomic coordinates (x 10^4) and equivalent isotropic displacement parameters ($Å^2$ x 10^3) for **71**. U(eq) is defined as one third of the trace of the orthogonalized U^{ij} tensor.

	x	y	z	U(eq)
Mn(1)	7312(1)	1697(1)	6414(1)	43(1)
Br(1)	7686(1)	-1029(1)	6630(1)	114(1)
C(1)	7144(6)	3931(8)	6816(4)	35(2)
C(2)	7874(6)	3985(7)	6189(4)	36(2)
C(3)	9062(6)	3105(8)	6170(4)	44(2)
C(6)	7605(6)	3037(8)	7412(3)	35(2)
C(13)	7205(6)	5056(8)	5651(4)	46(2)
C(5)	8758(6)	2131(8)	7373(4)	42(2)
C(7)	9050(7)	1269(9)	8059(4)	61(2)
O(1)	6692(7)	1163(9)	4879(4)	102(2)
C(16)	6942(8)	1335(10)	5469(6)	62(2)
O(2)	4381(6)	1411(8)	6579(3)	94(2)
C(15)	5961(7)	5001(8)	6731(4)	48(2)
C(17)	5534(8)	1478(9)	6518(4)	54(2)
C(4)	9505(6)	2167(8)	6746(4)	47(2)
C(14)	5774(7)	5287(9)	5921(4)	56(2)
C(10)	10759(8)	1305(11)	6597(5)	77(3)
C(9)	7006(7)	2817(9)	8116(4)	53(2)
C(12)	10026(7)	2934(10)	5574(4)	66(3)
C(8)	7722(8)	1392(11)	8408(5)	74(3)
C(11)	10853(9)	1523(14)	5801(6)	105(4)

Table A1.3: Bond lengths [Å] and angles [°] for **71**.

Mn(1)-C(17)	1.781(8)	C(17)-Mn(1)-C(2)	113.1(3)
Mn(1)-C(16)	1.802(10)	C(16)-Mn(1)-C(2)	90.6(3)
Mn(1)-C(1)	2.133(7)	C(1)-Mn(1)-C(2)	38.7(2)
Mn(1)-C(2)	2.157(7)	C(17)-Mn(1)-C(3)	150.6(3)
Mn(1)-C(3)	2.202(6)	C(16)-Mn(1)-C(3)	89.7(3)
Mn(1)-C(6)	2.209(7)	C(1)-Mn(1)-C(3)	68.2(2)
Mn(1)-C(5)	2.223(7)	C(2)-Mn(1)-C(3)	37.6(2)
Mn(1)-C(4)	2.226(6)	C(17)-Mn(1)-C(6)	91.5(3)
Mn(1)-Br(1)	2.4774(15)	C(16)-Mn(1)-C(6)	157.5(3)
C(1)-C(6)	1.410(9)	C(1)-Mn(1)-C(6)	37.9(2)
C(1)-C(2)	1.423(9)	C(2)-Mn(1)-C(6)	68.9(2)
C(1)-C(15)	1.498(9)	C(3)-Mn(1)-C(6)	79.6(2)
C(2)-C(3)	1.406(9)	C(17)-Mn(1)-C(5)	119.7(3)
C(2)-C(13)	1.496(9)	C(16)-Mn(1)-C(5)	152.0(3)
C(3)-C(4)	1.402(10)	C(1)-Mn(1)-C(5)	67.6(2)
C(3)-C(12)	1.528(9)	C(2)-Mn(1)-C(5)	80.7(3)
C(6)-C(5)	1.394(9)	C(3)-Mn(1)-C(5)	67.3(3)
C(6)-C(9)	1.499(9)	C(6)-Mn(1)-C(5)	36.7(2)
C(13)-C(14)	1.544(9)	C(17)-Mn(1)-C(4)	157.1(3)
C(5)-C(4)	1.433(10)	C(16)-Mn(1)-C(4)	114.6(3)
C(5)-C(7)	1.499(9)	C(1)-Mn(1)-C(4)	80.1(2)
C(7)-C(8)	1.509(10)	C(2)-Mn(1)-C(4)	67.7(3)
O(1)-C(16)	1.118(9)	C(3)-Mn(1)-C(4)	36.9(2)
O(2)-C(17)	1.147(8)	C(6)-Mn(1)-C(4)	67.0(2)
C(15)-C(14)	1.531(10)	C(5)-Mn(1)-C(4)	37.6(2)
C(4)-C(10)	1.495(9)	C(17)-Mn(1)-Br(1)	90.5(3)
C(10)-C(11)	1.510(12)	C(16)-Mn(1)-Br(1)	90.0(3)
C(9)-C(8)	1.527(11)	C(1)-Mn(1)-Br(1)	150.1(2)
C(12)-C(11)	1.534(12)	C(2)-Mn(1)-Br(1)	156.4(2)
C(17)-Mn(1)-C(16)	88.2(3)	C(3)-Mn(1)-Br(1)	118.8(2)
C(17)-Mn(1)-C(1)	87.6(3)	C(6)-Mn(1)-Br(1)	112.5(2)
C(16)-Mn(1)-C(1)	119.7(3)	C(5)-Mn(1)-Br(1)	87.9(2)

C(4)-Mn(1)-Br(1)	90.7(2)	C(9)-C(6)-Mn(1)	129.6(5)
C(6)-C(1)-C(2)	121.2(5)	C(2)-C(13)-C(14)	102.9(5)
C(6)-C(1)-C(15)	129.4(6)	C(6)-C(5)-C(4)	120.1(6)
C(2)-C(1)-C(15)	109.3(6)	C(6)-C(5)-C(7)	110.4(6)
C(6)-C(1)-Mn(1)	74.0(4)	C(4)-C(5)-C(7)	129.5(6)
C(2)-C(1)-Mn(1)	71.5(4)	C(6)-C(5)-Mn(1)	71.1(4)
C(15)-C(1)-Mn(1)	129.4(5)	C(4)-C(5)-Mn(1)	71.3(4)
C(3)-C(2)-C(1)	118.5(6)	C(7)-C(5)-Mn(1)	131.5(5)
C(3)-C(2)-C(13)	130.8(6)	C(5)-C(7)-C(8)	102.9(6)
C(1)-C(2)-C(13)	110.7(5)	O(1)-C(16)-Mn(1)	177.3(9)
C(3)-C(2)-Mn(1)	72.9(4)	C(1)-C(15)-C(14)	103.7(5)
C(1)-C(2)-Mn(1)	69.7(4)	O(2)-C(17)-Mn(1)	176.7(8)
C(13)-C(2)-Mn(1)	128.8(5)	C(3)-C(4)-C(5)	119.7(6)
C(4)-C(3)-C(2)	121.0(6)	C(3)-C(4)-C(10)	111.6(7)
C(4)-C(3)-C(12)	109.3(6)	C(5)-C(4)-C(10)	128.7(7)
C(2)-C(3)-C(12)	129.7(7)	C(3)-C(4)-Mn(1)	70.6(3)
C(4)-C(3)-Mn(1)	72.5(4)	C(5)-C(4)-Mn(1)	71.1(3)
C(2)-C(3)-Mn(1)	69.5(4)	C(10)-C(4)-Mn(1)	129.9(5)
C(12)-C(3)-Mn(1)	129.4(5)	C(15)-C(14)-C(13)	105.3(6)
C(5)-C(6)-C(1)	119.5(6)	C(4)-C(10)-C(11)	103.7(7)
C(5)-C(6)-C(9)	110.4(6)	C(6)-C(9)-C(8)	102.7(6)
C(1)-C(6)-C(9)	130.0(6)	C(3)-C(12)-C(11)	103.0(7)
C(5)-C(6)-Mn(1)	72.2(4)	C(7)-C(8)-C(9)	107.0(6)
C(1)-C(6)-Mn(1)	68.2(4)	C(10)-C(11)-C(12)	107.6(7)

Table A1.4: Anisotropic displacement parameters ($Å^2 \times 10^3$) for **71**. The anisotropic displacement factor exponent takes the form: $-2\pi^2[h^2a^{*2}U^{11} + ... + 2\ h\ k\ a^*\ b^*\ U^{12}]$.

	U^{11}	U^{22}	U^{33}	U^{23}	U^{13}	U^{12}
Mn(1)	40(1)	38(1)	49(1)	-2(1)	-5(1)	0(1)
Br(1)	128(1)	39(1)	164(1)	-1(1)	-47(1)	0(1)
C(1)	34(3)	36(4)	34(4)	1(4)	6(3)	-3(3)
C(2)	40(3)	35(4)	33(4)	-7(3)	6(3)	10(3)
C(3)	31(3)	45(5)	58(5)	-9(4)	6(3)	-6(3)
C(6)	30(3)	42(5)	33(4)	-2(4)	-5(3)	-10(3)
C(13)	55(4)	43(5)	41(5)	2(4)	9(4)	5(3)
C(5)	36(3)	34(5)	53(5)	6(4)	-7(3)	-2(3)
C(7)	49(4)	64(6)	67(6)	21(5)	-20(4)	2(4)
O(1)	129(6)	127(7)	49(4)	-29(4)	7(4)	-17(5)
C(16)	57(5)	63(7)	69(7)	-8(5)	12(5)	-5(4)
O(2)	52(3)	135(7)	93(5)	0(4)	4(3)	-32(4)
C(15)	50(4)	48(5)	45(5)	1(4)	1(4)	8(4)
C(17)	60(5)	52(6)	47(5)	-3(4)	-6(4)	-11(4)
C(4)	33(3)	43(5)	61(6)	-2(4)	-14(4)	6(3)
C(14)	58(4)	55(5)	55(6)	6(4)	-2(4)	17(4)
C(10)	56(5)	78(7)	95(8)	-8(6)	-7(5)	23(5)
C(9)	47(4)	67(6)	45(5)	3(4)	0(4)	-9(4)
C(12)	47(4)	86(7)	66(6)	-15(5)	14(4)	2(4)
C(8)	65(5)	86(8)	70(7)	27(5)	8(5)	0(5)
C(11)	77(6)	148(11)	90(9)	-14(7)	10(6)	62(7)

Table A1.5: Hydrogen coordinates (x 10^4) and isotropic displacement parameters ($Å^2$ x 10^3) for **71**.

	x	y	z	U(eq)
H(13A)	7139(6)	4626(8)	5172(4)	55
H(13B)	7704(6)	5998(8)	5647(4)	55
H(7A)	9800(7)	1717(9)	8357(4)	74
H(7B)	9270(7)	227(9)	7964(4)	74
H(15A)	6167(7)	5928(8)	6992(4)	57
H(15B)	5145(7)	4555(8)	6901(4)	57
H(14A)	5450(7)	6304(9)	5822(4)	68
H(14B)	5120(7)	4584(9)	5689(4)	68
H(10A)	10664(8)	248(11)	6713(5)	93
H(10B)	11563(8)	1704(11)	6871(5)	93
H(9A)	6023(7)	2678(9)	8049(4)	64
H(9B)	7208(7)	3666(9)	8434(4)	64
H(12A)	10616(7)	3805(10)	5550(4)	79
H(12B)	9518(7)	2792(10)	5110(4)	79
H(8A)	7900(8)	1455(11)	8926(5)	88
H(8B)	7153(8)	517(11)	8293(5)	88
H(11A)	10483(9)	652(14)	5538(6)	126
H(11B)	11801(9)	1648(14)	5700(6)	126

Table A2.1: Crystal data and structure refinement for **73**.

Empirical formula	$C_{17}H_{18}IO_2Mn$	
Formula weight	436.15	
Temperature	299(2) K	
Wavelength	0.71073 Å	
Crystal system	Orthorhombic	
Space group	Pbca	
Unit cell dimensions	a = 14.401(3) Å	α= 90°.
	b = 15.073(3) Å	β= 90°.
	c = 15.256(3) Å	γ = 90°.
Volume	3311.6(11) $Å^3$	
Z	8	
Density (calculated)	1.750 Mg/m^3	
Absorption coefficient	2.663 mm^{-1}	
F(000)	1712	
Crystal size	.14 x .28 x .33 mm^3	
Theta range for data collection	2.37 to 24.99°.	
Index ranges	$-18 \leq h \leq 18$, $-19 \leq k \leq 19$, $-19 \leq l \leq 19$	
Reflections collected	23086	
Independent reflections	2912 [R(int) = 0.0344]	
Refinement method	Full-matrix least-squares on F^2	
Data / restraints / parameters	2897 / 3 / 208	
Goodness-of-fit on F^2	1.047	
Final R indices [I>2sigma(I)]	R1 = 0.0260, wR2 = 0.0628	
R indices (all data)	R1 = 0.0343, wR2 = 0.0729	
Largest diff. peak and hole	0.642 and -0.585 $e.Å^{-3}$	

Table A2.2: Atomic coordinates (x 10^4) and equivalent isotropic displacement parameters ($Å^2$ x 10^3) for **73**. U(eq) is defined as one third of the trace of the orthogonalized U^{ij} tensor.

	x	y	z	U(eq)
C(1)	1204(2)	732(2)	9798(2)	51(1)
Mn(1)	2002(1)	1120(1)	8676(1)	41(1)
I(1)	2607(1)	2296(1)	7498(1)	61(1)
Mn(1A)	2002(1)	1120(1)	8676(1)	41(1)
I(1A)	3345(4)	1579(4)	9714(5)	74(1)
C(2)	1151(2)	55(2)	9161(2)	48(1)
C(3)	834(2)	260(2)	8311(2)	44(1)
C(4)	598(2)	1136(2)	8099(2)	42(1)
C(5)	637(2)	1810(2)	8739(2)	45(1)
C(6)	934(2)	1605(2)	9589(2)	50(1)
C(7)	911(3)	2435(2)	10147(3)	75(1)
C(8)	849(3)	3181(2)	9471(3)	83(1)
C(9)	398(3)	2777(2)	8670(3)	67(1)
C(10)	306(2)	1197(3)	7156(2)	63(1)
C(11)	656(3)	320(3)	6772(2)	80(1)
C(12)	713(3)	-333(2)	7529(2)	66(1)
C(13)	1449(3)	-825(2)	9545(3)	74(1)
C(14)	1977(3)	-536(3)	10372(3)	98(2)
C(15)	1552(3)	344(3)	10663(2)	80(1)
C(16)	2914(4)	1502(4)	9377(4)	66(1)
O(16)	3476(6)	1700(7)	9883(6)	138(6)
C(16A)	2781(2)	330(2)	8197(2)	56(1)
O(16A)	3271(2)	-193(2)	7907(2)	86(1)
C(17)	2781(2)	330(2)	8197(2)	56(1)
O(17)	3271(2)	-193(2)	7907(2)	86(1)
C(17A)	2400(16)	1927(23)	7899(20)	100(13)
O(17A)	2586(15)	2459(11)	7386(11)	0(4)

Table A2.3: Bond lengths [Å] and angles [°] for **73**.

C(1)-C(6)	1.410(4)	C(10)-C(11)	1.531(6)
C(1)-C(2)	1.411(4)	C(11)-C(12)	1.519(5)
C(1)-C(15)	1.527(4)	C(13)-C(14)	1.536(6)
C(1)-Mn(1A)	2.143(3)	C(14)-C(15)	1.527(6)
C(1)-Mn(1)	2.143(3)	C(16)-O(16)	1.158(11)
Mn(1)-C(16)	1.789(6)	C(16A)-O(16A)	1.146(4)
Mn(1)-C(17)	1.792(3)	C(17)-O(17)	1.146(4)
Mn(1)-C(2)	2.151(3)	C(17A)-O(17A)	1.152(2)
Mn(1)-C(3)	2.195(3)	C(6)-C(1)-C(2)	120.3(3)
Mn(1)-C(6)	2.200(3)	C(6)-C(1)-C(15)	130.0(3)
Mn(1)-C(4)	2.204(3)	C(2)-C(1)-C(15)	109.6(3)
Mn(1)-C(5)	2.226(3)	C(6)-C(1)-Mn(1A)	73.3(2)
Mn(1)-I(1)	2.6701(7)	C(2)-C(1)-Mn(1A)	71.1(2)
Mn(1A)-C(17A)	1.7924(12)	C(15)-C(1)-Mn(1A)	128.2(2)
Mn(1A)-C(16A)	1.792(3)	C(6)-C(1)-Mn(1)	73.3(2)
Mn(1A)-C(2)	2.151(3)	C(2)-C(1)-Mn(1)	71.1(2)
Mn(1A)-C(3)	2.195(3)	C(15)-C(1)-Mn(1)	128.2(2)
Mn(1A)-C(6)	2.200(3)	C(16)-Mn(1)-C(17)	89.9(2)
Mn(1A)-C(4)	2.204(3)	C(16)-Mn(1)-C(1)	90.2(2)
Mn(1A)-C(5)	2.226(3)	C(17)-Mn(1)-C(1)	118.66(14)
Mn(1A)-I(1A)	2.594(8)	C(16)-Mn(1)-C(2)	116.9(2)
C(2)-C(3)	1.409(4)	C(17)-Mn(1)-C(2)	90.07(13)
C(2)-C(13)	1.512(4)	C(1)-Mn(1)-C(2)	38.36(12)
C(3)-C(4)	1.401(4)	C(16)-Mn(1)-C(3)	154.7(2)
C(3)-C(12)	1.501(4)	C(17)-Mn(1)-C(3)	89.11(13)
C(4)-C(5)	1.410(4)	C(1)-Mn(1)-C(3)	68.32(12)
C(4)-C(10)	1.503(4)	C(2)-Mn(1)-C(3)	37.82(11)
C(5)-C(6)	1.400(4)	C(16)-Mn(1)-C(6)	91.5(2)
C(5)-C(9)	1.501(4)	C(17)-Mn(1)-C(6)	156.45(14)
C(6)-C(7)	1.513(4)	C(1)-Mn(1)-C(6)	37.85(12)
C(7)-C(8)	1.529(6)	C(2)-Mn(1)-C(6)	68.41(11)
C(8)-C(9)	1.513(5)	C(3)-Mn(1)-C(6)	79.71(11)

C(16)-Mn(1)-C(4)	155.2(2)	C(2)-Mn(1A)-C(6)	68.41(11)
C(17)-Mn(1)-C(4)	114.78(13)	C(3)-Mn(1A)-C(6)	79.71(11)
C(1)-Mn(1)-C(4)	80.24(11)	C(17A)-Mn(1A)-C(4)	91.3(6)
C(2)-Mn(1)-C(4)	67.87(11)	C(16A)-Mn(1A)-C(4)	114.78(13)
C(3)-Mn(1)-C(4)	37.13(10)	C(1)-Mn(1A)-C(4)	80.24(11)
C(6)-Mn(1)-C(4)	66.95(11)	C(2)-Mn(1A)-C(4)	67.87(11)
C(16)-Mn(1)-C(5)	118.2(2)	C(3)-Mn(1A)-C(4)	37.13(10)
C(17)-Mn(1)-C(5)	151.81(14)	C(6)-Mn(1A)-C(4)	66.95(11)
C(1)-Mn(1)-C(5)	67.66(11)	C(17A)-Mn(1A)-C(5)	89.7(11)
C(2)-Mn(1)-C(5)	80.26(11)	C(16A)-Mn(1A)-C(5)	151.81(14)
C(3)-Mn(1)-C(5)	67.06(10)	C(1)-Mn(1A)-C(5)	67.66(11)
C(6)-Mn(1)-C(5)	36.89(11)	C(2)-Mn(1A)-C(5)	80.26(11)
C(4)-Mn(1)-C(5)	37.11(10)	C(3)-Mn(1A)-C(5)	67.06(10)
C(16)-Mn(1)-I(1)	87.1(2)	C(6)-Mn(1A)-C(5)	36.89(11)
C(17)-Mn(1)-I(1)	87.87(11)	C(4)-Mn(1A)-C(5)	37.11(10)
C(1)-Mn(1)-I(1)	153.34(9)	C(17A)-Mn(1A)-I(1A)	89.1(8)
C(2)-Mn(1)-I(1)	155.94(9)	C(16A)-Mn(1A)-I(1A)	87.63(15)
C(3)-Mn(1)-I(1)	118.15(8)	C(1)-Mn(1A)-I(1A)	89.11(14)
C(6)-Mn(1)-I(1)	115.68(9)	C(2)-Mn(1A)-I(1A)	114.43(15)
C(4)-Mn(1)-I(1)	91.36(7)	C(3)-Mn(1A)-I(1A)	152.08(15)
C(5)-Mn(1)-I(1)	90.40(8)	C(6)-Mn(1A)-I(1A)	92.62(13)
C(17A)-Mn(1A)-C(16A)	88.9(14)	C(4)-Mn(1A)-I(1A)	157.59(13)
C(17A)-Mn(1A)-C(1)	152.3(15)	C(5)-Mn(1A)-I(1A)	120.49(13)
C(16A)-Mn(1A)-C(1)	118.66(14)	C(3)-C(2)-C(1)	119.5(3)
C(17A)-Mn(1A)-C(2)	156.4(8)	C(3)-C(2)-C(13)	129.9(3)
C(16A)-Mn(1A)-C(2)	90.07(13)	C(1)-C(2)-C(13)	110.6(3)
C(1)-Mn(1A)-C(2)	38.36(12)	C(3)-C(2)-Mn(1A)	72.8(2)
C(17A)-Mn(1A)-C(3)	118.6(8)	C(1)-C(2)-Mn(1A)	70.5(2)
C(16A)-Mn(1A)-C(3)	89.11(13)	C(13)-C(2)-Mn(1A)	128.8(2)
C(1)-Mn(1A)-C(3)	68.32(12)	C(3)-C(2)-Mn(1)	72.8(2)
C(2)-Mn(1A)-C(3)	37.82(11)	C(1)-C(2)-Mn(1)	70.5(2)
C(17A)-Mn(1A)-C(6)	114.6(14)	C(13)-C(2)-Mn(1)	128.8(2)
C(16A)-Mn(1A)-C(6)	156.45(14)	C(4)-C(3)-C(2)	119.9(3)
C(1)-Mn(1A)-C(6)	37.85(12)	C(4)-C(3)-C(12)	110.4(3)

C(2)-C(3)-C(12)	129.7(3)	C(9)-C(5)-Mn(1)	130.7(2)
C(4)-C(3)-Mn(1A)	71.8(2)	C(5)-C(6)-C(1)	120.0(3)
C(2)-C(3)-Mn(1A)	69.4(2)	C(5)-C(6)-C(7)	109.4(3)
C(12)-C(3)-Mn(1A)	129.9(2)	C(1)-C(6)-C(7)	130.6(3)
C(4)-C(3)-Mn(1)	71.8(2)	C(5)-C(6)-Mn(1A)	72.6(2)
C(2)-C(3)-Mn(1)	69.4(2)	C(1)-C(6)-Mn(1A)	68.9(2)
C(12)-C(3)-Mn(1)	129.9(2)	C(7)-C(6)-Mn(1A)	130.3(2)
C(3)-C(4)-C(5)	120.7(3)	C(5)-C(6)-Mn(1)	72.6(2)
C(3)-C(4)-C(10)	110.3(3)	C(1)-C(6)-Mn(1)	68.9(2)
C(5)-C(4)-C(10)	129.0(3)	C(7)-C(6)-Mn(1)	130.3(2)
C(3)-C(4)-Mn(1)	71.1(2)	C(6)-C(7)-C(8)	103.3(3)
C(5)-C(4)-Mn(1)	72.3(2)	C(9)-C(8)-C(7)	105.9(3)
C(10)-C(4)-Mn(1)	129.8(2)	C(5)-C(9)-C(8)	103.7(3)
C(3)-C(4)-Mn(1A)	71.1(2)	C(4)-C(10)-C(11)	102.7(3)
C(5)-C(4)-Mn(1A)	72.3(2)	C(12)-C(11)-C(10)	106.7(3)
C(10)-C(4)-Mn(1A)	129.8(2)	C(3)-C(12)-C(11)	103.0(3)
C(6)-C(5)-C(4)	119.6(3)	C(2)-C(13)-C(14)	102.2(3)
C(6)-C(5)-C(9)	110.4(3)	C(15)-C(14)-C(13)	106.6(3)
C(4)-C(5)-C(9)	130.0(3)	C(1)-C(15)-C(14)	102.3(3)
C(6)-C(5)-Mn(1A)	70.5(2)	O(16)-C(16)-Mn(1)	174.2(7)
C(4)-C(5)-Mn(1A)	70.6(2)	O(16A)-C(16A)-Mn(1A)	178.1(3)
C(9)-C(5)-Mn(1A)	130.7(2)	O(17)-C(17)-Mn(1)	178.1(3)
C(6)-C(5)-Mn(1)	70.5(2)	O(17A)-C(17A)-Mn(1A)	174.7(18
C(4)-C(5)-Mn(1)	70.6(2)		
)			

Table A2.4: Anisotropic displacement parameters ($Å^2 x\ 10^3$) for **73**. The anisotropic displacement factor exponent takes the form: $-2\pi^2[\ h^2a^{*2}U^{11} + ... + 2\ h\ k\ a^*\ b^*\ U^{12}\ ]$.

	U^{11}	U^{22}	U^{33}	U^{23}	U^{13}	U^{12}
C(1)	41(2)	74(2)	39(2)	5(2)	1(1)	1(2)
Mn(1)	34(1)	46(1)	42(1)	-2(1)	-2(1)	-1(1)
I(1)	60(1)	56(1)	66(1)	6(1)	10(1)	-11(1)
Mn(1A)	34(1)	46(1)	42(1)	-2(1)	-2(1)	-1(1)
I(1A)	49(2)	105(2)	69(3)	-17(2)	-6(2)	-7(2)
C(2)	38(2)	50(2)	56(2)	8(2)	4(1)	1(1)
C(3)	35(2)	47(2)	50(2)	-6(1)	2(1)	-4(1)
C(4)	33(1)	53(2)	41(2)	1(1)	-4(1)	-4(1)
C(5)	31(1)	48(2)	56(2)	0(1)	-1(1)	3(1)
C(6)	39(2)	62(2)	47(2)	-13(2)	1(1)	2(1)
C(7)	61(2)	90(3)	74(3)	-40(2)	3(2)	2(2)
C(8)	72(3)	59(2)	117(3)	-32(2)	4(2)	2(2)
C(9)	51(2)	52(2)	99(3)	1(2)	2(2)	10(2)
C(10)	53(2)	88(2)	49(2)	7(2)	-13(2)	-8(2)
C(11)	71(2)	117(3)	52(2)	-23(2)	-7(2)	-11(2)
C(12)	54(2)	69(2)	75(2)	-28(2)	-4(2)	-9(2)
C(13)	64(2)	64(2)	95(3)	25(2)	7(2)	9(2)
C(14)	93(3)	112(3)	87(3)	47(3)	-8(3)	23(3)
C(15)	71(2)	122(3)	48(2)	21(2)	0(2)	8(2)
C(16)	52(3)	92(3)	56(3)	-3(2)	-8(2)	-6(3)
O(16)	90(6)	219(10)	104(6)	-9(4)	-47(3)	-27(4)
C(16A)	43(2)	53(2)	71(2)	0(2)	6(2)	-4(2)
O(16A)	63(2)	71(2)	122(2)	-14(2)	25(2)	14(1)
C(17)	43(2)	53(2)	71(2)	0(2)	6(2)	-4(2)
O(17)	63(2)	71(2)	122(2)	-14(2)	25(2)	14(1)

Table A2.5: Hydrogen coordinates (x 10^4) and isotropic displacement parameters ($Å^2$x 10^3) for **73**.

	x	y	z	U(eq)
H(7A)	1470(3)	2488(2)	10498(3)	90
H(7B)	375(3)	2436(2)	10532(3)	90
H(8A)	475(3)	3667(2)	9695(3)	99
H(8B)	1462(3)	3405(2)	9330(3)	99
H(9A)	-269(3)	2865(2)	8678(3)	81
H(9B)	649(3)	3032(2)	8136(3)	81
H(10A)	594(2)	1701(3)	6868(2)	76
H(10B)	-363(2)	1246(3)	7103(2)	76
H(11A)	231(3)	104(3)	6328(2)	96
H(11B)	1263(3)	400(3)	6508(2)	96
H(12A)	149(3)	-681(2)	7575(2)	79
H(12B)	1238(3)	-730(2)	7462(2)	79
H(13A)	1850(3)	-1147(2)	9145(3)	89
H(13B)	917(3)	-1191(2)	9691(3)	89
H(14A)	1910(3)	-978(3)	10830(3)	117
H(14B)	2632(3)	-463(3)	10244(3)	117
H(15A)	1046(3)	252(3)	11072(2)	96
H(15B)	2014(3)	726(3)	10931(2)	96

Table A3.1: Crystal data and structure refinement for **80**.

Empirical formula	$C_{18}H_{15}O_3Mn$	
Formula weight	334.24	
Temperature	173(2) K	
Wavelength	0.71073 Å	
Crystal system	Monoclinic	
Space group	C2/c	
Unit cell dimensions	a = 16.567(18) Å	α= 90°.
	b = 9.919(14) Å	β= 98.09(5)°.
	c = 18.524(26) Å	γ = 90°.
Volume	3013.7(68) $Å^3$	
Z	8	
Density (calculated)	1.473 Mg/m^3	
Absorption coefficient	0.885 mm^{-1}	
F(000)	1376	
Crystal size	0.04 x 0.22 x 0.42 mm^3	
Theta range for data collection	2.40 to 24.99°.	
Index ranges	$-21 \leq h \leq 20$, $-7 \leq k \leq 11$, $-21 \leq l \leq 16$	
Reflections collected	2507	
Independent reflections	1717 [R(int) = 0.2486]	
Refinement method	Full-matrix least-squares on F^2	
Data / restraints / parameters	1679 / 0 / 199	
Goodness-of-fit on F^2	1.080	
Final R indices [I>2sigma(I)]	R1 = 0.1455, wR2 = 0.3683	
R indices (all data)	R1 = 0.1943, wR2 = 0.4620	
Extinction coefficient	0.0000(9)	
Largest diff. peak and hole	1.304 and -1.241 $e.Å^{-3}$	

Table A3.2: Atomic coordinates (x 10^4) and equivalent isotropic displacement parameters ($Å^2$ x 10^3) for **80**. U(eq) is defined as one third of the trace of the orthogonalized U^{ij} tensor.

	x	y	z	U(eq)
Mn(1)	1177(1)	3583(3)	1438(2)	48(1)
C(1)	2459(11)	3175(18)	1467(13)	53(6)
C(2)	2273(13)	4466(19)	1155(14)	55(7)
C(3)	1705(12)	4395(19)	508(13)	49(6)
C(4)	1584(9)	2933(17)	396(9)	47(7)
C(5)	2044(9)	2196(20)	970(11)	44(6)
C(6)	2031(12)	755(20)	989(13)	51(7)
C(7)	1566(11)	126(24)	385(12)	51(7)
C(8)	1101(11)	828(19)	-215(11)	39(6)
C(9)	1096(10)	2242(20)	-212(12)	44(6)
C(10)	571(13)	2762(19)	-876(13)	66(8)
C(11)	349(11)	1519(21)	-1371(13)	67(7)
C(12)	576(11)	247(19)	-868(12)	56(7)
C(13)	1634(12)	-1382(20)	443(14)	65(8)
C(14)	2177(13)	-1654(19)	1194(15)	66(8)
C(15)	2425(14)	-270(21)	1479(13)	70(8)
C(16)	1075(11)	2446(18)	2154(10)	42(4)
O(16)	1024(8)	1672(16)	2633(10)	85(6)
C(17)	1013(10)	5046(16)	1998(10)	37(4)
O(17)	919(8)	6015(11)	2314(9)	65(5)
O(18)	-570(8)	3529(14)	837(9)	66(4)
C(18)	123(10)	3560(18)	1069(11)	50(6)

Table A3.3: Bond lengths [Å] and angles [°] for **80**.

Mn(1)-C(16)	1.77(2)	C(16)-Mn(1)-C(2)	128.0(10)
Mn(1)-C(18)	1.78(2)	C(18)-Mn(1)-C(2)	136.7(9)
Mn(1)-C(17)	1.83(2)	C(17)-Mn(1)-C(2)	90.7(7)
Mn(1)-C(2)	2.15(2)	C(16)-Mn(1)-C(1)	93.3(8)
Mn(1)-C(1)	2.16(2)	C(18)-Mn(1)-C(1)	156.3(8)
Mn(1)-C(3)	2.19(2)	C(17)-Mn(1)-C(1)	111.0(8)
Mn(1)-C(5)	2.25(2)	C(2)-Mn(1)-C(1)	38.5(8)
Mn(1)-C(4)	2.228(15)	C(16)-Mn(1)-C(3)	156.2(7)
C(1)-C(2)	1.42(3)	C(18)-Mn(1)-C(3)	100.4(9)
C(1)-C(5)	1.44(3)	C(17)-Mn(1)-C(3)	105.2(7)
C(2)-C(3)	1.42(3)	C(2)-Mn(1)-C(3)	38.1(7)
C(3)-C(4)	1.47(3)	C(1)-Mn(1)-C(3)	65.7(8)
C(4)-C(5)	1.42	C(16)-Mn(1)-C(5)	91.8(7)
C(4)-C(9)	1.46(3)	C(18)-Mn(1)-C(5)	119.2(8)
C(5)-C(6)	1.43(3)	C(17)-Mn(1)-C(5)	149.2(8)
C(6)-C(7)	1.41(3)	C(2)-Mn(1)-C(5)	63.1(7)
C(6)-C(15)	1.46(3)	C(1)-Mn(1)-C(5)	38.2(7)
C(7)-C(8)	1.44(3)	C(3)-Mn(1)-C(5)	64.8(6)
C(7)-C(13)	1.50(3)	C(16)-Mn(1)-C(4)	122.5(7)
C(8)-C(9)	1.40(3)	C(18)-Mn(1)-C(4)	93.7(7)
C(8)-C(12)	1.50(3)	C(17)-Mn(1)-C(4)	144.0(7)
C(9)-C(10)	1.49(3)	C(2)-Mn(1)-C(4)	62.4(7)
C(10)-C(11)	1.55(3)	C(1)-Mn(1)-C(4)	63.2(8)
C(11)-C(12)	1.58(3)	C(3)-Mn(1)-C(4)	39.0(7)
C(13)-C(14)	1.57(3)	C(5)-Mn(1)-C(4)	37.0(2)
C(14)-C(15)	1.51(3)	C(2)-C(1)-C(5)	106.9(21)
C(16)-O(16)	1.19(2)	C(2)-C(1)-Mn(1)	70.4(10)
C(17)-O(17)	1.15(2)	C(5)-C(1)-Mn(1)	74.4(10)
O(18)-C(18)	1.17(2)	C(1)-C(2)-C(3)	112.3(17)
C(16)-Mn(1)-C(18)	95.1(8)	C(1)-C(2)-Mn(1)	71.0(9)
C(16)-Mn(1)-C(17)	92.5(8)	C(3)-C(2)-Mn(1)	72.6(10)
C(18)-Mn(1)-C(17)	90.7(8)	C(4)-C(3)-C(2)	103.2(16)

C(4)-C(3)-Mn(1)	71.9(8)	C(6)-C(7)-C(13)	110.9(20)
C(2)-C(3)-Mn(1)	69.2(10)	C(8)-C(7)-C(13)	124.3(21)
C(5)-C(4)-C(3)	110.7(18)	C(9)-C(8)-C(7)	119.0(19)
C(5)-C(4)-C(9)	121.0(20)	C(9)-C(8)-C(12)	112.5(19)
C(3)-C(4)-C(9)	128.3(17)	C(7)-C(8)-C(12)	128.5(20)
C(5)-C(4)-Mn(1)	72.3(9)	C(8)-C(9)-C(4)	118.0(19)
C(3)-C(4)-Mn(1)	69.2(9)	C(8)-C(9)-C(10)	110.2(19)
C(9)-C(4)-Mn(1)	126.9(9)	C(4)-C(9)-C(10)	131.8(18)
C(4)-C(5)-C(1)	106.7(19)	C(9)-C(10)-C(11)	105.9(18)
C(4)-C(5)-C(6)	121.7(22)	C(10)-C(11)-C(12)	105.6(20)
C(1)-C(5)-C(6)	131.6(19)	C(8)-C(12)-C(11)	103.4(16)
C(4)-C(5)-Mn(1)	70.7(9)	C(7)-C(13)-C(14)	105.2(18)
C(1)-C(5)-Mn(1)	67.3(10)	C(15)-C(14)-C(13)	104.4(17)
C(6)-C(5)-Mn(1)	126.1(10)	C(6)-C(15)-C(14)	110.0(23)
C(7)-C(6)-C(5)	115.5(22)	O(16)-C(16)-Mn(1)	178.6(15)
C(7)-C(6)-C(15)	109.4(21)	O(17)-C(17)-Mn(1)	175.8(16)
C(5)-C(6)-C(15)	135.0(23)	O(18)-C(18)-Mn(1)	178.7(16)
C(6)-C(7)-C(8)	124.8(24)		

Table A3.4: Anisotropic displacement parameters ($Å^2 x\ 10^3$) for **80**. The anisotropic displacement factor exponent takes the form: $-2\pi^2[\ h^2 a^{*2} U^{11} + ... + 2\ h\ k\ a^*\ b^*\ U^{12}\ ]$.

	U^{11}	U^{22}	U^{33}	U^{23}	U^{13}	U^{12}
Mn(1)	26(2)	49(2)	78(3)	0(1)	37(2)	4(1)
C(1)	31(10)	43(13)	93(20)	-11(10)	40(13)	-10(8)
C(2)	49(13)	43(13)	85(21)	-13(10)	51(15)	-10(8)
C(3)	30(11)	54(13)	70(19)	16(9)	34(13)	2(8)
C(4)	39(13)	46(13)	67(21)	-17(10)	46(15)	-14(9)
C(5)	11(10)	66(15)	58(19)	28(10)	20(12)	15(8)
C(6)	42(13)	49(14)	71(23)	-4(10)	39(16)	-5(9)
C(7)	28(13)	90(18)	43(22)	1(12)	33(16)	-2(10)
C(8)	27(12)	62(15)	31(19)	-18(10)	14(14)	-17(8)
C(9)	18(10)	64(15)	56(20)	13(11)	21(13)	8(8)
C(10)	66(15)	48(14)	99(22)	-6(11)	67(17)	-6(10)
C(11)	36(12)	75(16)	96(22)	-4(12)	35(14)	3(10)
C(12)	44(12)	51(13)	83(20)	-10(10)	40(14)	-16(9)
C(13)	53(13)	52(14)	101(24)	1(11)	47(16)	10(10)
C(14)	56(13)	31(13)	118(25)	11(10)	34(16)	4(8)
C(15)	82(17)	63(16)	74(21)	22(12)	44(16)	26(12)
O(16)	53(9)	76(12)	135(18)	24(9)	48(11)	-5(7)
O(17)	44(8)	35(8)	119(15)	-21(7)	26(9)	2(5)
O(18)	46(9)	59(9)	98(14)	-13(7)	28(9)	-2(7)
C(18)	24(10)	54(12)	80(17)	8(9)	33(11)	6(8)

Table A3.5: Hydrogen coordinates (x 10^4) and isotropic displacement parameters ($Å^2$x 10^3) for **80**.

	x	y	z	U(eq)
H(1A)	2858(11)	2976(18)	1912(13)	63
H(2A)	2515(13)	5326(19)	1368(14)	66
H(3A)	1495(12)	5148(19)	174(13)	58
H(10A)	869(13)	3439(19)	-1129(13)	79
H(10B)	72(13)	3187(19)	-742(13)	79
H(11A)	665(11)	1521(21)	-1787(13)	80
H(11B)	-239(11)	1519(21)	-1564(13)	80
H(12A)	81(11)	-180(19)	-727(12)	68
H(12B)	880(11)	-428(19)	-1116(12)	68
H(13A)	1894(12)	-1755(20)	36(14)	78
H(13B)	1089(12)	-1797(20)	432(14)	78
H(14A)	1863(13)	-2133(19)	1532(15)	80
H(14B)	2661(13)	-2200(19)	1127(15)	80
H(15A)	2266(14)	-151(21)	1971(13)	84
H(15B)	3025(14)	-173(21)	1520(13)	84

Table A4.1: Crystal data and structure refinement for **81**.

Empirical formula	$C_{20}H_{24}O_5PMn$	
Formula weight	430.30	
Temperature	299(2) K	
Wavelength	0.71073 Å	
Crystal system	Monoclinic	
Space group	P2(1)/c	
Unit cell dimensions	a = 9.7266(8) Å	α= 90°.
	b = 22.349(2) Å	β= 106.4810(10)°.
	c = 9.6034(8) Å	γ = 90°.
Volume	2001.8(3) $Å^3$	
Z	4	
Density (calculated)	1.428 Mg/m^3	
Absorption coefficient	0.767 mm^{-1}	
F(000)	896	
Crystal size	.08 x .33 x .35 mm^3	
Theta range for data collection	1.82 to 27.50°.	
Index ranges	$-12 \leq h \leq 12$, $-28 \leq k \leq 26$, $-12 \leq l \leq 11$	
Reflections collected	17829	
Independent reflections	4584 [R(int) = 0.0305]	
Refinement method	Full-matrix least-squares on F^2	
Data / restraints / parameters	4583 / 0 / 244	
Goodness-of-fit on F^2	1.029	
Final R indices [I>2sigma(I)]	R1 = 0.0349, wR2 = 0.0867	
R indices (all data)	R1 = 0.0533, wR2 = 0.0955	
Largest diff. peak and hole	0.259 and -0.206 $e.Å^{-3}$	

Table A4.2: Atomic coordinates (x 10^4) and equivalent isotropic displacement parameters ($Å^2$ x 10^3) for **81**. U(eq) is defined as one third of the trace of the orthogonalized U^{ij} tensor.

	x	y	z	U(eq)
Mn(1)	3710(1)	5676(1)	6636(1)	38(1)
P(1)	3863(1)	6502(1)	7853(1)	43(1)
C(6)	439(2)	5924(1)	6913(2)	38(1)
C(5)	1441(2)	5510(1)	6625(2)	38(1)
C(4)	1564(2)	5463(1)	5168(2)	40(1)
C(1)	2417(2)	5089(1)	7511(2)	45(1)
C(7)	-379(2)	6266(1)	5807(2)	42(1)
C(17)	5453(2)	5484(1)	7678(3)	50(1)
C(9)	714(2)	5837(1)	4064(2)	45(1)
C(16)	4351(2)	6029(1)	5294(3)	48(1)
C(8)	-241(2)	6221(1)	4382(2)	45(1)
C(3)	2606(2)	5004(1)	5180(3)	48(1)
C(15)	96(2)	6038(1)	8321(2)	53(1)
C(2)	3065(2)	4771(1)	6589(3)	51(1)
C(13)	-1363(2)	6666(1)	6340(3)	58(1)
C(10)	697(3)	5875(1)	2494(3)	66(1)
C(12)	-1037(3)	6575(1)	3064(3)	64(1)
C(14)	-924(3)	6564(1)	7985(3)	75(1)
C(11)	-415(4)	6352(2)	1873(3)	102(1)
O(2)	4773(2)	6242(1)	4391(2)	74(1)
O(1)	6593(2)	5341(1)	8360(2)	77(1)
O(5)	2744(2)	7036(1)	7332(2)	57(1)
O(4)	3664(2)	6506(1)	9455(2)	62(1)
O(3)	5388(2)	6813(1)	8052(2)	69(1)
C(20)	2478(3)	7272(1)	5893(3)	78(1)
C(19)	4471(4)	6100(2)	10539(3)	86(1)
C(18)	5765(4)	7366(1)	8847(5)	106(1)

Table A4.3: Bond lengths [Å] and angles [°] for **81**.

Mn(1)-C(17)	1.760(3)	O(4)-C(19)	1.435(3)
Mn(1)-C(16)	1.768(2)	O(3)-C(18)	1.445(3)
Mn(1)-C(2)	2.114(2)	C(17)-Mn(1)-C(16)	92.36(11)
Mn(1)-C(3)	2.125(2)	C(17)-Mn(1)-C(2)	90.66(10)
Mn(1)-C(1)	2.147(2)	C(16)-Mn(1)-C(2)	125.09(10)
Mn(1)-P(1)	2.1673(6)	C(17)-Mn(1)-C(3)	115.30(10)
Mn(1)-C(4)	2.214(2)	C(16)-Mn(1)-C(3)	93.03(10)
Mn(1)-C(5)	2.235(2)	C(2)-Mn(1)-C(3)	38.53(9)
P(1)-O(5)	1.597(2)	C(17)-Mn(1)-C(1)	101.86(10)
P(1)-O(3)	1.598(2)	C(16)-Mn(1)-C(1)	157.61(10)
P(1)-O(4)	1.604(2)	C(2)-Mn(1)-C(1)	38.80(8)
C(6)-C(7)	1.366(3)	C(3)-Mn(1)-C(1)	65.33(9)
C(6)-C(5)	1.426(3)	C(17)-Mn(1)-P(1)	89.61(8)
C(6)-C(15)	1.504(3)	C(16)-Mn(1)-P(1)	91.62(7)
C(5)-C(1)	1.433(3)	C(2)-Mn(1)-P(1)	143.23(7)
C(5)-C(4)	1.442(3)	C(3)-Mn(1)-P(1)	154.41(6)
C(4)-C(9)	1.417(3)	C(1)-Mn(1)-P(1)	105.53(6)
C(4)-C(3)	1.440(3)	C(17)-Mn(1)-C(4)	153.11(10)
C(1)-C(2)	1.416(3)	C(16)-Mn(1)-C(4)	95.47(9)
C(7)-C(8)	1.416(3)	C(2)-Mn(1)-C(4)	63.90(9)
C(7)-C(13)	1.503(3)	C(3)-Mn(1)-C(4)	38.71(8)
C(17)-O(1)	1.162(3)	C(1)-Mn(1)-C(4)	64.32(8)
C(9)-C(8)	1.362(3)	P(1)-Mn(1)-C(4)	115.77(6)
C(9)-C(10)	1.506(3)	C(17)-Mn(1)-C(5)	138.87(9)
C(16)-O(2)	1.161(3)	C(16)-Mn(1)-C(5)	128.47(9)
C(8)-C(12)	1.507(3)	C(2)-Mn(1)-C(5)	63.56(8)
C(3)-C(2)	1.399(3)	C(3)-Mn(1)-C(5)	64.26(8)
C(15)-C(14)	1.513(3)	C(1)-Mn(1)-C(5)	38.11(8)
C(13)-C(14)	1.533(4)	P(1)-Mn(1)-C(5)	93.47(5)
C(10)-C(11)	1.514(4)	C(4)-Mn(1)-C(5)	37.81(7)
C(12)-C(11)	1.523(4)	O(5)-P(1)-O(3)	103.86(9)
O(5)-C(20)	1.432(3)	O(5)-P(1)-O(4)	92.21(9)

O(3)-P(1)-O(4)	104.04(10)	C(8)-C(7)-C(13)	127.9(2)
O(5)-P(1)-Mn(1)	122.10(7)	O(1)-C(17)-Mn(1)	178.1(2)
O(3)-P(1)-Mn(1)	110.74(6)	C(8)-C(9)-C(4)	119.7(2)
O(4)-P(1)-Mn(1)	120.90(7)	C(8)-C(9)-C(10)	112.0(2)
C(7)-C(6)-C(5)	119.4(2)	C(4)-C(9)-C(10)	128.4(2)
C(7)-C(6)-C(15)	112.1(2)	O(2)-C(16)-Mn(1)	177.7(2)
C(5)-C(6)-C(15)	128.5(2)	C(9)-C(8)-C(7)	121.2(2)
C(6)-C(5)-C(1)	133.2(2)	C(9)-C(8)-C(12)	111.3(2)
C(6)-C(5)-C(4)	119.0(2)	C(7)-C(8)-C(12)	127.4(2)
C(1)-C(5)-C(4)	107.7(2)	C(2)-C(3)-C(4)	107.7(2)
C(6)-C(5)-Mn(1)	128.31(14)	C(2)-C(3)-Mn(1)	70.33(13)
C(1)-C(5)-Mn(1)	67.63(11)	C(4)-C(3)-Mn(1)	73.98(12)
C(4)-C(5)-Mn(1)	70.30(11)	C(6)-C(15)-C(14)	103.9(2)
C(9)-C(4)-C(3)	133.3(2)	C(3)-C(2)-C(1)	110.0(2)
C(9)-C(4)-C(5)	119.4(2)	C(3)-C(2)-Mn(1)	71.14(12)
C(3)-C(4)-C(5)	107.3(2)	C(1)-C(2)-Mn(1)	71.85(12)
C(9)-C(4)-Mn(1)	126.42(15)	C(7)-C(13)-C(14)	104.1(2)
C(3)-C(4)-Mn(1)	67.31(12)	C(9)-C(10)-C(11)	103.8(2)
C(5)-C(4)-Mn(1)	71.89(11)	C(8)-C(12)-C(11)	103.8(2)
C(2)-C(1)-C(5)	107.2(2)	C(15)-C(14)-C(13)	108.1(2)
C(2)-C(1)-Mn(1)	69.35(12)	C(10)-C(11)-C(12)	109.1(2)
C(5)-C(1)-Mn(1)	74.26(11)	C(20)-O(5)-P(1)	119.8(2)
C(6)-C(7)-C(8)	121.2(2)	C(19)-O(4)-P(1)	120.1(2)
C(6)-C(7)-C(13)	110.8(2)	C(18)-O(3)-P(1)	121.5(2)

Table A4.4: Anisotropic displacement parameters ($Å^2$ x 10^3) for **81**. The anisotropic displacement factor exponent takes the form: $-2\pi^2[h^2a^{*2}U^{11} + ... + 2 h k a^* b^* U^{12}]$.

	U^{11}	U^{22}	U^{33}	U^{23}	U^{13}	U^{12}
Mn(1)	37(1)	33(1)	45(1)	-4(1)	15(1)	1(1)
P(1)	39(1)	36(1)	55(1)	-8(1)	17(1)	-1(1)
C(6)	33(1)	43(1)	38(1)	-1(1)	11(1)	-2(1)
C(5)	37(1)	37(1)	41(1)	-2(1)	11(1)	-4(1)
C(4)	43(1)	38(1)	41(1)	-7(1)	13(1)	-6(1)
C(1)	45(1)	39(1)	50(1)	5(1)	13(1)	-2(1)
C(7)	36(1)	42(1)	46(1)	-3(1)	10(1)	-1(1)
C(17)	47(1)	45(1)	63(2)	-4(1)	20(1)	1(1)
C(9)	49(1)	48(1)	37(1)	-5(1)	12(1)	-8(1)
C(16)	48(1)	43(1)	57(1)	-7(1)	21(1)	-1(1)
C(8)	44(1)	44(1)	41(1)	2(1)	4(1)	-3(1)
C(3)	53(1)	38(1)	56(1)	-14(1)	20(1)	-4(1)
C(15)	47(1)	68(2)	48(1)	1(1)	21(1)	7(1)
C(2)	51(1)	32(1)	69(2)	-2(1)	17(1)	1(1)
C(13)	47(1)	65(2)	61(2)	-4(1)	12(1)	14(1)
C(10)	79(2)	80(2)	41(1)	-2(1)	18(1)	-2(2)
C(12)	70(2)	64(2)	50(2)	13(1)	3(1)	6(1)
C(14)	82(2)	85(2)	64(2)	-2(2)	31(2)	29(2)
C(11)	136(3)	117(3)	56(2)	30(2)	31(2)	36(2)
O(2)	90(1)	68(1)	80(1)	7(1)	52(1)	-4(1)
O(1)	47(1)	82(1)	96(2)	6(1)	9(1)	15(1)
O(5)	59(1)	38(1)	80(1)	0(1)	28(1)	7(1)
O(4)	75(1)	58(1)	53(1)	-13(1)	20(1)	7(1)
O(3)	46(1)	55(1)	112(2)	-35(1)	32(1)	-16(1)
C(20)	85(2)	52(2)	97(2)	20(2)	28(2)	12(1)
C(19)	111(3)	90(2)	50(2)	-1(2)	10(2)	16(2)
C(18)	77(2)	77(2)	169(4)	-66(2)	45(2)	-37(2)

Table A4.5: Hydrogen coordinates (x 10^4) and isotropic displacement parameters ($Å^2$ x 10^3) for **81**.

	x	y	z	U(eq)
H(1A)	2539(2)	5008(1)	8542(2)	54
H(3A)	2869(2)	4852(1)	4332(3)	58
H(15A)	955(2)	6136(1)	9089(2)	63
H(15B)	-357(2)	5691(1)	8611(2)	63
H(2A)	3716(2)	4430(1)	6886(3)	61
H(13A)	-2358(2)	6557(1)	5906(3)	70
H(13B)	-1231(2)	7082(1)	6114(3)	70
H(10A)	424(3)	5495(1)	2006(3)	80
H(10B)	1629(3)	5991(1)	2405(3)	80
H(12A)	-871(3)	7001(1)	3225(3)	77
H(12B)	-2060(3)	6498(1)	2819(3)	77
H(14A)	-458(3)	6918(1)	8486(3)	90
H(14B)	-1764(3)	6480(1)	8307(3)	90
H(11A)	-1172(4)	6186(2)	1080(3)	123
H(11B)	24(4)	6681(2)	1498(3)	123
H(20A)	1784(3)	7588(1)	5754(3)	117
H(20B)	2117(3)	6960(1)	5199(3)	117
H(20C)	3355(3)	7426(1)	5763(3)	117
H(19A)	4225(4)	6161(2)	11429(3)	129
H(19B)	5477(4)	6172(2)	10699(3)	129
H(19C)	4249(4)	5696(2)	10214(3)	129
H(18A)	6716(4)	7482(1)	8850(5)	158
H(18B)	5730(4)	7311(1)	9827(5)	158
H(18C)	5098(4)	7673(1)	8390(5)	158

Table A5.1: Crystal data and structure refinement for **98**.

Empirical formula	$C_{22}H_{36}O_7P_2MnBF_4$	
Formula weight	616.20	
Temperature	173(2) K	
Wavelength	0.71073 Å	
Crystal system	Triclinic	
Space group	P-1	
Unit cell dimensions	a = 9.338(3) Å	α= 97.530(7)°.
	b = 11.092(4) Å	β= 94.265(11)°.
	c = 12.973(5) Å	γ = 91.954(10)°.
Volume	1327.1(9) $Å^3$	
Z	2	
Density (calculated)	1.542 Mg/m^3	
Absorption coefficient	0.687 mm^{-1}	
F(000)	640	
Crystal size	0.18 x 0.42 x 0.44 mm^3	
Theta range for data collection	1.59 to 27.52°.	
Index ranges	$-9 \leq h \leq 7, -13 \leq k \leq 14, -16 \leq l \leq 3$	
Reflections collected	3442	
Independent reflections	3413 [R(int) = 0.0557]	
Refinement method	Full-matrix least-squares on F^2	
Data / restraints / parameters	3413 / 0 / 335	
Goodness-of-fit on F^2	1.056	
Final R indices [I>2sigma(I)]	R1 = 0.0456, wR2 = 0.1251	
R indices (all data)	R1 = 0.0534, wR2 = 0.1306	
Extinction coefficient	0.0034(15)	
Largest diff. peak and hole	0.870 and -0.532 $e.Å^{-3}$	

Table A5.2: Atomic coordinates (x 10^4) and equivalent isotropic displacement parameters ($Å^2$ x 10^3) for **98**. U(eq) is defined as one third of the trace of the orthogonalized U^{ij} tensor.

	x	y	z	U(eq)
Mn(1)	1050(1)	7233(1)	2436(1)	17(1)
P(1)	1198(1)	9131(1)	2118(1)	20(1)
C(1)	-229(5)	6750(3)	930(2)	17(1)
F(1)	5916(4)	13854(3)	2472(3)	76(1)
B(1)	5190(7)	12743(4)	2301(3)	31(2)
P(2)	3130(1)	7577(1)	3389(1)	21(1)
F(2)	6118(4)	11844(3)	2020(2)	67(1)
C(2)	-950(5)	6271(3)	1710(2)	18(1)
C(3)	-215(5)	5515(3)	2358(2)	19(1)
F(3)	4571(4)	12491(3)	3189(2)	63(1)
F(4)	4091(3)	12765(2)	1513(2)	38(1)
C(4)	1217(5)	5222(3)	2207(2)	21(1)
C(5)	1945(5)	5701(3)	1418(2)	18(1)
C(6)	1197(5)	6458(3)	772(2)	16(1)
C(7)	2141(5)	6732(3)	-73(2)	21(1)
C(8)	3657(5)	6465(3)	363(2)	22(1)
C(9)	3411(5)	5469(3)	1069(2)	24(1)
C(10)	1693(5)	4295(3)	2907(2)	24(1)
C(11)	610(5)	4460(3)	3759(2)	29(1)
C(12)	-788(5)	4860(3)	3211(2)	26(1)
C(13)	-2490(5)	6624(3)	1686(2)	25(1)
C(14)	-2570(5)	7613(3)	939(2)	26(1)
C(15)	-1237(5)	7454(3)	294(2)	22(1)
O(16)	-718(4)	8044(3)	4145(2)	41(1)
C(16)	45(5)	7758(3)	3498(2)	23(1)
O(17)	1753(4)	9383(2)	1026(2)	27(1)
C(17)	3139(6)	9882(4)	882(3)	38(2)
O(18)	2168(3)	10145(2)	2875(2)	27(1)
C(18)	1714(6)	10760(3)	3839(2)	41(2)

O(19)	-364(3)	9680(2)	2076(2)	24(1)
C(19)	-592(6)	10852(3)	1713(3)	40(2)
O(20)	4363(3)	8261(2)	2867(2)	24(1)
C(20)	5362(6)	9219(4)	3364(3)	38(2)
O(21)	3829(4)	6353(2)	3669(2)	28(1)
C(21)	5251(6)	6354(4)	4204(3)	35(1)
O(22)	3197(3)	8432(2)	4495(2)	28(1)
C(22)	2550(5)	8012(4)	5374(2)	40(2)

Table A5.3: Bond lengths [Å] and angles [°] for **98**.

Mn(1)-C(16)	1.772(4)	C(8)-C(9)	1.547(4)
Mn(1)-C(3)	2.194(4)	C(10)-C(11)	1.551(5)
Mn(1)-P(1)	2.1996(12)	C(11)-C(12)	1.546(5)
Mn(1)-C(2)	2.203(4)	C(13)-C(14)	1.556(4)
Mn(1)-C(1)	2.206(3)	C(14)-C(15)	1.553(6)
Mn(1)-P(2)	2.2174(14)	O(16)-C(16)	1.160(4)
Mn(1)-C(4)	2.224(3)	O(17)-C(17)	1.425(6)
Mn(1)-C(6)	2.232(3)	O(18)-C(18)	1.442(4)
Mn(1)-C(5)	2.237(3)	O(19)-C(19)	1.457(4)
P(1)-O(17)	1.598(3)	O(20)-C(20)	1.442(5)
P(1)-O(19)	1.599(3)	O(21)-C(21)	1.452(5)
P(1)-O(18)	1.600(3)	O(22)-C(22)	1.452(4)
C(1)-C(6)	1.405(6)	C(16)-Mn(1)-C(3)	85.7(2)
C(1)-C(2)	1.407(5)	C(16)-Mn(1)-P(1)	87.07(11)
C(1)-C(15)	1.509(5)	C(3)-Mn(1)-P(1)	149.29(11)
F(1)-B(1)	1.370(6)	C(16)-Mn(1)-C(2)	86.7(2)
B(1)-F(2)	1.375(5)	C(3)-Mn(1)-C(2)	37.69(12)
B(1)-F(3)	1.382(5)	P(1)-Mn(1)-C(2)	112.11(9)
B(1)-F(4)	1.397(6)	C(16)-Mn(1)-C(1)	114.9(2)
P(2)-O(20)	1.597(3)	C(3)-Mn(1)-C(1)	67.46(13)
P(2)-O(21)	1.599(2)	P(1)-Mn(1)-C(1)	88.88(9)
P(2)-O(22)	1.608(2)	C(2)-Mn(1)-C(1)	37.21(13)
C(2)-C(3)	1.420(4)	C(16)-Mn(1)-P(2)	92.89(14)
C(2)-C(13)	1.502(6)	C(3)-Mn(1)-P(2)	121.86(10)
C(3)-C(4)	1.409(6)	P(1)-Mn(1)-P(2)	88.28(4)
C(3)-C(12)	1.521(5)	C(2)-Mn(1)-P(2)	159.53(9)
C(4)-C(5)	1.418(5)	C(1)-Mn(1)-P(2)	151.86(12)
C(4)-C(10)	1.515(4)	C(16)-Mn(1)-C(4)	113.00(15)
C(5)-C(6)	1.426(4)	C(3)-Mn(1)-C(4)	37.2(2)
C(5)-C(9)	1.493(6)	P(1)-Mn(1)-C(4)	159.57(9)
C(6)-C(7)	1.512(5)	C(2)-Mn(1)-C(4)	67.36(15)
C(7)-C(8)	1.538(5)	C(1)-Mn(1)-C(4)	79.37(12)

P(2)-Mn(1)-C(4)	94.23(12)	O(20)-P(2)-O(21)	104.6(2)
C(16)-Mn(1)-C(6)	151.6(2)	O(20)-P(2)-O(22)	98.89(15)
C(3)-Mn(1)-C(6)	79.04(13)	O(21)-P(2)-O(22)	103.63(12)
P(1)-Mn(1)-C(6)	93.88(9)	O(20)-P(2)-Mn(1)	115.53(10)
C(2)-Mn(1)-C(6)	66.69(15)	O(21)-P(2)-Mn(1)	112.71(12)
C(1)-Mn(1)-C(6)	36.90(15)	O(22)-P(2)-Mn(1)	119.49(13)
P(2)-Mn(1)-C(6)	115.47(12)	C(1)-C(2)-C(3)	119.6(4)
C(4)-Mn(1)-C(6)	66.74(11)	C(1)-C(2)-C(13)	111.2(3)
C(16)-Mn(1)-C(5)	150.06(15)	C(3)-C(2)-C(13)	129.1(4)
C(3)-Mn(1)-C(5)	67.10(14)	C(1)-C(2)-Mn(1)	71.5(2)
P(1)-Mn(1)-C(5)	122.72(9)	C(3)-C(2)-Mn(1)	70.8(2)
C(2)-Mn(1)-C(5)	79.48(14)	C(13)-C(2)-Mn(1)	131.8(2)
C(1)-Mn(1)-C(5)	67.18(13)	C(4)-C(3)-C(2)	120.4(3)
P(2)-Mn(1)-C(5)	91.16(11)	C(4)-C(3)-C(12)	110.7(3)
C(4)-Mn(1)-C(5)	37.07(13)	C(2)-C(3)-C(12)	128.8(4)
C(6)-Mn(1)-C(5)	37.21(11)	C(4)-C(3)-Mn(1)	72.6(2)
O(17)-P(1)-O(19)	102.30(14)	C(2)-C(3)-Mn(1)	71.5(2)
O(17)-P(1)-O(18)	99.1(2)	C(12)-C(3)-Mn(1)	131.3(2)
O(19)-P(1)-O(18)	103.86(14)	C(3)-C(4)-C(5)	120.1(3)
O(17)-P(1)-Mn(1)	117.85(9)	C(3)-C(4)-C(10)	110.0(3)
O(19)-P(1)-Mn(1)	110.07(11)	C(5)-C(4)-C(10)	129.6(4)
O(18)-P(1)-Mn(1)	121.20(10)	C(3)-C(4)-Mn(1)	70.3(2)
C(6)-C(1)-C(2)	120.3(3)	C(5)-C(4)-Mn(1)	72.0(2)
C(6)-C(1)-C(15)	128.9(3)	C(10)-C(4)-Mn(1)	134.4(2)
C(2)-C(1)-C(15)	110.6(4)	C(4)-C(5)-C(6)	119.0(4)
C(6)-C(1)-Mn(1)	72.6(2)	C(4)-C(5)-C(9)	130.0(3)
C(2)-C(1)-Mn(1)	71.3(2)	C(6)-C(5)-C(9)	110.7(3)
C(15)-C(1)-Mn(1)	132.8(2)	C(4)-C(5)-Mn(1)	71.0(2)
F(1)-B(1)-F(2)	110.0(5)	C(6)-C(5)-Mn(1)	71.2(2)
F(1)-B(1)-F(3)	111.0(3)	C(9)-C(5)-Mn(1)	133.1(3)
F(2)-B(1)-F(3)	108.6(3)	C(1)-C(6)-C(5)	120.6(3)
F(1)-B(1)-F(4)	108.8(3)	C(1)-C(6)-C(7)	130.5(3)
F(2)-B(1)-F(4)	110.4(3)	C(5)-C(6)-C(7)	108.8(3)
F(3)-B(1)-F(4)	108.1(5)	C(1)-C(6)-Mn(1)	70.5(2)

C(5)-C(6)-Mn(1)	71.6(2)	C(15)-C(14)-C(13)	105.9(3)
C(7)-C(6)-Mn(1)	134.5(3)	C(1)-C(15)-C(14)	104.2(3)
C(6)-C(7)-C(8)	103.6(3)	O(16)-C(16)-Mn(1)	173.9(4)
C(7)-C(8)-C(9)	104.7(3)	C(17)-O(17)-P(1)	125.5(2)
C(5)-C(9)-C(8)	103.3(3)	C(18)-O(18)-P(1)	123.7(3)
C(4)-C(10)-C(11)	102.0(3)	C(19)-O(19)-P(1)	120.7(3)
C(12)-C(11)-C(10)	105.6(3)	C(20)-O(20)-P(2)	127.4(2)
C(3)-C(12)-C(11)	102.0(3)	C(21)-O(21)-P(2)	122.0(2)
C(2)-C(13)-C(14)	104.2(3)	C(22)-O(22)-P(2)	120.4(3)

Table A5.4: Anisotropic displacement parameters ($Å^2 \times 10^3$) for **98**. The anisotropic displacement factor exponent takes the form: $-2\pi^2[h^2a^{*2}U^{11} + ... + 2\ h\ k\ a^*\ b^*\ U^{12}]$.

	U^{11}	U^{22}	U^{33}	U^{23}	U^{13}	U^{12}
Mn(1)	16(1)	16(1)	18(1)	0(1)	-1(1)	3(1)
P(1)	19(1)	16(1)	22(1)	-1(1)	-2(1)	3(1)
C(1)	11(4)	19(2)	21(1)	-3(1)	-2(1)	-1(2)
F(1)	51(4)	53(2)	116(3)	7(2)	-34(2)	-21(2)
B(1)	27(5)	31(2)	34(2)	2(2)	-4(2)	5(3)
P(2)	19(1)	19(1)	22(1)	0(1)	-3(1)	4(1)
F(2)	65(3)	70(2)	74(2)	19(1)	17(2)	43(2)
C(2)	9(4)	21(2)	23(1)	-2(1)	-2(1)	0(2)
C(3)	13(4)	20(2)	23(1)	0(1)	2(1)	-2(2)
F(3)	52(3)	105(2)	39(1)	26(1)	5(1)	24(2)
F(4)	44(3)	32(1)	38(1)	10(1)	-14(1)	2(1)
C(4)	24(4)	11(2)	25(1)	-1(1)	1(2)	-1(2)
C(5)	17(4)	11(2)	24(1)	-1(1)	2(1)	1(2)
C(6)	9(4)	14(2)	22(1)	-2(1)	-2(1)	-3(2)
C(7)	21(4)	20(2)	23(1)	0(1)	3(1)	2(2)
C(8)	15(4)	20(2)	32(2)	4(1)	4(2)	0(2)
C(9)	25(4)	18(2)	29(2)	3(1)	5(2)	5(2)
C(10)	27(4)	16(2)	30(2)	6(1)	2(2)	3(2)
C(11)	32(4)	28(2)	30(2)	12(1)	9(2)	4(2)
C(12)	23(4)	26(2)	30(2)	7(1)	6(2)	-3(2)
C(13)	15(4)	31(2)	28(2)	2(1)	0(2)	-5(2)
C(14)	11(4)	33(2)	33(2)	5(1)	-2(2)	4(2)
C(15)	17(4)	25(2)	23(1)	2(1)	-5(1)	2(2)
O(16)	41(3)	51(2)	29(1)	-7(1)	13(1)	8(2)
C(16)	19(4)	24(2)	24(1)	-2(1)	-6(2)	-1(2)
O(17)	25(3)	26(1)	28(1)	3(1)	2(1)	-8(2)
C(17)	33(5)	45(3)	38(2)	12(2)	1(2)	-7(3)
O(18)	25(3)	20(1)	33(1)	-7(1)	-2(1)	-2(1)
C(18)	61(5)	27(2)	30(2)	-11(1)	-2(2)	14(2)

O(19)	15(3)	22(1)	36(1)	5(1)	-3(1)	5(1)
C(19)	47(5)	26(2)	49(2)	10(2)	-5(2)	20(2)
O(20)	13(3)	25(1)	32(1)	1(1)	-3(1)	-6(1)
C(20)	29(5)	33(2)	47(2)	2(2)	-6(2)	-12(3)
O(21)	22(3)	25(1)	36(1)	6(1)	-8(1)	6(2)
C(21)	26(5)	41(2)	39(2)	11(2)	-4(2)	14(2)
O(22)	28(3)	32(1)	23(1)	-3(1)	-3(1)	3(2)
C(22)	31(5)	67(3)	22(2)	3(2)	-1(2)	6(3)

Table A5.5: Hydrogen coordinates (x 10^4) and isotropic displacement parameters ($Å^2$ x 10^3) for **98**.

	x	y	z	U(eq)
H(7A)	2087(5)	7594(3)	-192(2)	26
H(7B)	1859(5)	6201(3)	-736(2)	26
H(8A)	4137(5)	7205(3)	771(2)	26
H(8B)	4255(5)	6169(3)	-209(2)	26
H(9A)	3443(5)	4646(3)	674(2)	29
H(9B)	4141(5)	5553(3)	1671(2)	29
H(10A)	2694(5)	4477(3)	3210(2)	29
H(10B)	1614(5)	3459(3)	2525(2)	29
H(11A)	435(5)	3686(3)	4042(2)	35
H(11B)	980(5)	5089(3)	4340(2)	35
H(12A)	-1428(5)	4150(3)	2914(2)	31
H(12B)	-1315(5)	5414(3)	3696(2)	31
H(13A)	-2743(5)	6958(3)	2392(2)	30
H(13B)	-3147(5)	5916(3)	1416(2)	30
H(14A)	-3467(5)	7494(3)	474(2)	31
H(14B)	-2544(5)	8437(3)	1341(2)	31
H(15A)	-1504(5)	6995(3)	-405(2)	27
H(15B)	-791(5)	8254(3)	210(2)	27
H(17A)	3211(6)	9945(4)	141(3)	57
H(17B)	3878(6)	9352(4)	1120(3)	57
H(17C)	3282(6)	10693(4)	1287(3)	57
H(18A)	2479(6)	11340(3)	4171(2)	61
H(18B)	1512(6)	10161(3)	4307(2)	61
H(18C)	843(6)	11197(3)	3692(2)	61
H(19A)	-1607(6)	11042(3)	1741(3)	60
H(19B)	-327(6)	10817(3)	993(3)	60
H(19C)	5(6)	11486(3)	2161(3)	60
H(20A)	5997(6)	9464(4)	2852(3)	56
H(20B)	5939(6)	8924(4)	3934(3)	56
H(20C)	4831(6)	9919(4)	3643(3)	56

H(21A)	5481(6)	5519(4)	4302(3)	52
H(21B)	5271(6)	6857(4)	4885(3)	52
H(21C)	5962(6)	6687(4)	3785(3)	52
H(22A)	2691(5)	8644(4)	5980(2)	60
H(22B)	3004(5)	7270(4)	5541(2)	60
H(22C)	1519(5)	7839(4)	5196(2)	60

Table A6.1: Crystal data and structure refinement for **102**.

Empirical formula	$C_{18}H_{14}O_3\ MnBF_4$	
Formula weight	420.04	
Temperature	173(2) K	
Wavelength	0.71073 Å	
Crystal system	Monoclinic	
Space group	P2(1)/n	
Unit cell dimensions	a = 7.733(2) Å	α= 90°.
	b = 7.774(2) Å	β= 96.660(4)°.
	c = 28.795(7) Å	γ = 90°.
Volume	1719.4(7) $Å^3$	
Z	4	
Density (calculated)	1.623 Mg/m^3	
Absorption coefficient	0.825 mm^{-1}	
F(000)	848	
Crystal size	.12 x .28 x .42 mm^3	
Theta range for data collection	1.42 to 27.50°.	
Index ranges	$-9 \leq h \leq 10, -9 \leq k \leq 10, -37 \leq l \leq 37$	
Reflections collected	14780	
Independent reflections	3936 [R(int) = 0.0290]	
Refinement method	Full-matrix least-squares on F^2	
Data / restraints / parameters	3935 / 0 / 240	
Goodness-of-fit on F^2	1.051	
Final R indices [I>2sigma(I)]	R1 = 0.0481, wR2 = 0.1208	
R indices (all data)	R1 = 0.0588, wR2 = 0.1272	
Extinction coefficient	0.0001(7)	
Largest diff. peak and hole	1.033 and -1.215 $e.Å^{-3}$	

Table A6.2: Atomic coordinates (x 10^4) and equivalent isotropic displacement parameters ($Å^2$ x 10^3) for **102**. U(eq) is defined as one third of the trace of the orthogonalized U^{ij} tensor.

	x	y	z	U(eq)
Mn(1)	3139(1)	7404(1)	822(1)	23(1)
C(1)	1065(3)	6179(4)	1200(1)	27(1)
B(1)	2131(5)	8298(5)	-877(1)	36(1)
F(1)	1189(4)	7359(4)	-1222(1)	85(1)
C(2)	335(4)	7366(4)	860(1)	32(1)
F(2)	1054(4)	8848(3)	-558(1)	78(1)
C(3)	638(4)	7247(4)	390(1)	34(1)
F(3)	2857(3)	9673(3)	-1082(1)	61(1)
C(4)	1724(4)	5961(4)	251(1)	32(1)
F(4)	3419(3)	7263(4)	-660(1)	76(1)
C(5)	2505(4)	4803(4)	588(1)	29(1)
C(6)	2199(3)	4879(3)	1064(1)	25(1)
C(7)	3080(4)	3522(4)	1390(1)	31(1)
C(8)	3980(4)	4170(4)	1853(1)	28(1)
C(9)	5757(4)	3960(4)	1962(1)	39(1)
C(10)	6576(4)	4494(5)	2388(1)	46(1)
C(11)	5641(5)	5291(5)	2709(1)	45(1)
C(12)	3861(4)	5510(4)	2602(1)	36(1)
C(13)	3005(4)	4940(4)	2176(1)	28(1)
C(14)	1069(4)	5129(4)	2066(1)	33(1)
C(15)	521(4)	6446(4)	1685(1)	33(1)
C(16)	4058(4)	8293(5)	1383(1)	43(1)
O(16)	4599(4)	8861(5)	1733(1)	70(1)
C(17)	5290(4)	6951(4)	666(1)	44(1)
O(17)	6598(3)	6662(4)	540(1)	76(1)
C(18)	3250(4)	9501(4)	547(1)	40(1)
O(18)	3265(4)	10781(3)	360(1)	72(1)

Table A6.3: Bond lengths [Å] and angles [°] for **102**.

Mn(1)-C(17)	1.807(3)	C(18)-O(18)	1.132(4)
Mn(1)-C(18)	1.819(3)	C(17)-Mn(1)-C(18)	88.6(2)
Mn(1)-C(16)	1.824(3)	C(17)-Mn(1)-C(16)	91.1(2)
Mn(1)-C(5)	2.169(3)	C(18)-Mn(1)-C(16)	90.7(2)
Mn(1)-C(4)	2.178(3)	C(17)-Mn(1)-C(5)	85.57(13)
Mn(1)-C(3)	2.179(3)	C(18)-Mn(1)-C(5)	136.11(12)
Mn(1)-C(2)	2.185(3)	C(16)-Mn(1)-C(5)	132.76(14)
Mn(1)-C(6)	2.232(3)	C(17)-Mn(1)-C(4)	96.19(14)
Mn(1)-C(1)	2.252(3)	C(18)-Mn(1)-C(4)	100.22(13)
C(1)-C(2)	1.415(4)	C(16)-Mn(1)-C(4)	166.95(13)
C(1)-C(6)	1.422(4)	C(5)-Mn(1)-C(4)	37.82(11)
C(1)-C(15)	1.518(4)	C(17)-Mn(1)-C(3)	128.93(15)
B(1)-F(1)	1.371(5)	C(18)-Mn(1)-C(3)	83.38(13)
B(1)-F(3)	1.372(4)	C(16)-Mn(1)-C(3)	139.13(14)
B(1)-F(4)	1.374(4)	C(5)-Mn(1)-C(3)	67.47(12)
B(1)-F(2)	1.376(4)	C(4)-Mn(1)-C(3)	37.31(12)
C(2)-C(3)	1.405(4)	C(17)-Mn(1)-C(2)	163.26(14)
C(3)-C(4)	1.394(4)	C(18)-Mn(1)-C(2)	97.54(13)
C(4)-C(5)	1.409(4)	C(16)-Mn(1)-C(2)	104.34(13)
C(5)-C(6)	1.419(4)	C(5)-Mn(1)-C(2)	79.22(11)
C(6)-C(7)	1.520(4)	C(4)-Mn(1)-C(2)	67.44(11)
C(7)-C(8)	1.515(4)	C(3)-Mn(1)-C(2)	37.57(11)
C(8)-C(9)	1.383(4)	C(17)-Mn(1)-C(6)	104.42(13)
C(8)-C(13)	1.399(4)	C(18)-Mn(1)-C(6)	163.23(13)
C(9)-C(10)	1.380(5)	C(16)-Mn(1)-C(6)	99.43(13)
C(10)-C(11)	1.383(5)	C(5)-Mn(1)-C(6)	37.57(10)
C(11)-C(12)	1.386(5)	C(4)-Mn(1)-C(6)	68.29(10)
C(12)-C(13)	1.396(4)	C(3)-Mn(1)-C(6)	80.20(11)
C(13)-C(14)	1.501(4)	C(2)-Mn(1)-C(6)	67.12(10)
C(14)-C(15)	1.524(4)	C(17)-Mn(1)-C(1)	139.97(14)
C(16)-O(16)	1.136(4)	C(18)-Mn(1)-C(1)	131.44(13)
C(17)-O(17)	1.137(4)	C(16)-Mn(1)-C(1)	87.58(12)

C(5)-Mn(1)-C(1)	66.92(10)	C(4)-C(5)-C(6)	122.3(3)
C(4)-Mn(1)-C(1)	79.88(10)	C(4)-C(5)-Mn(1)	71.4(2)
C(3)-Mn(1)-C(1)	67.54(11)	C(6)-C(5)-Mn(1)	73.6(2)
C(2)-Mn(1)-C(1)	37.15(10)	C(5)-C(6)-C(1)	118.2(2)
C(6)-Mn(1)-C(1)	36.98(10)	C(5)-C(6)-C(7)	117.0(2)
C(2)-C(1)-C(6)	118.8(2)	C(1)-C(6)-C(7)	124.7(2)
C(2)-C(1)-C(15)	114.6(2)	C(5)-C(6)-Mn(1)	68.79(15)
C(6)-C(1)-C(15)	126.6(3)	C(1)-C(6)-Mn(1)	72.2(2)
C(2)-C(1)-Mn(1)	68.8(2)	C(7)-C(6)-Mn(1)	131.6(2)
C(6)-C(1)-Mn(1)	70.77(15)	C(8)-C(7)-C(6)	116.0(2)
C(15)-C(1)-Mn(1)	132.5(2)	C(9)-C(8)-C(13)	119.9(3)
F(1)-B(1)-F(3)	108.2(3)	C(9)-C(8)-C(7)	120.2(3)
F(1)-B(1)-F(4)	108.3(3)	C(13)-C(8)-C(7)	119.9(3)
F(3)-B(1)-F(4)	109.9(3)	C(10)-C(9)-C(8)	120.5(3)
F(1)-B(1)-F(2)	109.6(3)	C(9)-C(10)-C(11)	120.5(3)
F(3)-B(1)-F(2)	110.8(3)	C(10)-C(11)-C(12)	119.2(3)
F(4)-B(1)-F(2)	109.9(3)	C(11)-C(12)-C(13)	121.0(3)
C(3)-C(2)-C(1)	121.8(3)	C(12)-C(13)-C(8)	118.9(3)
C(3)-C(2)-Mn(1)	71.0(2)	C(12)-C(13)-C(14)	121.0(3)
C(1)-C(2)-Mn(1)	74.0(2)	C(8)-C(13)-C(14)	120.2(3)
C(4)-C(3)-C(2)	119.8(3)	C(13)-C(14)-C(15)	113.9(2)
C(4)-C(3)-Mn(1)	71.3(2)	C(1)-C(15)-C(14)	119.1(2)
C(2)-C(3)-Mn(1)	71.4(2)	O(16)-C(16)-Mn(1)	178.6(3)
C(3)-C(4)-C(5)	119.0(3)	O(17)-C(17)-Mn(1)	175.8(4)
C(3)-C(4)-Mn(1)	71.4(2)	O(18)-C(18)-Mn(1)	177.0(3)
C(5)-C(4)-Mn(1)	70.8(2)		

Table A6.4: Anisotropic displacement parameters ($Å^2 \times 10^3$) for **102**. The anisotropic displacement factor exponent takes the form: $-2\pi^2[h^2a^{*2}U^{11} + ... + 2\ h\ k\ a^*\ b^*\ U^{12}]$.

	U^{11}	U^{22}	U^{33}	U^{23}	U^{13}	U^{12}
Mn(1)	21(1)	21(1)	26(1)	-1(1)	0(1)	-2(1)
C(1)	22(1)	27(1)	32(1)	-1(1)	3(1)	-4(1)
B(1)	39(2)	36(2)	32(2)	-2(1)	7(1)	-3(2)
C(2)	20(1)	31(2)	42(2)	1(1)	1(1)	0(1)
F(2)	109(2)	79(2)	53(1)	23(1)	45(1)	50(2)
C(3)	26(1)	37(2)	36(2)	6(1)	-7(1)	-7(1)
F(3)	66(2)	52(1)	66(1)	14(1)	11(1)	-17(1)
C(4)	33(2)	35(2)	26(1)	-2(1)	-3(1)	-11(1)
F(4)	60(2)	77(2)	93(2)	35(2)	23(1)	25(1)
C(5)	30(1)	27(1)	29(1)	-5(1)	3(1)	-8(1)
C(6)	24(1)	22(1)	28(1)	-1(1)	3(1)	-4(1)
C(7)	36(2)	25(1)	31(1)	0(1)	7(1)	5(1)
C(8)	30(1)	26(1)	29(1)	5(1)	6(1)	2(1)
C(9)	33(2)	47(2)	39(2)	7(1)	8(1)	5(1)
C(10)	29(2)	63(2)	44(2)	12(2)	-2(1)	-5(2)
C(11)	50(2)	49(2)	33(2)	4(1)	-5(1)	-18(2)
C(12)	45(2)	33(2)	30(1)	-1(1)	7(1)	-8(1)
C(13)	32(1)	24(1)	28(1)	2(1)	7(1)	-2(1)
C(14)	31(2)	38(2)	30(1)	0(1)	10(1)	0(1)
C(15)	29(1)	36(2)	36(2)	1(1)	10(1)	8(1)
C(16)	39(2)	55(2)	34(2)	-1(2)	4(1)	-20(2)
O(16)	79(2)	98(2)	33(1)	-14(1)	0(1)	-50(2)
C(17)	30(2)	30(2)	72(2)	-11(2)	8(2)	-6(1)
O(17)	34(1)	58(2)	141(3)	-31(2)	30(2)	-7(1)
C(18)	42(2)	30(2)	43(2)	-1(1)	-9(1)	-8(1)
O(18)	91(2)	33(1)	83(2)	19(1)	-25(2)	-17(1)

Table A6.5: Hydrogen coordinates (x 10^4) and isotropic displacement parameters ($Å^2$ x 10^3) for **102**.

	x	y	z	U(eq)
H(2A)	-235(4)	8426(4)	967(1)	38
H(3A)	262(4)	8206(4)	169(1)	41
H(4A)	2116(4)	5997(4)	-68(1)	38
H(5A)	3467(4)	4049(4)	502(1)	34
H(7A)	2192(4)	2666(4)	1456(1)	37
H(7B)	3952(4)	2916(4)	1224(1)	37
H(9A)	6419(4)	3443(4)	1741(1)	47
H(10A)	7792(4)	4314(5)	2463(1)	55
H(11A)	6213(5)	5683(5)	3000(1)	54
H(12A)	3214(4)	6056(4)	2821(1)	43
H(14A)	574(4)	5470(4)	2354(1)	39
H(14B)	567(4)	3998(4)	1966(1)	39
H(15A)	-765(4)	6521(4)	1652(1)	40
H(15B)	974(4)	7580(4)	1799(1)	40

Table A7.1: Crystal data and structure refinement for **117**.

Empirical formula	$C_{15}H_{21}O_5P_2F_6Mn$	
Formula weight	512.20	
Temperature	173(2) K	
Wavelength	0.71073 Å	
Crystal system	Orthorhombic	
Space group	Pnma	
Unit cell dimensions	a = 15.694(5) Å	α= 90°.
	b = 10.991(4) Å	β= 90°.
	c = 11.735(4) Å	γ = 90°.
Volume	2024.4(11) $Å^3$	
Z	4	
Density (calculated)	1.681 Mg/m^3	
Absorption coefficient	0.889 mm^{-1}	
F(000)	1040	
Crystal size	.32 x .45 x .70 mm^3	
Theta range for data collection	2.17 to 27.69°.	
Index ranges	$-20 \leq h \leq 18$, $-14 \leq k \leq 14$, $-14 \leq l \leq 15$	
Reflections collected	16907	
Independent reflections	2455 [R(int) = 0.0419]	
Refinement method	Full-matrix least-squares on F^2	
Data / restraints / parameters	2452 / 0 / 222	
Goodness-of-fit on F^2	1.164	
Final R indices [I>2sigma(I)]	R1 = 0.0343, wR2 = 0.0882	
R indices (all data)	R1 = 0.0469, wR2 = 0.0991	
Extinction coefficient	0.0000(3)	
Largest diff. peak and hole	0.538 and -0.712 e.$Å^{-3}$	

Table A7.2: Atomic coordinates (x 10^4) and equivalent isotropic displacement parameters ($Å^2$ x 10^3) for **117**. U(eq) is defined as one third of the trace of the orthogonalized U^{ij} tensor.

	x	y	z	U(eq)
P	6960(1)	-2500	-3556(1)	32(1)
Mn(1)	7021(1)	-2500	1129(1)	22(1)
P(1)	5649(1)	-2500	1470(1)	30(1)
C(1)	7304(2)	-1859(2)	2850(2)	35(1)
F(1)	6321(2)	-1496(2)	-3089(3)	68(1)
F(1A)	7774(23)	-1680(35)	-3077(33)	60(10)
C(2)	7818(2)	-1240(2)	2087(2)	34(1)
F(2)	7588(2)	-1491(2)	-4031(4)	85(2)
F(2A)	6724(20)	-1721(23)	-2581(22)	38(6)
C(3)	8349(2)	-1857(2)	1295(2)	32(1)
F(3)	6418(4)	-2500	-4685(3)	124(2)
F(3A)	6846(33)	-1839(33)	-4744(37)	64(12)
F(4)	7432(4)	-2500	-2407(5)	166(4)
F(4A)	7396(19)	-3300(26)	-4509(20)	13(6)
F(5A)	7555(33)	-3152(41)	-2556(40)	37(9)
F(6A)	6333(17)	-3367(25)	-3882(26)	45(7)
C(7)	9186(4)	-2091(6)	-564(5)	55(2)
C(7A)	9539(4)	-3278(7)	-102(6)	59(2)
C(8)	8894(2)	-1147(3)	475(3)	56(1)
O(11)	6733(1)	-583(2)	-585(2)	45(1)
C(11)	6832(1)	-1335(2)	73(2)	29(1)
O(13)	5240(1)	-1437(2)	2216(2)	44(1)
C(13)	5357(2)	-182(3)	1864(3)	55(1)
O(14)	5137(1)	-2500	302(2)	37(1)
C(14)	4209(2)	-2500	266(5)	53(1)

Table A7.3: Bond lengths [Å] and angles [°] for **117**.

P-F(6A)	1.42(3)	C(7A)-C(8)#1	1.372(8)
P-F(6A)#1	1.42(3)	C(8)-C(7A)#1	1.372(8)
P-F(2A)#1	1.48(3)	O(11)-C(11)	1.142(3)
P-F(2A)	1.48(3)	O(13)-C(13)	1.451(4)
P-F(3A)#1	1.58(4)	O(14)-C(14)	1.457(4)
P-F(3A)	1.58(4)	F(6A)-P-F(6A)#1	84.1(22)
P-F(4)	1.538(5)	F(6A)-P-F(2A)#1	69.3(18)
P-F(4A)#1	1.58(3)	F(6A)#1-P-F(2A)#1	115.0(16)
P-F(4A)	1.58(3)	F(6A)-P-F(2A)	115.0(16)
P-F(5A)#1	1.66(5)	F(6A)#1-P-F(2A)	69.3(18)
P-F(5A)	1.66(5)	F(2A)#1-P-F(2A)	70.9(19)
P-F(3)	1.574(4)	F(6A)-P-F(3A)#1	51.5(18)
Mn(1)-C(11)#1	1.807(2)	F(6A)#1-P-F(3A)#1	89.6(20)
Mn(1)-C(11)	1.807(2)	F(2A)#1-P-F(3A)#1	112.8(17)
Mn(1)-C(2)	2.179(2)	F(2A)-P-F(3A)#1	157.0(24)
Mn(1)-C(2)#1	2.179(2)	F(6A)-P-F(3A)	89.6(20)
Mn(1)-C(1)#1	2.184(2)	F(6A)#1-P-F(3A)	51.5(18)
Mn(1)-C(1)	2.184(2)	F(2A)#1-P-F(3A)	157.0(24)
Mn(1)-P(1)	2.1903(11)	F(2A)-P-F(3A)	112.8(17)
Mn(1)-C(3)#1	2.209(2)	F(3A)#1-P-F(3A)	54.7(29)
Mn(1)-C(3)	2.209(2)	F(6A)-P-F(4A)#1	118.9(16)
P(1)-O(14)	1.589(2)	F(6A)#1-P-F(4A)#1	74.7(14)
P(1)-O(13)#1	1.595(2)	F(2A)#1-P-F(4A)#1	168.8(15)
P(1)-O(13)	1.595(2)	F(2A)-P-F(4A)#1	109.6(14)
C(1)-C(2)	1.384(3)	F(3A)#1-P-F(4A)#1	71.4(15)
C(1)-C(1)#1	1.410(5)	F(3A)-P-F(4A)#1	33.8(18)
F(1A)-F(2A)	1.75(5)	F(6A)-P-F(4A)	74.7(14)
C(2)-C(3)	1.420(3)	F(6A)#1-P-F(4A)	118.9(16)
C(3)-C(3)#1	1.415(5)	F(2A)#1-P-F(4A)	109.6(14)
C(3)-C(8)	1.506(3)	F(2A)-P-F(4A)	168.8(15)
C(7)-C(7A)	1.518(9)	F(3A)#1-P-F(4A)	33.8(18)
C(7)-C(8)	1.665(7)	F(3A)-P-F(4A)	71.4(15)

F(4A)#1-P-F(4A)	67.7(19)	C(11)#1-Mn(1)-P(1)	87.95(7)
F(6A)-P-F(5A)#1	150.1(23)	C(11)-Mn(1)-P(1)	87.95(7)
F(6A)#1-P-F(5A)#1	106.8(19)	C(2)-Mn(1)-P(1)	118.03(7)
F(2A)#1-P-F(5A)#1	81.0(20)	C(2)#1-Mn(1)-P(1)	118.03(7)
F(2A)-P-F(5A)#1	49.0(20)	C(1)#1-Mn(1)-P(1)	91.76(7)
F(3A)#1-P-F(5A)#1	152.1(25)	C(1)-Mn(1)-P(1)	91.76(7)
F(3A)-P-F(5A)#1	119.2(25)	C(11)#1-Mn(1)-C(3)#1	89.33(9)
F(4A)#1-P-F(5A)#1	91.0(19)	C(11)-Mn(1)-C(3)#1	116.24(9)
F(4A)-P-F(5A)#1	119.8(19)	C(2)-Mn(1)-C(3)#1	67.46(9)
F(6A)-P-F(5A)	106.8(19)	C(2)#1-Mn(1)-C(3)#1	37.76(9)
F(6A)#1-P-F(5A)	150.1(23)	C(1)#1-Mn(1)-C(3)#1	67.88(9)
F(2A)#1-P-F(5A)	49.0(20)	C(1)-Mn(1)-C(3)#1	80.22(9)
F(2A)-P-F(5A)	81.0(20)	P(1)-Mn(1)-C(3)#1	155.67(7)
F(3A)#1-P-F(5A)	119.2(25)	C(11)#1-Mn(1)-C(3)	116.24(9)
F(3A)-P-F(5A)	152.1(25)	C(11)-Mn(1)-C(3)	89.33(9)
F(4A)#1-P-F(5A)	119.8(19)	C(2)-Mn(1)-C(3)	37.76(9)
F(4A)-P-F(5A)	91.0(19)	C(2)#1-Mn(1)-C(3)	67.46(9)
F(5A)#1-P-F(5A)	51.1(32)	C(1)#1-Mn(1)-C(3)	80.22(9)
F(4)-P-F(3)	176.0(3)	C(1)-Mn(1)-C(3)	67.88(9)
C(11)#1-Mn(1)-C(11)	90.26(14)	P(1)-Mn(1)-C(3)	155.67(7)
C(11)#1-Mn(1)-C(2)	154.00(10)	C(3)#1-Mn(1)-C(3)	37.35(12)
C(11)-Mn(1)-C(2)	89.85(10)	O(14)-P(1)-O(13)#1	105.64(10)
C(11)#1-Mn(1)-C(2)#1	89.85(10)	O(14)-P(1)-O(13)	105.64(10)
C(11)-Mn(1)-C(2)#1	154.00(10)	O(13)#1-P(1)-O(13)	94.24(14)
C(2)-Mn(1)-C(2)#1	78.97(12)	O(14)-P(1)-Mn(1)	109.86(9)
C(11)#1-Mn(1)-C(1)#1	116.04(9)	O(13)#1-P(1)-Mn(1)	119.74(7)
C(11)-Mn(1)-C(1)#1	153.68(9)	O(13)-P(1)-Mn(1)	119.74(7)
C(2)-Mn(1)-C(1)#1	67.15(9)	C(2)-C(1)-C(1)#1	119.45(13)
C(2)#1-Mn(1)-C(1)#1	36.99(9)	C(2)-C(1)-Mn(1)	71.29(13)
C(11)#1-Mn(1)-C(1)	153.68(9)	C(1)#1-C(1)-Mn(1)	71.17(6)
C(11)-Mn(1)-C(1)	116.04(9)	P-F(1A)-F(2A)	51.3(14)
C(2)-Mn(1)-C(1)	36.99(9)	C(1)-C(2)-C(3)	122.0(2)
C(2)#1-Mn(1)-C(1)	67.15(9)	C(1)-C(2)-Mn(1)	71.72(13)
C(1)#1-Mn(1)-C(1)	37.65(13)	C(3)-C(2)-Mn(1)	72.27(13)

P-F(2A)-F(1A)	61.3(16)	C(8)#1-C(7A)-C(7)	107.6(5)
C(3)#1-C(3)-C(2)	118.52(13)	C(7A)#1-C(8)-C(3)	119.8(4)
C(3)#1-C(3)-C(8)	121.2(2)	C(7A)#1-C(8)-C(7)	31.7(3)
C(2)-C(3)-C(8)	120.3(2)	C(3)-C(8)-C(7)	107.6(3)
C(3)#1-C(3)-Mn(1)	71.33(6)	O(11)-C(11)-Mn(1)	178.2(2)
C(2)-C(3)-Mn(1)	69.97(13)	C(13)-O(13)-P(1)	119.3(2)
C(8)-C(3)-Mn(1)	130.2(2)	C(14)-O(14)-P(1)	122.1(3)
C(7A)-C(7)-C(8)	112.0(4)		

Symmetry transformations used to generate equivalent atoms: #1 x,-y-1/2,z

Table A7.4: Anisotropic displacement parameters ($Å^2 x\ 10^3$) for **117**. The anisotropic displacement factor exponent takes the form: $-2\pi^2[\ h^2a^{*2}U^{11} + ... + 2\ h\ k\ a^*\ b^*\ U^{12}\ ]$.

	U^{11}	U^{22}	U^{33}	U^{23}	U^{13}	U^{12}
P	36(1)	26(1)	35(1)	0	9(1)	0
Mn(1)	24(1)	22(1)	21(1)	0	1(1)	0
P(1)	26(1)	35(1)	29(1)	0	5(1)	0
C(1)	38(1)	42(1)	24(1)	-7(1)	-4(1)	5(1)
F(1)	52(1)	38(1)	116(3)	-22(1)	41(2)	0(1)
C(2)	39(1)	26(1)	37(1)	-4(1)	-11(1)	0(1)
F(2)	68(2)	31(1)	156(4)	-2(1)	64(2)	-10(1)
C(3)	26(1)	38(1)	31(1)	3(1)	-5(1)	-7(1)
F(3)	70(3)	261(8)	39(2)	0	-4(2)	0
F(4)	74(4)	355(13)	69(3)	0	-28(3)	0
C(7)	34(3)	94(6)	36(3)	8(3)	3(2)	-12(3)
C(7A)	40(4)	89(5)	49(4)	-5(4)	16(3)	12(3)
C(8)	40(2)	77(2)	51(2)	22(2)	-5(1)	-26(2)
O(11)	60(1)	38(1)	37(1)	12(1)	-5(1)	2(1)
C(11)	31(1)	30(1)	28(1)	-1(1)	-2(1)	0(1)
O(13)	41(1)	49(1)	43(1)	-8(1)	14(1)	8(1)
C(13)	55(2)	46(2)	64(2)	-13(1)	8(2)	14(1)
O(14)	23(1)	49(1)	39(1)	0	-2(1)	0
C(14)	24(2)	63(3)	72(3)	0	-7(2)	0

Table A7.5: Hydrogen coordinates (x 10^4) and isotropic displacement parameters ($Å^2$x 10^3) for **117**.

	x	y	z	U(eq)
H(1A)	6921(16)	-1455(24)	3364(23)	39(7)
H(2)	7791(17)	-387(25)	2061(23)	43(8)
H(7A)	9633(4)	-1702(6)	-986(5)	66
H(7B)	8735(28)	-2142(38)	-1025(35)	23(13)
H(7AB)	10105(45)	-3198(57)	603(56)	71
H(7AC)	9809(44)	-3830(63)	-702(62)	71
H(8A)	9207(36)	-655(45)	846(43)	124(19)
H(8B)	8561(24)	-561(33)	81(33)	75(11)
H(13C)	5246(24)	-83(39)	1018(31)	89(12)
H(13B)	5894(24)	63(31)	2046(27)	63(10)
H(13A)	4957(23)	247(30)	2267(29)	70(10)
H(14B)	3988(22)	-1747(31)	681(30)	75(10)
H(14A)	4061(35)	-2500	-521(47)	81(16)

Table A8.1: Crystal data and structure refinement for **125**.

Empirical formula	$C_{18}H_{13}O_3Mn$	
Formula weight	332.22	
Temperature	173(2) K	
Wavelength	0.71073 Å	
Crystal system	Monoclinic	
Space group	C2	
Unit cell dimensions	a = 25.577(14) Å	α= 90°.
	b = 6.255(3) Å	β= 107.230(8)°.
	c = 9.362(5) Å	γ = 90°.
Volume	1430.5(14) $Å^3$	
Z	4	
Density (calculated)	1.543 Mg/m^3	
Absorption coefficient	0.932 mm^{-1}	
F(000)	680	
Crystal size	.03 x .05 x .50 mm^3	
Theta range for data collection	1.67 to 27.51°.	
Index ranges	$-32 \le h \le 32$, $-8 \le k \le 8$, $-12 \le l \le 11$	
Reflections collected	6352	
Independent reflections	2802 [R(int) = 0.0604]	
Refinement method	Full-matrix least-squares on F^2	
Data / restraints / parameters	2802 / 1 / 200	
Goodness-of-fit on F^2	1.034	
Final R indices [I>2sigma(I)]	R1 = 0.0520, wR2 = 0.0925	
R indices (all data)	R1 = 0.0894, wR2 = 0.1044	
Absolute structure parameter	0.50(3)	
Extinction coefficient	0.0000(7)	
Largest diff. peak and hole	0.412 and -0.372 $e.Å^{-3}$	

Table A8.2: Atomic coordinates (x 10^4) and equivalent isotropic displacement parameters ($Å^2$ x 10^3) for **125**. U(eq) is defined as one third of the trace of the orthogonalized U^{ij} tensor.

	x	y	z	U(eq)
Mn(1)	568(1)	2748(1)	8005(1)	22(1)
C(3)	1021(2)	2839(13)	10348(5)	32(1)
C(1)	1664(2)	2473(8)	8814(5)	18(1)
C(12)	3321(2)	2790(13)	7043(5)	40(1)
O(17)	729(2)	4853(6)	5351(4)	36(1)
C(16)	-22(2)	1266(8)	6937(6)	30(1)
C(17)	673(2)	4059(7)	6394(6)	25(1)
O(18)	-180(2)	6162(6)	8324(4)	36(1)
C(9)	2454(2)	143(7)	7182(5)	23(1)
C(18)	109(2)	4811(8)	8232(6)	26(1)
C(15)	2153(2)	3112(6)	8664(5)	20(1)
C(6)	1314(2)	696(7)	8066(5)	22(1)
C(14)	2508(2)	2188(6)	7846(5)	21(1)
C(8)	2010(2)	-1372(7)	7260(6)	26(1)
C(2)	1373(2)	3779(8)	9628(6)	30(1)
O(16)	-404(2)	298(6)	6283(5)	50(1)
C(5)	964(2)	-252(8)	8772(6)	27(1)
C(7)	1432(2)	-389(7)	6774(5)	25(1)
C(4)	808(2)	779(9)	9941(6)	32(1)
C(10)	2829(2)	-494(9)	6456(6)	32(1)
C(13)	2946(2)	3471(8)	7753(6)	30(1)
C(11)	3258(2)	765(10)	6378(6)	43(2)

Table A8.3: Bond lengths [Å] and angles [°] for **125**.

Mn(1)-C(18)	1.798(6)	C(16)-Mn(1)-C(4)	99.1(2)
Mn(1)-C(16)	1.801(5)	C(17)-Mn(1)-C(4)	153.9(2)
Mn(1)-C(17)	1.805(5)	C(18)-Mn(1)-C(5)	147.7(2)
Mn(1)-C(4)	2.126(5)	C(16)-Mn(1)-C(5)	88.3(2)
Mn(1)-C(5)	2.153(5)	C(17)-Mn(1)-C(5)	120.2(2)
Mn(1)-C(3)	2.157(5)	C(4)-Mn(1)-C(5)	38.9(2)
Mn(1)-C(2)	2.262(5)	C(18)-Mn(1)-C(3)	91.9(2)
Mn(1)-C(6)	2.287(5)	C(16)-Mn(1)-C(3)	133.5(2)
C(3)-C(2)	1.403(7)	C(17)-Mn(1)-C(3)	132.0(2)
C(3)-C(4)	1.407(9)	C(4)-Mn(1)-C(3)	38.3(2)
C(1)-C(15)	1.358(6)	C(5)-Mn(1)-C(3)	68.0(2)
C(1)-C(2)	1.462(7)	C(18)-Mn(1)-C(2)	102.3(2)
C(1)-C(6)	1.468(6)	C(16)-Mn(1)-C(2)	165.2(2)
C(12)-C(13)	1.386(7)	C(17)-Mn(1)-C(2)	95.8(2)
C(12)-C(11)	1.399(9)	C(4)-Mn(1)-C(2)	67.4(2)
O(17)-C(17)	1.141(6)	C(5)-Mn(1)-C(2)	77.3(2)
C(16)-O(16)	1.158(6)	C(3)-Mn(1)-C(2)	36.9(2)
O(18)-C(18)	1.143(6)	C(18)-Mn(1)-C(6)	165.6(2)
C(9)-C(10)	1.388(7)	C(16)-Mn(1)-C(6)	106.3(2)
C(9)-C(14)	1.411(6)	C(17)-Mn(1)-C(6)	86.9(2)
C(9)-C(8)	1.498(7)	C(4)-Mn(1)-C(6)	68.0(2)
C(15)-C(14)	1.469(6)	C(5)-Mn(1)-C(6)	36.4(2)
C(6)-C(5)	1.394(7)	C(3)-Mn(1)-C(6)	78.2(2)
C(6)-C(7)	1.493(7)	C(2)-Mn(1)-C(6)	63.6(2)
C(14)-C(13)	1.402(6)	C(2)-C(3)-C(4)	120.4(5)
C(8)-C(7)	1.540(7)	C(2)-C(3)-Mn(1)	75.6(3)
C(5)-C(4)	1.425(7)	C(4)-C(3)-Mn(1)	69.6(3)
C(10)-C(11)	1.371(8)	C(15)-C(1)-C(2)	121.0(4)
C(18)-Mn(1)-C(16)	88.1(2)	C(15)-C(1)-C(6)	128.5(4)
C(18)-Mn(1)-C(17)	92.1(2)	C(2)-C(1)-C(6)	109.8(4)
C(16)-Mn(1)-C(17)	94.5(2)	C(13)-C(12)-C(11)	119.1(6)
C(18)-Mn(1)-C(4)	110.4(2)	O(16)-C(16)-Mn(1)	178.3(5)

O(17)-C(17)-Mn(1)	178.1(5)	C(9)-C(8)-C(7)	114.1(4)
C(10)-C(9)-C(14)	118.9(5)	C(3)-C(2)-C(1)	120.9(5)
C(10)-C(9)-C(8)	119.1(4)	C(3)-C(2)-Mn(1)	67.5(3)
C(14)-C(9)-C(8)	121.9(4)	C(1)-C(2)-Mn(1)	89.6(3)
O(18)-C(18)-Mn(1)	177.1(4)	C(6)-C(5)-C(4)	122.5(5)
C(1)-C(15)-C(14)	132.0(4)	C(6)-C(5)-Mn(1)	77.0(3)
C(5)-C(6)-C(1)	118.9(4)	C(4)-C(5)-Mn(1)	69.6(3)
C(5)-C(6)-C(7)	120.2(4)	C(6)-C(7)-C(8)	110.4(4)
C(1)-C(6)-C(7)	119.3(4)	C(3)-C(4)-C(5)	116.6(5)
C(5)-C(6)-Mn(1)	66.5(3)	C(3)-C(4)-Mn(1)	72.0(3)
C(1)-C(6)-Mn(1)	88.5(3)	C(5)-C(4)-Mn(1)	71.5(3)
C(7)-C(6)-Mn(1)	127.0(3)	C(11)-C(10)-C(9)	122.8(5)
C(13)-C(14)-C(9)	117.9(5)	C(12)-C(13)-C(14)	122.2(5)
C(13)-C(14)-C(15)	115.9(4)	C(10)-C(11)-C(12)	119.0(5)
C(9)-C(14)-C(15)	126.2(4)		

Table A8.4: Anisotropic displacement parameters ($Å^2 \times 10^3$) for **125**. The anisotropic displacement factor exponent takes the form: $-2\pi^2[h^2a^{*2}U^{11} + ... + 2\ h\ k\ a^*\ b^*\ U^{12}]$.

	U^{11}	U^{22}	U^{33}	U^{23}	U^{13}	U^{12}
Mn(1)	17(1)	26(1)	21(1)	3(1)	4(1)	-1(1)
C(3)	19(2)	56(3)	21(2)	4(4)	3(2)	16(4)
C(1)	18(2)	18(3)	16(2)	1(2)	1(2)	2(2)
C(12)	22(3)	65(3)	35(3)	19(4)	10(2)	2(5)
O(17)	45(3)	40(2)	28(2)	0(2)	17(2)	-11(2)
C(16)	28(3)	30(3)	28(3)	10(2)	3(3)	-5(3)
C(17)	25(3)	25(3)	24(3)	-2(2)	5(3)	-5(2)
O(18)	34(2)	38(2)	43(3)	11(2)	21(2)	8(2)
C(9)	21(3)	30(3)	15(3)	4(2)	0(2)	6(2)
C(18)	22(3)	32(3)	25(3)	9(2)	11(3)	-5(3)
C(15)	18(2)	13(3)	23(2)	0(2)	-3(2)	-1(2)
C(6)	15(3)	20(2)	24(3)	-3(2)	-1(2)	-4(2)
C(14)	16(3)	27(3)	17(2)	7(2)	0(2)	4(2)
C(8)	32(3)	19(2)	25(3)	-5(2)	7(3)	5(2)
C(2)	18(3)	38(3)	24(3)	-7(2)	-7(2)	3(2)
O(16)	37(3)	49(2)	52(3)	16(2)	-8(2)	-18(2)
C(5)	17(3)	25(2)	34(3)	9(2)	1(3)	4(2)
C(7)	29(3)	20(2)	23(3)	-4(2)	6(3)	-2(2)
C(4)	19(3)	50(3)	26(3)	18(3)	7(3)	2(3)
C(10)	27(3)	43(3)	26(3)	-4(2)	9(3)	10(3)
C(13)	21(3)	39(3)	27(3)	9(2)	0(2)	-2(2)
C(11)	27(4)	78(4)	26(3)	7(3)	13(3)	17(3)

Table A8.5: Hydrogen coordinates (x 10^4) and isotropic displacement parameters ($Å^2$ x 10^3) for **125**.

	x	y	z	U(eq)
H(3A)	881(2)	3714(13)	11049(5)	39
H(12A)	3617(2)	3685(13)	7009(5)	48
H(15A)	2290(2)	4394(6)	9184(5)	24
H(8A)	2089(2)	-1896(7)	8300(6)	31
H(8B)	2015(2)	-2621(7)	6615(6)	31
H(2A)	1460(2)	5338(8)	9775(6)	35
H(5A)	772(2)	-1604(8)	8342(6)	32
H(7A)	1404(2)	659(7)	5962(5)	29
H(7B)	1158(2)	-1527(7)	6384(5)	29
H(4A)	533(2)	133(9)	10379(6)	38
H(10A)	2786(2)	-1860(9)	5993(6)	38
H(13A)	2988(2)	4854(8)	8192(6)	36
H(11A)	3509(2)	271(10)	5880(6)	51

Table A9.1: Crystal data and structure refinement for **148**.

Empirical formula	$C_{20}H_{30}O_2BrMn$	
Formula weight	437.29	
Temperature	173(2) K	
Wavelength	0.71073 Å	
Crystal system	Monoclinic	
Space group	P2(1)/n	
Unit cell dimensions	a = 9.004(6) Å	α= 90°.
	b = 16.690(11) Å	β= 105.688(10)°.
	c = 14.135(9) Å	γ = 90°.
Volume	2045.0(22) $Å^3$	
Z	4	
Density (calculated)	1.420 Mg/m^3	
Absorption coefficient	2.608 mm^{-1}	
F(000)	904	
Crystal size	0.55 x 0.32 x 0.25 mm^3	
Theta range for data collection	1.93 to 27.53°.	
Index ranges	$-11 \le h \le 11$, $-20 \le k \le 21$, $-18 \le l \le 18$	
Reflections collected	17809	
Independent reflections	4705 [R(int) = 0.0744]	
Refinement method	Full-matrix least-squares on F^2	
Data / restraints / parameters	4705 / 0 / 223	
Goodness-of-fit on F^2	1.049	
Final R indices [I>2sigma(I)]	R1 = 0.0490, wR2 = 0.1148	
R indices (all data)	R1 = 0.1070, wR2 = 0.1424	
Extinction coefficient	0.0024(6)	
Largest diff. peak and hole	0.583 and -0.783 $e.Å^{-3}$	

Table A9.2: Atomic coordinates (x 10^4) and equivalent isotropic displacement parameters ($Å^2$ x 10^3) for **148**. U(eq) is defined as one third of the trace of the orthogonalized U^{ij} tensor.

	x	y	z	U(eq)
Mn(1)	3817(1)	1458(1)	2175(1)	22(1)
C(1)	6020(4)	804(2)	2528(2)	22(1)
C(2)	6052(5)	1397(2)	3259(2)	23(1)
C(3)	4893(5)	1407(2)	3776(2)	23(1)
C(4)	3671(5)	844(2)	3534(2)	23(1)
C(5)	3610(5)	256(2)	2791(3)	26(1)
C(6)	4794(5)	240(2)	2296(3)	25(1)
C(7)	4767(5)	-399(2)	1529(3)	35(1)
C(8)	5658(6)	-1144(3)	1997(4)	51(1)
C(9)	2326(5)	-373(2)	2560(4)	41(1)
C(10)	906(6)	-154(3)	1712(4)	54(2)
C(11)	2427(5)	858(3)	4070(3)	33(1)
C(12)	2844(6)	334(3)	4992(4)	52(1)
C(13)	4989(5)	2007(3)	4605(3)	31(1)
C(14)	4188(6)	2806(3)	4300(3)	44(1)
C(15)	7357(5)	1993(2)	3509(3)	29(1)
C(16)	8739(5)	1684(3)	4324(3)	41(1)
C(17)	7312(5)	762(3)	2023(3)	33(1)
C(18)	7055(6)	1243(3)	1072(3)	44(1)
C(19)	4403(5)	2489(3)	1884(3)	33(1)
O(19)	4771(5)	3037(2)	1777(2)	48(1)
Br(1A)	1248(1)	2067(1)	2111(1)	40(1)
C(20B)	3218(12)	1325(6)	999(6)	69(3)
O(20B)	2838(2)	1177(1)	312(2)	72(1)
Br(1B)	2838(2)	1177(1)	312(2)	72(1)
C(20A)	2259(41)	1738(20)	2108(20)	114(10)
O(20A)	1248(1)	2067(1)	2111(1)	40(1)

Table A9.3: Bond lengths [Å] and angles [°] for **148**.

Mn(1)-C(20A)	1.46(4)	C(20A)-O(20A)	1.07(4)
Mn(1)-C(20B)	1.618(9)	C(20A)-Mn(1)-C(19)	90.9(12)
Mn(1)-C(19)	1.878(6)	C(20B)-Mn(1)-C(19)	86.3(4)
Mn(1)-C(2)	2.177(4)	C(20A)-Mn(1)-C(2)	138.7(11)
Mn(1)-C(1)	2.201(4)	C(20B)-Mn(1)-C(2)	134.8(4)
Mn(1)-C(6)	2.204(4)	C(19)-Mn(1)-C(2)	86.4(2)
Mn(1)-C(3)	2.210(4)	C(20A)-Mn(1)-C(1)	165.2(12)
Mn(1)-C(4)	2.213(4)	C(20B)-Mn(1)-C(1)	101.2(4)
Mn(1)-C(5)	2.216(4)	C(19)-Mn(1)-C(1)	102.4(2)
Mn(1)-O(20A)	2.506(2)	C(2)-Mn(1)-C(1)	38.02(14)
Mn(1)-Br(1A)	2.506(2)	C(20A)-Mn(1)-C(6)	131.1(12)
Mn(1)-Br(1B)	2.584(3)	C(20B)-Mn(1)-C(6)	88.2(3)
C(1)-C(6)	1.420(5)	C(19)-Mn(1)-C(6)	137.1(2)
C(1)-C(2)	1.426(5)	C(2)-Mn(1)-C(6)	68.18(15)
C(1)-C(17)	1.523(5)	C(1)-Mn(1)-C(6)	37.61(14)
C(2)-C(3)	1.426(5)	C(20A)-Mn(1)-C(3)	103.1(11)
C(2)-C(15)	1.506(6)	C(20B)-Mn(1)-C(3)	168.2(3)
C(3)-C(4)	1.418(6)	C(19)-Mn(1)-C(3)	100.9(2)
C(3)-C(13)	1.524(5)	C(2)-Mn(1)-C(3)	37.94(14)
C(4)-C(5)	1.427(5)	C(1)-Mn(1)-C(3)	68.28(14)
C(4)-C(11)	1.512(6)	C(6)-Mn(1)-C(3)	80.18(14)
C(5)-C(6)	1.426(6)	C(20A)-Mn(1)-C(4)	85.6(11)
C(5)-C(9)	1.530(6)	C(20B)-Mn(1)-C(4)	138.3(4)
C(6)-C(7)	1.517(5)	C(19)-Mn(1)-C(4)	134.5(2)
C(7)-C(8)	1.530(6)	C(2)-Mn(1)-C(4)	68.14(14)
C(9)-C(10)	1.541(7)	C(1)-Mn(1)-C(4)	80.48(14)
C(11)-C(12)	1.531(6)	C(6)-Mn(1)-C(4)	67.73(14)
C(13)-C(14)	1.521(6)	C(3)-Mn(1)-C(4)	37.40(15)
C(15)-C(16)	1.538(6)	C(20A)-Mn(1)-C(5)	97.7(12)
C(17)-C(18)	1.529(6)	C(20B)-Mn(1)-C(5)	103.8(4)
C(19)-O(19)	0.998(5)	C(19)-Mn(1)-C(5)	167.1(2)
C(20B)-O(20B)	0.970(8)	C(2)-Mn(1)-C(5)	80.83(15)

C(1)-Mn(1)-C(5)	68.15(15)	C(17)-C(1)-Mn(1)	132.3(3)
C(6)-Mn(1)-C(5)	37.63(15)	C(1)-C(2)-C(3)	120.4(4)
C(3)-Mn(1)-C(5)	67.82(14)	C(1)-C(2)-C(15)	119.3(3)
C(4)-Mn(1)-C(5)	37.59(14)	C(3)-C(2)-C(15)	120.3(3)
C(20A)-Mn(1)-O(20A)	5.5(12)	C(1)-C(2)-Mn(1)	71.9(2)
C(19)-Mn(1)-O(20A)	86.10(15)	C(3)-C(2)-Mn(1)	72.3(2)
C(2)-Mn(1)-O(20A)	135.47(11)	C(15)-C(2)-Mn(1)	130.4(3)
C(1)-Mn(1)-O(20A)	167.52(10)	C(4)-C(3)-C(2)	119.7(3)
C(6)-Mn(1)-O(20A)	136.25(11)	C(4)-C(3)-C(13)	120.0(4)
C(3)-Mn(1)-O(20A)	101.39(11)	C(2)-C(3)-C(13)	120.3(4)
C(4)-Mn(1)-O(20A)	87.04(11)	C(4)-C(3)-Mn(1)	71.4(2)
C(5)-Mn(1)-O(20A)	101.92(11)	C(2)-C(3)-Mn(1)	69.8(2)
C(20B)-Mn(1)-Br(1A)	88.3(4)	C(13)-C(3)-Mn(1)	132.8(3)
C(19)-Mn(1)-Br(1A)	86.10(15)	C(3)-C(4)-C(5)	120.5(4)
C(2)-Mn(1)-Br(1A)	135.47(11)	C(3)-C(4)-C(11)	120.0(3)
C(1)-Mn(1)-Br(1A)	167.52(10)	C(5)-C(4)-C(11)	119.5(4)
C(6)-Mn(1)-Br(1A)	136.25(11)	C(3)-C(4)-Mn(1)	71.2(2)
C(3)-Mn(1)-Br(1A)	101.39(11)	C(5)-C(4)-Mn(1)	71.3(2)
C(4)-Mn(1)-Br(1A)	87.04(11)	C(11)-C(4)-Mn(1)	130.8(3)
C(5)-Mn(1)-Br(1A)	101.92(11)	C(6)-C(5)-C(4)	119.3(4)
C(20A)-Mn(1)-Br(1B)	86.3(11)	C(6)-C(5)-C(9)	120.3(3)
C(19)-Mn(1)-Br(1B)	88.94(13)	C(4)-C(5)-C(9)	120.4(4)
C(2)-Mn(1)-Br(1B)	134.79(11)	C(6)-C(5)-Mn(1)	70.7(2)
C(1)-Mn(1)-Br(1B)	100.31(10)	C(4)-C(5)-Mn(1)	71.1(2)
C(6)-Mn(1)-Br(1B)	86.03(11)	C(9)-C(5)-Mn(1)	132.6(3)
C(3)-Mn(1)-Br(1B)	166.20(11)	C(1)-C(6)-C(5)	120.8(3)
C(4)-Mn(1)-Br(1B)	135.77(12)	C(1)-C(6)-C(7)	119.5(4)
C(5)-Mn(1)-Br(1B)	101.22(11)	C(5)-C(6)-C(7)	119.6(4)
O(20A)-Mn(1)-Br(1B)	88.84(5)	C(1)-C(6)-Mn(1)	71.1(2)
C(6)-C(1)-C(2)	119.3(3)	C(5)-C(6)-Mn(1)	71.6(2)
C(6)-C(1)-C(17)	120.4(3)	C(7)-C(6)-Mn(1)	131.7(3)
C(2)-C(1)-C(17)	120.3(3)	C(6)-C(7)-C(8)	110.9(4)
C(6)-C(1)-Mn(1)	71.3(2)	C(5)-C(9)-C(10)	115.1(4)
C(2)-C(1)-Mn(1)	70.1(2)	C(4)-C(11)-C(12)	111.9(4)

C(14)-C(13)-C(3)	115.7	O(19)-C(19)-Mn(1)	175.8(4)
(3)		O(20B)-C(20B)-Mn(1)	173.0(9)
C(2)-C(15)-C(16)	112.2(3)	O(20A)-C(20A)-Mn(1)	167.0(28)
C(1)-C(17)-C(18)	115.8(4)	C(20A)-O(20A)-Mn(1)	7.5(16)

Table A9.4: Anisotropic displacement parameters ($Å^2 \times 10^3$) for **148**. The anisotropic displacement factor exponent takes the form: $-2\pi^2[h^2a^{*2}U^{11} + ... + 2\ h\ k\ a^*\ b^*\ U^{12}]$.

	U^{11}	U^{22}	U^{33}	U^{23}	U^{13}	U^{12}
Mn(1)	27(1)	18(1)	21(1)	-1(1)	6(1)	3(1)
C(1)	21(2)	21(2)	24(2)	1(2)	5(2)	1(2)
C(2)	25(2)	22(2)	21(2)	4(2)	5(2)	3(2)
C(3)	23(2)	24(2)	22(2)	2(2)	6(2)	6(2)
C(4)	27(2)	19(2)	25(2)	9(2)	11(2)	7(2)
C(5)	26(2)	17(2)	36(2)	1(2)	10(2)	1(2)
C(6)	29(2)	14(2)	34(2)	-1(2)	10(2)	6(2)
C(7)	39(3)	22(2)	46(2)	-14(2)	15(2)	-3(2)
C(8)	59(4)	24(2)	77(3)	-10(2)	30(3)	6(2)
C(9)	35(3)	20(2)	76(3)	-12(2)	28(2)	-8(2)
C(10)	32(3)	39(3)	89(4)	-19(3)	12(3)	-8(2)
C(11)	32(3)	36(3)	36(2)	6(2)	16(2)	5(2)
C(12)	55(4)	59(4)	54(3)	25(3)	33(3)	9(3)
C(13)	33(3)	35(3)	26(2)	-9(2)	8(2)	0(2)
C(14)	56(3)	34(3)	42(2)	-12(2)	12(2)	8(2)
C(15)	28(3)	30(2)	29(2)	-5(2)	8(2)	-5(2)
C(16)	29(3)	49(3)	40(2)	0(2)	0(2)	-4(2)
C(17)	35(3)	34(3)	33(2)	-5(2)	16(2)	-3(2)
C(18)	48(3)	56(3)	34(2)	-2(2)	22(2)	-11(3)
C(19)	25(3)	42(3)	32(2)	-19(2)	5(2)	0(2)
O(19)	68(3)	38(2)	34(2)	12(2)	10(2)	12(2)
Br(1A)	45(1)	36(1)	36(1)	1(1)	6(1)	9(1)
C(20B)	86(7)	70(6)	38(4)	-28(4)	-3(4)	9(5)
O(20B)	59(1)	49(1)	107(2)	1(1)	23(1)	10(1)
Br(1B)	59(1)	49(1)	107(2)	1(1)	23(1)	10(1)
O(20A)	45(1)	36(1)	36(1)	1(1)	6(1)	9(1)

Table A9.5: Hydrogen coordinates (x 10^4) and isotropic displacement parameters ($Å^2$ x 10^3) for **148**.

	x	y	z	U(eq)
H(14A)	5233(5)	-183(2)	1023(3)	42
H(14B)	3685(5)	-548(2)	1203(3)	42
H(17A)	5625(6)	-1548(3)	1489(4)	76
H(17B)	5187(6)	-1363(3)	2491(4)	76
H(17C)	6733(6)	-999(3)	2312(4)	76
H(15A)	1983(5)	-467(2)	3159(4)	49
H(15B)	2759(5)	-883(2)	2394(4)	49
H(4AA)	148(6)	-589(3)	1616(4)	82
H(4AB)	1223(6)	-76(3)	1108(4)	82
H(4AC)	445(6)	341(3)	1875(4)	82
H(7A)	1446(5)	666(3)	3623(3)	40
H(7B)	2269(5)	1417(3)	4258(3)	40
H(3AA)	2013(6)	358(3)	5318(4)	79
H(3AB)	3805(6)	528(3)	5442(4)	79
H(3AC)	2982(6)	-222(3)	4807(4)	79
H(12A)	4535(5)	1756(3)	5097(3)	38
H(12B)	6091(5)	2112(3)	4930(3)	38
H(19A)	4315(6)	3147(3)	4881(3)	66
H(19B)	3088(6)	2714(3)	3995(3)	66
H(19C)	4647(6)	3071(3)	3828(3)	66
H(11A)	6983(5)	2500(2)	3726(3)	34
H(11B)	7696(5)	2107(2)	2913(3)	34
H(18A)	9559(5)	2089(3)	4464(3)	62
H(18B)	9126(5)	1187(3)	4107(3)	62
H(18C)	8413(5)	1580(3)	4920(3)	62
H(13A)	7470(5)	193(3)	1875(3)	39
H(13B)	8275(5)	952(3)	2490(3)	39
H(20A)	7946(6)	1177(3)	806(3)	66
H(20B)	6932(6)	1811(3)	1208(3)	66
H(20C)	6124(6)	1049(3)	592(3)	66